Interactions between dopamine neurons and radial glial cells in the adult goldfish forebrain

by

Lei Xing

Thesis submitted to the

Faculty of Graduate and Postdoctoral Studies

in partial fulfillment of the requirements

for the Doctorate in Philosophy degree in Biology

Department of Biology

Faculty of Science

University of Ottawa

Acknowledgements

Four years ago, I made a big decision to move to Canada and pursue my doctoral degree in Ottawa. As this great journey comes to an end, I would like to express my sincere gratitude to the many people who supported me and helped me.

With no doubt, I would like to thank my supervisor Dr. Vance Trudeau first. Vance, thank you for accepting me as one of your students and giving me the opportunity to study in your lab. I learned a great deal from you in the past four years, your guidance helped me in all the time of research and writing of this thesis. I could not have imagined having a better advisor for my Ph.D. studies and I am very proud to say that you are a great supervisor, great mentor and a great friend. Besides my supervisor, I would like to thank my committee members, Dr. Marc Ekker, Dr. Michael Jonz and Dr. Mario Tiberi for your direction, insightful comments and stimulating conversations, which encouraged me to widen my research from various perspectives. My sincere thanks also goes to Dr. Chris Martyniuk for performing proteomic studies and teaching me proteomics and bioinformatics, you are a great big brother mentor and a definite role model for being a well-rounded researcher.

Past and present teamENDO members: Thank You! We laughed together, we cried together, we worked hard together, and most importantly we had fun together! Laia, Christy and Lisa, thanks for showing me around the lab and for helping me with many techniques from the very beginning. Juan, thanks for all the inspiring discussion on the DHAA project and all the other crazy things we talked about. Brooke, thanks for all the assistance on the dissections and samplings. I will never forget the trip to Nova Scotia! Heather, Dillon and Crystal, thanks for all the hard work on cell culture, qPCR and cloning, I would not have been be able to finish in time without your valuable help. Maddie and Marilyn, thanks for

your contribution to my thesis and side projects. There are too many more to mention, thanks everyone, for everything.

Special thanks to Jing, for your help on my *in situ* experiments and being the "go to" person whenever I have a question or a problem; to Andrew Ochaski, for the training on confocal imaging; to Bill, for taking care of all the goldfish "volunteers". In terms of financial support I would like to acknowledge the Ontario Trillium Scholarship and University of Ottawa for supporting me.

And finally to my dear parents: thank you so much for all your love and care, for believing in me and supporting me financially and emotionally.

Abstract

Aromatase is the only enzyme that converts androgens into estrogens, which is found in the brain, testes and ovaries. In teleosts, brain aromatase is exclusively expressed in radial glial cells, which are the abundant stem-like non-neuronal progenitors involved in neuroendocrine functions and neurogenesis in the central nervous system. With little information about radial glial cell regulation by neurotransmitters and neurohormones available, the overall goal of this thesis is to investigate the interactions between dopamine neurons and radial glial cells in the adult goldfish (*Carassius auratus*) forebrain. Immunocytochemistry and confocal imaging revealed a close anatomical relationship between dopamine neurons and radial glial cells along the ventricular surface in the telencephalon. Transcriptional regulation of brain aromatase by dopamine indicated a brain region-specific pattern and suggested the involvement of other regulators in the goldfish forebrain. A novel goldfish primary radial glial cell culture model was established and characterized for brain aromatase regulation studies. Pharmacological studies demonstrated that specific activation of dopamine D1 receptors up-regulates brain aromatase through a cAMP-dependent molecular mechanism, which can be enhanced or attenuated by the product of aromatase action, 17β-estradiol. Proteome profiling and the response following treatment with the specific dopamine D1 receptor agonist SKF 38393 revealed that proteins involved in cell proliferation and growth are regulated through small molecules- and transcription factors-mediated signaling pathways. Analysis of genes related to radial glial cell and dopamine neuron functions demonstrated that glial activation and dopamine neuron recovery are estrogen-dependent in a neurotoxin MPTP-induced goldfish model of Parkinson's disease. This thesis illustrates novel molecular mechanisms underlying brain aromatase

regulation as well as radial glial cell function regulation and provides a framework for future investigation of existing endocrine disruptors modulating neurosteroid levels in the teleost brain.

Résumé

L'aromatase est la seule enzyme qui aromatise les androgènes pour produire des estrogènes et est retrouvée dans le cerveau, les testicules et les ovaires. L'aromatase située dans le cerveau des poissons téléostéens est exclusivement retrouvée dans les cellules gliales radiaires. Ces cellules progénitrices non-neuronales abondantes ressemblent aux cellules souches et jouent un rôle important dans le système nerveux central tel que la neurogénèse et la function neuroendocrine. Le but de cette thèse est d'étudier l'intéraction entre les neurones dopaminergiques et les cellules gliales radiaires dans le cerveau antérieur du poisson rouge *(Carassius auratus)* parce que l'information disponible sur la régulation de ces cellules gliales radiaires par divers neurotransmitteurs et neurohormones demeure incomplète. Les études d'imagerie par miscroscopie confocale et d'immunohistochimie suggèrent un lien anatomique étroint entre les neurones dopaminergiques et les cellules gliales radiaires à la surface ventriculaire du télencéphale. En outre, la régulation transcriptionnelle de l'aromatase dans le cerveau par la dopamine dépend spécifiquement du tissu observé. Cette observation suggère l'existence de régulateurs spécifiques pour la transcription de l'aromatase dans le cerveau antérieur du poisson rouge. Dans le but d'étudier la régulation de l'aromatase du cerveau, nous avons donc établi et caractérisé un nouveau modèle de cellules gliales radiaires du poisson rouge en culture. Nos études pharmacologiques montrent qu'une activation des récepteurs de la dopamine D1 augmente les niveaux d'aromatase du cerveau via une stimulation spécifique de la production intracellulaire d'adénosine monophosphate cyclique. Cette activation peut être aussi augmenter ou atténuer par 17ß-estradiol, le produit de l'activation de l'enzyme aromatase. Le profil protéomique observé des cellules gliales radiaires suite à un traitement avec le SKF 38393, un agoniste spécifique des récepteur

dopaminergiques D1, suggère que les protéines impliquées dans la prolifération et la croissance cellulaires sont contrôlées par des voies signalétiques que sont dépendantes de petites molécules et de facteurs transcriptionnels. Par ailleurs, l'activation de l'aromatase et la regénération des neurones dopaminergiques semblent dépendre de l'oestrogène. L'analyses des gènes liés aux fonctions neuronales dopaminergiques et des cellules gliales radiaires démontre que l'activation des cellules gliales et le rétablissment des neurones à la dopamine dans le poisson rouge injecté avec la neurotoxine MPTP, un modèle expérimental de la maladie de Parkinson, sont dépendants de l'oestrogène. En conclusion, cette thèse a mise àjour un nouveau mécanisme moléculaire qui permettra des études plus approfondies de l'activité de l'aromatase dans le cerveau du poisson rouge notamment celles liées au dérèglement fonctionnelle des cellules gliales radiaires par des pertubateurs endocriniens.

Table of contents

List of Figures

List of Tables

List of commonly used abbreviations in this thesis

5-HT	serotonin
AADC	aromatic amino acid decarboxylase
AC	adenylyl cyclase
ANOVA	analysis of variance
ATP	adenosine triphosphate
BDNF	brain-derived neurotrophic factor
BLBP	brain lipid binding protein
BrdU	bromodeoxyuridine
BSA	bovine serum albumin
cAMP	cyclic adenosine monophosphate
CNS	central nervous system
CRE	cAMP response element
CSF	cerebrospinal fluid
DA	dopamine
DAPI	4,6-diamino-2-phenylindole
DAT	dopamine transporters
ddPCR	droplet digital PCR
E2	17β-estradiol
EGF	epidermal growth factor
ER	estrogen receptor
ERE	estrogen response element
ERK	extracellular signal-regulated kinase
FBS	Fetal Bovine Serum
GDNF	glial cell line-derived neurotrophic factor
GFAP	glial fibrillary acidic protein
GLAST	glutamate aspartate transporter
GO	gene ontology
GPER	G protein-coupled estrogen receptor
GSI	gonadosomatic index
IGF-1	insulin growth factor 1
L-DOPA	L-3,4-dihydroxyphenylalanine
MAPK	mitogen-activated protein kinase
MPTP	1-methyl-4-phenyl-1,2,3,6-tetrahydropyridine
MS222	3-aminobenzoic acid ethylester
NPP	preoptic periventricular nucleus
NSAF	normalized spectral abundance factor
NURR1	nuclear receptor related 1 protein

p-CREB	phosphorylated cAMP response element binding protein
PANTHER	protein annotation through evolutionary relationship
PBR	peripheral benzodiazepine receptor
PBS	phosphate buffered saline
PCNA	proliferating cell nuclear antigen
PD	Parkinson's disease
PFA	paraformaldehyde
PINK1	PTEN-induced putative kinase 1
Pitx3	paired-like homeodomain transcription factor 3
PKA	protein kinase A
PKC	protein kinase C
PKG	protein kinase G
qPCR	quantitative real-time reverse transcription polymerase chain reaction
RGC	radial glial cell
RT	room temperature
SN	substantia nigra
SNEA	sub-network enrichment analysis
StAR	steroidogenic acute regulatory protein
TBST	Tris-Buffered Saline and Tween 20
TGFα	transforming growth factor α
TH	tyrosine hydroxylase
TIC	total ion current
TPI	triosephosphate isomerase
Vv	ventralis telencephali pars ventralis

Chapter 1: General Introduction [1]

1.1 Thesis outline and rationale

The overall goal of this thesis is to investigate the interactions between dopamine (DA) neurons and radial glial cells (RGCs) in the adult goldfish forebrain. Neurons and glia are two different cell types composing the vertebrate central nervous system (CNS). To maintain normal brain functions, communication between neurons and glia is essential. There is increasing evidence showing that glia not only serve as "glue" in the brain to support and separate neurons anymore, but that they also have many other important roles (Anthony et al., 2004; Campbell and Götz, 2002; Xing et al., 2014). In this thesis, DA neurons and RGCs were chosen as representatives of each cell type because of their abundance and crucial functions. In the CNS, DA is one of the key neurotransmitters involved in the control of reproduction, feeding, stress, motor behaviour and emotions across numerous vertebrate species (Beninger, 1983; Berridge and Robinson, 1998; Bressan and Crippa, 2005; Pfaus and Phillips, 1991; Wise, 2006). The degeneration of DA neurons in the midbrain is associated with the second most common neurodegenerative disease, Parkinson's disease (PD) (Calne et al., 1979; Langston and Ballard, 1983). Importantly, RGCs are the most abundant glial cell type in the teleost brain; they have many crucial roles in organizing brain structure and supporting neuroendocrine systems (Barry et al., 2014; Xing et al., 2014). There is increasing research revealing details of RGC functions, but there have been few studies on the regulation of RGCs by neurotransmitters, and none on the interaction between DA neurons

[1] *Partially based on Xing, L., Goswami, M., and Trudeau, V.L. (2014). Radial glial cell: critical functions and new perspective as a steroid synthetic cell. General and Comparative Endocrinology 203, 181-185.*

and RGCs in the teleost brain. Given the previous anatomical and pharmacological studies in other vertebrate species (Balthazart J, 1998; Popesku et al., 2008), I formulated the following hypotheses, which were addressed by the experiments described in subsequent chapters and appendices of this thesis, as outlined below (Fig. 1.1).

- ✧ Dopamine regulates gene expression and controls progenitor and steroidogenic functions of RGCs through a receptor dependent mechanism.
- ✧ Estrogens from RGCs contributes to DA neuron regeneration, development and functional maturation.

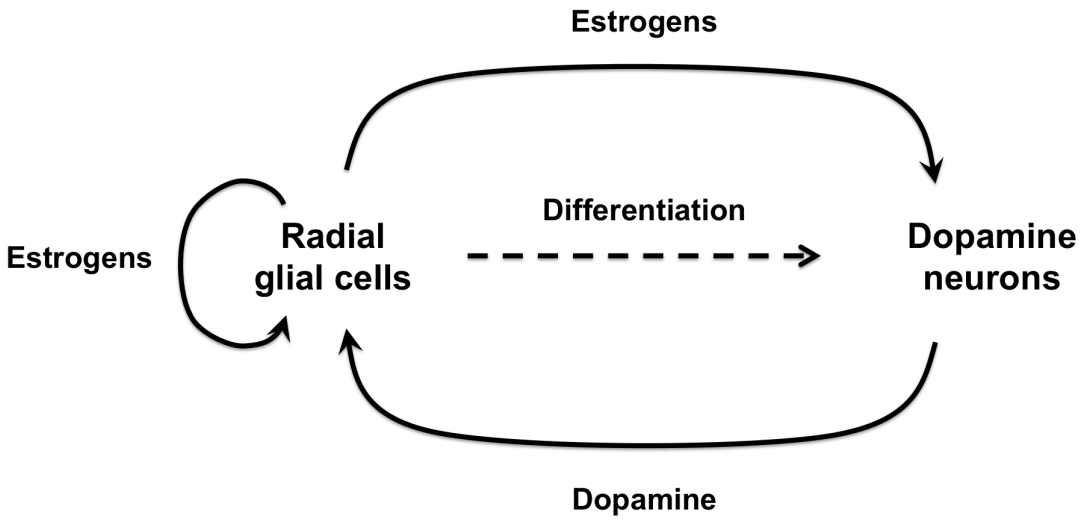

Figure 1.1. Hypothesized interactions between RGCs and DA neurons.

To address these two principal hypotheses, I first studied the distribution of catecholaminergic neurons and RGCs in goldfish forebrain. In order to better understand the functions of RGCs, aromatase B was used as a functional marker for RGCs. The anatomical relationships between DA neurons and aromatase B-positive RGCs were revealed, which showed the potential regulation of aromatase B expression in RGCs by DA. Next, I studied the dopaminergic regulation of aromatase B expression in the goldfish telencephalon and hypothalamus (Chapter 2). Results from these *in vivo* studies showed a brain region-specific and potentially estrogen receptor (ER)-dependent regulation pattern of aromatase B expression by DA. This suggests that there may be other regulators from other cells in the brain involved in aromatase B regulation. A primary RGC culture model was established in order to avoid influence from other cells in the brain and to study the direct effects of DA on RGCs. The *in vitro* studies showed that DA stimulates aromatase B expression through a DA D1 receptor (D1R)/cyclic adenosine monophosphate (cAMP) dependent signaling pathway (Chapter 3). Based on previous findings of positive feedback regulation of aromatase B by estrogens, I studied the combined effects of D1R activation and 17β-estradiol (E2) exposure on aromatase B expression in RGCs *in vitro* and also the involvement of ERs in aromatase B regulation (Chapter 4). After observing dose-dependent synergistic or antagonistic effects of DA and E2 on aromatase B expression and investigating the potential underlying mechanisms, discovering and better understanding RGCs functions through a large-scale study became my new objective. Proteomic profiling of RGCs and their response to dopaminergic treatment in culture provided novel insights about the RGC contribution to neuroendocrine functions and neurogenesis (Chapter 5). The potential roles of RGCs and estrogens in DA neuron recovery after neurotoxin insult were studied *in vivo*. The findings

suggested that both RGC activation and DA neuron recovery processes in the goldfish model of PD are estrogen-dependent (Chapter 6). The physiological relevance of my findings is discussed in this context, as well as new directions regarding future studies on RGC functions in neuroendocrine function and neurogenesis (Chapter 7).

In the following sections I review brain aromatase, RGCs and DA as well as the relationship between them, which provides the introduction to the major themes and concepts addressed in the chapters presenting experimental data. In each of these other chapters, I also provide more specific introductory material.

1.2 Brain aromatase

Aromatase cytochrome P450 (*cyp19*) is the only known enzyme that converts androgens into estrogens (Garcia-Segura et al., 2003; Lephart, 1996). In some species of vertebrates, including mammals, birds, amphibians and teleost fish, aromatase is found in the brain in addition to in testes and ovaries (Balthazart and Ball, 1998; Forlano et al., 2001; Iwabuchi et al., 2013). The distribution of aromatase varies between species and regions in the CNS, it has been studied at multiple levels, including mRNA, protein and enzyme activity (Azcoitia et al., 2011; Balthazart and Ball, 1998; Forlano et al., 2006; Garcia-Segura, 2008; Lephart, 1996). In mammals, brain aromatase is expressed in both neuronal and glial cell bodies, processes and synaptic terminals in specific brain regions, especially the pial surface and ventricular surface in the brain under normal conditions (Martinez-Cerdeno et al., 2006; Yague et al., 2006). Aromatase may also be expressed in reactive astrocytes and RGCs under conditions of cellular stress in mammalian brains (Azcoitia et al., 2003; Peterson et al., 2004). In contrast to mammals, teleosts express two structurally and functionally different

aromatase genes, aromatase A (*cyp19a1a*) and aromatase B (*cyp19a1b*), which are a result of a gene duplication event (Diotel et al., 2010a). The expression of aromatase B in the teleost brain is exclusive to one particular cell type, RGCs (Diotel et al., 2010a; Forlano et al., 2001), which allows for direct *in vivo* study of glial aromatase contributions without interference from neuronal compartments. Although it is very difficult to compare aromatase activity among species, Callard *et al*. demonstrated for the first time that goldfish exhibit the highest brain aromatase activity of vertebrates, with about 100-1000 times more active than in birds and mammals (Callard et al., 1981). More recently, Diotel *et al*. documented the distribution of *cyp11a1*, *hsd3b*, *cyp17* and *cyp19a1b* mRNAs and the ability of *de novo* synthesizing several steroids including estrone and E2 in the adult zebrafish brain (Diotel et al., 2011c). All these data indicate that teleost fish are excellent models to study function and regulation of glial aromatase. More importantly, recent studies indicate that RGCs are the progenitors of both neurons and glia during development, and are the source of new neuron generation in adult vertebrate brains (Alvarez-Buylla et al., 2001; Pellegrini et al., 2007; Zupanc and Clint, 2003).

1.3 Neuroprotective effects of estrogens

It is well known that E2 and other estrogens have multiple roles in reproduction, cognition, metabolism, socio-sexual behaviour and brain functions (Chen et al., 2013; Ervin et al., 2015; Garcia-Segura, 2008). In the adult CNS, estrogens produced locally can affect neighbouring steroid-sensitive neural circuits, which can be viewed as classic "paracrine" actions to modulate synaptic plasticity, cell growth, neurogenesis and long-term potentiation (Petrovska et al., 2012). Estrogens also protect the brain against apoptosis and injury in a

variety of experimental settings, including toxicity induced by excitatory neurotransmitters, neurotoxins, oxidative stress, and ischemia (Khalaj et al., 2011; Kuroki et al., 2001; Shahrokhi et al., 2012; Shughrue, 2004). A large body of research sought to understand the mechanisms underlying the neuroprotective effects of estrogens, especially E2, the most potent estrogen. Several mechanisms have been proposed that include:

1. Nuclear ER-mediated mechanisms. Importantly, ERs are widely distributed in the adult vertebrate brain in both neurons and glia (Al-Bader et al., 2011; Socorro et al., 2000), where they coordinate multiple neuroprotective signaling cascades. Classic ERs can function as a liganded transcription factor and also as co-activator to regulate gene expression (Arevalo et al., 2015). Morphological studies on ER knockout mice revealed a significant loss of neurons coupled with astrocyte proliferation, which supports the idea that ER-mediated mechanisms are involved in the neuroprotective actions of estrogens (Wang et al., 2001).

2. Membrane receptor-mediated rapid actions. An increasing number of studies have focused on the G protein-coupled estrogen receptor (GPER) on cell membrane and have reported that the activation of GPER stimulates mitogen-activated protein kinase (MAPK) and/or phosphotidylinositol-3-kinase (PI3K) signaling, which further mediate the neuritogenic actions of estrogens (Ruiz-Palmero et al., 2013). Studies applying a MAPK/ extracellular signal-regulated kinase (ERK) inhibitor to rat hippocampus demonstrated that MAPK/ERK mediates the neuroprotective actions of estrogens (Kuroki et al., 2001).

3. A receptor-independent antioxidant free radical scavenging mechanism. Both *in vitro* (Behl et al., 1995) and *in vivo* (Behl et al., 1997) studies have reported neuroprotective effects of estrogens under conditions associated with oxidative stress induced cell death.

These effects have been shown to be attributed to the presence of a hydroxyl group carried by the C3 position on the steroid A ring of the estrogens, which functions as a potent electron donor to scavenge free radicals (Behl et al., 1997). All these lines of information suggest that estrogens are neuroprotective and have potential for therapeutic applications in both acute damage and chronic neurodegenerative diseases.

1.4 Neuroestrogens and Parkinson's disease

Following Alzheimer's disease, PD is the second most common neurodegenerative disorder around the world. It is mainly characterized by a progressive degeneration of selective DA neurons in the substantia nigra (SN) (Hornykiewicz, 1989). Unfortunately, there is no cure for PD currently. All pharmaceutical treatments and medications including the use of oral preparations of L-3,4-dihydroxyphenylalanine (L-DOPA), DA receptor agonists and DA degrading enzyme inhibitors are focused on relieving the symptoms. Although these treatments have some effects on controlling symptoms, their adverse effects are considerable. A variety of epidemiological studies have reported sex difference in PD, the prevalence being higher in men than in women (Baldereschi et al., 2000; Czlonkowska et al., 2006; Van Den Eeden et al., 2003; Wooten et al., 2004). Research using animal models of PD induced by the neurotoxin 1-methyl-4-phenyl-1,2,3,6-tetrahydropyridine (MPTP) have also reported that there were sex differences observed in treated mice and demonstrated a greater neurotoxic effect in males than in females (Miller et al., 1998). Estrogen therapy prior to the initiation of L-DOPA treatment was reported to be beneficial to women with early PD onset (Saunders-Pullman et al., 1999), potentially through modulation of DA neuron activity at various steps of transmission including DA synthesis, release and metabolism by

regulating pre- and post-synaptic DA receptors and DA transporters (DAT) (Di Paolo, 1994). Furthermore, it has been reported that PD symptoms and L-DOPA-induced dyskinesia can be modulated by estrogens (Session et al., 1994). Studies showed that estrogens and estrogenic drugs protect existing nigrostriatal DA neuron activity including the DA concentration, TH expression, dopamine transporter (DAT) expression and neurotrophin release (D'Astous et al., 2004; Shughrue, 2004) and suggested that the implication of ERs rather than their antioxidant activities are involved in the effects of estrogens on DA neuron activity (Morissette et al., 2008). Besides stimulating DA neuron activity, estrogens have been reported to improve neural stem cell proliferation and decrease neuronal death through up-regulation of the antiapoptotic gene Bcl-2 and attenuation of inflammatory processes (Dubal et al., 2006; Okada et al., 2008). Taken together, all these lines of evidence suggest that estrogens have significant implication in PD treatment and that more knowledge of the underlying mechanisms of estrogenic action should be further explored in experimental PD models.

1.5 Radial glial cells

Radial glia are a cell type in the CNS of all vertebrates engaged in many key developmental processes. During CNS development, early progenitors - neuroepithelial cells give rise to RGCs, which represent the major cell type in the neural tube and comprise the neurogenic cell population (Schmechel and Rakic, 1979). At an early stage of development, RGCs predominantly divide to generate more RGCs and expand along the surface area of developing lateral ventricles. With developmental progression, RGCs generate less daughter RGCs but more intermediate progenitor cells and neurons. At later stages of CNS

development, RGCs transform into neurons and astrocytes (Fig. 1.2).

After differentiation from neuroepithelial cells, RGCs maintain a very similar morphology to their progenitors, with the soma positioned along the ventricle wall and a long radial process extending from its cell body reaching to the basement membrane at the pial surface (Stevenson and Yoon, 1982). This morphological feature enables its major function which is to serve as a guiding scaffold for newborn neurons to migrate to their final destination (Rakic, 1971b). In addition to their roles as a structural scaffold to guide neuronal migration (Radakovits et al., 2009). Adult neurogenesis in mammals has attracted great attention after the discovery of neural stem cells and the continuous generation of neurons in the adult CNS. This phenomenon has been observed both in mammalian and non-mammalian species. While the concept of adult neurogenesis is well accepted, mammals have very limited capacity for neurogenesis and neuroregeneration. The main reason is that there are only two proliferative and neurogenic regions in the adult mammalian brain. These include the anterior part of the subventricular zone of the lateral ventricle and subgranular zone of the dentate gyrus (Brunne et al., 2010; Ming and Song, 2011). In contrast to mammals, teleost fish exhibit an enormous potential to produce new neurons in the adult CNS and to replace damaged neurons by newly generated ones and neuronal differentiation. Persistent neurogenesis is maintained throughout development and also adulthood, as teleost fish have dozens of proliferative and neurogenic regions that can give rise to new neurons. This extensive neurogenic capacity may be largely due to the abundance of RGCs in the adult teleost brain (Strobl-Mazzulla et al., 2010). Abnormalities in RGC development, functions and differentiation, as well as in cellular interactions between RGCs, and interactions between RGCs and neurons could cause many developmental brain disorders

such as schizophrenia and lissencephaly (Hatten, 2002; Marín and Rubenstein, 2003).

1.6 Role of RGC in neuronal migration

The expression patterns of RGC marker proteins differ between embryonic and adult mammalian brain. Mammalian RGCs express brain lipid binding protein (BLBP) and glutamate aspartate transporter (GLAST) during development (Anthony et al., 2004). On the other hand, the RGCs along the ventricle in adult mouse brain have little to no GLAST immunoreactivity, yet these RGCs are glial fibrillary acidic protein (GFAP)- and vimentin-positive (Sundholm-Peters et al., 2004). In adult teleost brain, RGCs are BLBP-positive, which is similar to adult mammalian RGCs, but are also GFAP-positive (Takeuchi and Okubo, 2013). These GFAP or BLBP-positive RGCs are involved in neurogenesis and neuronal migration in both intact and injured adult brain and they contribute to the high capacity of neuroregeneration observed in teleost fish (Schmechel and Rakic, 1979; Zupanc and Clint, 2003). The hypothesis that RGCs in the adult brain guide neuronal migration has received strong support from several research groups studying the expression of RGC cell markers. First, the morphology and size of teleost RGCs in adult brain are extremely similar to RGCs in the developing brain, with a long process reaching the basal membrane playing a key structural role during neuronal migration (Diotel et al., 2010a; Stevenson and Yoon, 1982; Tong et al., 2009). Also, RGC fibre distribution and orientation in the adult fish brain matches the migration path of young neurons, indicating that young neurons use the radially-oriented glial fibres as a scaffold to reach their final destination within the cortical plate (Rakic, 1971a; Zupanc et al., 2012). This strategy appears to be employed when cells migrate over long trajectories. Second, the expression of microtubule-binding protein doublecortin in

migrating neurons has been observed in close apposition to radial processes in adult rat brain (Gubert et al., 2009; Radakovits et al., 2009). This close apposition between young neurons and RGCs can also be seen in electron microscopy images (Brunne et al., 2010; Rakic, 1971b). Interestingly, the triple staining result showed that elongated bromodeoxyuridine (BrdU)- and neuronal protein HuC/D-positive nuclei of newborn neurons overlap with GFAP immunoreactive fibres. This indicates that neurons are migrating along GFAP-positive RGC fibres (Hatten, 2002; Marín and Rubenstein, 2003; Zupanc and Clint, 2003).

1.7 Proliferative and neurogenic nature of RGCs

With the onset of neurogenesis, after neuroepithelial cells transform into RGCs, both neuroepithelial cells and RGCs are characterized by apical-basal polarity and nuclear migration (Anthony et al., 2004; Götz and Huttner, 2005). At the end of mammalian CNS development, RGCs withdraw their processes and differentiate into other types of glial cells when neurons reach their final destination (Fig. 1.2). It was thought that all RGCs disappear in the late stage of mammalian CNS development and differentiate into astrocytes. However, in the adult mammalian brain, RGCs can still be detected in some regions, such as the olfactory bulb, telencephalon, subventricular zone and dentate gyrus (Emsley et al., 2012; Liu et al., 2006; Sundholm-Peters et al., 2004). Bromodeoxyuridine (BrdU) labeling studies in adult rat brain also reveal strong proliferative sites at the ventricular zone, the region where high numbers of newborn cells and RGCs are located. These BrdU-positive cells also express GFAP, indicating that RGCs at the ventricular surface in the adult brain are proliferative (Pecchi et al., 2007; Takeuchi and Okubo, 2013). Live imaging observations confirmed bipolar RGC division as well as the generation of more than 4-5 daughter RGCs

within 40 hours (Pilz et al., 2013). Moreover, it has now been established that daughter RGCs can generate more RGCs, astrocytes, oligodendrocytes and neurons as well. For example, neurons in the rodent CNS originate from three classes of neural stem and progenitor cells - neuroepithelial cells, RGCs and intermediate neuronal progenitors. Neurogenic radial glia have also been observed in the outer subventricular zone of human neocortex (Hansen et al., 2010). The neurogenic nature of RGC is supported by the finding that most neurons in the adult mouse brain derive from GLAST-positive RGCs (Anthony and Heintz, 2008). These RGCs also express the transcription factor Pax6, which exists in neuronal RGCs during mammalian development (Gubert et al., 2013; Heins et al., 2002). Another study reported the triple staining of LIM homeobox transcription factor 1, alpha (LMX1α), which is expressed by DA neuronal progenitors, with condensed chromatin and phosphorylated vimentin, which is the marker of RGCs in M-phase. This result suggests that RGCs are the progenitors of DA neurons along the ventricle wall in the human brain (Hebsgaard et al., 2009). Bonilla et al. (2008) also showed that GLAST-positive RGCs in the brain floor plate of mouse could undergo neurogenesis and give rise to dopaminergic neuron progenitors, which then rapidly differentiate into dopaminergic neurons (Bonilla et al., 2008).

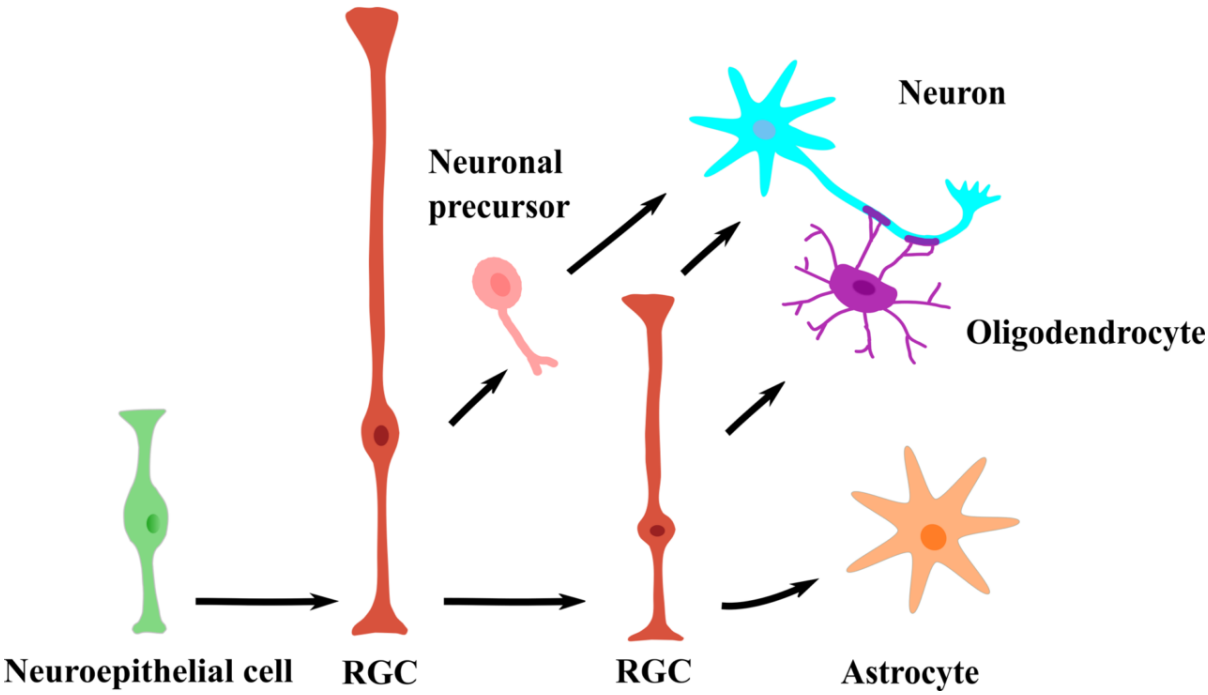

Figure 1.2. Differentiation of RGCs during CNS development.

In non-mammalian vertebrates, RGCs persist throughout an animal's entire life as a neuronal stem cell (Alvarez-Buylla et al., 2002). Indeed, several studies suggest that RGCs in adult fish brain express markers of a progenitor cell type, such as the intermediate filament nestin (Diotel et al., 2010a; Takeuchi and Okubo, 2013). The brains of teleosts keep growing and developing through adulthood, but very little is known about the underlying mechanisms. Several studies have reported remarkable regeneration capacity of adult fish brain, which relates to the abundance and persistence of RGCs (Diotel et al., 2013; Kroehne et al., 2011; Strobl-Mazzulla et al., 2010), showed the active proliferation in the adult zebrafish forebrain and reported that newborn cells arising from adult RGCs can differentiate into neurons. However, there is little information about the characterization and function of newborn

neurons with the exception of two studies describing newborn tyrosine hydroxylase (TH)-positive neurons in zebrafish telencephalon and newborn serotonin (5-HT) neurons at zebrafish paraventricular organ (Adolf et al., 2006; Pérez et al., 2013). Despite these exciting results from both mammals and teleost fish showing the possibility of RGC transformation into dopaminergic neurons, there is no direct *in vitro* data showing the process of this differentiation. One study showed that the transformation of RGCs into astrocytes is bidirectional in the mouse brain, based on the evidence that mature astrocytes can be dedifferentiated to RGCs by epidermal growth factor (EGF) and transforming growth factor α (TGFα) (Ghashghaei et al., 2007). These re-induced mouse RGCs regained the function of guiding neuronal migration. Additionally, with the delivery of transcriptional factors achaete-scute homolog 1 (ASCL1), LMX1B and nuclear receptor related 1 protein (NURR1) together in a polycistronic lentiviral vector, primary mature mouse astrocytes can be reprogrammed into functional dopaminergic neurons (Addis et al., 2011). Combining these two studies, RGCs could be the intermediate cell type of the differentiation process from astrocytes to dopaminergic neurons, but further experiments are needed to test this hypothesis. The presence of RGCs with proliferative and neurogenic characteristics in the adult brain suggests that they may have an important role in brain function maintenance, brain repair and neural plasticity.

1.8 New perspectives of RGC as a steroid synthesizing cell

Early studies reported that non-mammalian brains can synthesize estrogens locally (Callard et al., 1981). For the first time, Callard identified high levels of aromatase activity and correlated changes in aromatase activity to the seasonal reproductive cycles in goldfish

(Pasmanik and Callard, 1988). Subsequent work from the Bass and Kah research groups showed that aromatase, the only enzyme performing the conversion of androgens into estrogens, is exclusively expressed in RGCs of adult midshipman (*Porichthys notatus*) and zebrafish (*Danio rerio*) using double staining of brain aromatase and RGC cell markers BLBP or GFAP (Forlano et al., 2001; Tong et al., 2009). Therefore, RGCs are considered as the source of local estrogens in fish brain, and the estrogen-synthesizing role of RGC has now been established. The brains of teleost fish exhibit intense aromatase activity due to the strong expression of the aromatase B gene (Le Page et al., 2010), which arose from gene duplication events in teleosts.

In adult mammals and birds, aromatase expression is mainly localized in neurons, in the axons and terminals, as well as in reactive astrocytes (Balthazart and Ball, 1998; Peterson et al., 2005; Sanghera et al., 1991). Aromatase expression in adult mammalian and avian astrocytes and RGCs only occurs after induction by mechanical injury, excitotoxicity and inflammation (Garcia-Segura et al., 1999; Saldanha et al., 2013). One study showed the expression of aromatase in rat RGCs during CNS development (Martinez-Galan et al., 2004). However, with the disappearance of RGCs at the end of CNS development, it is difficult to study the neurosteroidogenic roles of RGCs using adult mammalian models. In contrast, the remarkable aromatase activity and exclusive expression of aromatase in RGCs in teleost brains indicate that they are excellent models to study the neurosteroidogenic functions of RGCs.

All steroid hormones are synthesized from cholesterol with the catalysis of cytochrome P450 enzymes, including cytochrome P450 side chain cleavage (*cyp11a1*), 3β-hydroxysteroid dehydrogenase (*hsd3b1*), cytochrome P450 17α-hydroxylase (*cyp17a1*), 17β-

hydroxysteroid dehydrogenase (*hsd17b1*), and cytochrome P450 aromatase (*cyp19a1b*) (Mellon et al., 2001). In all classes of vertebrates, the brain expresses the highest level of the steroid synthesizing enzymes (Diotel et al., 2011c; Do Rego et al., 2009). Studies in songbirds showed three possible sources of androgens for brain aromatase: 1) the circulating androgens secreted from gonads, although this source is very limited in females or non-breeding males; 2) androgen precursor dehydroepiandrosterone secreted by adrenal glands and gonads; 3) locally synthesized androgens in the brain (Schmidt et al., 2008). In zebrafish brain, the overall expression patterns of *cyp11a1*, *cyp17a1* and *hsd3b1* are similar to *cyp19a1b*, which is abundantly found in the telencephalon, the preoptic area, the hypothalamus and the cerebellum (Diotel et al., 2011c; Nagarajan et al., 2013). These data on the distribution of steroidogenic enzymes suggested that fish brain is use all three sources of aromatase to produce estrogens. However, the transfer of cholesterol from the outer to the inner mitochondrial membrane, where the cytochrome P450 enzymes are located, is the essential and rate-limiting step for steroid synthesis. There are very few studies showing the colocalization of cholesterol transferring proteins, such as the peripheral benzodiazepine receptor (PBR) and the steroidogenic acute regulatory protein (StAR), with aromatase. Moreover, very little ultrastructural data exists for teleost RGCs. The RGCs of the goldfish optic tectum were studied using electron microscopy. Specifically, the typical structures visualized were well-developed Golgi apparatus, smooth endoplasmic reticulum, granule-bearing mitochondria, and lipid droplets (Stevenson and Yoon, 1982). In this way, RGCs share some common organelle profiles typical of steroidogenic cells. However, direct ultrastructural and immunocytochemical comparisons of RGCs and well-described steroidogenic cells in the gonad or adrenal gland remain to be performed. Nevertheless, the

RGCs of the periventricular region of the goldfish optic tectum studied by Stevenson and Yoon (1982) are likely aromatase-positive (Le Page et al., 2010), given their location.

1.9 Dopamine

As one of the key neurotransmitters, DA belongs to the catecholamine family, which is structurally defined by a catechol ring and an amine side chain (Kopin, 1985). The production of DA occurs mainly in the CNS, but limited production is also observed in the adrenal medulla. Findings from past decades revealed that DA in the CNS is involved in many physiological functions, including locomotor activity (Beninger, 1983; Berridge and Robinson, 1998), learning, cognition, reproduction (Trudeau, 1997), sexual behaviour (Pfaus and Phillips, 1991), food intake and reward (Bressan and Crippa, 2005; Wise, 2006).

The biosynthesis of DA starts from tyrosine, which is an amino acid abundant in dietary proteins. As the main site of DA synthesis, the brain takes up blood borne tyrosine through a low-affinity amino acid transporting system, which further transfers tyrosine into DA neurons (Kopin, 1985). Once tyrosine has entered the DA neurons, the rate-limiting enzyme of DA synthesis, TH, catalyzes the conversion of tyrosine to L-DOPA. Aromatic amino acid decarboxylase (AADC) is another enzyme involved in DA synthesis in the neuronal cytoplasm, which is responsible for the conversion of L-DOPA to DA (Fig. 1.3) (Elsworth and Roth, 1997). Synthesized DA can be stored in specialized monoamine vesicles or in the smooth endoplasmic reticulum and released through selective membrane transporters from both neuron terminals and dendrites upon stimulation (Adrover et al., 2014; Kelly, 1993; Kopin, 1985).

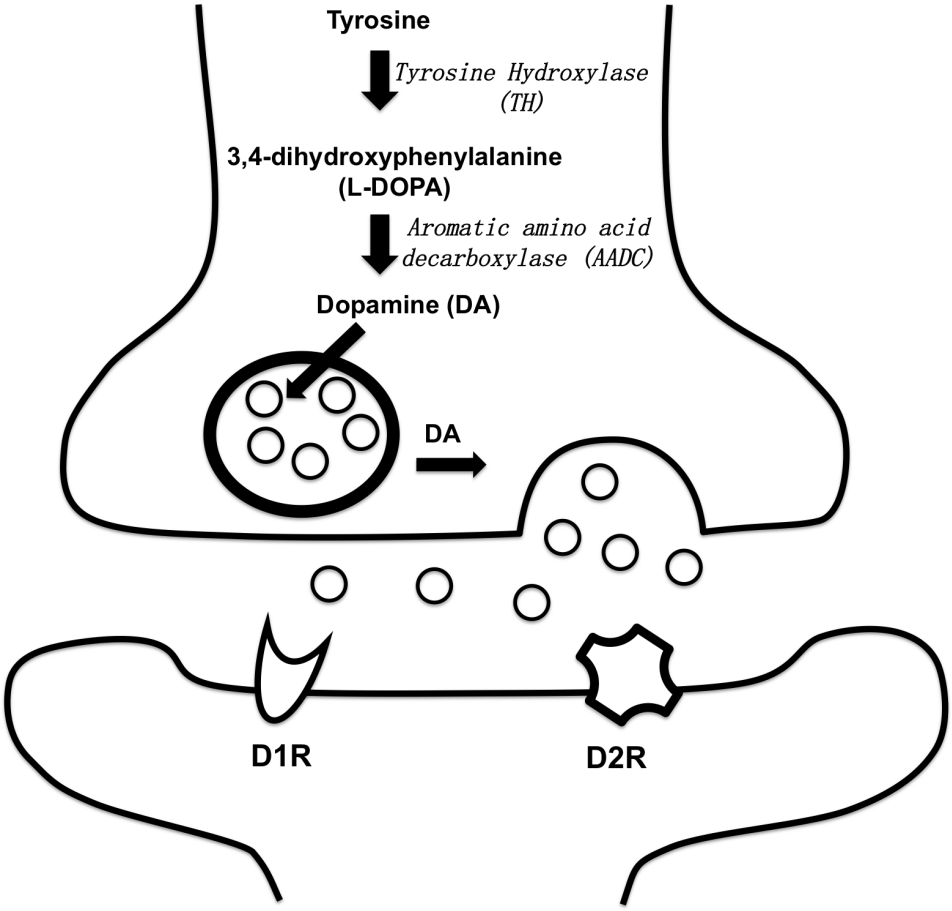

Figure 1.3. The biosynthesis, storage and release of DA.

Most actions of DA are through DA receptors. The existence of DA receptors in the CNS was first reported in 1972 (Baumgarten et al., 1972). The DA receptor includes five different subtypes (i.e. D1-D5), which belong to the seven transmembrane domain G protein-coupled receptor family and fall into two categories, the D1-like receptors (D1 and D5) and the D2-like receptors (D2, D3 and D4) in mammals (Strange, 1993). Members from this family display considerable amino acid sequence conservation in the transmembrane domains. The D1 and D5 receptors share 80% identity in their transmembrane domain, while the D2 and D3 receptors share 75% identity in their transmembrane domain (Kebabian and Calne, 1979). In teleost, extra dopamine receptor subtypes besides D1A (D1) and D1B (D5) are present, including D1C and D1X. The D1C receptor gene is well conserved among teleost, amphibians and other non-mammalian vertebrates, but not in mammalian species, suggesting that the D1C receptor gene was present in ancestral vertebrates, and secondarily lost in the mammalian lineage (Yamamoto et al., 2013a). The D1X receptor gene is exclusively expressed by teleost, likely to be teleost-specific paralogs of the D1B receptor genes that are probably a consequence of the genome duplication occurred early in the teleost lineage (Aparicio, 2000). Among all these receptor subtypes, the structural difference in transmembrane domains define their different characteristics (Missale et al., 1998). Indeed, D1-like receptors are coupled to stimulatory G protein Gs, which stimulates type 5 adenylate cyclase (AC) activity. The activation of AC mediated by the α unit of Gs protein (Gα) catalyzes the conversion of adenosine triphosphate (ATP) to cAMP. As one of the cAMP-dependent protein kinase members, PKA is an enzyme that phosphorylates other proteins. When the intracellular cAMP level rises, cAMP binds to the regulatory subunit of PKA. The conformational change of PKA enable the catalytic parts to phosphorylate the substrate

proteins (Corbin and Krebs, 1969). A number of proteins phosphorylated by PKA are involved in signal transduction and regulation of gene expression, including DA and cyclic AMP-regulated phosphoprotein, 32kDa (DARPP-32), voltage- and ligand-gated ion channels (calcium and sodium channels) and transcription factor cyclic AMP response element-binding protein (CREB)(Abekawa et al., 2000; Brami-Cherrier et al., 2002; Cantrell et al., 1997; Maroun and Akirav, 2009). Transcriptional activator CREB binds to CRE in the regulatory region of the gene and induces gene expression (Lonze and Ginty, 2002; Montminy, 1997). Several studies reported that D1-like receptors also activate MAPK, including ERK, p38MAP kinase, and c-jun amino-terminal kinase (Maroun and Akirav, 2009). In contrast, D2 receptor-induced inhibition of AC would decrease the phosphorylation of PKA substrates, which may be mediated by Gi dependent inhibition of cAMP (Huff, 1996). The activation of D2 receptors is able to stimulate MAPK (Luo et al., 1998), which is mediated at least in some cases by transactivation of a receptor tyrosine kinase (RTK). Another pathway activated by D2 receptors is phosphoinositide 3-kinase/protein kinase B pathway (Nair and Sealfon, 2003). As discussed above, DA receptor signal transduction pathways are complex, even one DA receptor subtype or isoform has a variety of effects by stimulating different but overlapping pathways. Through different mechanisms or pathways, activation of DA receptors results in modulations of peptide function, immediate early gene expression and enzyme activity (Baillien and Balthazart, 1997; Jaber et al., 1995; Keefe and Gerfen, 1995). Discovering new targets and the underlying signal transduction pathways could lead to a better understanding of the functions of DA and DA receptors.

Chapter 2: Dopaminergic regulation of radial glial cell functions in the goldfish forebrain [2]

2.1 Abstract

Aromatase is the only enzyme that converts of androgens into estrogens. Aromatase expression can be found in all vertebrate species, mainly in testes and ovaries as well as brains. While it is clear that brain aromatization plays important roles in neuroendocrine functions, neural plasticity and sexual behaviour, many questions about the regulation of brain aromatase still remain unanswered. In this study, we investigate the expression of brain-specific cytochrome P450 aromatase and D1R by RGCs along the ventricular surface, as well as the anatomical relationship between catecholaminergic neurons and RGCs in the female goldfish forebrain. An *in vivo* time course study (3h, 6h, 12h, 24h) was performed to determine the effects of injecting a selective D1R agonist (SKF 38393; 40μg/g body mass; intraperitoneally) on aromatase B and nuclear ERs in telencephalon and hypothalamus. Treatment with SKF 38393 significantly regulated *cyp19a1b* expression but had no effects on ER expression in telencephalon and significantly regulated the expression of *cyp19a1b, esr1*, *esr2a* and *gdnf* in hypothalamus. These neuroanatomical and pharmacological data indicate the existence of dopaminergic regulation of RGC functions in the adult teleost brain.

2.2 Introduction

---

[2] *Partially based on Xing, L., Mcdonald, H., Da Fonte, D.F., Gutierrez-Villagomez, J.M., and Trudeau, V.L. (2015). Dopamine D1 receptor activation regulates the expression of the estrogen synthesis gene aromatase B in radial glial cell. Front. Neurosci. 9. doi: doi: 10.3389/fnins.2015.00310. XL, designed the study, developed the methodology, conducted the majority of experiment and analysis and wrote the manuscript. MH contributed to imaging. DFDF, GVJM gave critical comments on the manuscript. TVL, helped with the design of the study and editing the article.*

The brain is an important site of estrogen synthesis in vertebrates along with ovaries and testes. The direct evidence that central neuroendocrine tissues are capable of converting androgens into estrogens suggests that many effects of gonadal androgens on neural cell functions are mediated by local metabolism of estrogens (Naftolin et al., 1971). Since the first report on the existence of brain aromatase, there have been active research efforts by several laboratories to investigate the physiological importance of and the potential regulators of brain aromatase. According to Kato's work, there are at least three promoters contained within the aromatase gene in the rat brain: hypothalamus type, ovarian type and cortical type. Through recruiting differential promoter types, brain aromatase expression can be regulated differently. This suggests that there may be many factors involved in brain aromatase expression regulation (Kato et al., 1997).

Several studies have showen that catecholaminergic neuronal inputs are proximal to aromatase positive cells in Japanese quail, which suggests that catecholamine may play a role in the control of brain aromatase (Absil et al., 2001; Baillien and Balthazart, 1997; Balthazart et al., 2000; Balthazart J, 1998). As one of the most abundant catecholamines, DA is a neurotransmitter implicated in many neural functions. There are many other independent lines of evidence to suggest that DA may be able to regulate aromatase expression, but the mechanisms under regulation are still unclear and controversial. Microarray results from previous studies showed that injecting the dopaminergic neurotoxin MPTP and D1R agonist (SKF 38393) can up-regulate or down-regulate *cyp19a1b* expression, respectively, which confirms that *cyp19a1b* expression can be regulated by neurotransmitter DA in goldfish. In the same study, injecting the D2 receptor agonist (LY 171555) is not able to change *cyp19a1b* expression, which indicates D1Rs, not D2 receptors, are involved in goldfish

cyp19a1b regulation (Popesku et al., 2010; Popesku et al., 2012).

Dopaminergic chemicals and DA are also able to regulate aromatase activity. As shown in the pioneering work by Baillien and colleagues (1997), aromatase activity in the quail brain was reduced by DA, DA Dl and D2 receptor agonists (apomorphine [Dl/D2], SKF-38393 [Dl] and RU-24213 [D2]) to different degrees. In contrast, DA antagonists (SCH-23390 [Dl] or spiperone [D2]) were not able to antagonize the inhibitory effect of the agonists. The results of this study suggested that DA receptors are not involved in the inhibitory effects of DA and dopaminergic drugs on aromatase activity (Baillien & Balthazart, 1997). Some studies have already shown brain aromatase activity may partially be regulated by a non-genomic mechanism Charlier *et al*., 2011). Balthazart's group has also shown that aromatase activity in quail brain is modulated by phosphatases (Balthazart et al., 2003), it is believed that aromatase enzymatic activities can be controlled by phosphorylation processes. This is supported by two pieces of evidence: 1) fifteen phosphorylation sites have been identified in quail aromatase, including sites for PKA and PKC; 2) The inhibitors of PKA and PKC are able to block the decrease of aromatase activity. Moreover, Sumiko and colleagues found that some neuropeptides, which act like neurotransmitters, including substance P, neurotensin, cholecystokinin and brain natriuretic peptide, could increase aromatase expression levels and the induction is PKC and PKG dependent (Abe-Dohmae et al., 1996). The study on DA receptor signaling showed that cAMP catalyzed by AC can bind to the regulatory subunit of PKA and PKC to stimulate their activities (Neve *et al*., 2004). It is therefore possible that the regulation of aromatase activity by dopaminergic drug is through DA receptor. Because of these controversial studies, the mechanisms involved in the dopaminergic regulation of aromatase must be resolved.

In this study, we demonstrate that adult RGCs express both aromatase B and D1R along the ventricular surface in goldfish telencephalon as well as the neuroanatomical relationships between DA neurons and RGCs. Moreover, pharmacological activation of the D1R *in vivo* indicates a dopaminergic regulation of *cyp19a1b* expression in the female goldfish forebrain.

2.3 Materials and Methods

2.3.1 Ethics Statement

All procedures used were approved by the University of Ottawa Protocol Review Committee and followed standard Canadian Council on Animal Care guidelines on the use of animals in research.

2.3.2 Experimental animals and design

Common adult female goldfish were purchased in April from a commercial supplier (Aleong's International Inc., Mississauga, ON, Canada) and acclimated for at least 3 weeks prior to experimentation. The fish were maintained at 18 °C under a natural simulated photoperiod and fed standard goldfish flakes. Sexually mature, pre-spawning female goldfish (20-35g) were anesthetised in 0.05% 3-aminobenzoic acid ethylester (MS222) for all handling, injection and dissection procedures.

Brains were rapidly dissected on ice and immediately placed in 4% paraformaldehyde (PFA) in RNase free phosphate buffered-saline (PBS; pH 7.4) for fixation overnight at 4 °C, then washed twice in PBS and twice in methanol for 5 m each and finally transferred to methanol. Fixed brains were stored at -20 °C until processed for cryo-sectioning. Following storage at -20 °C, fixed brains were rehydrated in a methanol-PBS series, then embedded in

1.5% agar/5% sucrose dissolved in PBS. Embedded brains were cut into blocks for cryo-sectioning and placed in 30% sucrose overnight. Blocks were frozen in Shandon Cryomatrix (Thermo Scientific) mounting medium in isopentane kept at -80 °C. Frozen blocks were sectioned with a 16 μm thickness. Sections were transferred onto Superfrost Plus slides (Fisher Scientific) and stored at -20 °C until needed for *in situ* hybridization or immunohistochemistry.

The selective D1R agonist 1-phenyl-2,3,4,5-tetrahydro-(1H)- 3-benzazepine-7,8-diol (SKF 38393) purchased from Tocris was dissolved in physiological fish saline (0.6% NaCl). Female goldfish were injected intraperitoneally with SKF 38393 (40μg/g body mass) (Popesku et al., 2010). Control fish received saline injection (5 μL/g body mass). This dose was chosen based on previous experiments showing dopaminergic modulation of LH release and gene expression (Popesku et al., 2010; Popesku et al., 2012). After 3, 6, 12 or 24 hours, fish were sacrificed by spinal transection, then the telencephalon and hypothalamus tissues were rapidly dissected and immediately frozen on dry ice for later RNA and protein extraction.

2.3.3 *In situ* hybridization

Frozen slides were thawed for 1 hour at room temperature (RT). Antisense RNA probes were synthesized *in vitro* using goldfish *cyp19a1b* cDNA fragments (1.6 kb). *In situ* hybridization on cryo-sections was performed as previously described (Smith et al., 2007). Briefly, probes were diluted in hybridization buffer at a dilution of 1:200. The probe mix was denatured at 70 °C for 10 min, then transferred on ice. Three hundred microliters of the probe mix was added to each slide that was then covered with a coverslip and placed in an oven at 70 °C overnight. For washes, slides were washed in solution A (1× SSC, 50%

formamide, and 0.1% Tween 20) at 70 °C, and in Tris-Buffered Saline and Tween 20 (TBST) at RT. Slides were then blocked in 10% calf serum in 1× TBST (blocking solution) for 1 hour at RT. For incubation with the antibody, 300µl of 1:2,000 diluted anti-DIG AP Fab fragment antibody (Roche) in blocking solution was added and then covered with a coverslip and incubated overnight at 4 °C. Slides were washed in 1× TBST and equilibrated in NTMT staining buffer (100 mM NaCl, 100 mM Tris HCL pH 9.5, 50 mM $MgCl_2$, and 0.1% Tween 20). For staining, slides were placed in Coplin jars with 40 ml NTMT containing 140 µl of BCIP and180 µl of NBT overnight at RT. Slides were subsequently washed and allowed to dry before mounting with coverslips using Aquamount (Polysciences).

2.3.4 Immunohistochemistry

Frozen slides were thawed for 1 hour at RT. Non-specific binding was blocked in blocking buffer (0.3% Triton PBS containing 1% bovine serum albumin (BSA)) for 45 m at RT. Slides were covered with anti-GFAP antibody (1:500, generated in mouse, ChemiconCat. # MAB360) (Forlano et al., 2001) and previously validated polyclonal rabbit anti-zebrafish aromatase B (Pellegrini et al., 2007) (1:800, generated in rabbit) or anti-D1R antibody (1:1000, generated in rabbit, Acris antibodies, Cat. # AP09962PU-N) or anti-TH antibody (1:500, generated in rabbit, Chemicon, Cat. # AB152) (Yamamoto et al., 2011) overnight at 4 °C. Sections were then washed in PBS and incubated with donkey anti-rabbit Alexa fluor 488 (1:500; Invitrogen Molecular Probes) and goat anti-mouse Alexa fluor 596 (1:500; Invitrogen Molecular Probes) for 1 hour at RT. Slides were washed in PBS and mounted with the antifading medium Vectashield with 4,6-diamino-2-phenylindole (DAPI) (Vector Laboratories), which permits visualization of cell nuclei. The anti-D1R antibody was generated against a conserved sequence in the rodent D1R (100% identity with goldfish) and

was validated for use in goldfish. Two negative controls were performed which demonstrated specificity of the reaction. First, anti-D1R antibody was pre-absorbed at 4°C overnight using the D1R peptide antigen (10 μg/ml, Acris Antibodies, Cat. # AP09962CP) prior to immunocytochemical testing on brain sections. Second, the D1R primary antibody was omitted for secondary antibody control (Fig A3.1). Images were taken with Nikon A1RsiMP confocal microscope with Nikon's Imaging Software NIS-Elements.

2.3.5 RNA extraction, quality control and cDNA synthesis

The RNeasy Plus Micro kit (Qiagen) was used to isolate RNA from the goldfish telencephalon and hypothalamus as described in the manufacturer's protocol. Upon purification, the concentration and quality of all samples was assessed using a NanoDrop ND-1000 spectrophotometer (Thermo Fisher Scientific) and 2100 Bioanalyzer (Agilent). RNA integrity values of samples ranged from 7.4 to 9.8, which is above the recommended minimum value of 5 for quantitative real-time reverse transcription polymerase chain reaction (qPCR) applications (Fleige and Pfaffl, 2006). Total cDNA was prepared from 1 μg of total RNA and 200 ng random hexamer primers (Life technologies) using Superscript II RNase H- reverse transcriptase (SSII) as described by the manufacturer (Life technologies). Each 20 μl reaction was diluted 100-fold in nuclease-free water and used as the template for qPCR assays. All brain cDNA samples from different time points were synthesized in parallel.

2.3.6 Quantitative real-time RT-PCR

Quantitative real-time RT-PCR assays based on SYBR green detection were used to evaluate relative gene expression. Primers used in the present study were designed using the

Primer3 (http://primer3.sourceforge.net/) and synthesized by Invitrogen (Table 2.1). The Maxima SYBR green qPCR Master Mix (Thermo Scientific) and Mx3000 Quantitative PCR System (Stratagene) were used to amplify and detect transcripts of interest. The thermal cycling parameters were an initial 1 cycle Taq activation at 95 °C for 15 min, followed by 40 cycles of 95 °C for 15 s, optimized annealing temperature (60-63 °C) for 5 s, 72 °C for 30 s, and a detection step at 80 °C for 8 s. Data were analyzed using the MxPro software package. The relative standard curve method was used to calculate relative mRNA abundance between samples, which were normalized by using NORMA-GENE algorithm (Heckmann et al., 2011) and then presented as means + SEM from 6 biological replicates (n = 6; assayed in duplicate) for each group. All data were first tested for normality and those data with non-normal distribution were subjected to $\log_{10}$ transformations prior to statistical analyses.

Table 2.1. Primer sets used for quantitative real-time RT–PCR in goldfish.

Gene	**Primer Sequence (Forward)**	**Primer Sequence (Reverse)**	**Amplicon size**	**Accession No.**
β-actin	CTGGGATGATATGGAGAAGA	CCAGTAGTACGACCTGAAGC	215	AB039726
cyp19a1b	TGCTGACATAAGGGCAATGA	GGAAGTAAAATGGGTTGTGGA	153	AB009335
esr1	GCAGGAGGGTTTGATTCTGAGA	CCATAATGATAGCCGGACGCA	76	AY055725
esr2a	TGACTACATCTGCCCTGCCA	CCAACTTCGTAACATTTTCGGAGA	72	AF061269
esr2b	TGGTCCCTTTAAATTCAGCAATCT	GTGTTTCCCTGTAGGCCAGTG	95	AF177465
gfap	CCTACGGCAAGAAGCAGAAA	TCCTTCAGGGCAGTGGTTAG	230	L23876
gdnf	ATGGACTCAGGAACCAAGCA	GTCTGTGACGTTGAGGTGGA	173	EU828244
bdnf	TTGAGGAGTTGCTTGAGGTG	GGCGTCCAGGTAGTTTTTGT	205	EU828243

2.3.7 Statistics

In all cases and before any analysis, normality and homogeneity of variances was verified using Shapiro-Wilk's and Levene's test, respectively. Comparison of more than two groups was performed using one-way analysis of variance (ANOVA) followed by a Tukey post-hoc test or Dunnett's post-hoc test if the data did not pass homogeneity test in IBM SPSS Statistics Version 22. P-values less than or equal to 0.05 were considered statistically significant. Data were presented as mean + SEM.

2.4 Results

2.4.1 Expression of aromatase B in female goldfish forebrain

We designed and synthesized the aromatase B probe to study the distribution of *cyp19a1b* mRNA in female goldfish forebrain. As shown in Fig. 2.1, positive expression of *cyp19a1b* mRNA was detected at ventral telencephalic area (Fig. 2.1A), especially along the ventricular surface (Fig. 2.1B). In order to localize aromatase B protein in goldfish telencephalon, double immunofluorescence detection was performed. The intermediate filament GFAP was used as a RGC cell marker (Zupanc and Sîrbulescu, 2011) to identify RGCs in female goldfish brain (Fig. 2.2A, E), combined with the aromatase B antibody (Fig. 2.2B, F). The yellow colour in double fluorescence detection showed that aromatase B was strongly expressed by the majority of GFAP-positive RGCs along the ventricular surface (Fig. 2.2D, H;).

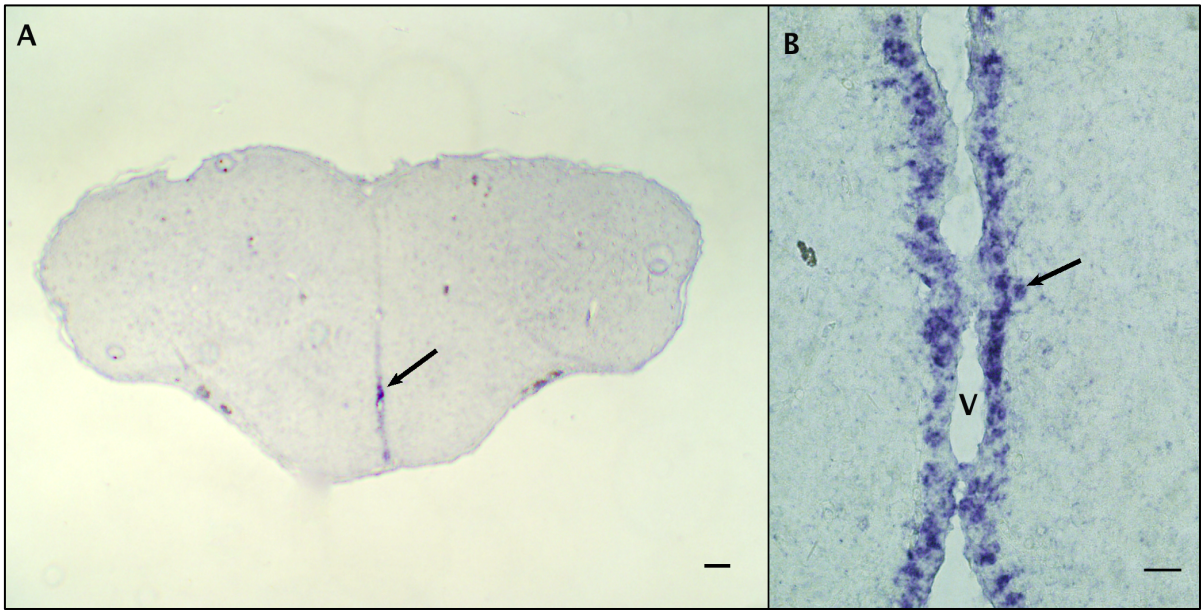

Figure 2.1. *In situ* hybridization on cryo-sections showing *cyp19a1b* transcripts in female goldfish telencephalon. (A) The black arrow indicates high density in the expression of cyp19a1b was detected in ventral area of telencephalon (scale bar = 100 μm). (B) Higher magnification view of the ventricular surface (V: ventricle) (scale bar = 20 μm).

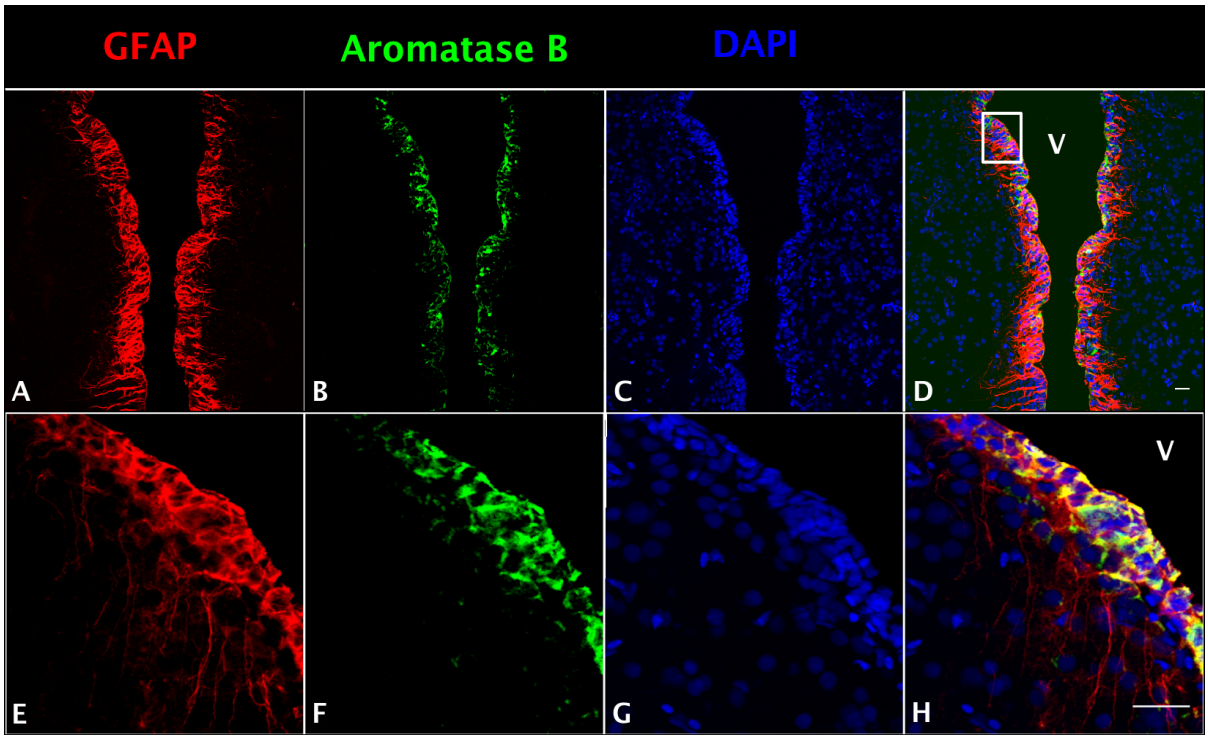

Figure 2.2. Double fluorescence detection of GFAP (red; A, E) and aromatase B (green; B, F) along the ventricular surface in female goldfish telencephalon. The confocal images show the expression of both aromatase B and GFAP along the ventricular surface (V; ventricle). The merged images show the colocalization of aromatase B and GFAP in RGCs (D, H). The nuclear stain DAPI (blue) is also shown (C, G). Scale bar = 20 μm.

2.4.2 Close anatomical relationship between catecholaminergic neurons and aromatase B-positive RGCs

Using TH and GFAP double fluorescence detection, we show that there is a close anatomical relationship between catecholaminergic neuronal cell bodies and RGC fibres (Fig. 2.3D, H) and between catecholaminergic neuronal processes and RGC fibres (Fig. 2.3L, P). Intensive TH-positive cell bodies were observed along the ventricular surface (Fig. 2.3B, F) and in the preoptic periventricular nucleus (NPP) with fibres extending to the area ventralis telencephali pars ventralis (Vv) (Fig. 2.3J, N). GFAP-immunoreactive RGCs were observed along the ventricular surface with fibres extending to the area Vv in telencephalon (Fig. 2.3A, E, I, M). Similar anatomical relationship was observed in *cyp19a1b*-GFP transgenic zebrafish (See Appendix 1).

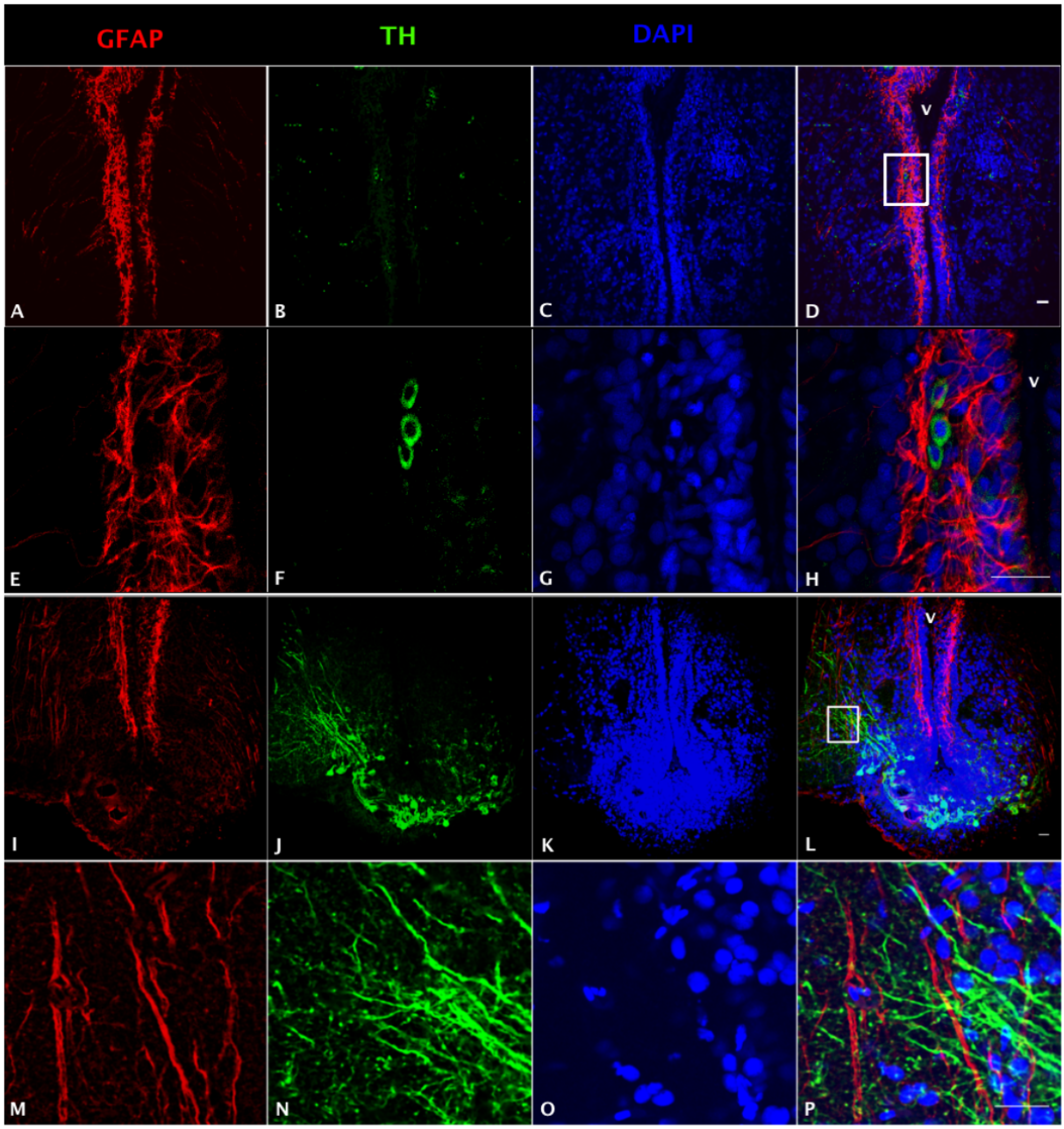
GFAP
TH
DAPI
A
B
C
D
v
E
F
G
H
v
I
J
K
L
v
M
N
O
P

Figure 2.3. Double fluorescence detection of GFAP (red) and TH (green) in the ventral telencephalic area of the female goldfish brain. The confocal images show that RGC cell bodies marked by GFAP are located along the ventricular surface (A, E). Some catecholaminergic neuron cell bodies marked by TH are located along the ventricular surface (B, F). Magnification of the boxed area in panel D shows that there are very close anatomical relationships between RGC fibres and catecholaminergic cell bodies (H). The confocal image shows RGC cell bodies marked by GFAP located along the ventricular surface with fibres extending from ventricular surface to the area Vv (I, M). Catecholaminergic neuron cell bodies marked by TH are located at NPP with fibres extending to the area Vv (J, N). Magnification of the boxed area in panel L shows that there are very close anatomical relationships between catecholaminergic neuronal processes and RGC fibres (V; ventricle, H, P). The nuclear stain DAPI (blue) is also shown (C, G, K, O). Scale bar = 20 μm.

2.4.3 Expression of D1R in RGCs

The presence of DA receptors on post-synaptic cells is required for direct regulation upon the release of DA by TH-positive catecholaminergic neurons. Both GFAP (Fig. 2.4A) and D1R (Fig. 2.4B)-positive staining can be observed along the ventricular surface (Fig. 2.4E, F), and in the area Vv (Fig. 2.4I, J). The merged confocal images show the colocalization of GFAP and D1R immunoreactivity (Fig. 2.4D, H, L), which indicates that RGCs express D1R.

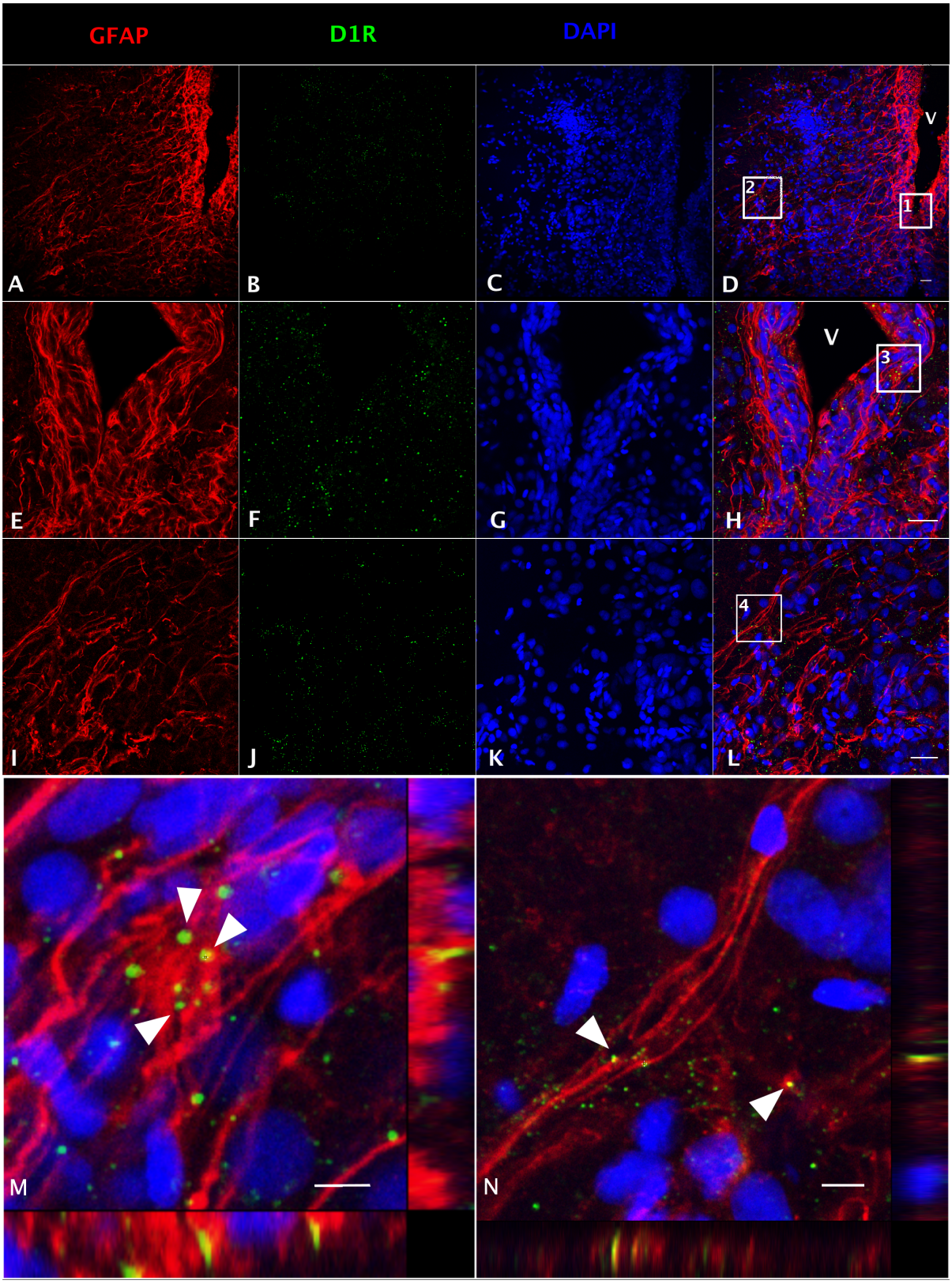
GFAP
D1R
DAPI
A
B
C
D
V
2
1
E
F
G
H
V
3
I
J
K
L
4
M
N

Figure 2.4. Double fluorescence detection of GFAP (red) and D1R (green) in the ventral telencephalic area of female goldfish brain. The confocal image shows that RGCs marked by GFAP are located at the ventricular surface (A, E) with fibres extending to the area Vv (I) and the expression of D1R at the ventricular surface and the area Vv (B, F, J). The expression of D1R in RGCs is shown in the merged images (V; ventricle, D, H, L). Magnification of the boxed area 1 in panel D shows that D1R is expressed by RGCs along the ventricular surface (H). Magnification of the boxed area 2 in panel D shows that D1R is expressed in RGC fibres in the area Vv (L). Single slice scanning view of the boxed area 3 in panel H shows the colocalization of D1R and GFAP in RGC fibres along the ventricular surface (M). Slice scan view of the boxed area 4 in panel L shows the colocalization of D1R and GFAP in RGCs in the area ventralis telencephali pars ventralis (N). The nuclear stain DAPI (blue) is also shown (C, G, K), arrowheads show the D1R location on RGC fibres. Scale bar = 20 μm in A-L; Scale bar = 5 μm in M and N.

2.4.4 The expression of *cyp19a1b* are regulated by SKF 38393

In telencephalon, after injection of the SKF 38393, there was a rapid, significant reduction of *cyp19a1b* expression ($P < 0.05$). The expression of *cyp19a1b* was decreased to 20%, 23%, 26% and 15% of control, at 3, 6, 12 and 24 hr, respectively. There were no significant differences ($P > 0.05$) between these 4 time points (Fig. 2.5A). In hypothalamus, after injection of the SKF 38393, the expression of *cyp19a1b* was decreased to 34% and 51% of control at 3 and 6 hr, respectively ($P < 0.05$) and increased to 287% at 12h ($P < 0.05$). The expression of *cyp19a1b* went back to 77% of control value at 24h ($P > 0.05$) (Fig. 2.5B).

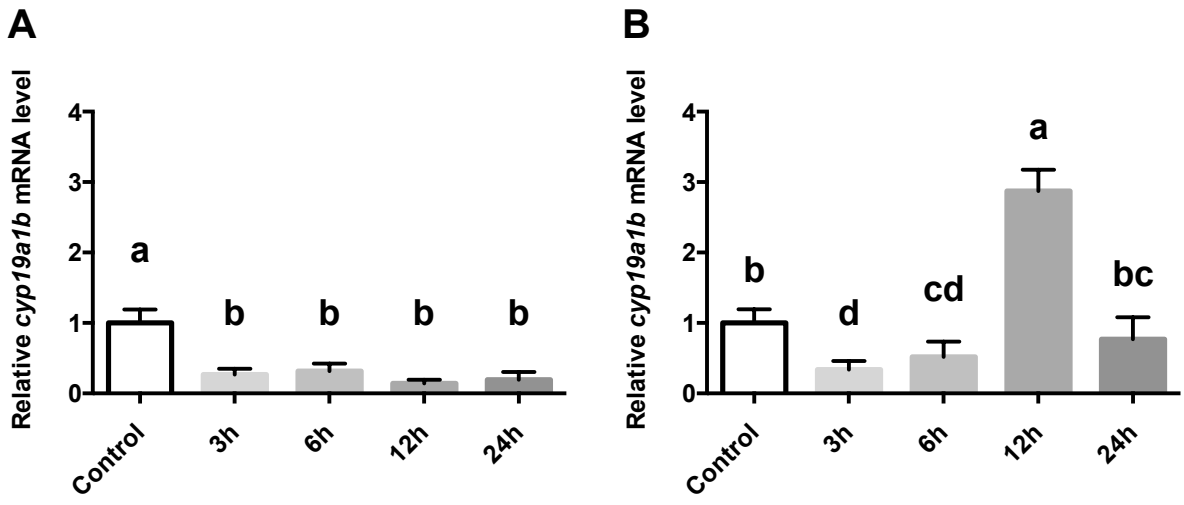

Figure 2.5. Quantitative real-time RT-PCR analysis showing variations in the relative levels of *cyp19a1b* mRNA in the female goldfish telencephalon (A) and hypothalamus (B) at 3, 6, 12, 24 hr after D1R agonist injection. Bars represent the mean + SEM of *cyp19a1b* levels in 6 different cDNA samples; values for each sample were determined in duplicate.

2.4.5 Estrogen receptor expression are regulated by SKF 38393

In telencephalon, after injection of the SKF 38393, there was no significant change in the expression of all three ERs ($P > 0.05$) (Fig. 2.6A). In hypothalamus, the expression of *esr1* and *esr2a* were increased at 3 and 6 hr ($P < 0.05$) (Fig. 2.6B).

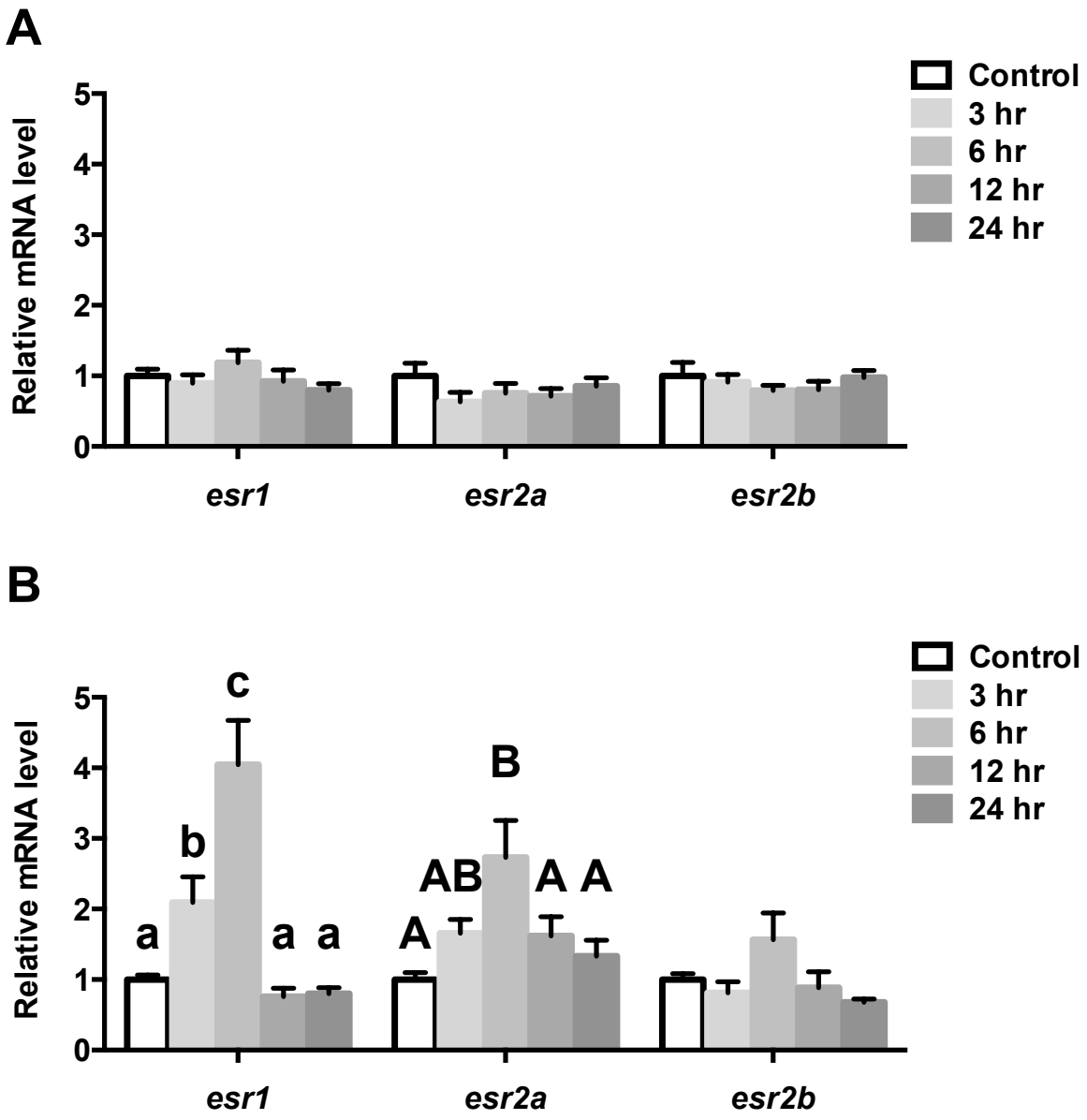

Figure 2.6. Quantitative real-time RT-PCR analysis showing variations in the relative amounts of RNA encoding for *esr1*, *esr2a* and *esr2b* in the female goldfish telencephalon and hypothalamus at 3, 6, 12, 24 hr after D1R agonist injection. Bars represent the mean + SEM of mRNA levels in 6 different cDNA samples; values for each sample were determined in duplicate.

2.4.6 Gene expression in RGCs are regulated by SKF 38393

In telencephalon, after injection of the SKF 38393, there was an increasing trend in the expression of *gfap, gdnf* and *bdnf,* but it was not significant ($P > 0.05$) (Fig. 2.7A, C, E). In hypothalamus, there was no significant change in the expression of *gfap* and *bdnf* ($P > 0.05$). The expression of *gdnf* was increased at 3 and 6 hr ($P < 0.05$), then back close to control value at 12 and 24 h ($P > 0.05$) (Fig. 2.7B, D, F).

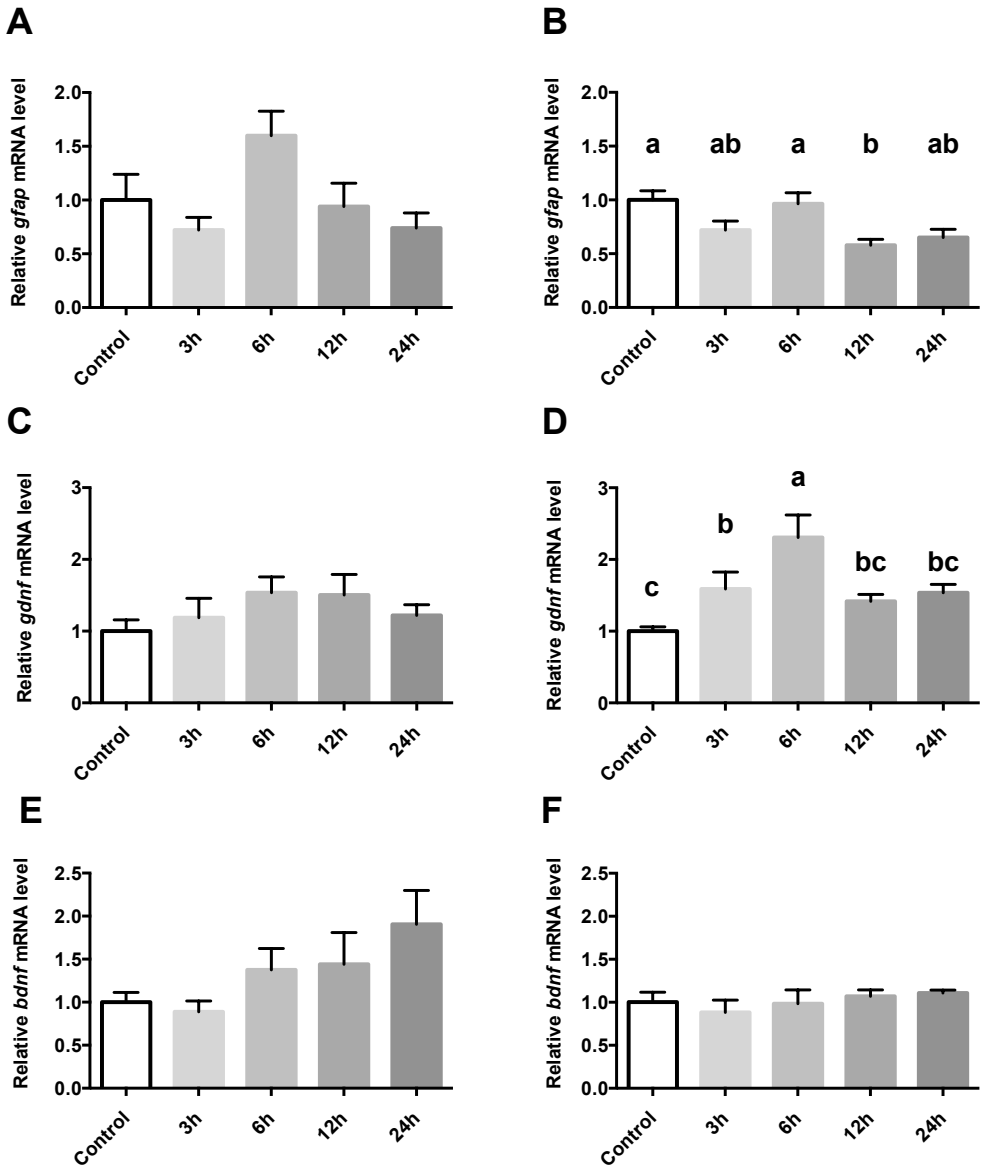

Figure 2.7. Quantitative real-time RT-PCR analysis showing variations in the relative amounts of RNA encoding for *gfap*, *gdnf* and *bdnf* in the female goldfish telencephalon (A, C, E) and hypothalamus (B, D, F) at 3, 6, 12, 24 hours after D1R agonist injection. Bars represent the mean + SEM of mRNA levels in 6 different cDNA samples; values for each sample were determined in duplicate.

2.5 Discussion

High expression of *cyp19a1b* is well known in adult fish forebrain, including telencephalon, preoptic region and hypothalamus (Diotel et al., 2010a; Nagarajan et al., 2013). In this study, we extend these observations to the female goldfish. *In situ* hybridization and immunofluorescence data showed the expression of aromatase mRNA and protein in goldfish ventral telencephalic area, especially along the ventricular surface. Very similar expression patterns of brain aromatase along the ventricular surface have been documented in other teleost fish species (Diotel et al., 2011a; Forlano et al., 2001; Nagarajan et al., 2013; Strobl-Mazzulla et al., 2008; Vizziano-Cantonnet et al., 2011). At the cellular level, brain aromatase is exclusively expressed by teleost RGCs, which has been reported in zebrafish and midshipman (Diotel et al., 2010a; Forlano et al., 2001; Tong et al., 2009). The colocalization of GFAP and aromatase B indicates that the goldfish RGCs in the ventral telencephalic area are a site for neuroestrogen synthesis. TH-positive catecholaminergic neurons are in close proximity to GFAP-positive RGCs expressing D1R, which raises the distinct possibility for dopaminergic regulation of RGCs. Our *in vivo* pharmacological studies suggested that *cyp19a1b* expression in the RGCs could be regulated by D1R activation.

The ventricular surface in the teleost forebrain is considered an active neurogenic niche that can generate new neurons during adulthood, due to the abundance of persisting RGCs, which are progenitor cells due to their proliferative and neurogenic nature (Pellegrini et al., 2007; Strobl-Mazzulla et al., 2008). Most importantly, expression of the estrogen synthesis enzyme aromatase in teleost RGCs suggests strong relationships with neurogenic and neuroendocrine activities. The expression of aromatase B enables RGCs to produce

estrogens, so they are important steroidogenic cells in the fish brain. Upon brain injury, local formation of neuroestrogens by astrocytes in the brain can decrease apoptosis and act as neurotrophic factors to stimulate neuron survival in mammals (Azcoitia et al., 2003; Garcia-Segura et al., 2003; Garcia-Segura et al., 1999; Saldanha et al., 2009; Tanapat et al., 1999). However, one recent study showed that E2 has an inhibitory effect on adult neurogenesis but not brain repair in zebrafish (Diotel et al., 2013). Therefore, because the inconclusive effects of E2 on cell proliferation in different species, the role of brain aromatase and estrogen synthesis in neurogenesis need to be further understood. Several studies have reported that steroid hormones, including both androgens and estrogens, can increase aromatase B expression (Forlano and Bass, 2005; Jeng et al., 2012a; Mouriec et al., 2009a; Mouriec et al., 2009b), but little else is known about the regulation of aromatase expression and enzyme activity in adult brain. Here, we show that aromatase B can be regulated via D1R receptor activation by *in vivo* injection of an agonist in fish.

Along the ventricle surface, RGCs synthesize and produce estrogens presumably by aromatizing circulating androgens that enter the brain. Recent studies further suggest that RGCs may be able to *de novo* synthesize estrogens, given the expression of numerous steroid synthetic enzymes leading to both androgen and estrogen synthesis, along with the expression of StAR protein (Xing et al., 2014). Previous studies in quail brain showed that there were catecholaminergic inputs close to aromatase-positive cells (Balthazart J, 1998). The double staining of TH and GFAP in this study indicates that catecholaminergic, presumptive dopaminergic neurons are in close proximity to aromatase-positive RGCs along the female goldfish ventricle. Moreover, there have been many studies suggesting the existence of DA in cerebrospinal fluid (CSF) due to some DA neurons in the periventricular

regions of female goldfish and the catfish paraventricular organ, which make contact with CSF in the third ventricle through their apical processes (Corio et al., 1991; Hornby and Piekut, 1990; Meek and Joosten, 1993; Smeets and González, 2000). Therefore, DA may originate either directly from neurons adjacent to RGCs or from the CSF, because RGCs are lying along the surface of the ventricle. This anatomical and biochemical data is strongly supported by our discovery of D1R and GFAP colocalization in RGCs along the ventricular surface. Therefore, it is possible that DA may regulate RGC functions through activation of DA receptors. On the other hand, the close associations between DA neuron cell bodies and RGC fibres also indicates that estrogens produced by RGCs might have effects on the neighbouring DA neurons to control DA synthesis and release.

The possibility that brain aromatase can be regulated by DA is supported by the transcriptional studies. Data demonstrated that injection of the SKF 38393 rapidly decreased *cyp19a1b* mRNA level in female goldfish telencephalon and hypothalamus. In the telencephalon, this suppressive effect lasted until 24 hr post injection. The observation in the hypothalamus revealed a more complex regulatory pattern of *cyp19a1b* expression. After the initial acute decrease at 3 hr, *cyp19a1b* mRNA levels rebounded at 12 hr, and then returned to control value at 24 hr. According to previous findings on the up-regulating *cyp19a1b* expression by estrogens and androgens (Bowman et al., 2002; Denslow et al., 2001), it is believed that nuclear ERs may play a role in the unexpected and transient increase in hypothalamic *cyp19a1b* expression at 12 hr following SKF 38393 injection. Due to duplication of the ERß gene, teleost have three ERs (*esr1, esr2a* and *esr2b*). All three types of ERs are expressed in the brain of fish, mainly in the preoptic area, hypothalamus and ventral telencephalon, with an expression pattern similar to that of aromatase (Pellegrini et

al., 2005). Most actions of estrogens are mediated by ERs, and the involvement of ERs in brain aromatase up-regulation has been reported (Mouriec et al., 2009a; Mouriec et al., 2009b). Here, we report that a D1R agonist can regulate ERs in goldfish hypothalamus but not telencephalon. The up-regulation of *esr1* and *esr2a* expression in the hypothalamus may be part of the mechanism whereby D1R agonist affects *cyp19a1b* expression, since *esr1* and *esr2a* can regulate estrogen synthesis positively (Pellegrini et al., 2005).

After observing the different regulation patterns of *cyp19a1b* expression in the goldfish telencephalon and hypothalamus, treatment with the D1R agonist regulates other functions of RGC, such as neurotrophic factor production was hypothesized. Therefore, the expression of genes, including *gfap*, *gdnf* and *bdnf*, were studied following D1R agonist injection. However, our data did not show a significant time-dependent regulation of *gfap* or *bdnf* expression, except *gdnf* expression in the hypothalamus. In fish, D1R expression in the brain is region -specific (Kapsimali et al., 2000; Li et al., 2007). The differential distribution of D1R or the various D1R subtypes may be at the basis of the contrasting responses to SKF 38393 as regards *cyp19a1b* expression in the telencephalon versus hypothalamus. For example, in the European eel (*Anguilla anguilla*) where DA receptor distributions are well described, there are clear differences in the expression patterns of D1A, D1B and D1C in the adult telencephalon and hypothalamus (Kapsimali et al., 2000). The *in situ* hybridization analysis on D1R subtype distribution indicated that D1B receptor transcripts are abundant along ventricular wall of the telencephalon where RGCs are located. In contrast, D1A is more abundant in the ventral periventricular area of the hypothalamus (Kapsimali et al., 2000). This is also a region previously noted to contain aromatase-positive RGCs in adult brain (Balthazart et al., 2002; Menuet et al., 2003; Menuet et al., 2005; Strobl-Mazzulla et al.,

2008). Because of the time-dependent effects of *cyp19a1b* expression and the tissue-dependent regulation of *gdnf* may indicate may indicate a combination of direct effects of SKF 38393 on RGCs, and indirect regulation of *cyp19a1b* expression via D1Rs on neurons impinging on RGCs. Development of cell isolation and culture methods (Xing et al., 2014; Xing et al., 2015) may lead to a better understanding of direct actions of DA on RGCs (see Chapter 3).

In summary, aromatase B and D1R are expressed by RGCs along the ventricular surface of the goldfish telencephalon. In the ventral telencephalic area of the goldfish forebrain, there is a close anatomical relationship between catecholaminergic neurons and RGCs, which indicates the possibility of catecholaminergic regulation of brain aromatase. The colocalization of brain aromatase and D1R in RGCs reveals the potential regulation of aromatase B by DA. Injection of D1R agonist rapidly regulated the expression of *cyp19a1b* and other genes related to RGC functions in female goldfish telencephalon and hypothalamus, which supports the proposal that DA is a regulator of brain aromatase, and possibly other RGC functions.

Chapter 3: Dopamine D1 receptor activation regulates aromatase B expression in goldfish RGCs [3]

3.1 Abstract

Radial glial cells are abundant stem-like non-neuronal progenitors that are important for adult neurogenesis and brain repair, yet little is known about their regulation by neurotransmitters. Here we provide evidence for neuronal-glial interactions via a novel role for DA to stimulate RGC functions. Goldfish were chosen as the model organism due to the abundance of RGCs and regenerative abilities of the adult CNS. A primary cell culture system was established and immunofluorescence analysis indicates that RGCs from female goldfish *in vitro* retain their major *in vivo* characteristics, including expression of GFAP and BLBP. Pharmacological experiments using the cultured RGCs established that specific activation of DA D1 receptors up-regulates *cyp19a1b* expression through a cAMP-dependent molecular mechanism. These data indicate that DA enhances the steroidogenic function of this neuronal progenitor cell.

3.2 Introduction

The RGC is a glial cell type in the CNS of all vertebrate species. As the key organizer and contributor of both nervous system development and adult neurogenesis, RGCs function

---

[3] *Partially based on Xing, L., Mcdonald, H., Da Fonte, D.F., Gutierrez-Villagomez, J.M., and Trudeau, V.L. (2015). Dopamine D1 receptor activation regulates the expression of the estrogen synthesis gene aromatase B in radial glial cell. Front. Neurosci. 9. doi: doi: 10.3389/fnins.2015.00310. XL, designed the study, developed the methodology, conducted the majority of experiments and analysis and wrote the manuscript. MH, DFDF maintained cell culture and helped with qPCR analysis. GVJM gave critical comments on the manuscript. TVL, helped with the design of the study and editing the article.*

as scaffolding to support neuron migration (Bentivoglio and Mazzarello, 1999; Schmechel and Rakic, 1979), and as stem cells that give rise to both neurons and other glial cells (Zupanc and Clint, 2003; Zupanc et al., 2012). Despite these essential functions, RGCs are transient in mammals as the majority differentiate into other cell types during the developmental process (Malatesta et al., 2000; Rakic, 2003b). In comparison, RGCs are highly abundant and persistent throughout the entire lifespan of fish, explaining the high regenerative capacity of the teleost CNS. To maintain normal brain function, regulation and termination of the regenerative process is critical. Therefore, RGCs must be under tight control by specific regulators to prevent the overproduction of newborn cells.

Studies in mammalian model systems indicate that neurotransmitters such as GABA and DA influence neurogenesis by modulating stem and progenitor cell functions (Ge et al., 2007; Hoglinger et al., 2004; Kippin et al., 2005). Our earlier work was suggestive of DA neuron-glia interaction since we observed rapid *in vivo* effects of DA receptor selective pharmacological agents on GFAP expression in goldfish hypothalamus (Popesku et al., 2010). In zebrafish, a close anatomical relationship exists between RGCs and 5-HT neurons in the hypothalamic paraventricular organ (Pérez et al., 2013); 5-HT being another potential neurotransmitter that may regulate this critical cell type, although specific receptors or functions for 5-HT or any other neurotransmitters in RGCs have not yet been identified.

Here we took advantage of the high abundance of RGCs in goldfish, and developed an *in vitro* culture system to specifically investigate DA signaling pathways. The teleost RGC culture system also represents the only native cell model to date that allows the distinction between glial and non-glial estrogens because it is the unique cell type in the adult teleost brain that expresses the estrogen synthesis enzyme aromatase B in normal brain or after

damage (Diotel et al., 2010a; Forlano et al., 2001). Aromatase B expression is lost as RGCs differentiate into neurons, therefore the overexpression of aromatase B is a key signal for maintaining the progenitor characteristics of this cell type (Coumailleau et al., 2015; Diotel et al., 2010a; Xing et al., 2014). Aromatase B is the specific marker and functional target herein investigated.

3.3 Materials and Methods

3.3.1 Experimental animals

All procedures used were approved by the University of Ottawa Protocol Review Committee and followed standard Canadian Council on Animal Care guidelines on the use of animals in research. Common adult female goldfish were maintained at 18 °C under a natural simulated photoperiod and fed standard goldfish flakes. Sexually mature female goldfish (18-35 g) were anaesthetized in 0.05% MS222 for all handling and dissection procedures.

3.3.2 Cell culture

The hypothalamus and telencephalon were dissected from female goldfish and minced into small pieces. Goldfish RGCs were dissociated with trypsin (0.25%, Gibco) and cultured in Leibovitz's L-15 medium (Gibco) with 15% Fetal Bovine Serum (FBS, Gibco) and antibiotic-antimycotic solution. Cell culture medium was changed once a week after initial isolation. Goldfish RGCs were subcultured by trypsinization (0.125%) for 3 passages to obtain high purity (>95%) cultures and then used for experiments.

3.3.3 Immunohistochemistry

Cultured cells on coverslips were fixed in 4% PFA for 20 m and washed in PBS, then

covered with the anti-BLBP (rabbit, 1:500, Millipore, ABN14), anti-Hu C/D (mouse, 1:500, Thermo Fisher Scientific, A-21271), anti-zn-12 (mouse, 1:500, Zebrafish International Resource Centre, zn-12), anti-GFAP (mouse, 1:500, Millipore, MAB360) (Forlano et al., 2001), anti-aromatase B (rabbit, 1:500, from the lab of O. Kah) (Menuet et al., 2003; Pellegrini et al., 2007) and anti-D1R antibody (rabbit, 1:500, Acris, AP09962PU-N), then incubated with donkey anti-rabbit Alexa fluor 488 (1:500, Molecular Probes) and goat anti-mouse Alexa fluor 596 (1:500, Molecular Probes) for 1 hour at RT. Slides were washed and mounted with the antifading medium Vectashield with DAPI. Images were taken by Nikon A1RsiMP confocal microscope with Nikon's Imaging Software NIS-Elements.

3.3.4 *In situ* hybridization

Antisense RNA probes were synthesized *in vitro* using goldfish aromatase B cDNA fragments (1.6 kb). *In situ* hybridization on cultures was performed as previously described with minor modifications (Chapter 1). Briefly, cells were fixed and incubated with probe mix in an oven at 70 °C overnight, and blocked in 10% calf serum for 1 hour at RT. Anti-DIG AP Fab fragment antibody (Roche) was added and incubated overnight at 4 °C, then incubated with NTMT containing BCIP and NBT overnight at RT.

3.3.5 RNA extraction, cDNA synthesis and qPCR

Cells were exposed to selective D1 agonist (SKF 38393, Tocris) and selective D2 agonist (Quinpirole, Tocris) for 24 hr at various concentrations to study the dose-dependent effects on *cyp19a1b* mRNA. To investigate DA receptor activation, cAMP and PKA involvement in *cyp19a1b* mRNA regulation by SKF 38393, cells were pre-exposed to 5 μM Flupentixol (Tocris), 100μM SKF 83566 (Tocris), 100 μM DOM (Sigma) or 10 μM H89

(Tocris) for 1 hr, then exposed to 10 μM SKF 38393 and 8-Br-cAMP (Tocris) for 24 hr. The isolation of total RNA was performed by using RNeasy Micro kit (Qiagen). Total cDNA was prepared using Maxima cDNA synthesis kit (Thermo Scientific) and used as the template for the qPCR assays. Primers used in the present study were designed using Primer3 (http://primer3.sourceforge.net/) and synthesized by Invitrogen (cyp19a1bFw, TGCTGACATAAGGGCAATGA; cyp19a1bRv, GGAAGTAAAATGGGTTGTGGA; 18sFw, AAACGGCTACCACATCCAAG; 18sRv, CACCAGATTTGCCCTCCA). The Maxima SYBR green qPCR Master Mix (Thermo Scientific) and CFX96 Real-Time PCR Detection System (Bio-Rad) were used to amplify and detect the transcripts of interest. Data were analyzed using the Bio-Rad software package. The relative standard curve method was used to calculate relative mRNA abundance between samples based on the Cq values, which were then normalized by using NORMA-GENE algorithm (Heckmann et al., 2011). Normalized data were used to calculate fold-change against the average value of control and then presented as means + SEM of gene expression from 4 biological replicates (n = 4) (assayed in duplicate) for each group.

3.3.6 Measurement of cAMP production

To examine the induction of cAMP production by DA compounds in RGC culture, RGCs were seeded in 25 cm^2 flasks and pre-incubated with IBMX (0.1mM, Sigma) for 15 min, then treated with SKF 38393 (10 μM) for 30 min. Cell culture medium and cell extract were quantified with a cyclic AMP select EIA Kit (Cayman, 501040) according to the manufacturer's instructions.

3.3.7 Western Blot

Cells were exposed to 10 μM SKF 38393 for 24h to study phosphorylated CREB protein (p-CREB) stimulation. Total protein was denatured and separated by electrophoresis on a 10% SDS-polyacrylamide gel and transferred to a PVDF membrane as described previously (Zhao et al., 2006). Membranes were incubated separately with primary anti-actin (Cedarlane, CLT9001) and anti-Phospho-CREB (Ser133, Cell Signaling Technology, 9198S) antibodies overnight at 4 °C and then incubated separately with goat anti-mouse IgG-HRP (Santa Cruz, sc-2005) and donkey anti-rabbit IgG antibody (GE Health Care, NA934VS). Blots were visualized using the Amersham ECL Prime Western Blotting Detection System (GE Health Care, RPN2232). Images were obtained using a Fusion FX5 and analyzed with Image J.

3.3.8 Statistics

In all cases and before any analysis, normality and homogeneity of variances was verified using Shapiro-Wilk's and Levene's test, respectively. Comparison of two groups was performed using Student's t-test in IBM SPSS Statistics Version 22. Comparison of more than two groups was performed using one-way analysis of variance (ANOVA) followed by a Tukey post-hoc test or Dunnett's post-hoc test if the data did not pass homogeneity test in IBM SPSS Statistics Version 22. P-values less than or equal to 0.05 were considered statistically significant. Data were presented as mean + SEM.

3.4 Results

3.4.1 Isolation and characterization of RGCs from goldfish brain

We developed a protocol to isolate and culture RGCs from goldfish brain and propose this as an excellent technique since it yields a relatively pure RGC culture for functional

studies, and a platform to screen potential drugs affecting RGCs. Both GFAP and BLBP are highly expressed RGC markers *in vivo* (Forlano et al., 2001; Tong et al., 2009) and were used to identify cells in culture. At the third passage, most cells showed positive expression of GFAP (97%, Fig. 3.1A) and BLBP (98%, Fig. 3.1B) indicating that the cells maintained essential *in vivo* characteristics. The merged image indicates that cells co-express GFAP and BLBP (Fig. 3.1D). Confocal images (Fig. 3.2A-D) strengthen this conclusion and indicate that the majority of cells in culture are RGCs (>95%). Both *in situ* hybridization (Fig. 3.2E) and immunofluorescence (Fig. 3.2F) images indicate that RGCs in culture express *cyp19a1b* mRNA and aromatase B protein, further demonstrating the conservation of fundamental *in vivo* functions in culture conditions.

We next set out to determine the role of D1R in the regulation of aromatase B *in vitro*. The yellow colour in merged confocal images shows the colocalization of GFAP and D1R (Fig. 3.2G-J). Following the establishment of both D1R and aromatase B in culture, we proceeded to determine the effects of a D1R agonist in *cyp19a1b* expression, as well as the signal transduction cascades associated with D1R activation and *cyp19a1b* expression.

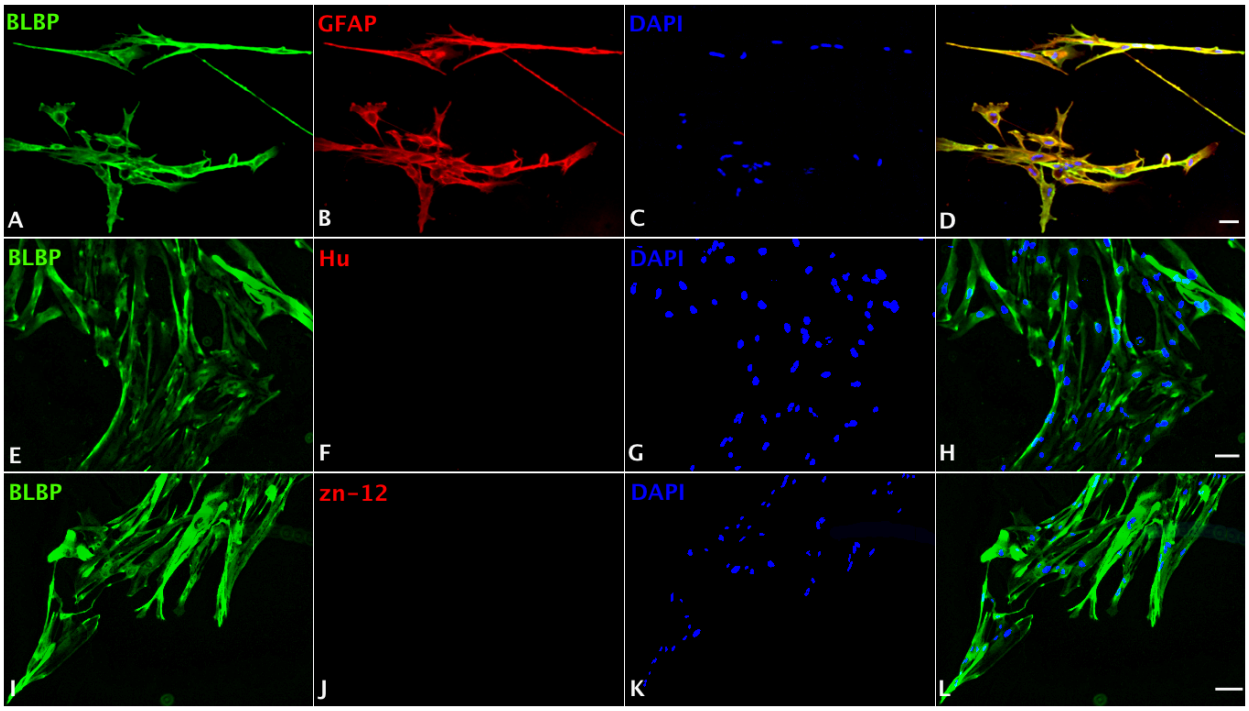

Figure 3.1. Double immunofluorescence labeling of BLBP and GFAP, BLBP and Hu and BLBP and zn-12. (A,E,I) BLBP labeling (green) of RGC in culture. (B) GFAP staining (red) in the same cells in panel A. (F) Hu staining (red) in the same cells in panel E. (J) zn-12 staining (red) in the same cells in panel I. (C, G, K) RGC nuclei were visualized by DAPI staining (blue). (D, H, L) Merged image shows expression of BLBP and GFAP, BLBP and Hu, BLBP and zn-12 in RGC primary culture. Scale bar = 20 μm. The percentage of positive GFAP and BLBP stained cells were counted out of total cells from 10 different views on one coverslip and six different coverslips with image J. Most cells in culture showed positive expression of GFAP (97±0.4%, A) and BLBP (98±0.3%, B). No immunoreactivity for Hu and zn-12 was detected.

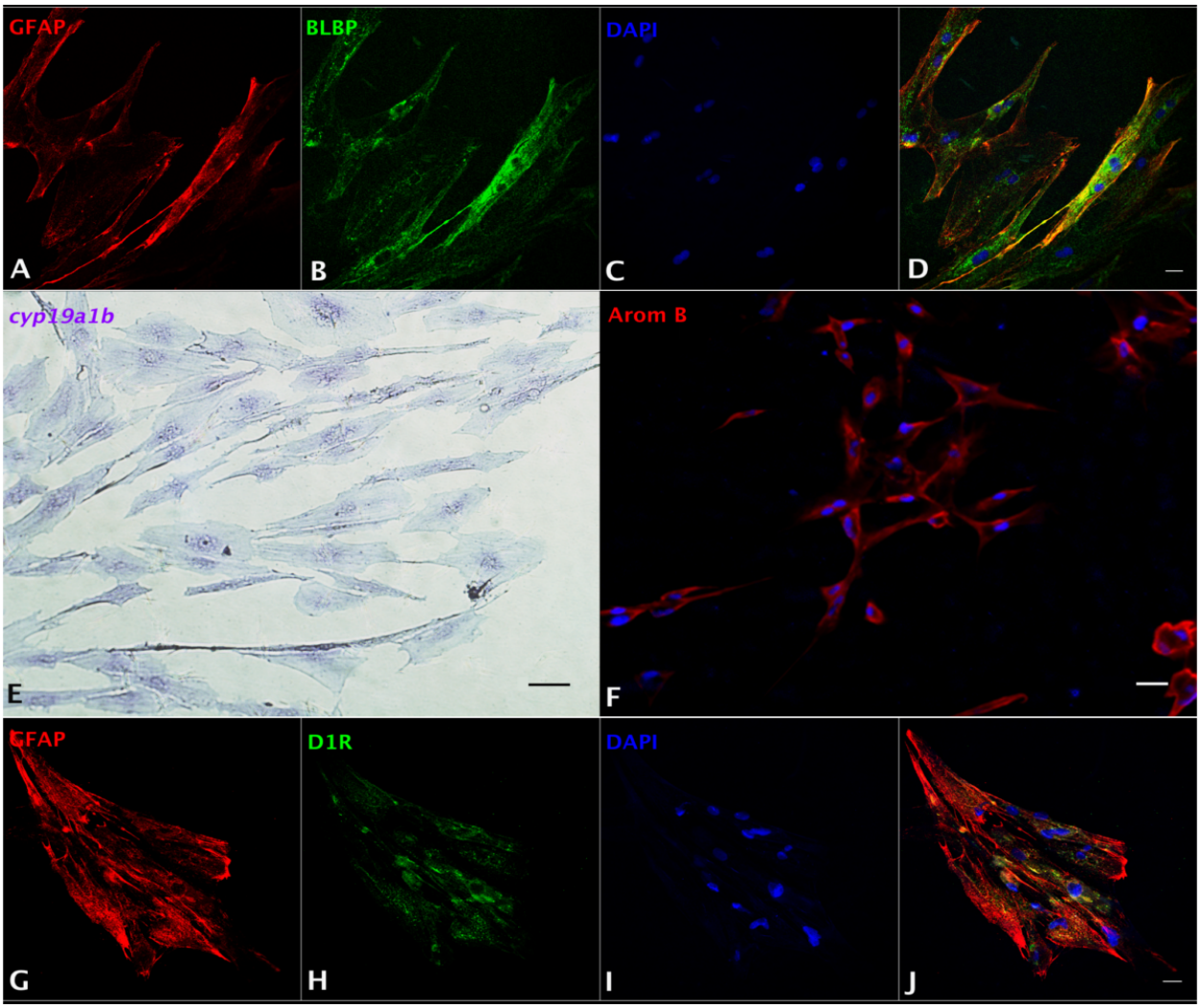

Figure 3.2. Characterization of RGCs in primary culture by *in situ* hybridization and immunofluorescence. Confocal image of double immunofluorescence labeling of GFAP (red, A) and BLBP (green, B) shows the colocalization of GFAP and BLBP in RGCs in culture (D). Positive staining of *cyp19a1b* mRNA (E) and aromatase B protein (AromB) in RGC culture (F) indicates the expression of aromatase B in RGC cultures. Confocal imaging of double immunofluorescence labeling of GFAP (red, G) and D1R (green, H) shows the colocalization of GFAP and D1R in RGC culture. The nuclear stain DAPI (blue) is also shown (C, I). Scale bar = 10 μm.

3.4.2 Dopamine D1 receptor activation regulates *cyp19a1b* mRNA in cultured RGCs

The RGC cultures were exposed to selective DA D1 (SKF 38393) or DA D2 (Quinpirole) agonists to investigate *cyp19a1b* mRNA regulation. After 24 hr incubation with SKF 38393 in the 1-100 μM ranges, qPCR data showed that 10 μM SKF 38393 effectively increased aromatase B mRNA by 2.1 fold ($P < 0.05$, Fig. 3.3A). In contrast, Quinpirole at 1 nM, 10 nM, 100 nM, 1 μM and 10 μM had no effect on *cyp19a1b* mRNA level ($P > 0.05$, Fig. 3.3B). Based on the dose-response study, 10 μM SKF 38393 was chosen to investigate the specificity of *cyp19a1b* expression regulation in RGC culture. First, the non-selective DA receptor antagonist, Flupentixol (Flup), was used to block DA receptors. The data showed that Flup alone did not affect *cyp19a1b* mRNA level ($P > 0.05$), but the stimulatory effects of SKF 38393 on *cyp19a1b* mRNA ($P < 0.05$) were completely inhibited ($P > 0.05$), indicating a receptor-dependent mechanism (Fig. 3.3C). Second, the selective D1R antagonist, SKF 83566 alone did not alter *cyp19a1b* mRNA ($P > 0.05$), but the stimulatory effects of SKF 38393 on *cyp19a1b* mRNA ($P < 0.05$) were completely blocked by SKF 83566 ($P > 0.05$), indicating D1R binding and activation involved in *cyp19a1b* mRNA regulation (Fig. 3.3D). Furthermore, it was confirmed that DA D2 receptors were not involved by using the selective DA D2 receptor antagonist Domperidone (DOM). The data showed that DOM alone did not have any effects on *cyp19a1b* mRNA ($P > 0.05$), and did not affect ($P < 0.05$) SKF 38393 action (Fig. 3.3E).

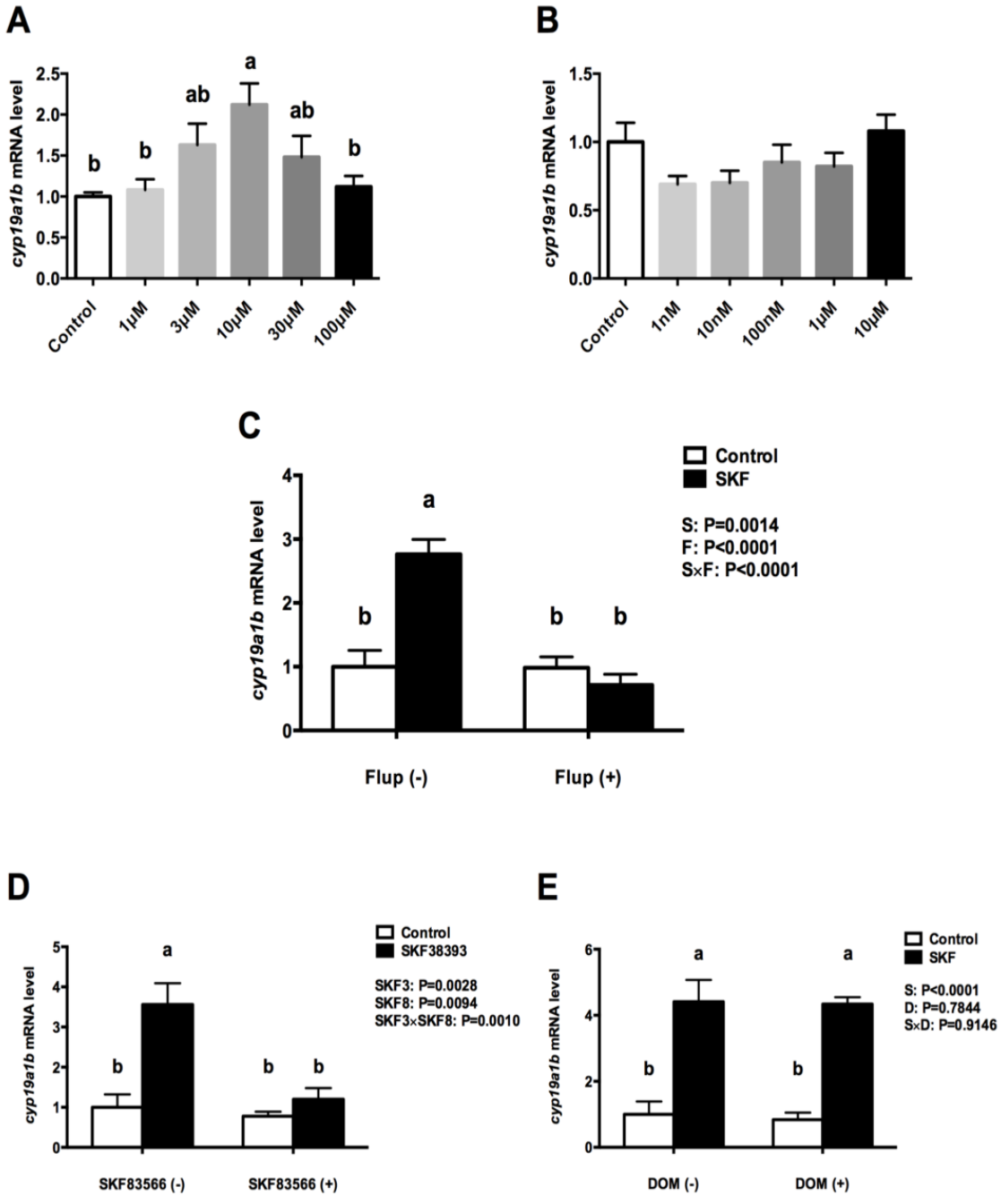
A
cyp19a1b mRNA level
2.5
2.0
1.5
1.0
0.5
0.0
b
b
ab
a
ab
b
Control
1μM
3μM
10μM
30μM
100μM
B
cyp19a1b mRNA level
1.5
1.0
0.5
0.0
Control
1nM
10nM
100nM
1μM
10μM
C
Control
SKF
S: P=0.0014
F: P<0.0001
S×F: P<0.0001
cyp19a1b mRNA level
4
3
2
1
0
b
a
b
b
Flup (-)
Flup (+)
D
Control
SKF38393
SKF3: P=0.0028
SKF8: P=0.0094
SKF3×SKF8: P=0.0010
cyp19a1b mRNA level
5
4
3
2
1
0
b
a
b
b
SKF83566 (-)
SKF83566 (+)
E
Control
SKF
S: P<0.0001
D: P=0.7844
S×D: P=0.9146
cyp19a1b mRNA level
6
4
2
0
b
a
b
a
DOM (-)
DOM (+)

Figure 3.3. The effects of dopaminergic compounds on *cyp19a1b* mRNA levels in RGC culture. Quantitative real-time RT-PCR analysis of *cyp19a1b* mRNA, normalized to *18s* in primary RGC culture after exposure of different dosages of SKF 38393 (A), different dosages of Quinpirole (B), SKF 38393 and/or Flup (C), SKF 38393 and/or SKF 83566 (D), SKF 38393 and/or DOM (E). DMSO was used as a vehicle to dissolve SKF 83566 and DOM, which showed no effects on *cyp19a1b* mRNA levels in RGC culture ($P > 0.05$) (Fig. A3.2). Data were defined as fold change relative to control, the bars represent the mean + SEM (n = 4), each sample was analyzed in duplicate. a,b-Groups marked by different letters are significantly different ($P < 0.05$).

3.4.3 Regulation of RGC *cyp19a1b* mRNA is through the D1R/cAMP/PKA/p-CREB signaling pathway

Activation of D1R by SKF 38393 increased total cAMP production by 25% ($P < 0.05$, Fig. 3.4A). Furthermore, 10 μM 8-Br-cAMP increased *cyp19a1b* mRNA by 1.8 fold, similar to the 2 fold increases following 10 μM SKF 38393 ($P < 0.05$, Fig. 3.4B). Therefore, we focused on the classic cAMP-dependent signaling pathway. The PKA inhibitor H89 blocked ($P > 0.05$) the D1R-dependent increase in *cyp19a1b* mRNA induced by SKF 38393 ($P < 0.05$) in cultured RGCs (Fig. 3.4C). It is known that PKA activation leads to phosphorylation of CREB. Exposure to SKF 38393 increased p-CREB protein levels by 1.8 fold ($P < 0.05$, Fig. 3.4D, E).

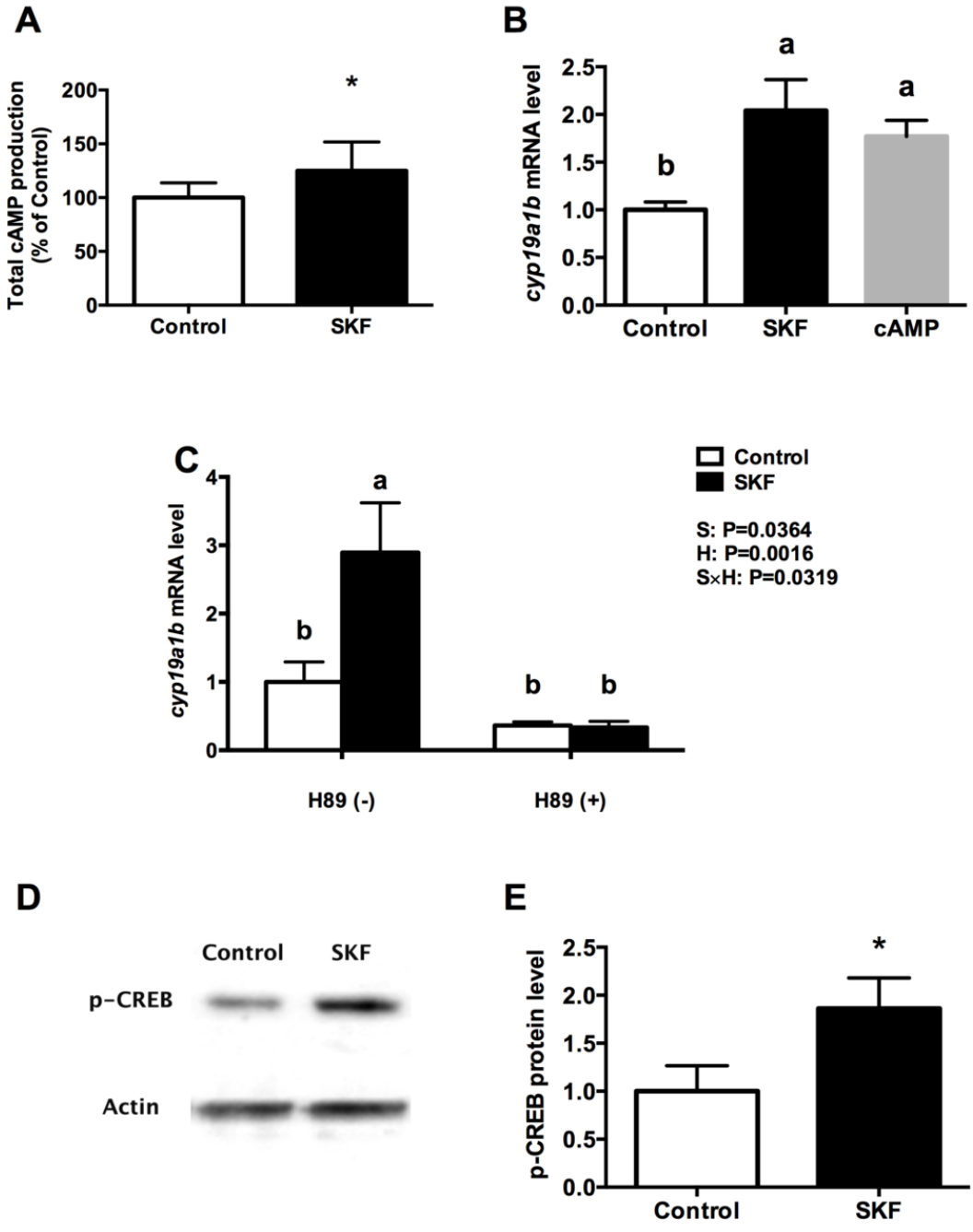
A
Total cAMP production (% of Control)
200
150
100
50
0
*
Control
SKF
B
cyp19a1b mRNA level
2.5
2.0
1.5
1.0
0.5
0.0
a
a
b
Control
SKF
cAMP
C
cyp19a1b mRNA level
4
3
2
1
0
a
b
b
b
H89 (-)
H89 (+)
Control
SKF
S: P=0.0364
H: P=0.0016
S×H: P=0.0319
D
Control
SKF
p-CREB
Actin
E
p-CREB protein level
2.5
2.0
1.5
1.0
0.5
0.0
*
Control
SKF

Figure 3.4. Involvement of D1R/cAMP/PKA/p-CREB signaling pathway in dopaminergic regulation of *cyp19a1b* mRNA in RGC culture. Total cAMP production rapidly increased by 10 μM SKF 38393 (30 min). Data were normalized to control value and defined as % of control, bars represent the mean + SEM (n = 3), and values for each sample were determined in duplicate. (A) Regulation of *cyp19a1b* mRNA in primary RGC culture after 24 hr exposure of 8-Br-cAMP (B), SKF 38393 and/or H89 (C). Western blot image showing the effects of SKF 38393 on p-CREB immunoreactivity, where actin served as an internal control (D). The densitometric analysis of western blot is reported as an arbitrary value relative to the average of all bands on the same blot. Data were normalized and defined as fold change relative to control, and bars represent the mean + SEM (n = 6) (E). a,b-Groups marked by different letters are significantly different ($P < 0.05$).

3.5 Discussion

Together the results show that RGCs possess a functional D1R/cAMP/PKA/p-CREB signalling pathway that is associated with the control of *cyp19a1b* mRNA production. To develop the protocol for goldfish RGC culture system, we combined different primary glial cell culture protocols of mammalian astrocytes, fish astroglia, goldfish microglial cells and zebrafish brainstem cells (Crocker et al., 2008; Houalla and Levine, 2003; Mack and Tiedemann, 2013; Tapanes-Castillo et al., 2014). There were several crucial differences between the protocols previously described and ours in order to optimize the isolation of RGCs. First, the trypsin dissociation was performed at RT instead of at 37 °C for mammalian cells since higher temperature yielded much fewer adhered cells at day 4 after seeding. Second, even though RGCs are extremely abundant in teleost brain compared to neurons

(Mack and Tiedemann, 2013; Reichenbach and Pannicke, 2008; Sherwood et al., 2006), regular cell culture medium still could not completely deprive neurons in glial culture systems. Here a relatively higher percentage (15%) of FBS was used to increase the glial cell attachment to the dish and inhibit neuronal cell survival and growth, because certain components in serum, like glutamate, are toxic to neurons (Ye and Sontheimer, 1998). Furthermore, microglia and oligodendrocytes were separated and removed from the culture because of their differential adhesive properties compared to RGCs, as they need suitable cell culture medium supplements and take relatively longer time to adhere (Houalla and Levine, 2003). Oligodendrocytes and oligodendrocyte precursor cells are the least adhesive cell population in the brain, and can therefore be easily removed during changing of the cell culture medium (Itoh, 2002). According to Houalla et al., trypsin (0.25%) is toxic to goldfish microglial cells during the tissue dissociation step (Houalla and Levine, 2003), which was an advantage to our RGC culture development. However, trypsin solely is not enough for separating microglia from RGCs since in the first two passages some microglia-like cells appear on top of the RGC cell layer. This encouraged us to subculture and passage using trypsin to remove the existing microglia in culture. In summary, our protocol requires (a) trypsinization for tissue dissociation and subculture, (b) a complete cell culture medium with 15% FBS, and (c) changing the cell culture medium within a week after isolation. We propose this technique yields a relatively pure primary RGC culture for future characterization and other functional studies.

The first suggestion that DA may regulate aromatase in the brain came from studies in quail. There are catecholaminergic inputs close to aromatase-positive neurons in the sexually dimorphic medial preoptic nucleus and bed nucleus striae terminalis (Balthazart et al., 2002)

but the mechanisms that are involved in this process remain unclear. Regardless, these pioneering studies indicated a relationship between DA receptors, aromatase and the control of sexual behaviour in male birds (Absil et al., 2001; Balthazart et al., 2000; Ubuka et al., 2014).

The current study differs significantly from the earlier research because of the focus on neuron-RGC interactions. There were no prior *in vitro* studies on fish RGCs to allow investigation of direct neurotransmitter regulation of this critical cell type. An important advance is therefore the development and validation of the first RGC culture system for a teleost model. Our approach is efficient with at least 95% of the cells expressing major radial glial markers *in vitro*. Markers for RGCs include GFAP, BLBP, vimentin, nestin, GLAST and S100β (Brunne et al., 2010; Diotel et al., 2010b; Forlano et al., 2005; Li et al., 2008a). There is no single marker that identifies all the RGCs in the teleost brain. Combinations of GFAP, BLBP and aromatase B are considered ideal (Diotel et al., 2010a; Tong et al., 2009; Verwer et al., 2007; Zupanc et al., 2012), and all were unequivocally present and colocalized in the cultured RGCs. The RGC cultures were also negative for Hu and zn-12, which are highly expressed in the nucleus and by the cell adhesion glycoproteins located on cell surface of mature neurons (Metcalfe et al., 1990), respectively. *In situ* hybridization, direct sequencing (Xing et al., 2014) and immunofluorescence were used to confirm the expression of *cyp19a1b* and aromatase B protein. The three independent techniques show that RGCs in culture are aromatase B-positive as they are *in vivo* (Forlano et al., 2001; Tong et al., 2009). Aromatase B is exclusively expressed by RGCs *in vivo* in fish (Forlano et al., 2001; Tong et al., 2009), and never in neurons as in mammals and birds (Azcoitia et al., 2011). Aromatase B is therefore a specific RGC protein with major roles in the control of neuroendocrine

function and neurogenesis in teleost brain (Pellegrini et al., 2007).

Previous to this research the only known neuroendocrine factor up-regulating aromatase B in the teleost brain was estradiol itself (Diotel et al., 2010a; Forlano and Bass, 2005; Menuet et al., 2005), presumably from either peripheral sources, or by local conversion of testosterone. Teleost *cyp19a1b* genes contain functional estrogen response elements (ERE) that explain these positive autoregulatory effects (Callard et al., 2001; Diotel et al., 2010a; Menuet et al., 2005). Immunocytochemistry, western blotting and direct sequencing all indicated the presence of D1R in goldfish RGCs (Fig. A3.3). The D1R belongs to the G protein-coupled receptor superfamily, and activates AC to promote cAMP accumulation (Kebabian and Calne, 1979). Previous studies identified the presence of a cAMP response element (CRE) located in the rat ovarian aromatase gene promoter (Hickey et al., 1990) and that aromatase gene transcription can be regulated by cAMP/CREB-dependent mechanisms (Richards, 1997; Wang et al., 2012). Teleosts possess independent gonadal and brain type aromatases, which arose from a presumptive ancient genome duplication event in this lineage (Chiang et al., 2001). There are CRE-like sites located in *cyp19a1a* and *cyp19a1b* promoters of zebrafish and other species (Callard et al., 2001; Tchoudakova et al., 2001; Tong and Chung, 2003), which indicate that fish aromatases may be regulated by cAMP/CREB. We report that the levels of cAMP and p-CREB can be rapidly increased by SKF 38393. Also, 8-Br-cAMP can stimulate *cyp19a1b* mRNA, and SKF 38393-stimulated *cyp19a1b* mRNA is inhibited by the PKA inhibitor H89. These results indicate that D1R activation via a cAMP/PKA/p-CREB pathway enhances *cyp19a1b* expression in RGCs.

The discovery that D1R activation stimulates aromatase B in RGCs is important for two main reasons: (A) it establishes that a catecholamine regulates a non-neuronal stem-like

progenitor cell that gives rise to both neurons and other glial cells (Bentivoglio and Mazzarello, 1999; Schmechel and Rakic, 1979; Zupanc and Clint, 2003; Zupanc et al., 2012), and (B) the data demonstrate that receptor activation regulates the estrogen synthesis enzyme aromatase B, which has many fundamental roles in brain differentiation, neural plasticity, neural regeneration, and neuroendocrine functions (Azcoitia et al., 2003; Garcia-Segura et al., 2003; Lephart, 1996; Ubuka et al., 2014). While it is well-known that estradiol stimulates neurogenesis in mammals (Garcia-Segura et al., 1999; Martinez-Cerdeno et al., 2006), emerging data in zebrafish indicate that estradiol inhibits neurogenesis (Diotel et al., 2013; Makantasi and Dermon, 2014). Moreover, chronic deprivation of estrogens by fadrozole inhibition of aromatase *in vivo* altered expression of numerous genes and pathways, include ependymins, synaptosomal-associated protein 25, neuropeptide Y and pituitary adenylyl cyclase-activating polypeptide, amongst others, implicated in the control of neuronal plasticity and neuroendocrine function in female goldfish brain (Zhang et al., 2009b). By increasing *cyp19a1b* mRNA, D1R activation maintains the non-neuronal characteristic of estrogen synthesis in RGCs, and in turn these estrogens may signal locally to modulate adult neurogenesis. Together with recent data indicating an important role for DA in homeostasis and regeneration in the salamander brain (Berg et al., 2011), the involvement of neurotransmitters in controlling RGC functions could be a plausible manner to link physiological variation or pathological loss of neuronal function to the need for repair of the adult CNS.

Chapter 4: Direct regulation of aromatase B expression by 17β-estradiol and dopamine in adult radial glial cells [4]

4.1 Abstract

Neuroestrogens, which are produced locally in the vertebrate brain, play many fundamental roles in neuroendocrine functions, reproductive functions, socio-sexual behaviours and neurogenesis. In fish brains, RGCs are neuronal progenitor cells that are abundant and are the exclusive site of aromatase B expression and neuroestrogen synthesis. Using a novel *in vitro* RGC culture preparation we studied the regulation of *cyp19a1b* expression by E2 and DA. We have established that activation of the D1R by SKF 38393 up-regulates *cyp19a1b* expression through the phosphorylation of CREB. This up-regulation can be enhanced by low dose of E2 (100 nM) through increasing the expression of D1R and the level of p-CREB protein. However, a high dose of E2 (1 μM) and D1R agonist together failed to up-regulate *cyp19a1b* expression, potentially due to attenuation of *esr2b* expression and p-CREB level up-regulation. Furthermore, we found the up-regulation of *cyp19a1b* expression by E2 and DA both requires the involvement of *esr1* and *esr2a*. The combined effect of E2 and DA agonist indicates that aromatase B in the adult teleost brain is under tight control by both neurotransmitters and steroids to precisely regulate neuroestrogen levels.

---

[4] *Partially based on Xing L., Esau C., and Trudeau VL. (2015). Direct regulation of aromatase B expression by 17β-estradiol and DA in adult radial glial cells. Submitted to Frontiers in Neuroscience. XL, designed the study, developed the methodology, conducted the majority of experiment and analysis and wrote the manuscript. EC, maintained cell culture and helped with qPCR analysis. TVL, helped with the design of the study and editing the article.*

4.2 Introduction

Brain aromatization plays numerous important roles including brain differentiation, neural plasticity, neural regeneration, neuroendocrine functions, reproductive functions and socio-sexual behaviours. It is possible that these processes are in part regulated by aromatization of androgen and thus local estrogen formation (Azcoitia et al., 2003; Garcia-Segura et al., 2003; Garcia-Segura et al., 1999; Lephart, 1996; Ubuka et al., 2014). However, while the essential functions of aromatase have been well studied, the regulation of aromatase in different regions of the brain is not well understood.

There are many response elements located at the promoter region of teleost *cyp19a1b* (Callard et al., 2001; Tchoudakova et al., 2001), including ERE and CRE. Through differential response element recruitment, *cyp19a1b* expression can be regulated differently, which suggests there should be multiple factors implicated in the regulation of *cyp19a1b* expression (Kato et al., 1997). It is well known that estrogens can up-regulate *cyp19a1b* expression in fish brain, which is mediated by ERs, some of which act as ligand-activated transcription factors (Belcher and Zsarnovszky, 2001). Upon binding to classical nuclear ERs, activated ER homo-dimerizes and binds to ERE at the promoter of *cyp19a1b*, and then mediates gene transcription (Marlatt et al., 2008; Strobl-Mazzulla et al., 2008). Due to duplication of the ERα gene, teleost have three ERs (*esr1*/ERα, *esr2a*/ERβ and *esr2b*/ERγ), all of which are expressed in the brain of fish with an distribution pattern similar to that of aromatase (Fergus and Bass, 2013; Forlano et al., 2005; Pellegrini et al., 2005; Strobl-Mazzulla et al., 2008). There is evidence showing that moderate up-regulation of *esr1* expression by estrogens precedes a dramatic up-regulation of aromatase by its own products (Bowman et al., 2002; Denslow et al., 2001; Marlatt et al., 2008; McEwen, 2002). The

possibility that *cyp19a1b* expression is up-regulated by estrogens is intriguing and suggests the presence of a positive feedback loop within the aromatase- and ER-positive cells, whereby estrogens enhance aromatase expression and therefore the subsequent products, estrogens.

In addition to estrogenic regulation of the *cyp19a1b* gene, our previous neuroanatomical and pharmacological studies in goldfish reveal that there is a close relationship between catecholaminergic neurons and aromatase B- and D1R-positive RGCs in goldfish forebrain. Activation of D1R but not D2R up-regulates *cyp19a1b* mRNA in cultured RGCs (Xing et al., 2015). The signaling pathway underlying activated D1R regulation of *cyp19a1b* involves cAMP, PKA and p-CREB. Whether this regulation involves nuclear ERs has yet to be determined. Since it is likely that both mechanisms are acting simultaneously to affect multifactorial control over neuroestrogen synthesis, and given the close association between RGCs and DA neurons we directly tested for interactive effects on RGCs *in vitro*.

We have shown that E2 and SKF 38393 alone significantly increased the expression of *cyp19a1b*. Moreover, the expression of *cyp19a1b* in RGCs may be synergistically up-regulated or antagonistically down-regulated, respectively, under low-dose or high-dose exposure to E2 and SKF 38393.

4.3 Materials and Methods

4.3.1 Experimental animals

All procedures used were approved by the University of Ottawa Protocol Review Committee and followed standard Canadian Council on Animal Care guidelines on the use of animals in research. Common adult female goldfish were maintained at 18 °C under a natural

simulated photoperiod and fed standard goldfish flakes. Sexually mature female goldfish (18-35 g) were anaesthetized in 0.05% MS222 for all handling and dissection procedures.

4.3.2 Cell culture

The hypothalamus and telencephalon were dissected from female goldfish and minced into small pieces. Goldfish RGCs were dissociated with trypsin (0.25%, Gibco) and cultured in Leibovitz's L-15 medium (Gibco) with 15% Fetal Bovine Serum (FBS, Gibco) and antibiotic-antimycotic solution. Cell culture medium was changed once a week after initial isolation. Goldfish RGCs were subcultured by trypsinization (0.125%) for 3 passages to obtain high purity (>95%) cultures and then used for experiments.

4.3.3 Drugs and exposures

Cells were exposed to E2 (Sigma-Aldrich) and selective SKF 38393 (Tocris) for 24 hr to study their effects on *cyp19a1b*, *esr1*, *esr2a*, *esr2b* and *drd1a* mRNA and p-CREB protein level. To investigate ERs involvement in *cyp19a1b* mRNA regulation by E2 and SKF 38393, cells were pre-exposed to ER antagonist MPP (Tocris) for 1 hr, and then exposed to E2 or SKF 38393 for 24 hr.

4.3.4 RNA extraction, quality control and cDNA synthesis

RNA was isolated using the RNeasy Micro kit (Qiagen) as described in the manufacturer's protocol. Upon purification, the concentration and quality of all samples were assessed using the NanoDrop ND-1000 spectrophotometer (Thermo Scientific) and the 2100 Bioanalyzer (Agilent). RNA integrity values of samples were above the recommended minimum value of 5 for quantitative real-time RT PCR applications and ranged from 8.5 to 9.8 (Fleige and Pfaffl, 2006). Total cDNA was prepared using Maxima First Strand cDNA

Synthesis Kit for RT-qPCR (Thermo Scientific). Each 20 µl reaction was diluted 10-fold in nuclease-free water and used as the template for qPCR assays.

4.3.5 Quantitative real-time RT-PCR

Quantitative real-time RT-PCR assays based on SYBR green detection were used to validate relative gene expression. Primers used in this study were designed using the Primer3 (http://primer3.sourceforge.net/) software and synthesized by Integrated DNA Technologies (Table 4.1). The Maxima SYBR green qPCR Master Mix (Thermo Scientific) and CFX96 Real-Time PCR Detection System (Bio-Rad) were used to amplify and detect the transcripts of interest. Data were analyzed using the CFX Manager™ Software package (Bio-Rad). The relative standard curve method was used to calculate relative mRNA abundance between samples, which were normalized by using NORMA-GENE algorithm (Heckmann et al., 2011) and then presented as means + SEM of fold change to control group (n = 4; assayed in duplicate).

Table 4.1. Primer sets used for qPCR and ddPCR.

Gene	**Primer Sequence (Forward)**	**Primer Sequence (Reverse)**	**Amplicon size**	**Accession No.**
β-actin	CTGGGATGATATGGAGAAGA	CCAGTAGTACGACCTGAAGC	215	AB039726
18s	AAACGGCTACCACATCCAAG	CACCAGATTTGCCCTCCA	165	AF047349
cyp19a1b	TGCTGACATAAGGGCAATGA	GGAAGTAAAATGGGTTGTGGA	153	AB009335
esr1	GCAGGAGGGTTTGATTCTGAGA	CCATAATGATAGCCGGACGCA	76	AY055725
esr2a	TGACTACATCTGCCCTGCCA	CCAACTTCGTAACATTTTCGGAGA	72	AF061269
esr2b	TGGTCCCTTTAAATTCAGCAATCT	GTGTTTCCCTGTAGGCCAGTG	95	AF177465
drd1a	CCCTTTGGTGCGTTTTGT	GAGCCTTGTGCCATTTGAG	210	L08602

4.3.6 Droplet digital PCR

The low expression of D1R (*drd1a*) in RGC cultures is not quantifiable using qPCR, so we used a more sensitive method to measure *drd1a* mRNA level. Droplet digital PCR (ddPCR) was performed using 40 ng of each cDNA sample and QX200™ ddPCR™ EvaGreen Supermix by employing QX200™ Droplet Digital™ PCR System (Bio-Rad). The ddPCR conditions were as follows: an initial denaturation for 5 m at 95 °C followed by 40 cycles of denaturation for 30 s at 95 °C and annealing and extension for 1 m at 56 °C, then signal stabilization for 5 m at 4 °C and 5 m at 90 °C. Template DNA was omitted from the ddPCR reaction as a no template control and the results of ddPCR were analyzed using the QuantaSoft Software (Bio-Rad). The absolute copy number of the targeted gene was divided by the average of the absolute copy number of two reference genes *β-actin* and *18s*, and presented as means + SEM of fold change to control group (n = 4; assayed in duplicate).

4.3.7 Western blot

Total protein extract from RGCs was denatured and separated by electrophoresis on a 10% SDS–polyacrylamide gel and transferred to a PVDF membrane as described previously (Zhao et al., 2006). Membranes were incubated with anti-Phospho-CREB (Ser133, Cell signaling technology, 9198S) antibodies overnight at 4 °C and then incubated with donkey anti-rabbit IgG antibody (GE Health Care, NA934VS). Blots were visualized using the Amersham ECL Prime Western Blotting Detection System (GE Health Care, RPN2232). Images were obtained using a ChemiDoc XRS+ system (Bio-Rad) and analyzed with image lab (Bio-Rad). Same blot incubated with anti-Phospho-CREB antibodies previously was stripped and re-probed with primary anti-actin (Cedarlane, CLT9001) antibodies overnight at

4 °C and then incubated with goat anti-mouse IgG-HRP (Santa Cruz, sc-2005), where actin served as an internal control.

4.3.8 Statistics

In all cases and before any analysis, normality and homogeneity of variances was verified using Shapiro-Wilk's and Levene's test, respectively. Comparison of two groups was performed using Student's t-test in IBM SPSS Statistics Version 22. Comparison of more than two groups was performed using one-way analysis of variance (ANOVA) followed by a Tukey post-hoc test or Dunnett's post-hoc test if the data did not pass homogeneity test in IBM SPSS Statistics Version 22. P-values less than or equal to 0.05 were considered statistically significant. Data were presented as mean + SEM.

4.4 Results

4.4.1 Regulation of *cyp19a1b* and ER expression by SKF 38393 and E2

Here, the qPCR data show that 10 μM SKF 38393 was able to increase *cyp19a1b,* but not *esr1, esr2a* and *esr2b* mRNA levels after 24 hr incubation (Fig. 4.1A). The 100 nM dose of E2 did not affect *cyp19a1b, esr1, esr2a* and *esr2b* mRNA levels after 24 hr incubation (Fig. 4.1B). However, when the concentration of E2 was increased to 1 μM, the expression of *cyp19a1b* and *esr2b* were increased dramatically 6.7-fold and 2.9-fold, respectively, but not *esr1* and *esr2a* (Fig. 4.1C). These data suggest that the up-regulation of *esr2b* may contribute to the stimulatory effect of E2 in *cyp19a1b* expression.

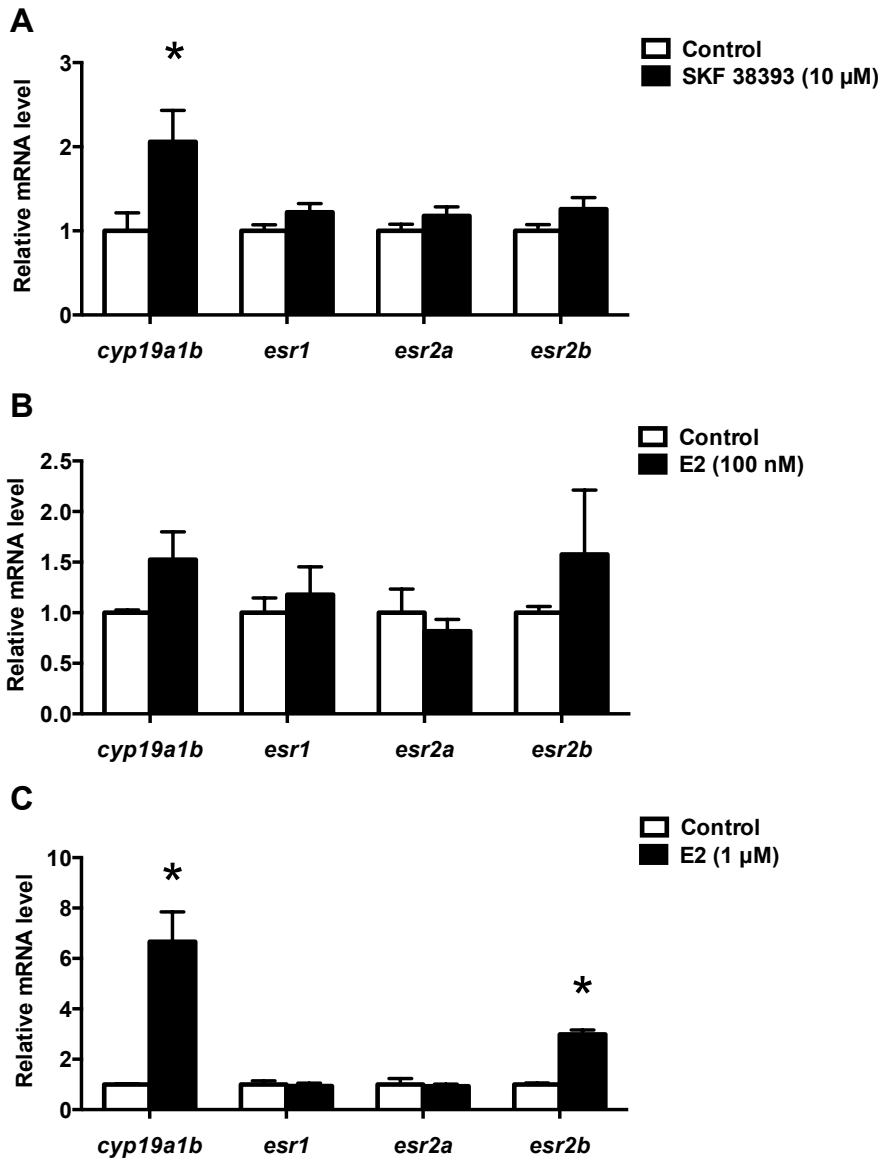

Figure 4.1. Quantitative real-time RT-PCR analysis showing variations in the relative amounts of the *cyp19a1b*, *esr1*, *esr2a* and *esr2b* mRNAs in primary RGCs culture exposed to 10 µM SKF 38393 (A), 100 nM E2 (B) and 1 µM E2 (C). Data were normalized and defined as fold change relative to control, and bars represent the mean + SEM. Treatment groups marked by asterisks have significantly different mRNA levels compared to control (P

< 0.05).

4.4.2 The involvement of ERs in *cyp19a1b* regulation by E2 and SKF 38393

When RGC cultures are exposed to SKF38393 and E2 for 24 hr there was no change in the expression of *esr1* and *esr2a*. This result led us to investigate the possible contribution of pre-existing ERs in RGCs to *cyp19a1b* up-regulation. The ERα and ERβ antagonist MPP was administered to RGC cultures 1 hr before SKF 38393 and E2. Data revealed that MPP alone decreases the expression of all three ERs by 29.9-57.6% (Fig. 4.2A), but has no effects in *cyp19a1b* expression (Fig. 4.2B, C). A two-way ANOVA was conducted that examined the effect of MPP and SKF 38393 as well as MPP and E2 on *cyp19a1b* expression. There was a statistically significant interaction between MPP and SKF 38393, and between MPP and E2. The stimulatory effect of SKF 38393 and E2 on *cyp19a1b* mRNA was completely blocked by MPP (Fig. 4.2B, C).

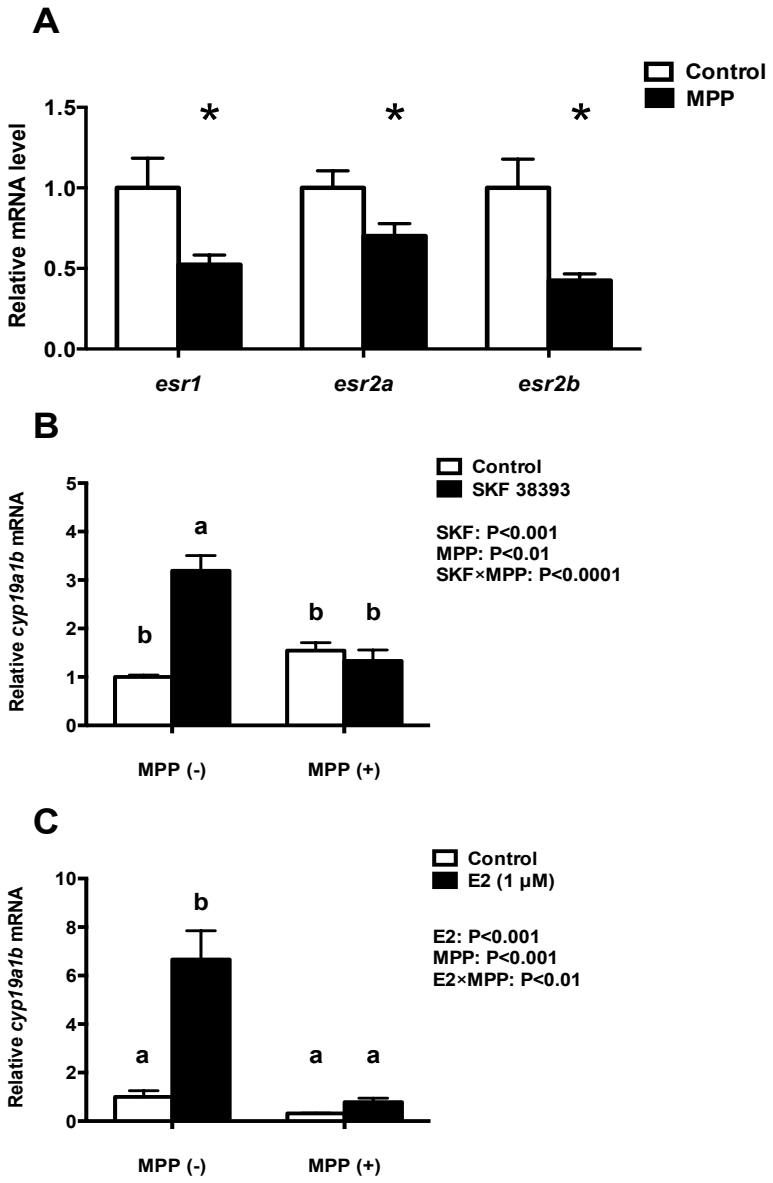

Figure 4.2. Quantitative real-time RT-PCR analysis showing variations in the relative amounts of the *cyp19a1b*, *esr1*, *esr2a* and *esr2b* mRNAs in primary RGCs cultures exposed to 100 nM MPP (A), 100 nM MPP and 10 μM SKF 38393 (B), 100 nM MPP and 1 μM E2 (C). Data were normalized and defined as fold change relative to control, and bars represent the mean + SEM. Treatment groups marked by asterisks or different letters have significantly

different mRNA levels compared to each other or to control ($P < 0.05$).

4.4.3 The combined effects of E2 and SKF 38393 on *cyp19a1b* regulation

Based on the previous dose-dependent studies, we examined the combined effects of two concentrations of SKF 38393 and E2. Our results indicate that there is either a synergistic or antagonistic effect in *cyp19a1b* regulation by E2 and SKF 38393, which is dependent on the concentration of E2. A two-way ANOVA was conducted that examined the effects of SKF 38393 and E2 on *cyp19a1b* expression. Both the low dose of E2 (100 nM) and the high dose of E2 (1 μM) increased *cyp19a1b* expression 1.5- and 6.7-fold, respectively, but there were no statistically significant interactions with SKF 38393 (1 μM) (Fig. 4.3A, B). When the dose of SKF 38393 was increased to 10 μM, statistically significant interactions between SKF 38393 and both low dose and high dose of E2 were evident. The two-way ANOVA indicated that both 10 μM SKF 38393 and 100 nM E2 increased *cyp19a1b* expression 2.8-fold and 1.5-fold, a result consistent with the earlier experiment shown in Fig. 4.1A and Fig. 4.1B, respectively. Post-hoc tests showed that the combination of the high dose of SKF 38393 and the low dose of E2 synergistically up-regulated *cyp19a1b* expression 8.0-fold (Fig. 4.3C). Contrasting this is the experiment where high doses of both SKF 38393 and E2 were used. Exposure of RGCs to 1 μM E2 alone increased *cyp19a1b* expression 6.7-fold, and the high dose of SKF 38393 inhibited this effect (Fig. 4.3D).

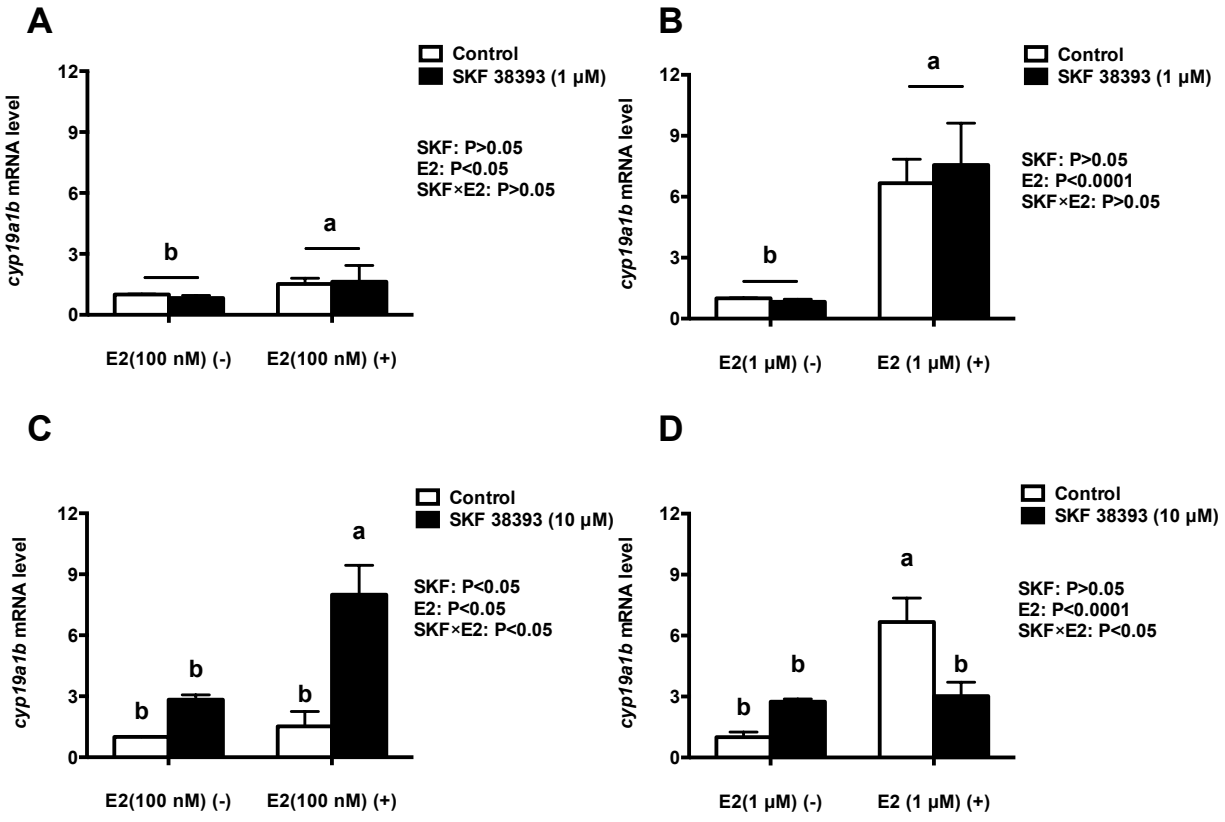

Figure 4.3. Quantitative real-time RT-PCR analysis showing variations in the relative amounts of the *cyp19a1b* mRNA in primary RGCs cultures exposed to 100 nM E2 and 1 μM SKF 38393 (A), 1 μM E2 and 1 μM SKF 38393 (B), 100 nM E2 and 10 μM SKF 38393 (C), 1 μM E2 and 10 μM SKF 38393 (D). Data were normalized and defined as fold change relative to control, and bars represent the mean + SEM. Treatment groups marked by different letters have significantly different mRNA levels ($P < 0.05$).

4.4.4 Synergistic effects of low levels of E2 on SKF 38393-induced *cyp19a1b* expression are associated with parallel increases in p-CREB

To further understand the underlying mechanisms underlying synergistic up-regulation of *cyp19a1b* by the low dose of E2 and the high dose of SKF 38393, we studied two components of the D1R/cAMP/PKA/p-CREB pathway, *drd1a* in mRNA level and p-CREB in protein level as well as the expression of *esr1*, *esr2a* and *esr2b*. A two-way ANOVA was conducted that examined the effect of SKF 38393 and E2 on *drd1a, esr1 esr2a* and *esr2b* mRNA levels and p-CREB protein level in cultured RGCs. There was a statistically significant interaction between SKF 38393 and E2 for *drd1a* mRNA level. Post-hoc tests showed that the combination of SKF 38393 and E2 up-regulated *drd1a* mRNA level (Fig. 4.4A), although increases were not very large, in the range of 1.7 fold. There was also a statistically significant interaction between SKF 38393 and E2 for p-CREB protein level (Fig. 4.4D). The SKF 38393 alone increased p-CREB 2.2-fold, and this was enhanced to 3.5-fold in the presence of E2, paralleling these results of *cyp19a1b* mRNA level (Fig. 4.3C). No effects on ER expression were observed for the E2 and SKF 38393 treatments (Fig. 4.5).

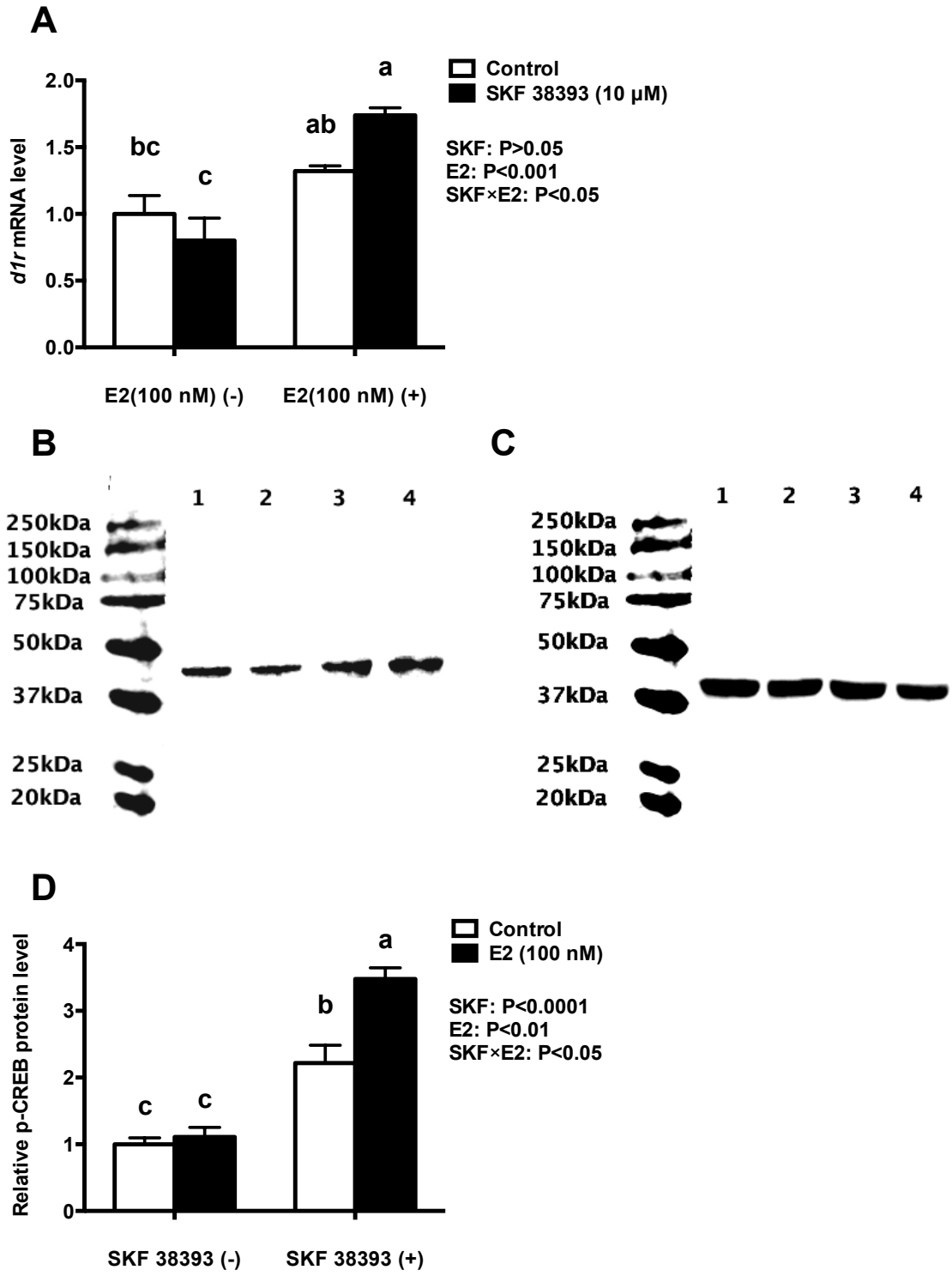
A
2.0
1.5
1.0
0.5
0.0
d1r mRNA level
bc
c
ab
a
Control
SKF 38393 (10 μM)
SKF: P>0.05
E2: P<0.001
SKF×E2: P<0.05
E2(100 nM) (-)
E2(100 nM) (+)
B
1
2
3
4
250kDa
150kDa
100kDa
75kDa
50kDa
37kDa
25kDa
20kDa
C
1
2
3
4
250kDa
150kDa
100kDa
75kDa
50kDa
37kDa
25kDa
20kDa
D
4
3
2
1
0
Relative p-CREB protein level
c
c
b
a
Control
E2 (100 nM)
SKF: P<0.0001
E2: P<0.01
SKF×E2: P<0.05
SKF 38393 (-)
SKF 38393 (+)

Figure 4.4. Synergistic up-regulation of D1R and p-CREB by E2 and SKF 38393. Droplet digital PCR analysis showing variations in the absolute amounts of the *drd1a* mRNA in primary RGCs culture exposed to 100 nM E2 and 10 μM SKF38393 (A). Western blot showing variations in the relative protein level of p-CREB in primary RGCs culture exposed to 100 nM E2 and 10 μM SKF 38393. Western blot image (B) showing the p-CREB immunoreactivity in control (lane 1), 100 nM E2 treated (lane 2), 10 μM SKF 38393 treated (lane3) and both 100 nM and 10 μM SKF 38393 treated (lane 4) groups, where actin served as internal control (C). The densitometric analysis of western blot is reported as an arbitrary value relative to the average of all bands on the same blot. Data were normalized and defined as fold change relative to control, and bars represent the mean + SEM (n = 4, D). Treatment groups marked by different letters have significantly different mRNA or protein levels ($P < 0.05$).

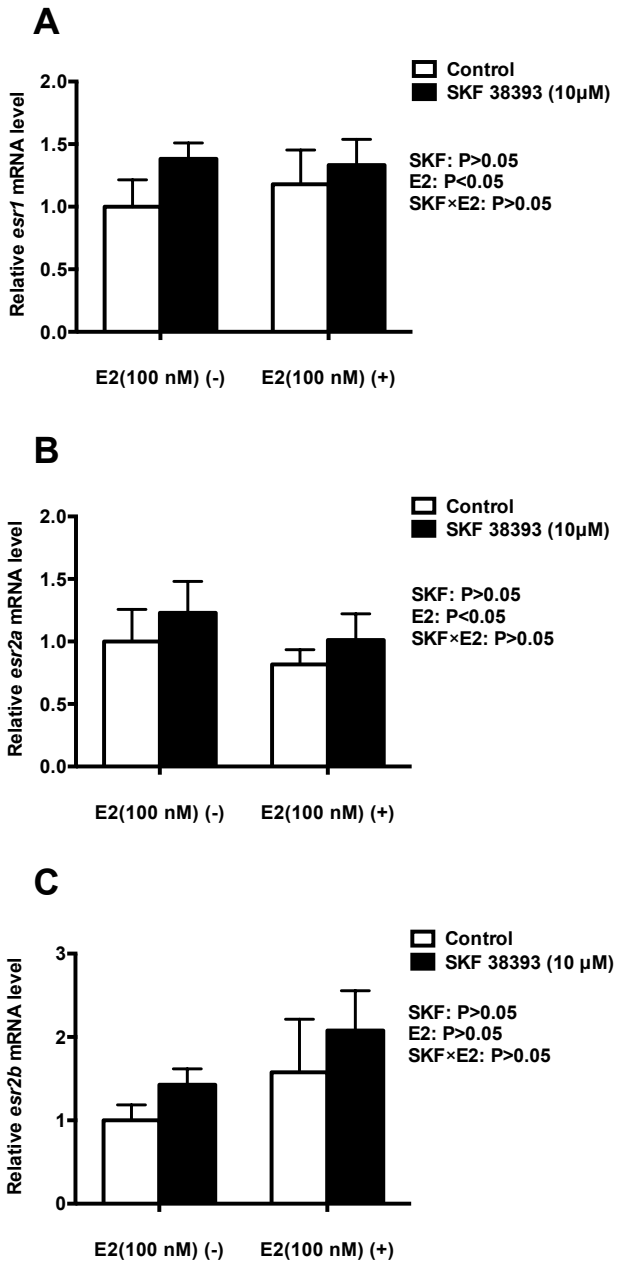

Figure 4.5. Quantitative real-time RT-PCR analysis showing variations in the relative amounts of the *esr1* (A), *esr2a* (B) and *esr2b* mRNA (C) in primary RGC cultures exposed to 100 nM E2 and 10 μM SKF 38393. Data were normalized and defined as fold change relative to control, and bars represent the mean + SEM.

4.4.5 Antagonistic effects of high levels of E2 on SKF 38393-induced *cyp19a1b* expression are associated with parallel decreases in p-CREB protein and *esr2b* mRNA

Further analysis was essential in understanding the potential mechanisms underlying antagonistic regulation of *cyp19a1b* expression by the combined high dose of E2 and high dose of SKF 38393. As with the previous experiment, a two-way ANOVA was conducted that examined the potential interactive effects of SKF 38393 and E2 on *drd1a, esr1 esr2a* and *esr2b* mRNA levels and p-CREB protein level. Exposure to 10 μM SKF 38393 and 1 μM E2 alone did not affect *drd1a* mRNA levels in cultured RGCs (Fig. 4.6A). In contrast, there was a statistically significant interaction between SKF 38393 and E2 on p-CREB protein and *esr2b* mRNA levels. Post-hoc tests showed that E2 inhibited the up-regulation of p-CREB protein induced by SKF 38393 (Fig. 4.6D) and that SKF 38393 inhibited the up-regulation of *esr2b* mRNA induced by E2 (Fig. 4.7C) in RGCs, both following a similar pattern to that of *cyp19a1b* expression (Fig. 4.3D).

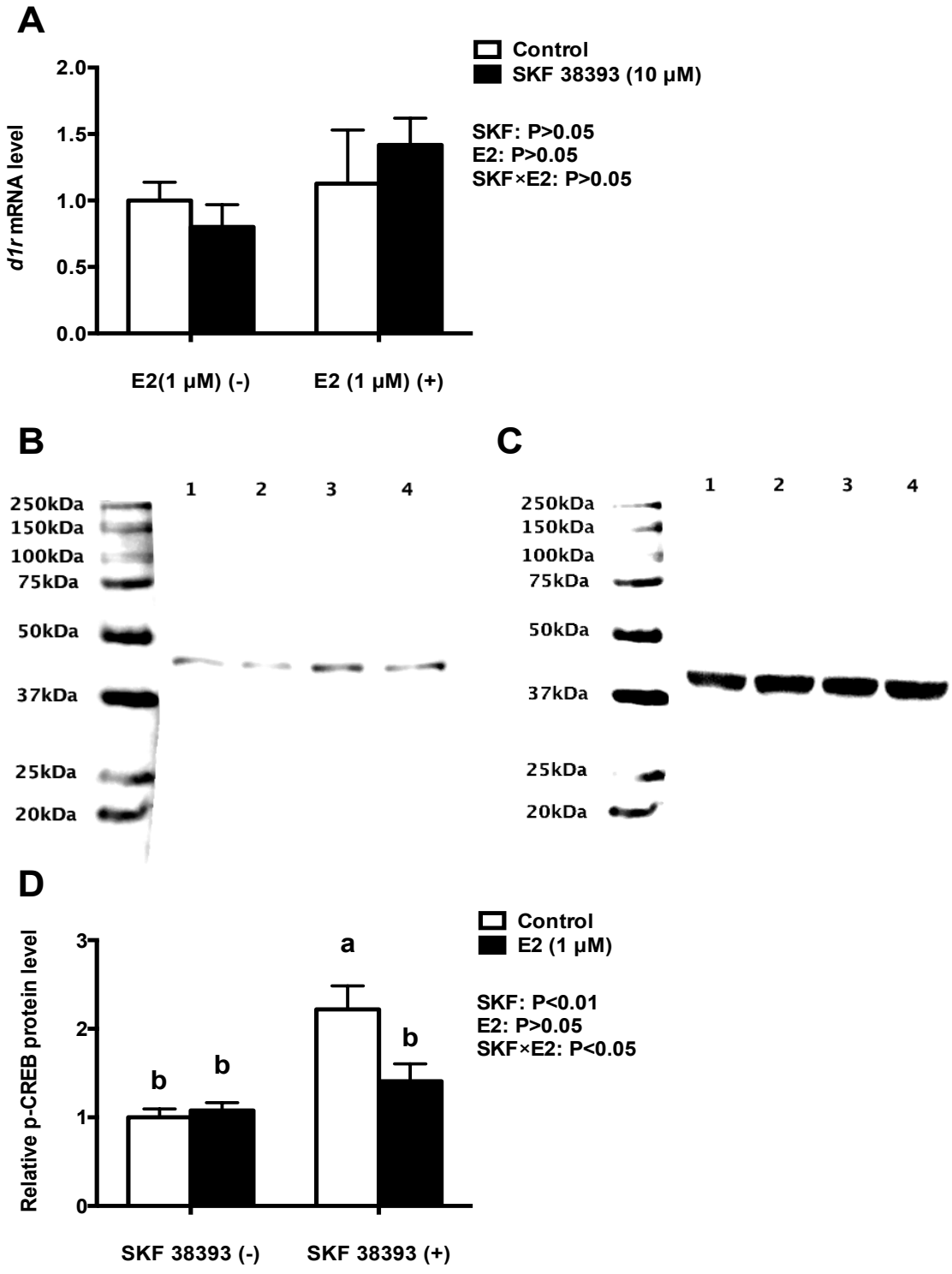
A
Control
SKF 38393 (10 μM)
SKF: P>0.05
E2: P>0.05
SKF×E2: P>0.05
d1r mRNA level
2.0
1.5
1.0
0.5
0.0
E2(1 μM) (-)
E2 (1 μM) (+)
B
1
2
3
4
250kDa
150kDa
100kDa
75kDa
50kDa
37kDa
25kDa
20kDa
C
1
2
3
4
250kDa
150kDa
100kDa
75kDa
50kDa
37kDa
25kDa
20kDa
D
Control
E2 (1 μM)
SKF: P<0.01
E2: P>0.05
SKF×E2: P<0.05
Relative p-CREB protein level
3
2
1
0
a
b
b
b
SKF 38393 (-)
SKF 38393 (+)

Figure 4.6. Antagonistic regulation of *drd1a* and p-CREB by E2 and SKF 38393. Droplet digital PCR analysis showing variations in the absolute amounts of the *drd1a* mRNA in primary RGCs culture exposed to 1 μM E2 and 10 μM SKF 38393 (A). Western blot image (B) showing the p-CREB immunoreactivity in control (lane 1), 1 μM E2 treated (lane 2), 10 μM SKF 38393 treated (lane3) and both 1 μM and 10 μM SKF 38393 treated (lane 4) groups, where actin served as internal control (C). The densitometric analysis of western blot is reported as an arbitrary value relative to the average of all bands on the same blot. Data were normalized and defined as fold change relative to control, and bars represent the mean + SEM (n = 4, C). Treatment groups marked by different letters have significantly different mRNA or protein levels ($P < 0.05$).

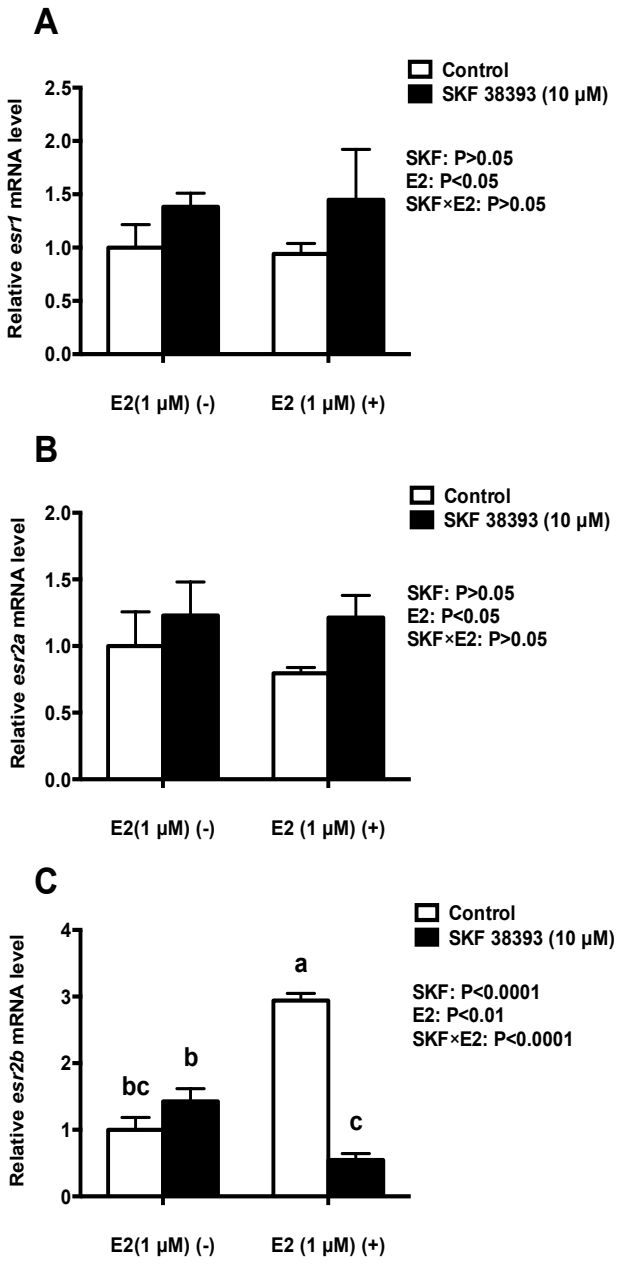

Figure 4.7. Quantitative real-time RT-PCR analysis showing variations in the relative amounts of the *esr1* (A), *esr2a* (B) and *esr2b* mRNA (C) in primary RGCs culture exposed to 1 μM E2 and 10 μM SKF 38393. Data were normalized and defined as fold change relative to control, and bars represent the mean + SEM. Treatment groups marked by different letters have significantly different mRNA levels ($P < 0.05$).

4.5 Discussion

The findings of this study indicate that *cyp19a1b* expression is up-regulated in goldfish RGC cultures in response to individual treatments with E2 or D1R agonist. However, co-exposure to these substances leads to either a further up-regulation or a down-regulation of *cyp19a1b* mRNA levels that are dependent on the concentration of E2. This is the first evidence for direct multifactorial control of aromatase in stem-like RGCs from the adult teleost brain. In mammals, aromatase is expressed in both neurons and glia (Tsuruo et al., 1995;Azcoitia et al., 2003). In contrast, RGCs are the exclusive cells to express aromatase in teleost brains (Forlano et al., 2001;Tong et al., 2009). This makes teleosts amenable models to delineate direct control of glial aromatase expression. Our data provides the foundation for further analysis of neurotransmitter and estrogenic regulation of RGCs, and contributes to our understanding of neuronal-glial interactions. This is important because estrogens in the CNS control fundamental processes such as sexual behavior and neurogenesis (Okada et al., 2008; Pellegrini et al., 2015; Ubuka et al., 2014).

The ability of E2 to regulate brain aromatase has been reported for a variety of species, including fish, birds and rats (Hutchison and Steimer, 1986; Pellegrini et al., 2005; Strobl-Mazzulla et al., 2008; Ubuka et al., 2014; Zhao et al., 2007). Here we confirm and extend these observations by showing a direct effect of E2 on isolated goldfish RGCs. It has been previously suggested that estrogenic regulation of brain aromatase may be controlled through a classical nuclear ER-dependent mechanism because aromatase and ERs are co-localized in CNS neurons in rodents and birds (Balthazart et al., 1991; Lassiter and Linney, 2007; Perlman and Arnold, 2003; Tsuruo et al., 1995; Zhao et al., 2007). Our pharmacological

experiments using goldfish RGCs in culture indicate the involvement of ERs since the up-regulation of *cyp19a1b* caused by exogenous E2 was completely blocked by the ER antagonist MPP, consistent with previous findings in zebrafish *in vivo* (Diotel et al., 2010a). Here, we report that E2 *in vitro* can increase *esr2b* mRNA only at a relatively high concentration. Contrary to *in vivo* reports in teleost, we did not find effects of exogenous E2 on *esr1* and *esr2a* expression in RGC cultures (Marlatt et al., 2008; Menuet et al., 2005). To further understand the involvement of ERs, we administrated MPP, an effective ERα/ERβ antagonist (Pinto et al., 2014). Exposure to MPP decreased the expression of all three nuclear ERs, suggesting that endogenous estrogens may be involved. Moreover, MPP blocked the stimulatory effect of added E2 on *cyp19a1b* expression. This finding indicates that the up-regulation of *cyp19a1b* mRNA by E2 is potentially due to the recruitment of the existing *esr1* and *esr2a* and/or increasing expression of *esr2b* to contribute to the positive feedback loop between aromatase, estrogens and ERs (Diotel et al., 2010a). Further studies on the involvement of *esr2b* are currently limited by the lack of a selective *esr2b* antagonist, although we do hypothesize that *esr2b* may be contributing to the up-regulation of *cyp19a1b* in RGCs, given the potency of *esr2b* to drive reporter gene expression for a consensus ERE construct (Menuet et al., 2002) or for the zebrafish *cyp19a1b* promoter construct in transfected cell assays (Menuet et al., 2002). It is unlikely that the G-protein coupled membrane estrogen receptor (GPER) is involved because we have been unable to identify GPER in RGCs using targeted PCR and RNA sequencing (data not shown).

We confirm here the results from our recent study (Xing et al., 2015) on the direct stimulatory effect of the p-CREB signaling pathway mediated by D1R activation to increase *cyp19a1b* expression in adult female goldfish RGCs. Similar to the observations of the

effects of E2, we believe that DA does not increase the expression of ERs but somehow activates or recruits the pre-existing ERs that contribute to the increase in *cyp19a1b* expression. This is shown by the results from the experiment where pre-treatment with MPP completely blocks SKF 38393-stimulated *cyp19a1b* expression. Moreover, exposure to E2 had no effect on *esr1 and esr2a,* and at a high dose sometimes increased *esr2b*, so at least new receptor resulting from translation of new mRNA appears unlikely under the conditions of our *in vitro* experiments.

While it is clear from our data that treatments with E2 or SKF 38393 alone can increase *cyp19a1b* expression, this is unlikely to represent situations *in vivo* where RGCs would be responding to neurotransmitters and endogenous estrogens simultaneously. Therefore, we treated RGCs with combinations of low and high doses of SKF 38393 and E2. It is evident that the RGC *cyp19a1b* response to D1R activation is dependent on the level of E2. The maximal response in *cyp19a1b* expression (i.e., 8.0-fold) was obtained from RGCs exposed to the lower E2 level of 100 nM plus the dose of 10 μM SKF 38393, which we showed previously to be the highest effective dose in the culture system (Xing et al., 2015). These experiments revealed a synergistic interaction between E2 and SKF 38393 that was supported statistically. Additionally, the levels of cellular p-CREB most closely followed the pattern of *cyp19a1b* expression, however, a more complex effect on D1R and ER expression was evident. The low level E2 treatment appears to amplify signaling via D1R/cAMP/PKA/p-CREB. Our absolute quantification of *drd1a* mRNA abundance showed that the low dose of E2 increased *drd1a* expression, especially in the presence of the SKF 38393. With the increased expression level of D1R, we hypothesized the activity of downstream signal transduction will be higher than control level. Our data showed that the

protein level of p-CREB also increased upon exposure to E2 and SKF 38393, similar to the *drd1a* expression regulatory pattern. While it is known that nuclear ERs bind to ERE at specific gene-regulatory regions thereby enhancing gene transcriptional activity, our findings do not support involvement of the up-regulation of ERs in the synergistic up-regulation of *cyp19a1b* by E2 and SKF 38393 since no increase in expression was observed for any of the three ERs.

While we do not have an estimate of the intracellular or extracellular levels of estrogens at or near regions of high RGC density in the brain, we consider the high 1 μM dose of E2 to be supraphysiological and the low 100 nM dose to be physiological relative to circulating E2 according to previous *in vivo* responses to exogenous estrogens in goldfish (Kobayashi et al., 1988; Martyniuk et al., 2006). Nevertheless, we originally hypothesized that the higher combined doses of E2 and SKF 38393 would cause up-regulation of *cyp19a1b* expression. Exposure of RGCs to a high dose of 1 μM E2 alone up-regulated *cyp19a1b* expression to a high level (6.7-fold). In this case, co-treatment with 10 μM SKF 38393 significantly reduced the high *cyp19a1b* expression induced by 1 μM E2. This was also evident at the level of intracellular signaling because p-CREB protein levels were also reduced by the co-treatment of high doses of E2 and SKF 38393. Moreover, 10 μM SKF 38393 reduced the increase in *esr2b* expression caused by the high dose of 1 μM E2.

In summary, we have described an example of complex control of aromatase B expression in adult teleost RGCs. Anatomical and physiological data (Xing et al., 2015) indicate a close relationship between catecholaminergic cell bodies and fibres and D1R-expressing RGCs in female goldfish brain. Pharmacological activation of D1R up-regulates *cyp19a1b* expression in RGCs, which ultimately would increase estrogen synthesis. It has

been previously shown and confirmed here that teleost RGCs respond positively to E2. We extend these observations to demonstrate a potentiating or synergistic interaction between dopaminergic and estrogenic stimulation of *cyp19a1b* expression. On the other hand, it appears that overstimulation of RGCs with the combined high doses of both E2 and SKF 38393 may limit *cyp19a1b* expression, and thus reduce estrogen synthesis in a manner similar to classical negative feedback control. In the teleost brain, the two main roles of estrogens that have been documented thus far are regulation of neuroendocrine-related genes (Martyniuk et al., 2006) and the inhibition of neurogenesis (Zhang et al., 2009a). For example, fadrozole inhibition of aromatase *in vivo* to lower estrogen levels altered expression of numerous genes implicated in the control of neuronal plasticity and neuroendocrine function in female goldfish brain (Zhang et al., 2009a). Interactive regulation of aromatase B by DA and estrogens therefore, would finely regulate local estrogen levels that in turn could regulate adjacent RGCs that express nuclear ERs, or neurons in the vicinity that express these receptors or GPER. Given the array of neurotransmitter and neuropeptide-expressing neurons and fibres in the neurogenic regions where *cyp19a1b* expressing RGCs are found, it is likely that many other neurohormones regulate the steroidogenic function of this critical cell.

Chapter 5: Proteomic profiling reveals dopaminergic regulation of progenitor cell functions of goldfish radial glial cells *in vitro* [5]

5.1 Abstract

Radial glial cells are stem-like cells found in the developing and adult central nervous system. They function as both a scaffold to guide neuron migration and as progenitor cells that support neurogenesis. Our previous study revealed a close anatomical relationship between DA neurons and RGCs in the telencephalon of female goldfish. In this study, label-free proteomics was used to identify the proteins in a primary RGC culture and to determine the proteome response to the selective SKF 38393 (10 μM), in order to better understand dopaminergic regulation of RGCs. A total of 689 unique proteins were identified in the RGCs and these were classified into biological and pathological pathways. Proteins such as nucleolin (6.9-fold) and ependymin-related protein 1 (4.9-fold) were increased in abundance while proteins triosephosphate isomerase (10-fold) and phosphoglycerate dehydrogenase (5-fold) were decreased in abundance. Pathway analysis revealed that proteins that consistently changed in abundance across biological replicates were related to small molecules such as ATP, lipids and steroids, hormones, glucose, cyclic AMP and Ca^{2+}. Sub-network enrichment analysis suggested that ERα signaling, among other transcription factors, is regulated by D1 receptor activation. This suggests that these signaling pathways are correlated to dopaminergic regulation of RGC functions. Most proteins down-regulated by SKF 38393

---

[5] *Xing L., Martyniuk, CJ., Esau C, Da Fonte DF., Trudeau VL. Proteomic profiling reveals dopaminergic regulation of progenitor cell functions of goldfish radial glial cells in vitro. Submitted to Journal of Proteomics. XL, designed the study, developed the methodology, conducted the majority of experiment and analysis and wrote the manuscript. MCJ, helped with bioinformatics analysis and article editing. EC, DFDF, maintained cell culture and helped with qPCR analysis. TVL, helped with the design of the study and editing the article.*

were involved in cell cycle/proliferation, growth, death, and survival, which suggests that DA inhibits the progenitor-related processes of RGCs. Examples of differently expressed proteins including triosephosphate isomerase, nucleolin, phosphoglycerate dehydrogenase and capping protein (actin filament) muscle Z-line beta were validated by qPCR and western blot, which were consistent with MS/MS data in the direction of change. This is the first study to characterize the RGC proteome on a large scale in a vertebrate species. These data provide novel insight into glial protein networks that are associated with neuroendocrine function and neurogenesis in the teleost brain.

5.2 Introduction

Radial glial cells are stem-like non-neuronal cells that are widely distributed in the developing CNS and have a unique bipolar morphological form (Schmechel and Rakic, 1979). At early stages of CNS development, RGCs are among the first specialized cells derived from primitive neuroepithelial cells at the cellular level, coincident with the appearance of early neurons (Hartfuss et al., 2001). With an ovoid cell body located close to the ventricular surface, RGCs extend an elongated radial process that terminates by conical endfoot at the walls of blood vessels or at the opposing pial surface (Barry et al., 2014). The most well characterized role for RGCs is that they serve as a scaffold for newborn neurons, enabling the cells to migrate to their final destination during embryonic brain development (Rakic, 1971a; Rakic, 1971b; Rakic, 1972). In mammals, most RGCs are transient and transform into fibrous or protoplasmic astrocytes at the end of neuron migration during the completion of cortical development (Levitt and Rakic, 1980; Schmechel and Rakic, 1979). However, there are exceptions, and not all RGCs undergo this transformation, but rather

move to other destinations in the CNS where they reside until adulthood (Schnitzer et al., 1981). Continuous neuronal generation in the adult brain has been reported in a variety of vertebrates, including human, although the extent and degree of neuronal generation varies greatly (Alvarez-Buylla et al., 2002; Zupanc, 2001). Among the vertebrates studied to date, the highest regenerative capacity of the CNS is observed in teleosts and amphibians, while the lowest frequency of regeneration is reported to be in mammals (Zupanc, 2008). Modern cell fate determination and lineage tracing have revealed that radial glia are also multifunctional neural stem cells in two discrete regions of adult mammalian brain; the subventricular zone and hippocampal dentate gyrus (Bonfanti and Peretto, 2007; Doetsch, 2003; Malatesta et al., 2003; Namba et al., 2005). Isolated RGCs from rats have been shown to generate neurons *in vitro* (Malatesta et al., 2000). This raises the possibility of RGCs contributing to adult neurogenesis and brain repair. Following this pivotal study, additional studies have demonstrated that the high capacity of regeneration of the teleost brain is attributed to the stem-like progenitor characteristic of RGCs (Lindsey et al., 2014; Strobl-Mazzulla et al., 2010; Zupanc and Clint, 2003). As the most abundant progenitor cell type in the teleost CNS, RGCs are in close anatomical contact with a variety of neurons including those synthesizing 5-HT (Pérez et al., 2013) and DA (Xing et al., 2015). Since the dynamics of cell proliferation and cell death are critical for normal brain function and maintaining physiological systems, it is essential to fully characterize these progenitor cells, as well as their regulators.

Recent investigations have determined that the neurotransmitter DA is capable of inhibiting the proliferation of progenitor cells in the salamander midbrain (Berg et al., 2011). Our previous work in goldfish has demonstrated that DA regulates aromatase B expression in

RGCs, the enzyme that converts androgens into estrogens. Thus, DA may regulate both neuroendocrine as well as progenitor functions of RGCs, as aromatase B expression is lost when RGCs differentiate into neurons. These findings expanded the roles of DA beyond its involvement in emotion and motivation, sensory-motor control, feeding and reproduction (Bjorklund and Dunnett, 2007). Data show that fish RGCs express D1R and can receive signals released from DA neurons, suggesting that RGCs are responsive to a DA regulatory system (Xing et al., 2015). Upon DA binding, D1R mediates the effects of DA and dopaminergic compounds via a variety of signaling transduction mechanisms that intersect to regulate cellular function (Cadet et al., 2010; Yamamoto et al., 2013b).

Despite the knowledge that there are multiple roles of RGCs, there is limited information about the RGC proteome, which can provide valuable insight into other capabilities and regulatory pathways. This knowledge has been limited due to a lack of pure isolated RGCs. To better understand the complex intracellular signaling in RGCs under normal conditions, and how these cells respond to DA, it is necessary to first describe the range and functionality of proteins expressed by RGCs. Our group has previously developed a method of isolating and culturing RGCs from goldfish forebrain for *in vitro* studies on RGC function and regulation. The objectives of this study were to (1) characterize the goldfish RGC proteome *in vitro*, (2) characterize the RGC proteomic response to the specific SKF 38393, (3) and identify RGC gene regulatory networks associated with DA stimulation to better understand neuroendocrine regulation and neurogenesis.

5.3 Materials and Methods

5.3.1 Experimental animals

All procedures used were approved by the University of Ottawa Protocol Review Committee and followed standard Canadian Council on Animal Care guidelines on the use of animals in research. Common adult female goldfish were maintained at 18 °C under a natural simulated photoperiod and fed standard goldfish flakes. Sexually mature female goldfish (18-35 g) were anaesthetized in 0.05% MS222 for all handling and dissection procedures.

5.3.2 Cell culture

The hypothalamus and telencephalon were dissected from female goldfish and minced into small pieces. Goldfish RGCs were dissociated with trypsin (0.25%, Gibco) and cultured in Leibovitz's L-15 medium (Gibco) with 15% FBS (Gibco) and antibiotic-antimycotic solution. Cell culture medium was changed once a week after initial isolation. Goldfish RGCs were subcultured by trypsinization (0.125%) for three passages to obtain high purity (>95%) cultures and then used for experiments.

5.3.3 Protein extraction, digestion, and LC-MS/MS

Cells were exposed to 10 μM SKF 38393, a D1R agonist (Tocris), for 24 hr as described previously (Xing et al., 2015). Proteins were extracted in 25 mM ammonium bicarbonate, pH 8.0 with Amicon Ultra-0.5 ml Centrifugal filter (EMD Millipore Inc., Billerica, MA, USA) and were quantified using EZQ® Protein Quantitation Kit (Invitrogen) with the SoftMax Pro Software v5.3 (Molecular Devices) as previously described (Koh et al., 2012). For each sample, a total of 16 μg of protein were reduced with 40 mM DTT, alkylated with 100 mM of iodoacetamide, and trypsin-digested overnight at 37 °C. Tryptic digested peptides were desalted with C18-solid phase extraction. A hybrid quadrupole Orbitrap (Q Exactive plus) Mass Spectrometer (MS) system (Thermo Fisher Scientific) was used with high-energy

collision dissociation (HCD) in each MS and MS/MS cycle. The MS system was interfaced with an automated Easy-nLC 1000 system (Thermo Fisher Scientific). Two micrograms of each sample was loaded with 50 fmol of peptides retention time calculation mixture (PRTC; Pierce, Thermo Fisher Scientific) as an internal standard (spike) and separation was carried out using an Acclaim Pepmap 100 pre-column (20 mm × 75 μm; 3 μm-C18) and a PepMap RSLC analytical column (500 mm × 75 μm; 2 μm-C18) at a flow rate at 300 nl/min over a linear gradient from the solvent A (0.1% formic acid (v/v)) to 25% solvent B (0.1% formic acid and 99.9% acetonitrile) for 150 min. This was followed by a gradient with 100% solvent B for an additional 32 min.

5.3.4 Database searching

The raw MS/MS data files were processed by a thorough database search considering biological modification and amino acid substitution against the National Centre for Biotechnology Information (NCBI) Teleostei database (downloaded on Mar. 25. 2015; 729,330 entries) using Scaffod Q+S (Proteome Software Inc.) and MASCOT 2.4 (Matrix Science Inc.) with the following parameters: peptide tolerance at 10 ppm, tandem MS tolerance at ± 0.01 Da, peptide charge of 2^+ or 3^+, trypsin as the enzyme, Carbamidomethyl at cysteine as fixed modifications, and oxidation at methionine and phosphorylation at serine, threonine, and tyrosine, as variable modifications.

5.3.5 Protein identification and classification

Scaffold (version Scaffold_4.4.3, Proteome Software Inc.) was used to validate MS/MS based peptide and protein identifications. Peptide identifications were accepted if they could be established at greater than 80% probability by the Peptide Prophet algorithm (Keller et al.,

2002) with Scaffold delta-mass correction. Protein identifications were accepted if they could be established at greater than 95% probability and contained at least 1 identified peptide. Proteins identified in less than four out of six biological replicates were removed from spectral counting data. The Protein Prophet algorithm (Nesvizhskii et al., 2003) assigned protein probabilities. Proteins that contained similar peptides and could not be differentiated based on MS/MS analysis alone were grouped to satisfy the principles of parsimony. After protein identification, protein annotation through evolutionary relationship (PANTHER) was used to classify all proteins detected in RGC cultures with gene ontology (GO) terms (Mi et al., 2013). The GO categories for biological processes, molecular functions or cellular components were individually sorted to determine the most abundant GO categories in RGC cultures.

5.3.6 Quantification and pathway analysis of proteins altered by SKF 38393

For quantification, protein identifications were accepted if they could be established at greater than 95% probability and contained at least 2 identified peptide. To be identified as differentially expressed, a protein had to be quantified with at least two unique spectra in at least four of six biological replicates. Both average total ion current (Average TIC) and normalized spectral abundance factor (NSAF) were used to normalize data and quantify protein abundance. Two normalization approaches were used to increase confidence in protein quantitation and proteins most likely regulated by SKF 38393 were reasoned to be those ones that were different than controls using both Average TIC and NSAF normalization. A student's t-test ($\alpha = 0.05$) was used to determine whether the abundance of proteins differed between groups. An additional strict selection criterion was also employed. Fold change range of >1.3 or <0.7 was used as the cut-off for differentially expressed

proteins.

Differentially expressed proteins were used to construct a protein network to better understand how proteins related to one another and to small molecules. Pathway Studio 9.0 (Ariadne) was used for pathway analysis. Protein networks based upon expression, binding, and regulatory interactions were constructed using direct connections with one neighbour. Functional class, small molecules, and cell processes were also mapped onto the pathway. In order to simplify pathways, only those interactions with the highest scores (most well supported by literature) are shown (>3000 connectivity; local connectivity >5). This is considered to be a strongly supported protein network based upon the literature of known interaction between proteins and molecules. However, it is important to note that the pathways are built with additional information that is not shown in the figures (i.e., those connections with <3000 connectivity).

5.3.7 Sub-network enrichment analysis

Sub-network enrichment analysis (SNEA) for expression targets, binding partners and proteins/chemicals regulating cell processes was performed to determine if there were common protein targets affected after SKF 38393 treatment. Unique proteins significantly regulated by SKF 38393, based on the Average TIC method, were considered for analysis. SNEA creates a central ″seed″ from all relevant entities in the database in order to find common effectors. The enrichment p-value for gene seeds was set at $p < 0.05$ and the criteria of greater than 5 members per group were required for inclusion as a significantly regulated gene network (Martyniuk et al., 2012).

5.3.8 Western blot

The protein level of triosephosphate isomerase (TPI) was measured by western blot to validate the differentially expressed proteins identified by MS. Total protein extract from RGCs was denatured and separated by electrophoresis on a 10% SDS–polyacrylamide gel and transferred to a PVDF membrane as described previously (Zhao et al., 2006). Membranes were incubated with primary anti-TPI (Abcam, ab96696) and anti-actin (Cedarlane, CLT9001) antibodies overnight at 4 °C and then incubated with donkey anti-rabbit IgG antibody (GE Health Care, NA934VS). Blots were visualized using the Amersham ECL Prime Western Blotting Detection System (GE Health Care, RPN2232). Images were obtained using a ChemiDoc XRS+ system (Bio-Rad) and analyzed with image lab (Bio-Rad). Same blot incubated with anti-Phospho-CREB antibodies previously was stripped and re-probed with primary anti-actin (Cedarlane, CLT9001) antibodies overnight at 4 °C and then incubated with goat anti-mouse IgG-HRP (Santa Cruz, sc-2005), where actin served as an internal control. Images were obtained using a ChemiDoc XRS+ system (BIO-RAD) and analyzed with image lab (BIO-RAD, n = 6).

5.3.9 Quantitative real-time RT-PCR

Quantitative real-time RT-PCR was also employed to validate the differentially expressed proteins and study gene-protein relationships. Relative transcript levels of *tpi1b, capzb, nuc, phdgh* and *fam1141a* were measured by qPCR assays based on SYBR green detection. Primers used in this study were designed using Primer3 (Untergasser et al., 2012) and synthesized by Integrated DNA Technologies (Table 5.1). The Maxima SYBR green qPCR Master Mix (Thermo Scientific) and CFX96 Real-Time PCR Detection System (Bio-

Rad) were used to measure the transcripts of interest. Data were analyzed using the CFX Manager™ Software package (Bio-Rad). The relative standard curve method was used to calculate relative mRNA abundance between samples, which were normalized using NORMA-GENE algorithm (Heckmann et al., 2011). Data are presented as mean + SEM of fold change relative to the control group (n = 4; assayed in duplicate).

Table 5.1. Primer sets used for quantitative real-time RT–PCR.

Gene	Primer Sequence (Forward)	Primer Sequence (Reverse)
tpi	TGAACGGCGACAAAAAGAG	CGTAGTCGAGGTAGATGGATGG
capzb	TGCCGTCTGTCTGTCTGTCT	CGTAGCCTTTTCTCCTTTTTCC
ncl	ACATCCTCCTCTTGCGGT	CGCCCTTCTGACTCTTTTCTC
phgdh	TCACAGTCCACACTCCTCTC	GTTCACCACCTTCACACCCT
fam114a1	GCTGCTGTTGCCTGTTCTT	TCTGTGGATGCTGCTTCTGG

5.3.10 Statistics

In all cases and before any analysis, normality was verified using Shapiro-Wilk's test. Comparison of two groups was performed using Student's t-test in IBM SPSS Statistics Version 22. P-values less than or equal to 0.05 were considered statistically significant. Data were presented as mean + SEM.

5.4 Results

5.4.1 Profiling proteins in primary RGC cultures

There were 689 unique proteins identified using one unique peptide criteria in primary RGC cultures (Protein Prophet FDR = 0.5%, Spectra Prophet FDR = 1.12%). There was a broad range in the biological functions represented by these proteins and the number of unique biological processes represented was 1130. The biological processes were most represented by the identified proteins included cellular process, cellular component organization or biogenesis, developmental process, biological regulation and localization (Fig. 5.1A). The figure represents the most abundant GO terms categories (biological processes) represented by the RGC proteins. There was also a wide range in the molecular functions with 724 unique molecular functions being identified. The number of unique cellular components represented by RGC proteins was 430. Proteins that were detected are localized to organelles, macromolecular complex and membranes (Fig. 5.1B). Molecular functions most represented by proteins detected in RGCs included binding, catalytic activity, structural molecule activity, enzyme regulator activity, nucleic acid binding transcription factor activity, transporter activity and receptor activity (Fig. 5.1C). Most proteins represent those classified as nuclei binding proteins, skeletal proteins, and enzyme modulator proteins (Fig. 5.1D). The number of proteins representing unique protein classes was 692, and within these classes, there were 356 unique pathways identified. While numerous pathways were represented by identified proteins, those most represented in the analysis included the integrin signaling pathway, cytoskeletal regulation by Rho GTPase, inflammation mediated by chemokine and cytokine signaling pathway, Parkinson disease, glycolysis, nicotinic acetylcholine receptor signaling pathway, gonadotropin releasing hormone receptor pathway and DA receptor mediated signaling pathway (Fig. 5.1E).

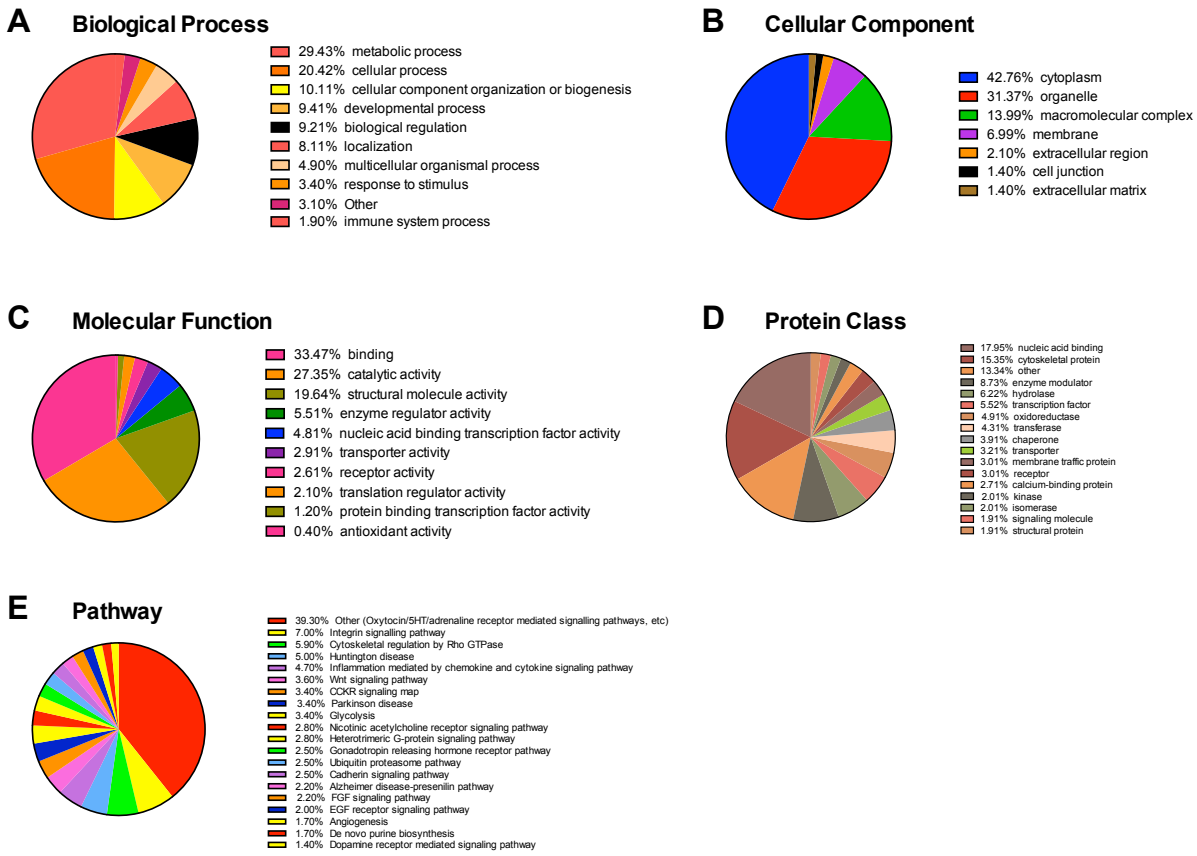

Figure 5.1. Proteins were classified according to (A) biological process, (B) cellular component, (C) molecular function, (D) protein class and (E) pathway. Protein ontology terms shown in the graph are the top categories (by percent) that are represented by proteins identified in primary RGC culture.

5.4.2 Proteins affected by SKF 38393 in primary RGC culture

The number of proteins identified using the two unique peptides criteria was 365 (Protein FDR = 0.2%, Spectra FDR = 1.1%). There were 62 proteins significantly regulated by SKF 38393 in primary RGC culture using Average TIC (Fig. 5.2), 45 proteins that were decreased and 17 proteins that were increased in relative abundance compared to the control group. There were 61 proteins significantly regulated by SKF 38393 in primary RGC culture using NSAF, 39 proteins that were decreased and 22 proteins that were increased in relative abundance compared to the control group (Table A3.1). Proteins that are most likely regulated by SKF 38393 were reasoned to be those that were significantly different than controls by using both Average TIC and NSAF quantitative methods ($P < 0.05$). Using this selection criterion, 22 proteins were affected by SKF 38393 (Table 5.2).

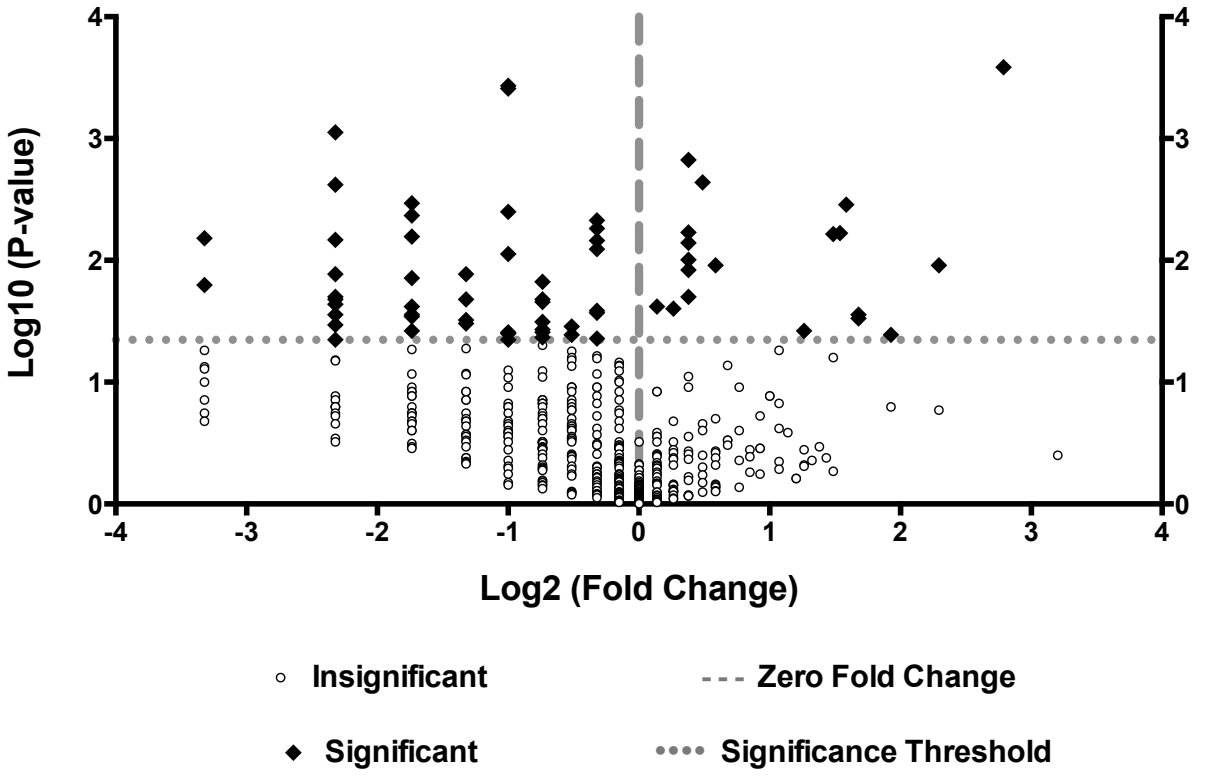

Figure 5.2. Volcano plot of proteins following treatment with SKF 38393.

Table 5.2. Proteins quantified with unique peptides that showed significant changes in abundance between control and SKF 38393-treated RGCs. These proteins were significant using both normalization methods ($P < 0.05$).

Protein ID	Accession	Average TIC		NSAF	
		P-Value	Fold change	P-Value	Fold change
60 kDa heat shock protein, mitochondrial	gil315585122	0.00089	0.2	0.00057	0.2
78 kDa glucose-regulated protein	gil410903448	0.0034	0.3	0.031	0.3
ADP-ribosylation factor GTPase-activating protein 2	gil528508501	0.021	0.6	0.0088	0.7
annexin A2-like	gil410908016	0.015	0.6	0.044	0.7
capping protein (actin filament) muscle Z-line beta	gil197631853	0.021	0.2	0.02	0.1
cellular retinoic acid-binding protein 2b	gil145337928	0.0059	1.3	0.013	1.7
collagen, type I, alpha 3	gil208609649	0.00039	0.5	0.02	0.2
collagen, type I, alpha 1	gil208609645	0.041	0.7	0.0053	0.4
drebrin	gil528514290	0.0061	2.8	0.021	3.1
endophilin-a2	gil551488208	0.011	0.0	0.014	0.0
endophilin-b1	gil308321574	0.013	0.2	0.024	0.2
ependymin related protein 1	gil49902917	0.011	4.9	0.012	4.8
nervous system overexpressed protein 20	gil141795527	0.034	0.2	0.045	0.2
microtubule-associated protein RP/EB family member 1	gil225707292	0.012	0.0	0.02	0.0
mitochondrial serine hydroxymethyltransferase	gil144954334	0.024	0.3	0.0078	0.2
nascent polypeptide-associated complex alpha polypeptide	gil112419004	0.038	2.4	0.025	2.7
nucleolin	gil27804344	0.00026	6.9	0.0015	5.8
phosphoglycerate dehydrogenase	gil33990002	0.0068	0.2	0.023	0.2
ribosomal protein L4	gil29436531	0.027	0.0	0.027	0.0
stress-70 protein, mitochondrial	gil182890510	0.0024	0.2	0.00075	0.1
synaptotagmin binding, cytoplasmic RNA interacting protein	gil28422490	0.021	0.4	0.038	0.5
triosephosphate isomerase 1b	gil156230739	0.016	0.1	0.025	0.1

5.4.3 Sub-networks underlying SKF 38393 effects in primary RGC culture

To learn more about relationships among regulated proteins that may underlie SKF 38393 effects in primary RGC culture, the 22 significantly regulated proteins were imported into Pathway Studio to construct protein pathways. The protein network contained many small molecules that could be associated with the regulation of RGC functions (Fig. 5.3). These molecules, surrounded by a purple hue, included those related to energy production (ATP), fatty acids (lipids and steroids), hormones (estrogen), stress (ROS), glucose, cellular second messenger (cAMP) and ions (Ca^{2+}).

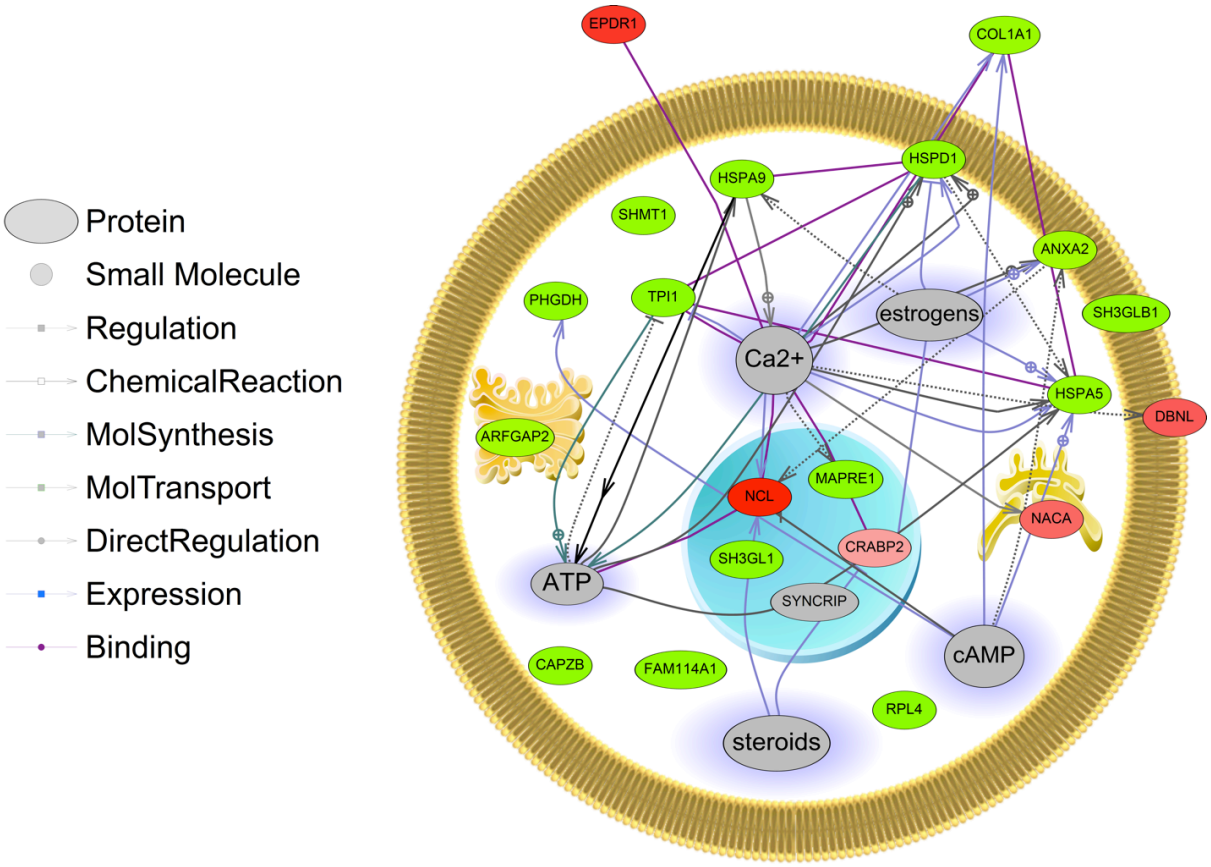

Figure 5.3. Protein network representing differentially expressed proteins following SKF 38393 treatment in primary RGC culture. Green indicates the protein is decreased in abundance and red indicates that the protein is increased in abundance. Small molecules with a purple hue are those that have been mapped to the protein network and are associated with the differentially expressed proteins.

SNEA was also performed to identify cell process, expression, and binding networks in primary RGC cultures on experimental data set acquired using Average TIC method. For the SNEA, 365 proteins were used in the final analysis as they were quantified with 2 or more unique peptides and were successfully mapped to human homologues. Cell processes including cell growth, cell proliferation, cell survival protein folding and RNA processing were affected by SKF 38393 (Fig. 5.4). SKF 38393 also regulated expression targets of ESR1, NFIC, E2F1, CEBPB, MYC and CTNNB1 in this network (Fig. 5.5). Downstream protein networks of each expression target are also regulated by SKF 38393, which may affect RGC functions. Binding partners among regulated proteins revealed 6 groups of binding partners of PTBP1, RNR2, AR, PCNA, HSP90AA1 and HSPD1 (Fig. 5.6).

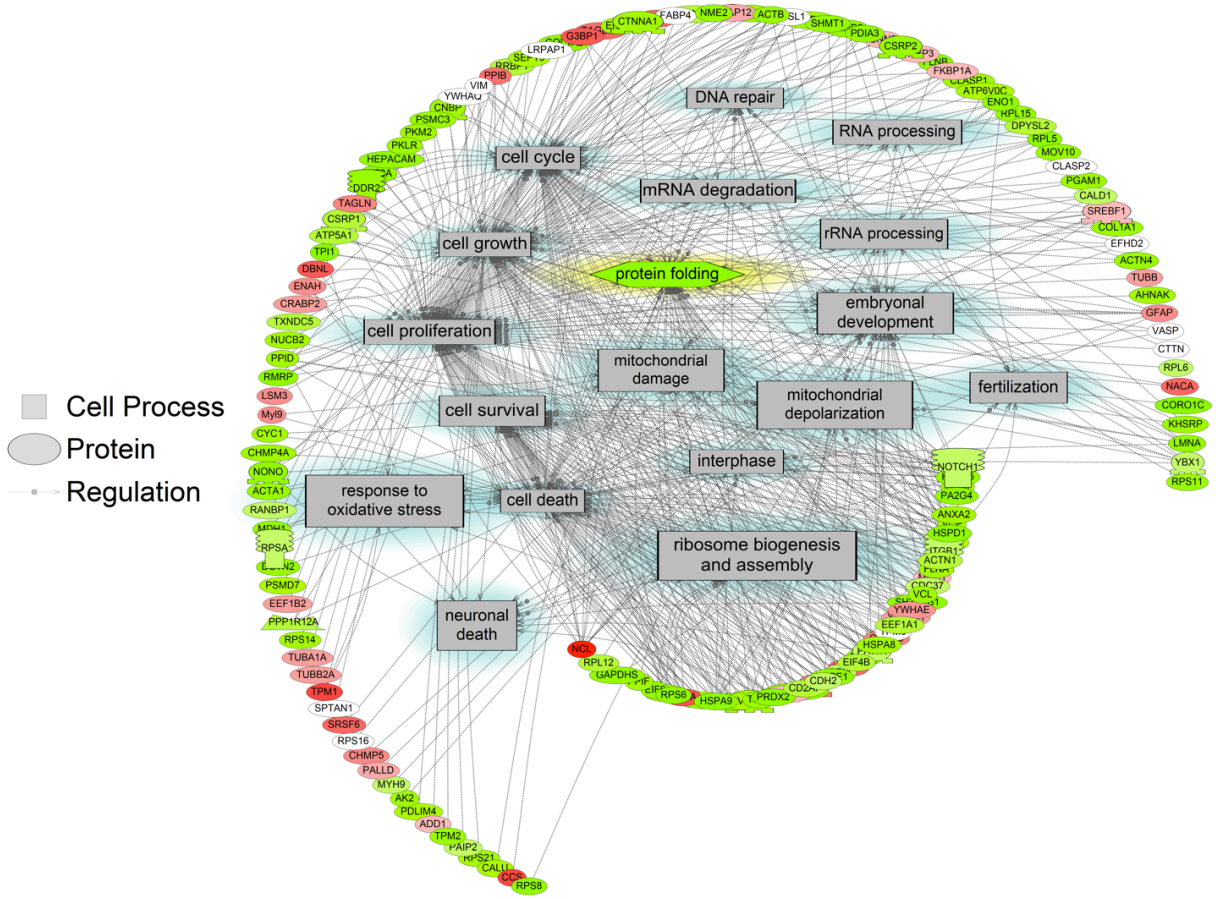

Figure 5.4. Cell Processes identified by SNEA were regulated by SKF 38393 in primary RGC culture. Green indicates that the protein is decreased in abundance and red indicates that the protein is increased in abundance.

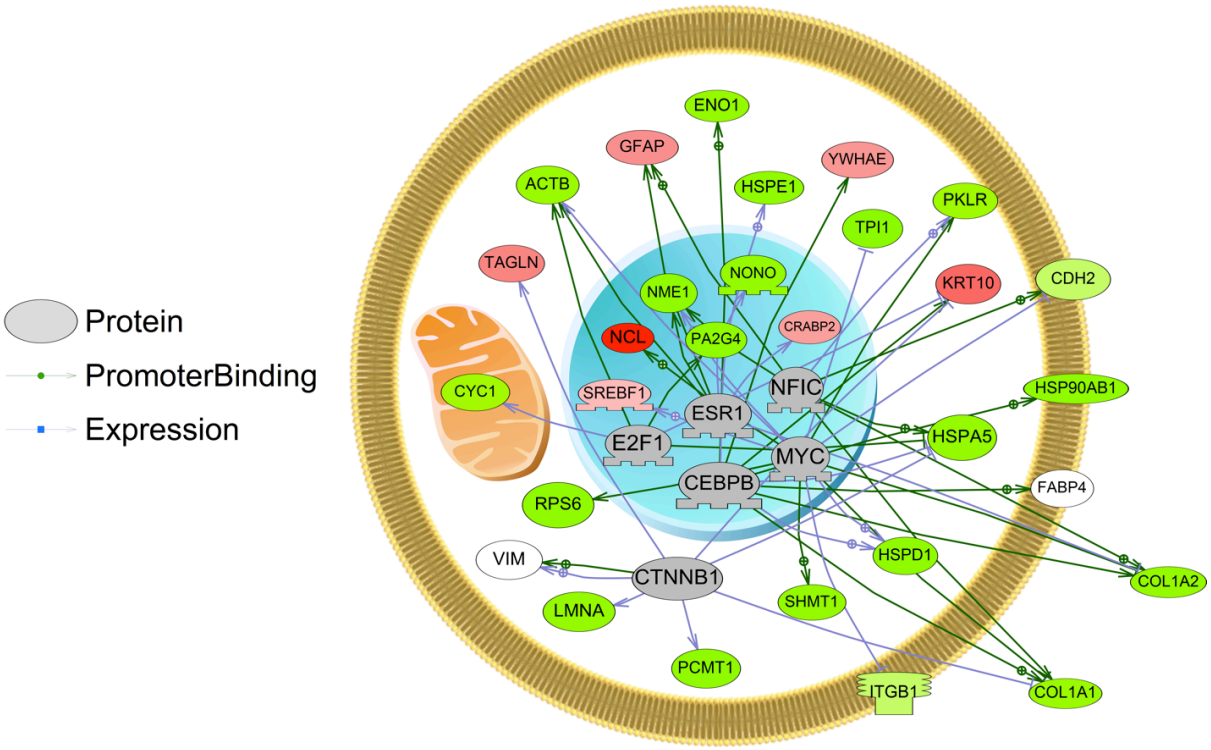

Figure 5.5. Expression targets identified by SNEA that are regulated by SKF 38393 in primary RGC culture. Green indicates the protein is decreased in abundance and red indicates the protein is increased in abundance. Proteins in grey are upstream regulators of the regulated proteins and were not directly measured by mass spectrometry but were determined to be related to the network.

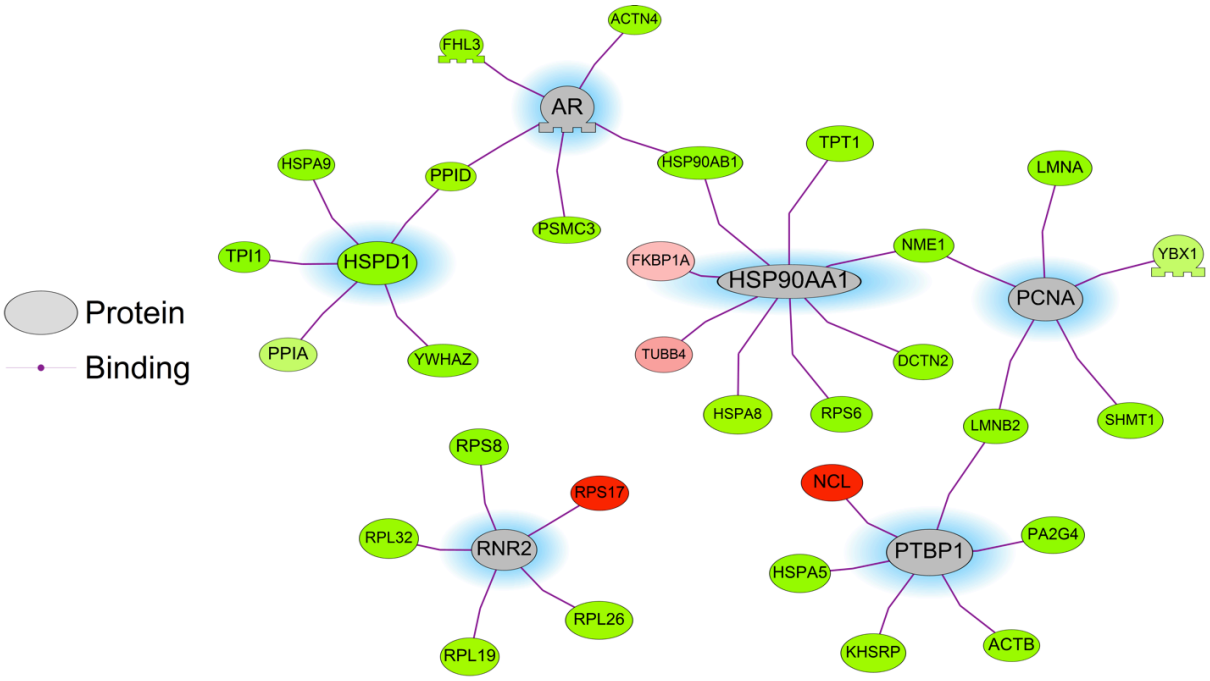

Figure 5.6. Binding partners identified by SNEA are regulated by SKF 38393 in primary RGC culture. Green indicates the protein is decreased in abundance and red indicates the protein is increased in abundance.

5.4.4 Validation by Western Blot and qPCR

We validated the results of the proteomic analysis by western blot for TPI, for which there was an antibody available (Fig. 5.7). Additionally to further investigate the effects of SKF 38393, we used qPCR to determine the levels of mRNAs encoding five regulated proteins (Fig. 5.8). The protein level of TPI was significantly down-regulated following SKF 38393 exposure ($P < 0.05$). The relative mRNA levels of *ncl* was significantly up-regulated following SKF 38393 exposure ($P < 0.05$) and the transcript levels of *tpi*, *capzb* and *phgdh* were significantly down-regulated following SKF 38393 exposure ($P < 0.05$). These data were all consistent with the direction of change as determined by MS/MS except for *fam1141a* for which the mRNA level did not change.

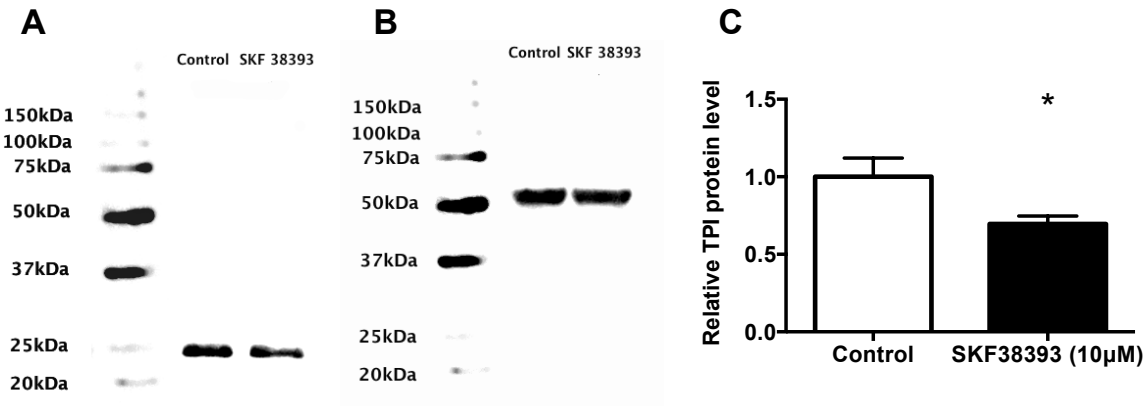

Figure 5.7. Western blot analysis showing TPI protein in primary RGCs culture exposed to 10 μM SKF 38393. (A) TPI immunoreactivity, where (B) actin served as internal control. The densitometric analysis of western blot is reported as an arbitrary value relative to the average of all bands on the same blot. Data were normalized and defined as fold change relative to control, and bars represent the mean + SEM (n = 6, C). Treatment group marked by asterisk has statistically different protein levels to control ($P < 0.05$).

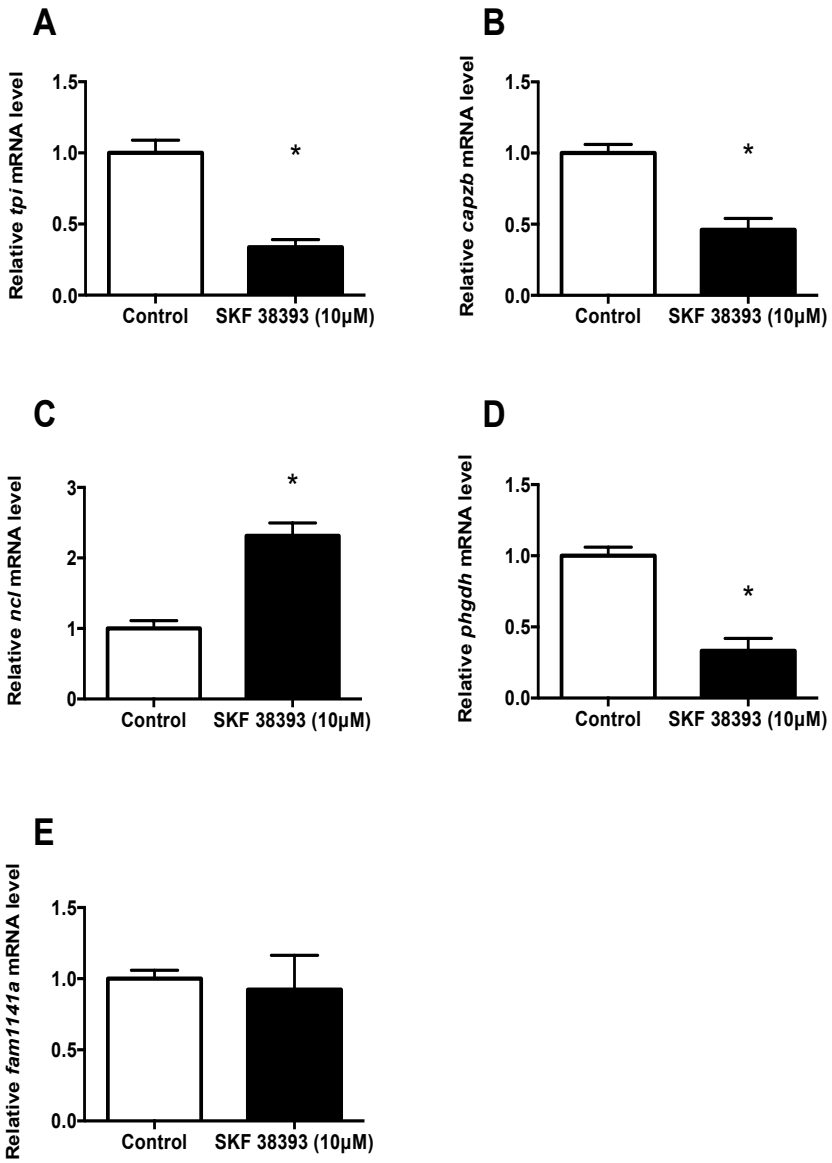

Figure 5.8. Quantitative real-time RT-PCR analysis for (A) *tpi1b*, (B) *capzb*, (C) *ncl*, (D) *phgdh* and (E) *fam114a1* mRNAs in primary RGCs culture exposed to 10 μM SKF 38393. Data were normalized and defined as fold change relative to control. Bars represent the mean + SEM (n = 4). Treatment groups marked by asterisks have significantly different mRNA levels to control ($P < 0.05$).

5.5 Discussion

Label free proteomics and MS were used to characterize female goldfish RGCs in culture and to define their cellular responses to specific activation of the D1R signaling pathway. A total of 689 unique proteins were identified and classified in the primary RGC cultures. A total of 62 differentially expressed proteins were identified using Average TIC method after SKF 38393 exposure, while 22 proteins were determined to be differentially expressed using two different algorithms for quantitation. Regulated proteins were associated with the processes of cell proliferation, growth, cycle, survival, and embryonic development. These proteins also interacted with small molecules including calcium, steroids, ATP and cAMP, along with several other transcription factors, some of which are ESR1, CTNNB1, NFIC and MYC. These proteomic data are the first to provide insight into the function and dopaminergic regulation of RGCs derived from adult teleost brain.

Functional annotations of these proteins indicate that goldfish RGCs express proteins known to play roles in human neurological diseases including Alzheimer's, Parkinson's and Huntington's disease. The presence of proteins such as 20β-hydroxysteroid dehydrogenase confirmed the steroidogenic role of teleost RGCs as we previously demonstrated (Xing et al., 2014). Several identified receptor-mediated signaling pathways also indicate that RGCs may be under the control of many neurotransmitters, neurohormones and neuropeptides. These results support previous findings that RGCs are a neuroendocrine cell that is regulated by neurotransmitters (Pérez et al., 2013; Xing et al., 2014; Xing et al., 2015). Perhaps most significant is that we identified D1R in the protein dataset. This strengthens our proposal that D1R is localized to RGCs, and supports our previous gene sequencing and immunocytochemistry data indicating the presence of this functional receptor (Xing et al.,

2015).

The protein networks underlying SKF 38393 exposure contained many small molecules that are associated with cell signaling and cell function regulation, including second messengers cAMP and Ca^{2+}, each involved in numerous intracellular signaling pathways. Proteins with an integral role in Ca^{2+} signaling that were regulated by SKF 38393 included annexin II (ANXA2) and calmodulin (CaM). As a member of the annexin protein family, which can bind to membrane phospholipids in a Ca^{2+}-dependent manner, ANXA2 is necessary for integrating Ca^{2+} signaling and membrane function (Gerke et al., 2005). The ubiquitous Ca^{2+} receptor protein CaM mediates a variety of signaling processes involved in cell proliferation, apoptosis, and autophagy (Berchtold and Villalobo, 2014). Therefore, we hypothesize that SKF 38393 may regulate RGCs membrane dynamics through Ca^{2+}-dependent pathways. Similarly, many transcription factors were identified as expression targets regulated by SKF 38393, such as ERα (ESR1). The actions of estrogens in the brain are primarily mediated by ERs, which are ligand responsive transcription factors (Tora et al., 1989). The dimerization of ERs can regulate gene transcription by binding to the ERE in the promoter of target genes, including the estrogen-synthetic enzyme aromatase in a positive manner in both mammals and teleost (Belcher and Zsarnovszky, 2001; Bowman et al., 2002; Simpkins et al., 2012). Our previous studies have shown that DA regulates aromatase B expression in goldfish RGCs by recruiting ESRs. This study strongly supports the involvement of ESR1 in dopaminergic regulation of RGC functions and presents several other putative protein candidates for regulation through ESR1, including NME1, NONO, COL1A2, ACTB, GFAP and CRABP2.

Cell processes that may also underlie DA regulation of RGCs function were identified

by network analysis. Among all the proteins decreased by DA, phosphoglycerate dehydrogenase (PHGDH) is an enzyme preferably expressed in RGCs and astrocytes at the adult mouse subventricular zone, whereby new neurons are generated from neural stem cells and RGCs (Kinoshita et al., 2009; Yamasaki et al., 2001). The expression of PHGDH in RGCs at neurogenic sites suggests that this enzyme may be involved in neurogenesis and brain repair. Indeed, PHGDH catalyzes the transition of 3-phosphoglycerate into 3-phosphohydroxypyruvate, which is the first and rate-limiting step in the phosphorylated pathway of serine biosynthesis (Ehmsen et al., 2013). It is assumed that RGCs supply serine and its derivatives to newborn, migrating neurons and that PHGDH is involved in cell proliferation since patients with PHGDH deficiency have impaired brain development (de Koning et al., 2003). Recent findings suggest that down-regulation of PHGDH inhibited proliferation and enhanced neuronal differentiation in neurogenic regions of adult human brain (Jing et al., 2015; Nakano et al., 2007). We have also identified goldfish PA2G4, a homolog of the human proliferation-associated 2G4 protein (also termed Ebp1), which is decreased by SKF 38393. Importantly, Ebp1 is a well-conserved DNA/RNA binding protein that is implicated in cell proliferation, growth, survival and differentiation in many mammalian cell types (Norris-Mullins et al., 2014). The Ebp1 knockdown studies in mouse have shown the inhibition of muscle stem cell as well as myoblast proliferation and differentiation (Figeac et al., 2014). The reduced proliferation could be linked to the negative effect of Ebp1 on the normal rRNA processing and/or ribosome assembly, since alterations of ribosome biogenesis can induce cell cycle arrest (Squatrito et al., 2004). On the other hand, enhanced expression of Ebp1 was observed during the process of cAMP-induced differentiation of another glial cell type, Schwann cells, in rats (Liu et al., 2014).

Furthermore, one of the most highly induced proteins by SKF 38393 was nucleolin, a protein that has a role in cell proliferation and survival. Previous studies have shown that nucleolin supresses Fas- and angiotensin-II- induced apoptosis in human cell lines, potentially through modulating Fas ligand binding and interacting with anti-apoptotic members of the Bcl-2 family (Lee et al., 2010; Wise et al., 2013). Furthermore, cellular model of PD revealed that nucleolin alters the generation of oxidative stress, which suggests the role of nucleolin in PD pathogenesis (Caudle et al., 2009). Here, we report that DA regulates cell proliferation-, differentiation- and survival-related proteins, PHGDH, PA2G4 and nucleolin in goldfish RGCs, which is consistent with previous studies that showed the inhibitory effects of DA in neurogenesis through inhibition of proliferation of progenitor cells in salamander (Berg et al., 2011). The present data also generate mechanistic understanding of the proteins that are potentially involved in this process. The tight regulation of progenitor cell proliferation and survival under physiological condition could act to preserve the capacity of neuron generation and may even be critical for brain repair after injury.

To characterize gene-protein relationships in RGCs and validate MS/MS data, transcripts from specific functional groups (cell proliferation, metabolism, apoptosis, ribosomal proteins, oxidative stress) were analyzed with qPCR or western blot and compared to relative protein abundance generated using mass spectrometry. We measured the protein level of TPI, which was significantly down-regulated by SKF 38393. The enzyme TPI catalyzes the interconversion of D-glyceraldehyde 3-phosphate to dihydroxyacetone phosphate and plays an important role in glycolysis and energy production. Findings on TPI enzymopathy demonstrated that TPI deficiency is coupled with neurodegeneration, especially the initiation process in humans (Olah et al., 2002). For example, in Alzheimer's

disease, to ensure the proper insertion of P-amyloid precursor protein into the cellular or synaptic membranes, sufficient energy is required. Glucose synthesis and ATP turnover rates are regulated by TPI, which is crucial to the progression of the disease (Meier-Ruge and Bertoni-Freddari, 1997). Therefore, our findings on the regulation of TPI by DA provide additional knowledge on the role of DA in neurodegenerative diseases. The qPCR data showed that the mRNA levels of *tpi, capzb* and *phgdh* were significantly down-regulated by SKF 38393, and the mRNA level of *ncl* was increased by SKF 38393; thus data were consistent between mass spectrometry and qPCR/Western blot in the direction of change. Our previous studies showed that dopaminergic compounds can also regulate the mRNA abundance of these transcripts (Popesku et al., 2010). For example, the mRNA and protein levels of TPI were regulated by SKF 38393 in goldfish hypothalamus after intraperitoneal injection.

In conclusion, this study utilized a label free proteomic approach to determine the protein profiles of the adult goldfish RGCs and to generate new knowledge regarding the regulation of proteins by the key neurotransmitter DA. For the first time, the RGC proteome in a vertebrate was characterized and gene network analysis has identified a DA-regulated protein network that involves steroids, cAMP, ATP, Ca^{2+} and stress-related molecules that are associated with intracellular signaling pathways in RGCs. In terms of the proteomic response, proteins involved in RGC progenitor functions were generally inhibited, likely through transcription factor-mediated pathways. This study provides the foundation for gene and protein regulatory networks in the fish RGCs, and identifies cellular processes and signaling pathways in these cells with roles in neurogenesis and neuroendocrine function. To fully understand glial contribution to normal adult brain functions through interactions with

neurotransmitters, the pathways regulated by DA must be further investigated in RGCs. Thus, additional studies are needed to evaluate the RGC proteome response to DA or other potential regulators in adult brain in closer detail. This approach may yield specific signatures and biomarkers for specific neuroendocrine and neurogenesis disruptors.

Chapter 6: Roles of estrogens and radial glial cells in MPTP-induced dopamine neuron degeneration and regeneration [6]

6.1 Abstract

Following Alzheimer's disease, PD is the second most common neurodegenerative disorder in the world. Significant glial cell reaction and DA neuron regeneration have been found both in human PD and MPTP-induced PD animal models. In teleost brain, RGCs are known as progenitor cells and secrete a number of neurosteroids, antioxidants and neurotrophic factors. The neuroprotective effects of neuroestrogens and RGCs in PD have not yet been clarified, and it is not known whether they are critical for brain repair and neurogenesis. Using a goldfish model of PD, we investigated the possible roles of RGCs, especially estrogen synthetic function, in the process underlying DA neuron regeneration in the brain. The data indicate that DA neuron degeneration and aromatase activity inhibition could be successfully induced using the neurotoxin MPTP and fadrozole in female goldfish, respectively. The expression of genes related to RGC functions including *gfap*, *gdnf* and *bdnf* as well as genes related to mature DA neuron functions including *th*, *slc6a3* and *pitx3* are under modulation of estrogens. Together these results revealed that the activation of RGCs and DA neuron recovery after MPTP insult is estrogen-dependent. Findings in this study provided some support for the hypothesis that estrogens are protective in PD. Future studies should be focused on finding the most plausible molecular pathways for enhancing

[6] *Partially based on Xing L., Venables M., and Trudeau VL. (2015). Role of estrogens and RGCs in MPTP-induced DA neuron degeneration and regeneration. Submitted to General and Comparative Endocrinology. XL, designed the study, developed the methodology, conducted the majority of experiment and analysis and wrote the manuscript. VM helped with RNA extractions and gave critical comments on the manuscript. TVL, helped with the design of the study and editing the article.*

protective functions of estrogens and understanding global effects of estrogens in treating neurodegenerative diseases in the CNS.

6.2 Introduction

Parkinson's disease is the second most common neurodegenerative disorder in the world (Dauer and Przedborski, 2003). The exact cause of PD is not clear, but it is well established that the pathology of PD is characterized by an accumulation of α-synuclein into Lewy bodies and the loss of DA neurons in the SN located in the midbrain of mammals (Giraldez-Perez et al., 2014). The main features of PD are tremors, rigidity, bradykinesia and postural instability, which can be accompanied by non-motor symptoms such as olfactory deficits, sleep impairments and neuropsychiatric disorders (Blesa et al., 2012).

The chemical MPTP is a common neurotoxin causing neurodegeneration and PD-like syndromes in humans (Langston and Ballard, 1983) and in various animal models including primates (Burns et al., 1983), rodents (Heikkila et al., 1984) and teleost fish (McKinley et al., 2005; Youdim et al., 1992). The chemical MPTP is highly lipophilic and able to rapidly cross the blood-brain barrier after systemic administration. Once in the brain, monoamine oxidase-B in glial cells metabolizes MPTP into neurotoxic 1-methyl-4-phenylpyridinium (MPP^+), which is then released into the extracellular space where it can be selectively taken up by DAT located on the DA nerve terminals. The accumulation of MPP^+ in the mitochondria of DA neurons disrupts the electron transport chain specifically at complex I, which leads to energy depletion and then cell death (Segura Aguilar and Kostrzewa, 2004). Studies using the goldfish have demonstrated that intraperitoneal administration of MPTP leads to a selective loss of DA neurons and induces a parkinsonian syndrome. This goldfish

model of PD was characterized by Weinreb and Youdim (Weinreb and Youdim, 2007), who reported profound bradykinesia (slow movement), reduction in movement paralleled with depletion of DA from the forebrain and midbrain after a single MPTP injection (50 μg/g body mass). Moreover, studies have shown significant glial cell activation associated with the loss of DA neurons in MPTP-induced PD disease models (Blesa et al., 2012; Yokoyama et al., 2010). However, the exact functions of activated glial cells in DA neurodegeneration and regeneration are not well understood, especially in teleost models.

Teleost fish serve as an excellent model to study neuroregeneration because of the remarkable capacity of plasticity within the fish brain compared to the mammalian brain (Zupanc and Clint, 2003). The higher regenerative capacity of the teleost brain is partially due to the abundance of neuronal progenitor cells such as RGCs. In mammals, most RGCs disappear following the development of the CNS by differentiating into other cell types, including astrocytes, oligodendrocytes and neurons (Schmechel and Rakic, 1979). As a result, there are very few RGCs in the adult mammalian brain. On the contrary, teleost RGCs are abundant and persist throughout their whole lifespan, which keep their progenitor nature and serve as "stem cells" (Zupanc, 2008). The RGCs are able to divide and differentiate into new neuronal cells, which can use the processes of RGCs as a scaffold to migrate to their final destination (Rakic, 2003a). This active proliferative nature of RGCs has been reported by several groups that have performed BrdU and proliferating cell nuclear antigen (PCNA) labeling in the zebrafish forebrain (Pellegrini et al., 2007; Zupanc and Sîrbulescu, 2011; Zupanc et al., 2012). It is suggested that the proliferative role of RGCs supports the regeneration of the adult brain and the activation of RGCs after brain injury or neuroinflammation is considered an essential process of brain repair (Zupanc and Clint,

2003).

In the adult fish brain, RGCs are not only known as the progenitor cells but also produce a number of neurosteroids and neurotrophic factors, such as glial cell line-derived neurotrophic factor (GDNF) and brain-derived neurotrophic factor (BDNF) (Pellegrini et al., 2007). Importantly, GDNF enhances the survival and morphological differentiation of newborn DA neurons and decreases apoptosis of damaged DA neurons (Lin et al., 1993; Yasuhara et al., 2007). On the other hand, BDNF stimulates axon regeneration and growth, regulates the expression of DA D3 receptor and improves motor difficulties in PD animal models (Lykissas et al., 2007). Recently, RGCs have been confirmed as a steroidogenic cell type in fish brain (Xing et al., 2014). It is well known that the enzyme aromatase catalyzes the conversion of androgens to estrogens and it is exclusively expressed in RGCs in the adult fish brain (Diotel et al., 2010a; Forlano et al., 2001). The expression of other steroidogenic enzymes such as 3β-hydroxysteroid dehydrogenase (*hsd3b1*), cytochrome P450 17α-hydroxylase (*cyp17a1*) and 17β-hydroxysteroid dehydrogenase (*hsd17b4*) in RGCs have been reported recently, which indicates the capability of RGCs to produce steroids *de novo* using the common steroid precursor cholesterol (Xing et al., 2014). Neurosteroids, especially neuroestrogens, have been extensively studied in many mammalian models for their neuroprotective and neuroregenerative functions (Garcia-Segura, 2008; Saldanha et al., 2009; Scott et al., 2012). The neuroprotective actions of neuroestrogens are partially mediated through nuclear ERs to regulate gene transcription (Coumailleau et al., 2015; Pietranera et al., 2015). Neuroestrogens have been shown to increase pro-survival *bcl-2* family members and decrease pro-apoptotic *bad* and *bim* factors in numerous mammalian animal and cell culture models thereby promoting cell survival (Dubal et al., 1999; McCullough et al., 2003; Wu et

al., 2005; Yao et al., 2007). Furthermore, estrogens are able to attenuate oxidative damage by reducing the level of reactive oxygen species (ROS) (Numakawa et al., 2007) and promote the secretion of growth factors such as BDNF and insulin growth factor 1 (IGF-1) in rats (Cardona-Gomez et al., 2001; Dhandapani et al., 2005). However, controversial findings about the roles of estrogens in fish neurogenesis have been reported in the last two years (Diotel et al., 2013; Makantasi and Dermon, 2014). For example, Diotel *et al*. found an inhibitory effect of estrogens and ERs on adult zebrafish neurogenesis (Diotel et al., 2013), but did not detect any stimulating effect on cellular proliferation, which significantly contrasts with findings from studies using mammalian models.

We have used the MPTP-injected adult goldfish model to determine the effects of estrogens and radial glia. We combined MPTP treatments with the aromatase inhibitor fadrozole to reduce estrogen levels. To assess possible effects on the dopaminergic system, we also determined expression of tyrosine hydroxylase (TH, *th*) and DAT (*slc6a3*). Both are indicators of the mature DA neuron functioning, since they are closely related to DA synthesis and reuptake, which tightly controls DA levels in brain (Yamamoto et al., 2011). The PTEN-induced putative kinase 1 (PINK1, *pink1*) is a mitochondria-targeted serine/threonine kinase, which is linked to autosomal recessive familial PD and may help protect mitochondria from malfunctioning during periods of cellular stress (Matsuda et al., 2013). Transcription factor paired-like homeodomain transcription factor 3 (Pitx3, *pitx3*) has roles in the regulation of TH expression and long-term survival and maintenance of the midbrain DA neurons (Li et al., 2009; Reddy et al., 2011). Our results indicate that RGC activation and neurotrophic factor production as well as DA neuron recovery after MPTP injection is estrogen-dependent.

6.3 Materials and Methods

6.3.1 Ethics Statement

All procedures used were approved by the University of Ottawa Protocol Review Committee and followed standard Canadian Council on Animal Care guidelines on the use of animals in research.

6.3.2 Experimental animals and design

Common adult female goldfish were purchased in April from a commercial supplier (Mt. Parnell Fisheries Inc.) and acclimated for at least 3 weeks prior to experimentation. The fish were maintained at 18 °C under a natural simulated photoperiod and fed standard goldfish flakes. Sexually mature, pre-spawning female goldfish (20-35 g) were anaesthetized in 0.05% MS222 for all handling, injection, and dissection procedures.

There are four different experiment groups in this study. The control group only received a saline injection intraperitoneally (5 μL/g body mass). Fish in Fadrozole group were exposed to 50 μg/L fadrozole (Sigma-Aldrich) dissolved in the goldfish tanks (70 L), 15 fish per tank. Fish in MPTP group received MPTP (50 μg/g body mass) injection and fish in Fadrozole+MPTP group received both fadrozole exposure and MPTP injection. The 11-day experimental protocol is summarized in Figure 6.1. The water and fadrozole were renewed every 3 days, at day 3, 6, 9. At day 4, fish in MPTP and Fadrozole+MPTP were injected with MPTP. The fish exposed to fadrozole only also received a saline injection. Fifteen fish in

each group were anaesthetized and sacrificed by spinal transection at day 8 and day 11, respectively (Figure 6.1). Whole body mass and ovary mass were weighed for calculating the gonadosomatic index (GSI = [Gonad Mass / Total Tissue Mass] x 100). Telencephalon (Tel) and hypothalamus (Hyp) tissues of 12 fish were rapidly dissected and immediately frozen on dry ice for later RNA extraction. Brains of 8 fish were rapidly dissected on ice and immediately fixed in 4% PFA dissolved in RNase free PBS (pH 7.4) overnight at 4 °C, then washed twice in PBS and twice in methanol for 5 m each to finally be transferred in methanol. Fixed brains were stored at -20 °C until processed for cryo-sectioning. Following storage at -20 °C, fixed brains were rehydrated in a methanol-PBS dilution series, then embedded in 1.5% agar/5% sucrose dissolved in PBS. Embedded brains were cut into blocks for cryo-sectioning and placed in 30% sucrose overnight. Blocks were frozen in Shandon Cryomatrix (Thermo Scientific) mounting medium in isopentane kept at -80 °C. Frozen blocks were sectioned with a 16 µm thickness. Sections were transferred onto Superfrost Plus slides (Fisher) and stored at -20 °C until needed for immunohistochemistry.

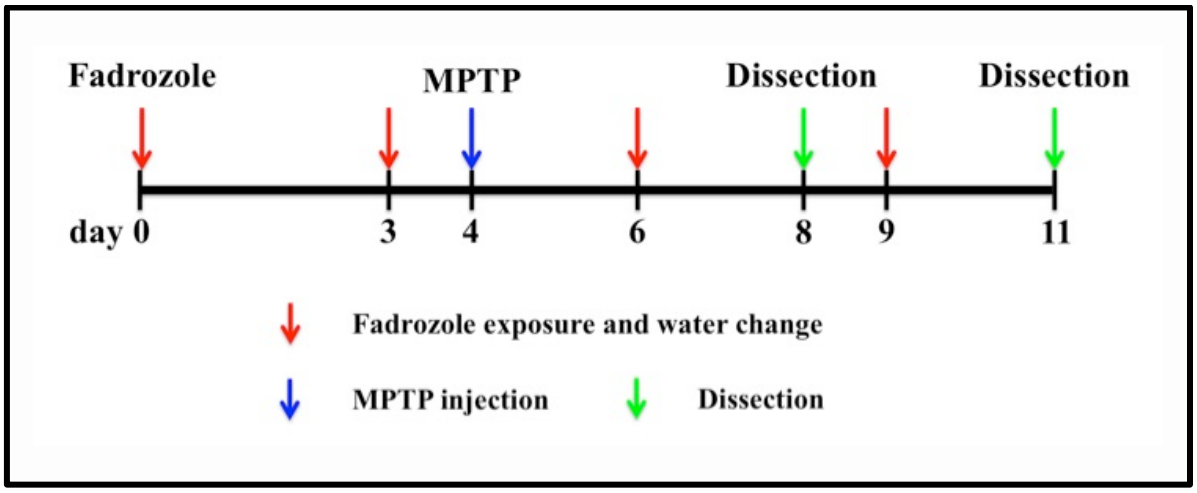

Figure 6.1. Timeline and process of experimental design.

6.3.3 Immunohistochemistry

Frozen slides were thawed for 1 hour at RT. Non-specific binding was blocked in blocking buffer (0.3% Triton PBS containing 1% BSA) for 45min at RT. Slides were covered with anti-GFAP antibody (1:500, generated in mouse, Chemicon, Temecula, CA, USA, Cat. # MAB360), which was previously validated in midshipman (Forlano et al., 2001) and anti-TH antibody (1:500, generated in rabbit, Chemicon, Tamecula, CA, USA, Cat. # AB152), which was previously validated in zebrafish (Yamamoto et al., 2011) overnight at 4 °C. Sections were then washed for 2× 10 m in PBS and incubated with a donkey anti-rabbit Alexa fluor 488 (1:500; Invitrogen Molecular Probes) and goat anti-mouse Alexa fluor 596 (1:500; Invitrogen Molecular Probes) for 1 hour at RT. Slides were washed 2× 10 m in PBS and mounted with the antifading medium Vectashield with DAPI (Vector Laboratories) that permits visualization of cell nuclei. A grading system from 0-3 was used to evaluate the protein level based on the intensity of immunohistochemistry staining (n = 6; Table 6.1). Four independent evaluators were asked to grade immunohistochemistry images in a blind design. The median score from each group are presented as the numbers of plus (+) symbols.

Table 6.1. Semi-quantitative grading system for evaluating immunohistochemistry images

Score	0	1	2	3
Intensity of staining	Negative	Weak	Intermediate	Strong

6.3.4 RNA extraction, quality control and cDNA synthesis

RNA was isolated using the RNeasy Micro kit (Qiagen) as described in the

manufacturer's protocol. Upon purification, the concentration and quality of all samples was assessed using NanoDrop ND-1000 spectrophotometer (Fisher) and 2100 Bioanalyzer (Agilent). RNA integrity values of samples ranged from 8.1 to 9.9, which is above the recommended minimum value of 5 for quantitative real-time RT PCR applications (Fleige and Pfaffl, 2006). Total cDNA was prepared using Maxima First Strand cDNA Synthesis Kit for RT-qPCR (Thermo Scientific). Each 20 µl reaction was diluted 100-fold in nuclease-free water and used as the template for qPCR assays. All brain cDNA samples from different time points were synthesized in parallel.

6.3.5 Quantitative real-time RT-PCR

Quantitative real-time RT-PCR assays based on SYBR green detection were used to validate relative gene expression. Primers used in the present study were designed using Primer3 (http://primer3.sourceforge.net/) and synthesized by Integrated DNA Technologies (Table 6.2). The Maxima SYBR green qPCR Master Mix (Thermo Scientific) and CFX96 Real-Time PCR Detection System (Bio-Rad) were used to amplify and detect the transcripts of interest. Data were analyzed using the CFX Manager™ Software package (Bio-Rad). The relative standard curve method was used to calculate relative mRNA abundance between samples, which were normalized using NORMA-GENE algorithm (Heckmann et al., 2011) and then presented as means + SEM of the fold change of gene expression from 8 biological replicates (n = 8; assayed in duplicate) for each group.

Table 6.2. Primer sets used for quantitative real-time RT–PCR in goldfish.

Gene	Primer Sequence (Forward)	Primer Sequence (Reverse)	Amplicon size	Accession No.
β-actin	CTGGGATGATATGGAGAAGA	CCAGTAGTACGACCTGAAGC	215	AB039726
gfap	CCTACGGCAAGAAGCAGAAA	TCCTTCAGGGCAGTGGTTAG	230	L23876
th	AGCACACTGGTCAGCTCTCTC	ATCATCTTCCGGCGTTTTC	193	AY644727
slc6a3	TGGTGATCGCTGGGATGCC	GAAGCCCACACCTTTGAAGAGG	112	EF371919
pink1	AGGGACGCACTTATCAGGAA	ACCCTTCAGCAGCACCAC	244	EF396231
pitx3	ATGGAGAAAGCGTGAAAGGA	ATGTTCATGGAAGGGATGGA	248	EU531569
cyp19a1b	TGCTGACATAAGGGCAATGA	GGAAGTAAAATGGGTTGTGGA	153	AB009335
gdnf	ATGGACTCAGGAACCAAGCA	GTCTGTGACGTTGAGGTGGA	173	EU828244
bdnf	TTGAGGAGTTGCTTGAGGTG	GGCGTCCAGGTAGTTTTTGT	205	EU828243

6.3.6 Statistics

In all cases and before any analysis, normality and homogeneity of variances was verified using Shapiro-Wilk's and Levene's test, respectively. Comparison of two groups was performed using Student's t-test or Mann-Whitney test if data did not pass normality test in IBM SPSS Statistics Version 22. Comparison of more than two groups was performed using one-way analysis of variance (ANOVA) followed by a Tukey post-hoc test or Dunnett's post-hoc test if the data did not pass homogeneity test in IBM SPSS Statistics Version 22. P-values less than or equal to 0.05 were considered statistically significant.

Normally distributed data were presented as a mean + SEM and data with non-normal distribution were presented scattered graphs.

6.4 Results

6.4.1 Effects of fadrozole on GSI

Fadrozole treatment induced significant reduction of female goldfish GSI compared to control fish at 8 d (Fig. 6.2A) and 11 d (Fig. 6.2B) after exposure (Mann-Whitney test, $P < 0.05$). This confirms the effectiveness of waterborne fadrozole, as we have reported previously for female goldfish (Zhang et al., 2009a).

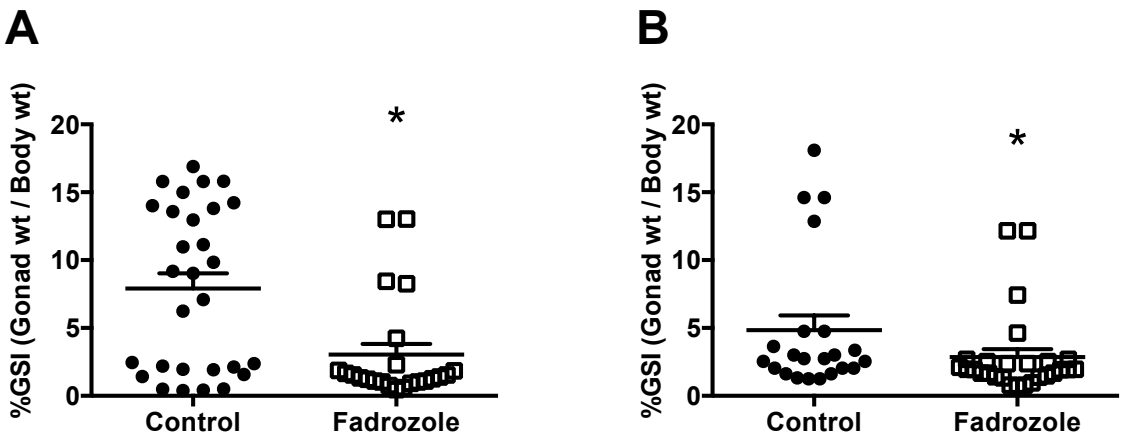

Figure 6.2. The effects of fadrozole on female goldfish GSI. Female goldfish GSI exposed to fadrozole was significantly lower than non-exposed at 8d (A) and at 11d (B). A Mann-Whitney test was performed to determine the effects of fadrozole on GSI. Treatment groups marked by asterisks have significantly different GSI compared to control ($n = 22$, $P < 0.05$).

6.4.2 Effects of MPTP and fadrozole on TH and GFAP-immunoreactivity

Our anatomical assessments focused on the ventral telencephalon, since previous data showed that this is the major brain region negatively impacted by the neurotoxin MPTP (Goping et al., 1995), and is a major site for RGCs and neurogenesis (Elisabeth et al., 2015). Additionally, by using TH and GFAP double fluorescence detection, we revealed a close anatomical relationship between catecholaminergic neurons and RGCs (Fig. 6.3A,B), confirming our previous report (Xing et al., 2015). Intense GFAP-positive RGCs were observed along the ventricular surface with fibres extending to the ventral telencephalic area. Additionally, TH-positive catecholaminergic neurons were observed in the NPP with fibres extending to the ventral telencephalic area. Sections from three goldfish brain samples were stained with GFAP and TH from each group and semi-quantification was performed to study the dynamic changes of RGCs and DA neurons. Four days after MPTP treatment, confocal images (Fig. 6.3A) and semi-quantification data (Fig. 6.3C) showed an up-regulation of GFAP and reduction of TH, but no changes were observed in the fadrozole only exposure. However, pre-treatment with fadrozole blocked the increase in GFAP immunoreactivity observed with MPTP injection (Fig. 6.3A). Seven days after MPTP treatment, confocal images (Fig. 6.3B) and semi-quantification data (Fig. 6.3C) indicated continued up-regulation of GFAP, however, the fish treated with both MPTP and fadrozole had lower intensity of GFAP than the other groups (Fig. 6.3B, C).

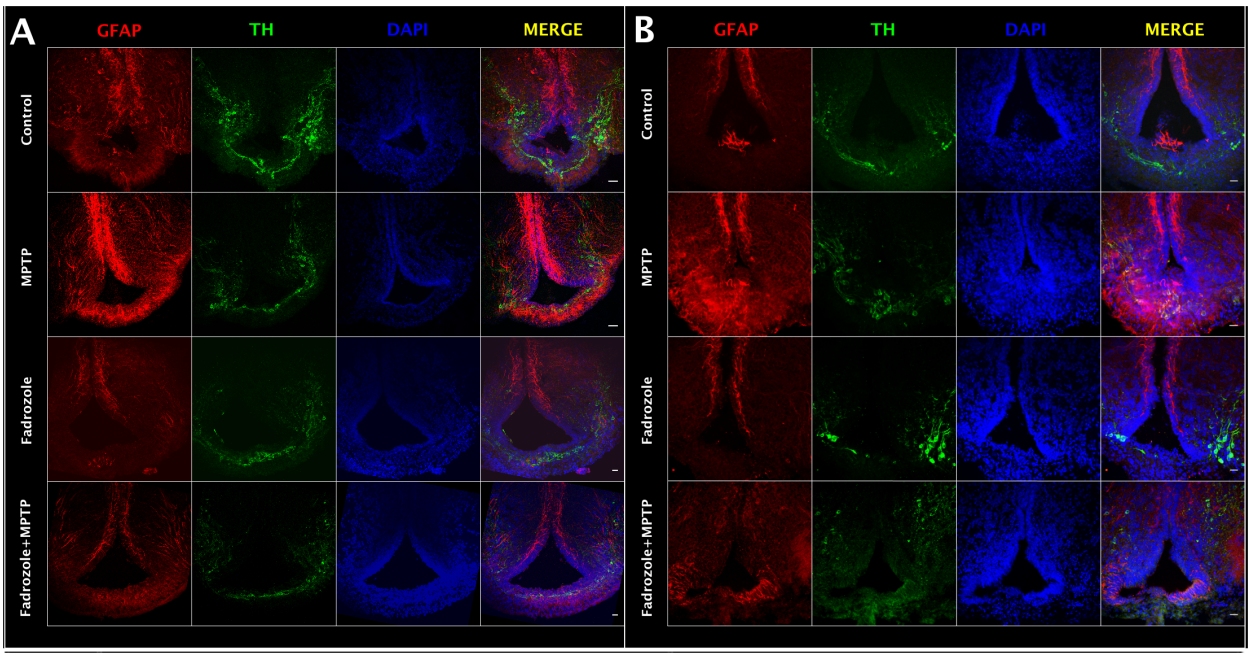

C	DAY 4				DAY 7			
	Control	MPTP	Fadrozole	Fadrozole+MPTP	Control	MPTP	Fadrozole	Fadrozole+MPTP
GFAP	++	+++	++	++	++	+++	++	+
TH	++	+	++	+	++	++	++	++

Figure 6.3. Double fluorescence detection of GFAP (red) and TH (green) in female goldfish ventral telecephalic area at 4 or 7-days post MPTP injection and 8 days (A) or 11 days (B) post fadrozole exposure. The confocal image shows RGCs marked by GFAP located along the ventricular surface. Catecholaminergic neurons marked by TH are close to RGCs. The nuclear stain DAPI (blue) is also shown. Scale bar = 10 μm. Results of semi-quantification of staining intensity of GFAP and TH (n = 3) are shown (C).

6.4.3 DA neuron regeneration and cell turnover is estrogen-dependent

A two-way ANOVA analysis was performed to reveal the effects of MPTP and fadrozole on the expression of genes related to DA neuronal function. In the telencephalon, *th* expression was unaffected by MPTP (Fig. 6.4A), which did not parallel the effects observed for loss of TH immunoreactivity (Fig. 6.3). In contrast, there was a statistically significant interaction between MPTP and fadrozole on *slc6a3* expression in telencephalon (Fig. 6.4C). Post-hoc tests indicated that injection of MPTP increased *slc6a3* expression 2.5-fold and that pre-treatment with fadrozole blocked the effect of MPTP to increase s*lc6a3* in the telencephalon (Fig. 6.4C). There were no effects of treatment on *pink1* (Fig. 6.4E) and *pitx3* (Fig. 6.4G) in the telencephalon at this time point.

After 4 days of MPTP injection (experimental day 8), the *th* expression in hypothalamus was significantly decreased by MPTP, but there were no effects of fadrozole alone (Fig. 6.4B). However, hypothalamic patterns of expression of *slc6a3* were very similar to those observed in telencephalon. There was a statistically significant interaction between MPTP and fadrozole on the *slc6a3* expression in the hypothalamus (Fig. 6.4D). Post-hoc tests indicated that injection of MPTP increased *slc6a3* expression 1.9-fold and that pre-treatment with fadrozole blocked the effect of MPTP to increase s*lc6a3* expression in the hypothalamus (Fig. 6.4D). There were no effects of treatment on *pink1* (Fig. 6.4F) in the hypothalamus. While 2-way ANOVA indicated significant interactions between MPTP and fadrozole for *pitx3* expression, effects of treatments were relatively minor; post-hoc analysis indicated that the lowest levels of expression were found in the hypothalamus of females treated with both MPTP and fadrozole (Fig. 6.4H)

At 7 days following MPTP injection (experimental day 11) treatment effects and

patterns of gene expression in the telencephalon were different to the results presented for day 4 (Fig. 6.4). There were no effects of MPTP or fadrozole on the expression of *th* (Fig. 6.5A), *slc6a3* (Fig. 6.5C) or *pink1* (Fig. 6.4E). On the other hand, we detected a statistically significant interaction between MPTP and fadrozole on the expression of *pitx3* in the telencephalon (Fig. 6.5D). Post-hoc tests revealed that MPTP increased *pitx3* expression while fadrozole blocked this effect.

Although two-way ANOVA indicated statistically significant interaction between MPTP and fadrozole on the expression of *th* (Fig. 6.5B), *slc6a3* (Fig. 6.5D), *pitx3* (Fig. 6.5H) in the hypothalamus, effects were generally of low magnitude. While there was a statistically significant main effect of fadrozole on *th*, a reduction was only clearly evident in the hypothalamus of those fish receiving both MPTP and fadrozole (Fig. 6.5B). Similarly, *slc6a3* (Fig. 6.5D) was highest in MPTP-injected fish and lowest in those treated with both MPTP and fadrozole. The pattern of hypothalamic *pitx3* expression (Fig. 6.5H) was similar to that of *slc6a3* (Fig. 6.5D); *pitx3* was highest in MPTP-injected fish and similar to control values in the other groups. There were no effects of treatments on *pink1* (Fig. 6.5F) in the hypothalamus at this time point.

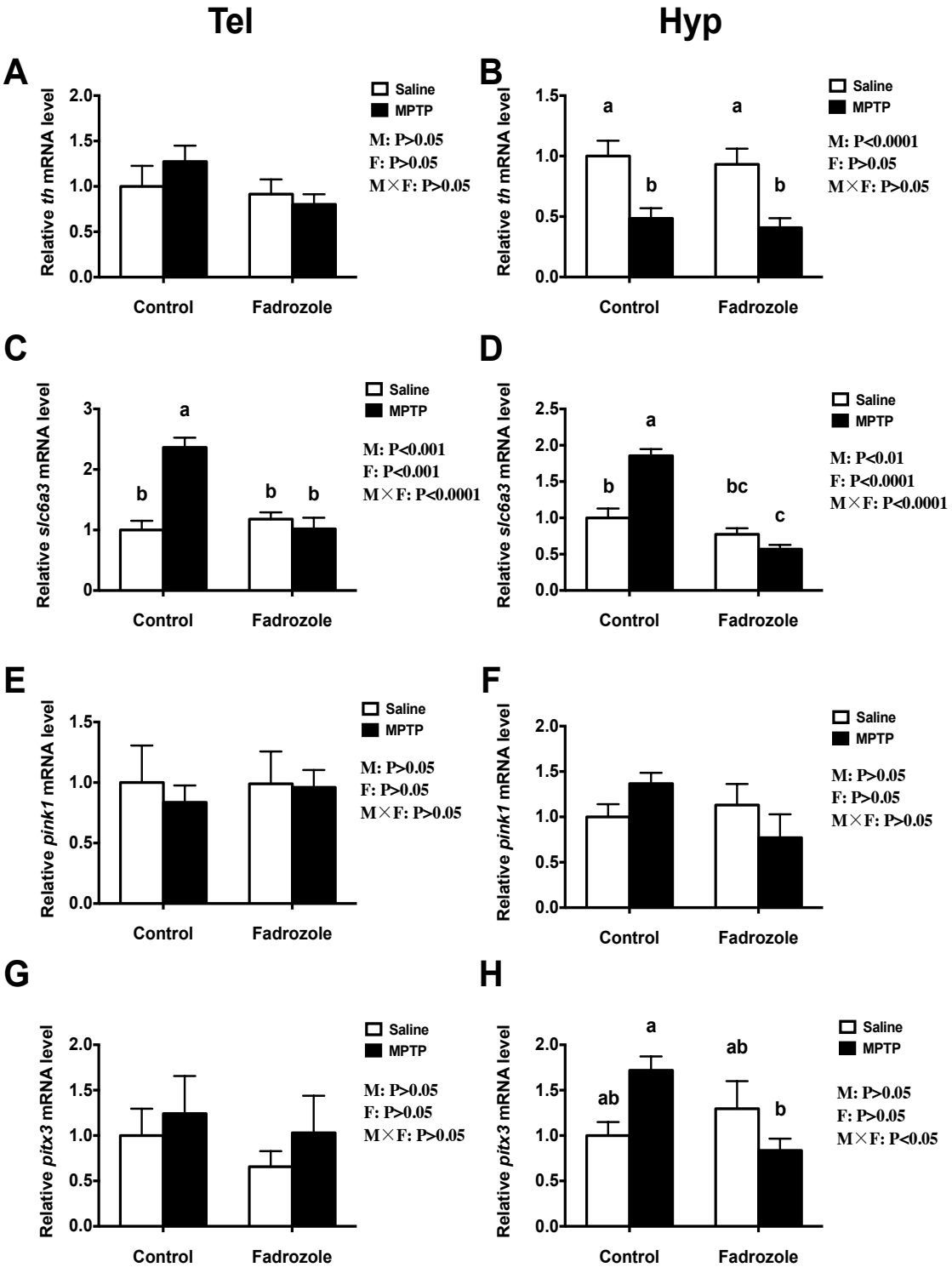
Tel
Hyp
A
Relative th mRNA level
2.0
1.5
1.0
0.5
0.0
Control
Fadrozole
Saline
MPTP
M: P>0.05
F: P>0.05
M×F: P>0.05
B
a
a
b
b
M: P<0.0001
F: P>0.05
M×F: P>0.05
C
Relative slc6a3 mRNA level
3
2
1
0
a
b
b
b
M: P<0.001
F: P<0.001
M×F: P<0.0001
D
2.5
a
b
bc
c
M: P<0.01
F: P<0.0001
M×F: P<0.0001
E
Relative pink1 mRNA level
M: P>0.05
F: P>0.05
M×F: P>0.05
F
G
Relative pitx3 mRNA level
H
ab
a
ab
b
M: P>0.05
F: P>0.05
M×F: P<0.05

Figure 6.4. Quantitative real-time RT-PCR analysis showing variations in the relative amounts of the mRNA encoding genes related to DA neuron regeneration in the telencephalon (A,C,E,G) and hypothalamus (B,D,F,H) of female goldfish injected with MPTP (4d) and exposed to fadrozole (8d). Bars represent the mean + SEM in 8 different cDNA samples; values for each sample were determined in duplicate. Two-way ANOVA followed by Tukey's test was performed to determine the effects of MPTP and fadrozole treatments. Treatment groups marked by different letters have significantly different mRNA levels ($P < 0.05$).

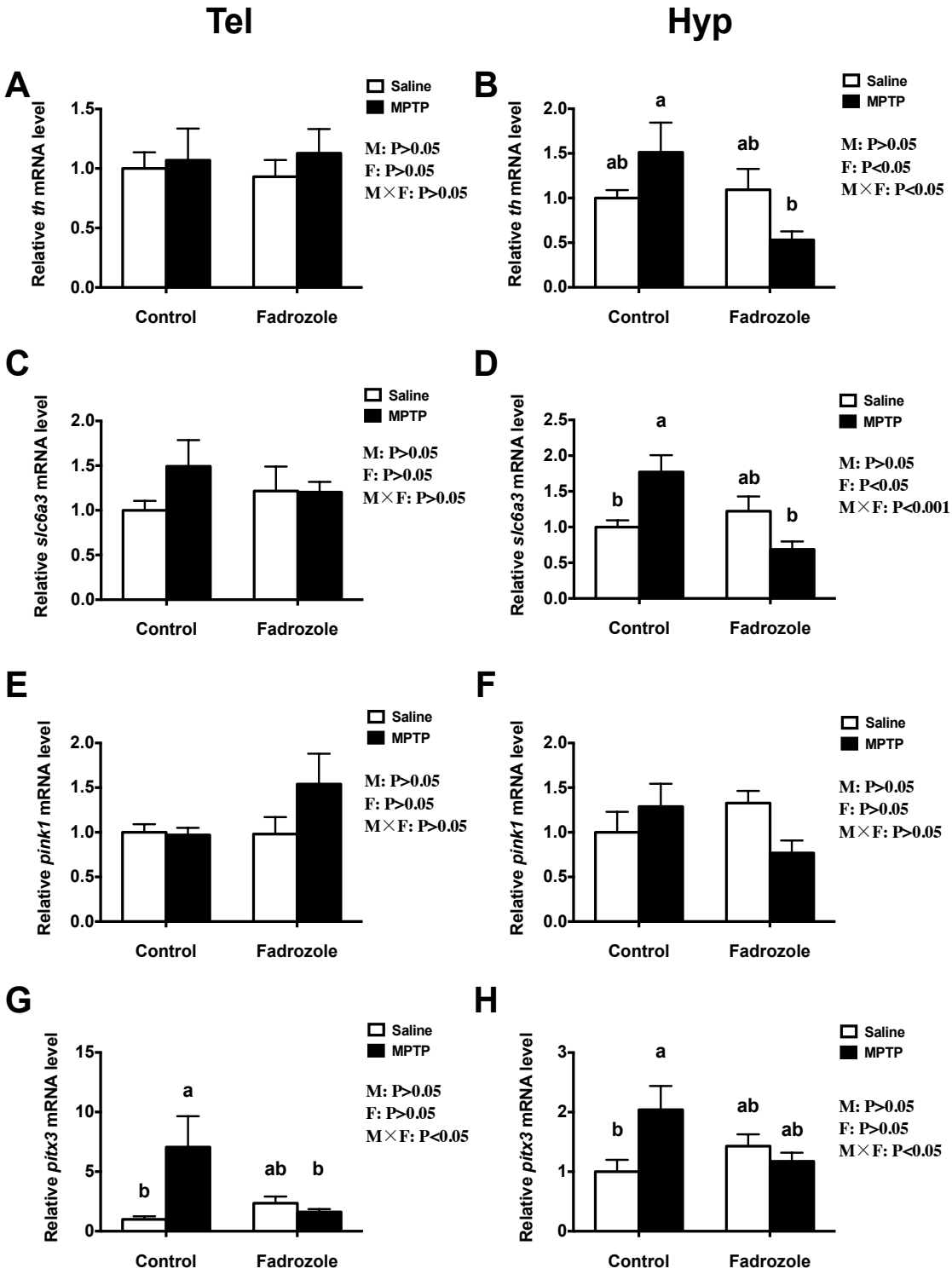
Tel
Hyp
A
B
C
D
E
F
G
H
Relative th mRNA level
Relative slc6a3 mRNA level
Relative pink1 mRNA level
Relative pitx3 mRNA level
Saline
MPTP
M: P>0.05
F: P>0.05
M×F: P>0.05
M: P>0.05
F: P<0.05
M×F: P<0.05
M: P>0.05
F: P<0.05
M×F: P<0.001
M: P>0.05
F: P>0.05
M×F: P>0.05
M: P>0.05
F: P>0.05
M×F: P<0.05
Control
Fadrozole
a
ab
b

Figure 6.5. Quantitative real-time RT-PCR analysis showing variations in the relative amounts of the mRNA encoding genes related to DA neuron regeneration in the telencephalon (A,C,E,G) and hypothalamus (B,D,F,H) of female goldfish injected with MPTP (7d) and exposed to fadrozole (11d). Bars represent the mean + SEM in 8 different cDNA samples; values for each sample were determined in duplicate. Two-way ANOVA followed by Tukey's test was performed to determine the effects of MPTP and fadrozole treatments. Treatment groups marked by different letters have significantly different mRNA levels ($P < 0.05$).

6.4.4 Activation of RGC functions is estrogen-dependent

Two-way ANOVA analysis was performed to determine the effects of MPTP and fadrozole on the expression of genes related to RGC functions in the goldfish telencephalon. Here we also studied the hypothalamus since there are abundant dopaminergic fibres yet few cell bodies (Hornby and Piekut, 1990), and it is an important target area for DA action (Popesku et al., 2010; Popesku et al., 2012).

At 4 days following a single MPTP injection (experimental day 8; Fig. 6.1), there was a statistically significant interaction between MPTP and fadrozole on *gfap* expression in the telencephalon (Fig. 6.6A) and the hypothalamus (Fig. 6.6B) and on *gdnf* expression only in the hypothalamus (Fig. 6.6D). For the telencephalon, post-hoc tests showed that MPTP increased *gfap* expression 4-fold and that the up-regulation was completely inhibited by fadrozole (Fig. 6.6A); there was no effect of fadrozole treatment alone. This data on *gfap* expression directly supports the GFAP immunofluorescence data for the telencephalon (Fig. 6.3A). This indicates the activation of RGCs after MPTP injection and RGC activation as

assessed using *gfap* can be blocked by fadrozole. While *gdnf* expression was increased by MPTP in the telencephalon (Fig. 6.6C), there were no effects of fadrozole alone. There was no statistically significant effect of fadrozole on MPTP-induced *gdnf* expression in the telencephalon, although expression was reduced close to control levels (Fig. 6.6C). Post-hoc tests indicated that MPTP increased hypothalamic *gdnf* expression 1.7-fold, while fadrozole blocked the effect of MPTP (Fig. 6.6D).

There was no treatment effect detected for *bdnf* expression in the telencephalon (Fig. 6.6E). In contrast, hypothalamic *bdnf* expression was reduced by fadrozole alone (Fig. 6.6E); there were no effects of MPTP evident. Fadrozole exposure significantly reduced *cyp19a1b* expression in telencephalon, and there were no effects of MPTP detected (Fig. 6.6G). Similarly, fadrozole significantly reduced *cyp19a1b* expression in the hypothalamus, and there were no effects of MPTP detected (Fig. 6.6H).

At 7 days following MPTP injection (experimental day 11) treatment effects in the telencephalon were lessened compared to day 4 (Fig. 6.6). The two-way ANOVA indicated an overall main effect of MPTP to increase *gfap* in telencephalon, and there were no effects or interactions with fadrozole. Post-hoc tests indicated that MPTP increased *gfap* expression 2.5 fold (Fig. 6.7A), which should be compared to the 4-fold increase observed at day 4 (Fig. 6.7A). The PCR data on the effects of MPTP induced *gfap* expression directly supports the GFAP immunofluorescence data for the telencephalon at this time point (Fig. 6.7). However, while GFAP immunofluorescence remained very low in the fish treated with both MPTP and fadrozole, *gfap* mRNA levels were similar to control values at 7 days following MPTP injection (Fig. 6.7A). There were no observable effects detected for *gdnf* expression in the telencephalon (Fig. 6.7C). As reported at the previous time point (Fig. 6.7E), there were no

major effects on *bdnf* in the telencephalon (Fig. 6.7E). Fadrozole exposure significantly reduced *cyp19a1b* expression in the telencephalon, and there were no effects of MPTP detected (Fig. 6.7G).

Complex, and statistically significant interactions were evident for MPTP and fadrozole on the expression of *gfap*, *gdnf* and *bdnf* in the hypothalamus (Fig. 6.7B,D,F) at 7 days following MPTP injection (experimental day 11). While the two-way ANOVA did not reveal main effects of MPTP or fadrozole alone, post-hoc tests indicated that *gfap* expression was lowest in the hypothalamus of those fish treated with both MPTP and fadrozole (Fig. 6.7B). There was a main effect of fadrozole to reduce *gdnf* expression, and this was more pronounced in fish treated with both MPTP and fadrozole (Fig. 6.7D).

Two-way ANOVA indicated that fadrozole but not MPTP alone decreased hypothalamic *bdnf* expression; the post-hoc test indicated that the expression of *bdnf* was lowest in the hypothalamus of those fish treated with both MPTP and fadrozole (Fig. 6.7F). Hypothalamic *cyp19a1b* expression was significantly affected by both MPTP and fadrozole (Fig. 6.7H). At this time point, MPTP was found to increase *cyp19a1b*, but no interaction with fadrozole was detected by two-way ANOVA analysis.

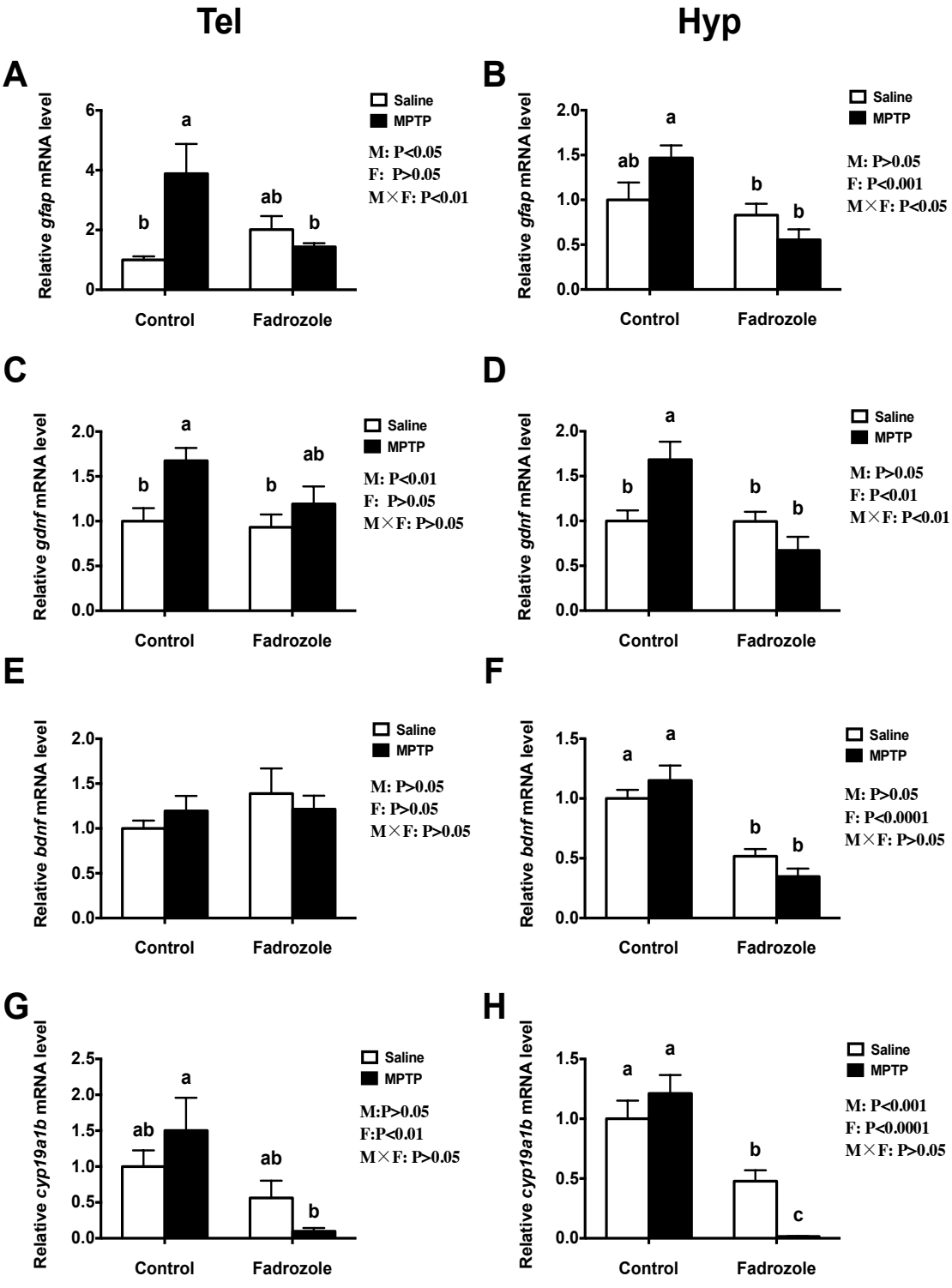
Tel
Hyp
A
Relative gfap mRNA level
Saline
MPTP
M: P<0.05
F: P>0.05
M×F: P<0.01
Control
Fadrozole
B
Relative gfap mRNA level
M: P>0.05
F: P<0.001
M×F: P<0.05
C
Relative gdnf mRNA level
M: P<0.01
F: P>0.05
M×F: P>0.05
D
Relative gdnf mRNA level
M: P>0.05
F: P<0.01
M×F: P<0.01
E
Relative bdnf mRNA level
M: P>0.05
F: P>0.05
M×F: P>0.05
F
Relative bdnf mRNA level
M: P>0.05
F: P<0.0001
M×F: P>0.05
G
Relative cyp19a1b mRNA level
M:P>0.05
F:P<0.01
M×F: P>0.05
H
Relative cyp19a1b mRNA level
M: P<0.001
F: P<0.0001
M×F: P>0.05

Figure 6.6. Quantitative real-time RT-PCR analysis showing variations in the relative amounts of the mRNA encoding genes related to RGC function in the telencephalon (A,C,E,G) and hypothalamus (B,D,F,H) of female goldfish injected with MPTP (4d) and exposed to fadrozole (8d). Bars represent the mean + SEM in 8 different cDNA samples; values for each sample were determined in duplicate. Two-way ANOVA followed by Tukey's test was performed to determine the effects of MPTP and fadrozole treatments. Treatment groups marked by different letters have significantly different mRNA levels ($P < 0.05$).

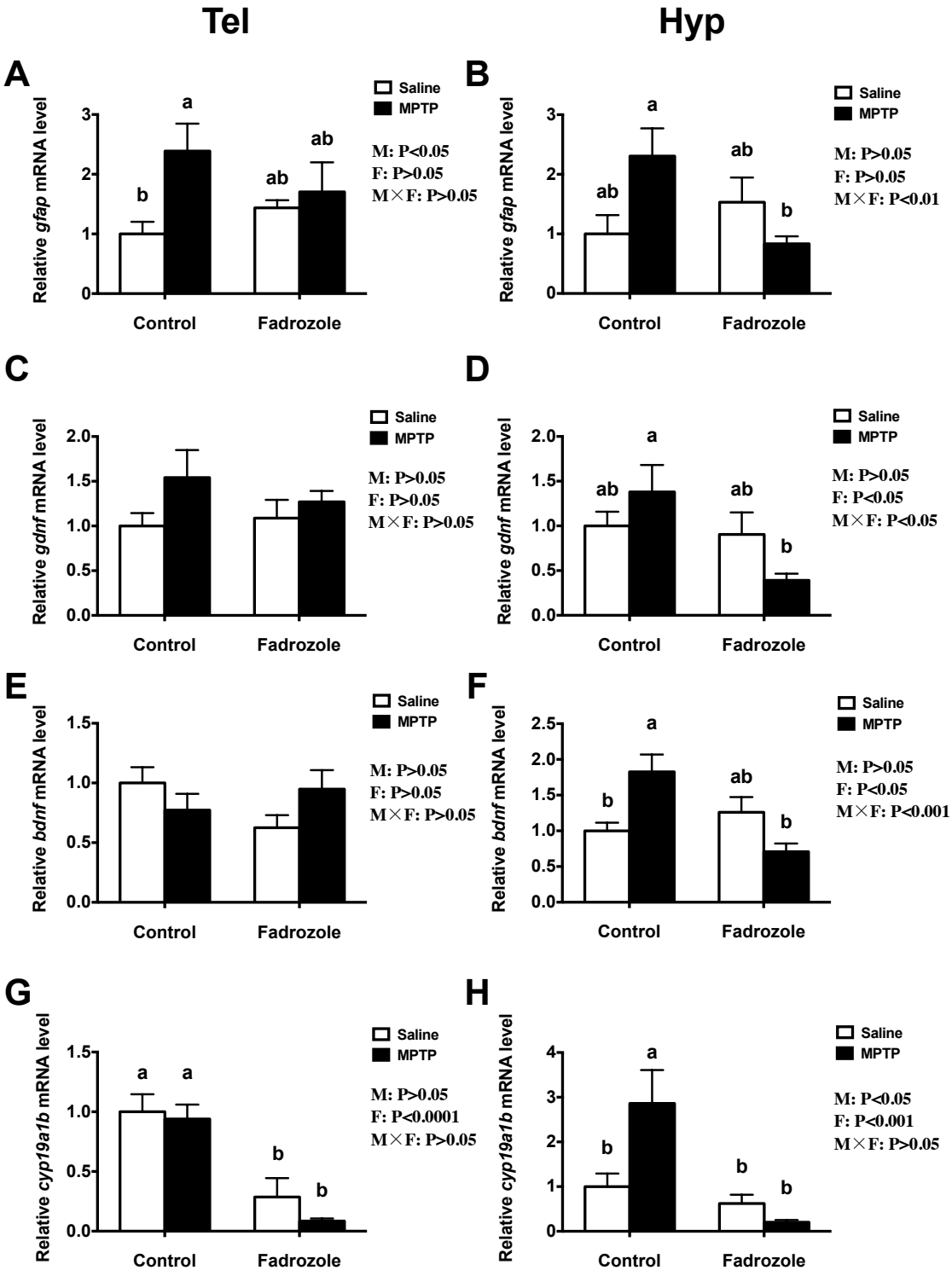
Tel
Hyp
A
B
C
D
E
F
G
H
Saline
MPTP
Relative gfap mRNA level
M: P<0.05
F: P>0.05
M×F: P>0.05
M: P>0.05
F: P>0.05
M×F: P<0.01
Relative gdnf mRNA level
M: P>0.05
F: P>0.05
M×F: P>0.05
M: P>0.05
F: P<0.05
M×F: P<0.05
Relative bdnf mRNA level
M: P>0.05
F: P>0.05
M×F: P>0.05
M: P>0.05
F: P<0.05
M×F: P<0.001
Relative cyp19a1b mRNA level
M: P>0.05
F: P<0.0001
M×F: P>0.05
M: P<0.05
F: P<0.001
M×F: P>0.05
Control
Fadrozole

Figure 6.7. Quantitative real-time RT-PCR analysis showing variations in the relative amounts of the mRNA encoding genes related to RGC function in the telencephalon (A,C,E,G) and hypothalamus (B,D,F,H) of female goldfish injected with MPTP (7d) and exposed to fadrozole (11d). Bars represent the mean + SEM in 8 different cDNA samples; values for each sample were determined in duplicate. Two-way ANOVA followed by Tukey's test was performed to test the effects of MPTP and fadrozole treatments. Treatment groups marked by different letters have significantly different mRNA levels ($P < 0.05$).

6.5 Discussion

In this study, we successfully induced DA neuron degeneration using the neurotoxin MPTP and inhibited aromatase activity using fadrozole in adult female goldfish. We demonstrated the important roles of estrogens and RGCs in DA neuron regeneration in female goldfish brain. Data showed that the activation of RGCs and DA neuron recovery processes are estrogen-dependent.

We first confirmed that the physiological effects of fadrozole and MPTP. Fadrozole is a potent selective inhibitor for estrogen-synthesizing aromatase, which decreases the circulating estrogen levels in the goldfish serum and impair gonadal development and maturation (Zhang et al., 2009a). Here, the effects of fadrozole were observed through the reduction of ovary mass as well as the decrease of *cyp19a1b* mRNA in fadrozole treated groups at both 8 and 11 days after exposure. The MPTP model of goldfish has been validated and widely used for PD research by numerous research groups (Hibbert et al., 2004; Popesku et al., 2010; Weinreb and Youdim, 2007). Our previous studies showed that DA neuron degeneration starts within 4 days post injection of MPTP and that DA levels reach their

lowest value in the hypothalamus at day 4, followed by full recovery to baseline levels at day 7 in goldfish (Popesku, 2009). This suggests that DA neurons in the goldfish hypothalamus are regenerating from day 4 to day 7 post injection of MPTP (Popesku et al., 2012). Pollard et al. showed full recovery of DA levels in the brain of goldfish after 8 days using the same dose of MPTP (50 μg/g) (Pollard and Conti, 2007). Poli et al. (Poli et al., 1992) previously showed spontaneous recovery of DA and norepinephrine levels in the goldfish telencephalon, diencephalon and medulla after 6 weeks following injection of MPTP at a lower dose (10 μg/g) for three consecutive days. Neither of the previous studies, however, conducted any gene expression analyses as presented here. In our study, a single injection of MPTP (50 μg/g body mass) was used to induce DA neuron degeneration. Reduction of TH protein level observed by immunohistochemistry suggested that there is a significant TH-positive neuron damage or loss in the area of preoptic periventricular nucleus. Our transcriptional data showed no decrease on *th* mRNA level at day 4 post-injection of MPTP in the telencephalon, which could be due to the compromised DA neurons are up-regulating *th* transcription to compensate decreased TH protein level. As the rate-limiting enzyme in DA synthesis, *th* mRNA up-regulation could be a very important early compensatory mechanism, especially in animals with high regenerative capacity like goldfish. This compensation can also be seen in our transcriptional data on *slc6a3* expression, which suggests the compromised DA neurons were preparing to increase re-uptake of DA in an attempt to maintain an overall normal DA levels. In the hypothalamus, DA neuron recovery after neurotoxin MPTP insult is characterized by the changes in the *th*, *slc6a3* and *pitx3* expression. The expression of *th* was decreased at day 4 post injection of MPTP, which directly supports our immunohistochemistry data, indicating the compromise of DA synthesis system and the DA

neuron loss. The up-regulation of *slc6a3* and *pitx3* expression started at 4 days and continued until 7 days post-injection of MPTP showing the compensation and regeneration of DA neurons. Data also showed the up-regulation of *slc6a3* and *pitx3* expression was attenuated upon the exposure to fadrozole indicating that the DA neuron regeneration induced by MPTP is estrogen-dependent.

Significant glial scar formation is associated with a DA neuron depletion in PD affected humans and MPTP-treated squirrel monkeys (Forno et al., 1992; Forno et al., 1996). Emerging evidence indicates that the roles played by glial cells in PD may not be restricted to its basic function, that is gliosis, but also include actions which significantly and actively contribute to the regeneration of DA neurons (Elisabeth et al., 2015; Episcopo et al., 2013). Prior to this study, there was little information about the RGC activation and their potential roles in DA neuron regeneration in teleost models of PD. Here, we observed that GFAP immunostaining was increased at both day 4 and 7 post-injection of MPTP, directly supported by the *gfap* gene expression data, showing the activation of RGCs in the goldfish telencephalon. An increase in GFAP mRNA and protein levels is a prominent feature of degenerative diseases such as PD and a hallmarker for glial cell activation (Episcopo et al., 2013; Schuster et al., 2010). Even though the full functions of GFAP are not well understood, as an intermediate filament protein, GFAP is believed to be involved in gap junctional communication between glial cells and neurons (Li et al., 2008b), which could be potentially beneficial to compromised neurons after brain injury or insult. In the hypothalamus, the expression of *gfap*, *gdnf* and *bdnf* had a similar up-regulation pattern following MPTP injection, showing the activation of RGCs in the goldfish hypothalamus as well. Although we found that gene expression of *gdnf* and *bdnf* were regulated differently in the

telencephalon and hypothalamus, up-regulation after MPTP injection is common to both tissues. This is consistent with a variety of findings on the activation of glial cells, especially astrocytes, in MPTP-induced mammalian PD models (Episcopo et al., 2013; Forno, 1996). Reactive astrocytes in mammals have been shown to secrete a number of neurotrophic factors including GDNF, BDNF and mesencephalic astrocyte-derived neurotrophic factor (MANF) (Chen et al., 2006; Petrova et al., 2003), which have been proven to be beneficial to damaged DA neurons. Furthermore, we found that MPTP-induced up-regulation of neurotraphic factor mRNAs was attenuated by inhibiting aromatase with fadrozole. This finding indicates that estrogens are involved in neurotrophic factor synthesis after neurotoxin insult and supports the hypothesis that estrogens are neuroprotective.

Estrogenic modulation of brain functions has strong implications on the management of inflammation, trauma, ischemia and neurodegeneration caused by aging and neurological disorders (Pietranera et al., 2015). Therefore, estrogens qualify as the "neuroprotectants" in the adult brain. The protective effects of estrogens in the adult brain involves the prevention of excitotoxicity, inflammation and oxidant injury, the inhibition of apoptosis, the promotion of neuronal survival, the regulation of dendritic remodelling, synaptogenesis and steroidogenesis and the regulation of a plethora of neurotransmitters: acetylcholine, DA, 5-HT, glutamate and GABA (Azcoitia et al., 2003; Brinton, 2008; Garcia-Segura et al., 2003; Lephart, 1996; McEwen, 2002; Suzuki et al., 2007; Ubuka et al., 2014). Moreover, chronic deprivation of estrogens by fadrozole inhibition of aromatase *in vivo* altered expression of numerous genes and pathways implicated in the control of neuronal plasticity and neuroendocrine function in female goldfish brain (Zhang et al., 2009b). We demonstrated that the reaction of RGCs to MPTP is estrogen-dependent. However, more studies on the

direct effects of estrogens in brain repair and the underlying molecular mechanisms in adult teleosts are needed.

In conclusion, estrogens in female goldfish brain have essential roles in glial reaction in the MPTP-induced PD model. The production of neurotrophic factors GDNF and BDNF in adult brain and genes involved in DA neuron development including *th, slc6a3* and *pitx3* are under modulation of estrogens, especially after damage. It is imperative that the evaluation of global effects of estrogens should be fully explored, especially with regard to their neuroprotective efficacy in neurodegenerative disorders, as they may serve as a broad-spectrum therapeutic agent for use in humans.

Chapter 7: General Discussion

Estrogens are gonadal hormones yet exert diverse non-reproductive actions on the vertebrate CNS. Although discovered more than a century ago, knowledge of the functions of estrogen is still expanding. Numerous studies have focused on the neuroprotective roles of estrogens in adult mammalian brain, but without any comparative aspects in the teleost brain in the past 20 years. A thorough understanding of the roles and regulation of estrogens in fish brain would not only provide comprehensive knowledge of estrogenic actions on the brain, but also reveal more information on the high regenerative capacity of the teleost brain. Until now, the only known regulator of neuroestrogen synthesis in the teleost brain is estradiol-17β through a positive feedback system, which has mainly been studied during development. In this thesis, the regulation of the estrogen-synthetic enzyme aromatase in adult teleost RGCs, which are the primary source of neuroestrogen synthesis, by DA was discovered. The effects of endogenous estrogens on compromised DA neurons caused by neurotoxin insult were also investigated. In this chapter, estrogens are also the focus of discussion to understand the interactions between DA neurons and RGCs in both directions, from DA neurons to RGCs and from RGCs to DA neurons, in the goldfish brain. Here I interpret and place my findings within larger context of what else is already known about neuroestrogens, RGCs and DA. The main results of the research are summarized in Fig. 7.1.

7.1 Actions of DA neurons on RGCs

In Chapter 2, both immunofluorescence and *in situ* hybridization data confirmed the similar expression pattern of *cyp19a1b* in goldfish RGCs along the ventricular surface, with

a similar expression patter as in other teleost species, including eel, zebrafish and midshipman (Forlano et al., 2001; Jeng et al., 2012b; Tong et al., 2009). Due to the special location of these aromatase-positive RGCs, they are potentially under tight regulation by neurotransmitters, neuropeptides and neurohormones from cerebrospinal fluid (CSF) in the ventricle and from surrounding cells in the forebrain. The immunohistochemical studies on RGCs and DA neurons revealed a close anatomical relationship between them and the expression of D1R on aromatase-positive RGCs (Chapter 2). This suggests that DA released from DA neurons located at the NPP and perhaps also from CSF could regulate aromatase in RGCs. Previous microarray studies also provided fundamental information on the dopaminergic regulation of brain aromatase in goldfish hypothalamus (Popesku et al., 2010), however the underlying mechanisms were unexplored. The establishment of the first teleost RGC culture serves as an excellent platform for detailed studies on neuroendocrine function of RGCs, and thus is a novel and important contribution of my work. Data from gene expression studies (Chapter 3 and Chapter 4) and proteomic studies (Chapter 5) also confirmed the existence of D1R and ERs in cultured RGCs. Together, all these findings suggests a potential regulation of aromatase in RGCs by DA and estrogens through modulation of D1R and ERs.

In Chapter 2 and Chapter 3, both *in vivo* and *in vitro* studies were performed to better understand the regulation of *cyp19a1b* expression in RGCs by DA and the mechanisms involved. In adult goldfish brain, *in vivo* time course studies on dopaminergic regulation of *cyp19a1b* expression by the SKF 38393 in goldfish telencephalon and hypothalamus revealed a brain region-specific and time-specific regulation pattern. The established primary RGC culture system eliminates the influence from other cells in the goldfish forebrain, so

direct action of neurotransmitters and hormones can be determined. This *in vitro* model was used for pharmacological studies to show that D1R activation increases *cyp19a1b* mRNA level in cultured RGCs through the D1R/cAMP/PKA/p-CREB signaling pathway (Fig. 7.1). The results from *in vitro* studies (Chapter 3) did not correlate to the *in vivo* findings (Chapter 2) in the direction of *cyp19a1b* regulation, which suggests the regulation network of *cyp19a1b* expression in goldfish brain is complicated. The difference between the regulation pattern in the hypothalamus and in the telencephalon as well as the difference between *in vivo* and *in vitro* observations could be due to 1) the recruitment of different DA D1R subtypes; 2) the involvement of different ERs; 3) different abundance levels of RGCs and *cyp19a1b* mRNA; 4) indirect effects of DA on other regulatory neurons for RGCs in the brain. However, all together, both *in vivo* and *in vitro* studies suggested a regulatory role of DA on aromatase expression.

Aromatase B is only expressed in RGCs, and never in neurons in teleosts. Thus, the up-regulation of *cyp19a1b* expression caused by DA may maintain the non-neuronal characteristics of RGCs and keep them as progenitors in the brain. This hypothesis was further confirmed by the proteomic studies performed in Chapter 5, which identified and quantified proteins differentially expressed by RGCs treated with D1R agonist and revealed much more information about RGCs in culture and the effects of D1R agonist on them. The SNEA on proteins regulated by D1R agonist detected that many of them, including PHGDH, PA2G4, nucleolin and TPI, are involved in cell proliferation, cell cycle and cell survival (Fig. 7.1). The regulation of these proteins indicates that DA has a role in regulating the progenitor functions of RGCs likely through steroids, cAMP, ATP, Ca^{2+}, stress-related molecules and transcription factor-mediated pathways.

The goldfish model of PD was also used to investigate the effects of dopaminergic chemicals on RGCs in the goldfish brain (Chapter 6). The injection of neurotoxin MPTP induced DA neuron damage and loss in the goldfish NPP, as determined by TH immunocytochemistry. Glial scar formation has been observed in conjunction with a DA neuron depletion in PD affected humans and MPTP-treated squirrel monkeys (Forno et al., 1992; Forno et al., 1996). After MPTP injection, GFAP immunoreactivity along the goldfish brain ventricle was increased, which is a sign of RGC activation. Activated RGCs after MPTP injection tend to have higher transcript levels of neurotrophic factors *gdnf* and *bdnf* as well as the intermediate filament protein *gfap,* which is consistent with previous findings on reactive astrocytes in mammalian models of PD (Chen et al., 2006; Petrova et al., 2003). Findings from Chapter 6 also suggest that either the signals from the comprised DA neurons or the low DA levels in goldfish brain after MPTP injection activates RGCs, which indicates an inhibitory role of DA on RGC functions.

7.2 Actions of RGCs on DA neurons

Studies on the roles of estrogens in female goldfish performed in Chapter 6 confirmed the important functions of estrogens in DA neuron loss, compensation and recovery processes. The goldfish model of PD using MPTP injection and of chronic estrogen deprivation by fadrozole inhibition of aromatase were established for the studies. The findings that the up-regulation of *th*, *slc6a3* and *pitx3* was attenuated by fadrozole-induced estrogen derivation (Fig. 7.1) suggested that the DA neuron recovery process is at least partially estrogen-dependent and provides key information on the roles of estrogens in animal models of PD. As the only cell type expresses aromatase in teleost brain, RGCs have

an essential role in supplying neuroestrogens and many other neurotropic factors to the brain, especially to damaged neurons. The production of neurotrophic factors GDNF and BDNF in adult brain are also under the modulation of estrogens, especially after damage. This suggests that estrogens are involved the neurotrophic factor synthesis after neurotoxin insult and supports the hypothesis that estrogens are neuroprotective. Studies in mammalian models of PD have also reported on the neuroprotective roles of estrogens (Saunders-Pullman, 2003; Sawada and Shimohama, 2003). Epidemiologic and clinical findings have also suggested that estrogens play a role in modulating PD onset and progress (Saunders-Pullman et al., 1999; Schapira and Jenner, 2011; Wooten et al., 2004). Furthermore, both reactive astrocytes and RGCs are stem-like cells, which can differentiate into other cell types in the CNS (Addis et al., 2011; Episcopo et al., 2013; Li et al., 2008b; Malatesta et al., 2000; Mashanov et al., 2013; Pilz et al., 2013). In the adult teleost brain, the differentiation of RGCs into other neurons including DA neurons after neurotoxin insult should be an area of focus for future studies.

7.3 Actions of RGCs on RGCs

In teleost brain, communications between RGCs also exist. It is hypothesized that estrogens synthesized and released from RGCs are autoregulatory and can also affect neighbouring RGCs through paracrine mechanisms (Fig. 7.1). Previous studies have shown that the primary estrogen, E2, can increase the expression of aromatase in a positive feedback manner in brain and gonads. In this thesis, similar positive feedback regulation pattern was also observed in RGC cultures, indicating for the first time direct estrogen action on RGCs. The up-regulation of *cyp19a1b* expression in RGCs by E2 is potentially occurring

through recruiting existing ERα and ERβ as well as increasing ERγ expression. Moreover, E2 is able to modify the effects of DA on *cyp19a1b* expression. This estrogenic modulation is concentration-dependent; a lower level of E2 increased D1R-dependent *cyp19a1b* expression by up-regulating the mRNA level of *drd1a* and the protein level of p-CREB. With simultaneous stimulation from DA and E2, there is a synergistic up-regulation of *cyp19a1b* expression. However, with high E2 added to the cultures, the up-regulation of *cyp19a1b* expression induced by the D1R agonist was attenuated. This control mechanism of *cyp19a1b* expression suggests a tight regulation of brain aromatase and potentially of neuroestrogen levels by both DA and E2 (Fig. 7.1). It also demonstrates that there is a feedback system for estrogen production in the teleost brain under normal conditions (Chapter 4). On the other hand, when the brain is damaged by neurotoxin MPTP insult, significant glial cell activation associated with DA neuron loss was observed in goldfish brain. The expression of RGC- related genes including *gfap*, gdnf, *bdnf* and *cyp19a1b* were affected by MPTP, and these responses were estrogen-dependent (Fig. 7.1). Studies performed under physiological situations and following MPTP indicate that estrogens have important functions under both normal and injury conditions (Chapter 6).

7.4 Conclusions

The research presented in this thesis provides evidence in support of the hypotheses that DA regulates RGC functions and that estrogens affect the recovery and actions of DA neurons. In the goldfish forebrain, DA released from DA neurons affects *cyp19a1b* expression in neighbouring RGCs, through a D1R-dependent manner. The activation of D1R has an inhibitory role in RGC proliferation and differentiation through small molecule-

mediated and transcription factor-mediated pathways. Estrogens are essential in the process of DA neuron recovery and RGC activation after neurotoxin insult. They could also further enhance or attenuate the actions of DA on *cyp19a1b* regulation in RGCs. Findings from this thesis provide evidence for novel mechanisms underlying estrogen synthesis control by DA and E2 in adult brain (Fig. 7.1). The mechanistic framework discovered will facilitate future research on other molecular mechanisms involved in aromatase regulation, and therefore contribute to studies investigating the combined effects of DA and E2 on estrogen synthesis in the adult brain with other potential regulators. The information on RGCs revealed by proteomic studies allows new hypotheses to be proposed about underlying molecular mechanisms of RGC function regulation by DA or other potential regulators. Possible roles of estrogens uncovered in a goldfish model of PD are partially conserved with regard to neuroprotective effects in mammals, providing evidence for new perspectives on the involvement of estrogens in PD. To conclude, this thesis 1) established a primary RGC culture system and characterized the proteome of goldfish RGCs; 2) identified a novel mechanism of neuroestrogen synthesis control by DA and E2; 3) elucidated the involvement of estrogens in DA neuron recovery and RGC activation after neurotoxin insult.

7.5 Future directions

In addition to what has been outlined in the individual chapters of this thesis, some future directions could include:

1. Dopaminergic regulation of aromatase activity and estrogen release. The studies on the regulation of aromatase B by dopamine in this thesis are mainly focused on the transcriptional level, future studies should be performed to better understand this regulation

on the protein, enzyme activity and functionality levels of aromatase B in goldfish forebrain as well as in cultured RGCs.

2. Searching for other regulators of RGCs. In teleost, RGCs are not in close proximity not only to DA neurons, but also to 5-HT- and to secretoneurin-positive neurons. Future studies should explore other potential regulators of RGC functions and investigate the mechanisms of their actions.

3. Screening endocrine disruptors using primary RGC culture system. The primary RGC culture system served as an excellent platform for studies on dopaminergic regulation of aromatase B. It would also be a great model to study the neurotoxic effects of environmental endocrine disruptors, because RGC is a steroidogenic cell in goldfish brain with the presence of most key steroidogenesis enzymes (See Appendix 2).

4. Transcriptome and secretome profiling of cultured RGCs. The proteome profiling studies provide significant information on the function and regulation of RGCs, studies on the transcriptome and secretome of RGCs should be performed to better understand the roles of these important progenitor cells. By directly comparing the time- and dose-dependent actions of neurotransmitters simultaneously on the RGC transcriptome, cellular proteome and secretome, the direct relationship between receptor activation, cellular processes and secretion can be established for the first time.

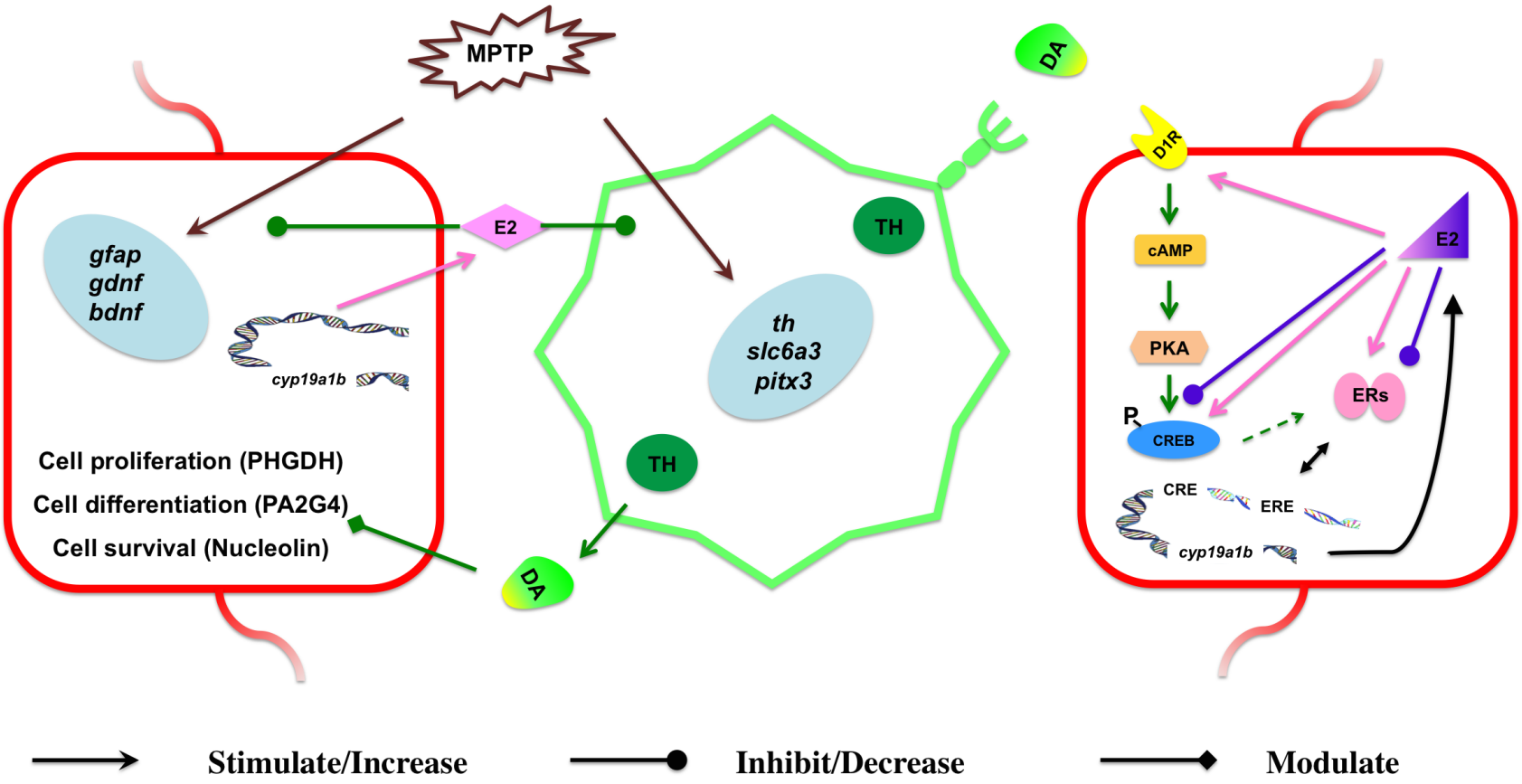

Figure 7.1 Proposed mechanisms underlying interactions between DA neurons and RGCs in goldfish forebrain. See text for details.

Appendix 1: Anatomical relationship between dopamine neurons and radial glial cells in zebrafish

A1.1 Introduction

The zebrafish is an important model organism for genetic, developmental and toxicological studies, especially of the CNS (Kimmel, 1993). Closely related to goldfish, zebrafish also belongs to the family of cyprinidae. Due to the complete transparency of embryos and shorter life span in zebrafish, research on generating transgenic zebrafish using multiple genetic tools have revived great success in the past decades (Stuart et al., 1988; Stuart et al., 1990). Tong *et al*. generated an aromatase B (*cyp19a1b*) transgenic zebrafish line by injecting a green fluorescent protein gene driven by zebrafish *cyp19a1b* promoter and revealed that aromatase B is exclusively expressed in RGCs in zebrafish (Tong et al., 2009). Using the same transgenic zebrafish line, Pérez *et al*. revealed the relationship between RGCs and 5-HT neurons (Pérez et al., 2013). Here, we sought out to study the anatomical relationship between RGCs and DA neurons in zebrafish and the potential effects of DA on RGCs gene expression and function.

A1.2 Materials and Methods

Adult transgenic zebrafish were kept in the zebrafish facilities at University of Ottawa (Ottawa, Canada). For materials and methods on immunohistochemistry and confocal imaging, please refer to Chapter 2, as the same protocol was used for female goldfish.

A1.3 Results

A1.3.1 Anatomical relationship between cyp19a1b-positive RGCs and TH-positive DA neurons.

We show that there is a close anatomical relationship between catecholaminergic neuronal cell bodies and *cyp19a1b*-positive RGCs. Aromatase B is widely distributed along the ventricular surface in zebrafish telencephalon. Intensive TH-positive cell bodies and fibres were observed close to *cyp19a1b*-positive RGCs (Fig. A1.1).

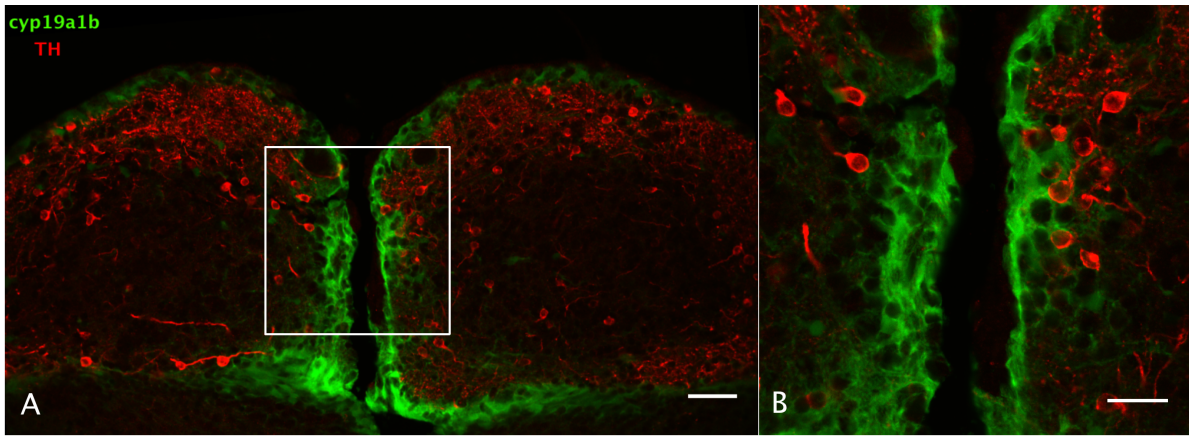

Figure A1.1. Double fluorescence detection of TH (red) and *cyp19a1b*-GFP (green) in zebrafish telencephalon. The confocal images show *cyp19a1b*-positive RGC cell bodies located along the ventricular surface (A). Some catecholaminergic neuron cell bodies and fibres marked by TH are widely distributed in zebrafish telencephalon (A). Magnification of the boxed area in panel A shows that there are very close anatomical relationships between RGCs and catecholaminergic cell bodies and fibres (B). Scale bar = 20 μm in A; Scale bar = 5 μm in B.

A1.3.2 Expression of dopamine D1 receptor in RGCs

The presence of DA receptors on post-synaptic cells is required for direct regulation upon the release of DA by TH-positive catecholaminergic neurons. The D1R-positive staining can be observed along the ventricular surface. The merged confocal images show the colocalization of *cyp19a1b* and D1R immunoreactivity (Fig. 3D, H, L), which indicates that *cyp19a1b*-RGCs express D1R.

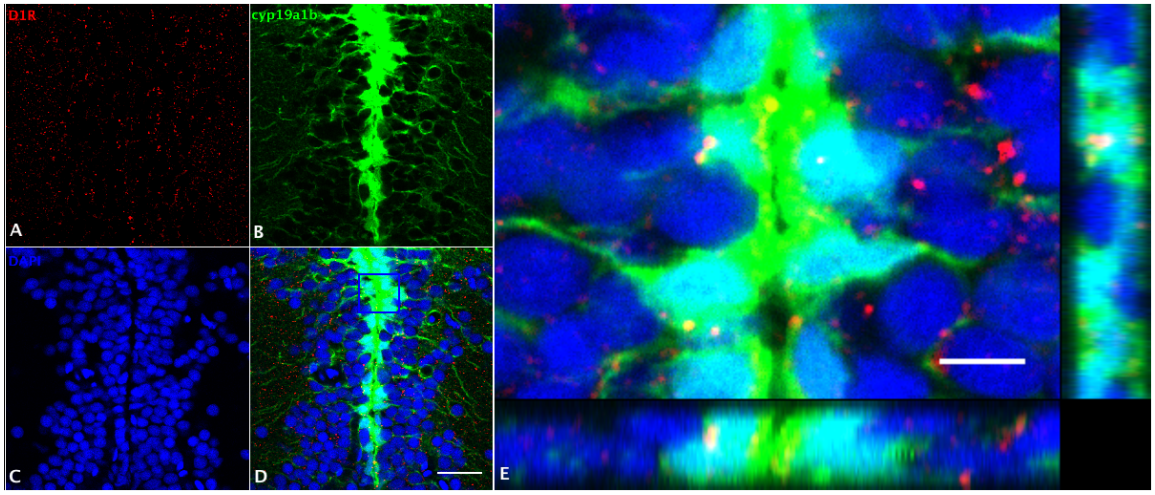

Figure A1.2. Double fluorescence detection of D1R (red,A) and *cyp19a1b*-GFP (green,B) along ventricular surface in zebrafish telencephalon. The confocal image shows that *cyp19a1b*-positive RGCs are located at the ventricular surface and the expression of D1R close to the ventricular surface. The expression of D1R by RGCs is shown in the merged images. Magnification of the boxed area in panel D shows that D1R is expressed by RGCs along the ventricular surface (E). The nuclear stain DAPI (blue) is also shown (C,D,E). Scale bar = 20 μm in A-D; Scale bar = 5 μm in E.

A1.4 Discussion

Data from Chapter 2 showed that aromatase B is exclusively expressed by RGCs in goldfish telencephalon and that there is a close anatomical relationship between TH-positive catecholaminergic neurons and GFAP-positive RGCs in adult goldfish telencephalon. Due to the lack of available aromatase B antibody generated in a different host animal, we could not study the relationship between DA neurons and aromatase B. In this study, we took advantage of *cyp19a1b*-GFP transgenic zebrafish and investigated the relationship between aromatase B and DA neurons directly. The present study provides the information regarding a close anatomical relationship between TH-positive catecholaminergic neurons and *cyp19a1b*-RGCs in adult zebrafish CNS for the first time. Furthermore, D1R staining in *cyp19a1b* transgenic zebrafish showed that *cyp19a1b*-positive RGCs express D1R as well, which suggests that the RGCs in zebrafish telencephalon could potentially receive signals from neighbouring DA neurons and that the activation of D1R may change the functions of RGCs, as I established in goldfish. Together, these two lines of evidence in zebrafish are consistent with our previous findings in goldfish (Chapter 2), which showed that it is conserved between zebrafish and goldfish in this anatomical aspect and strengthened our hypothesis on dopaminergic regulation of aromatase B in RGCs in teleost brain.

Appendix 2: Dehydroabietic acid cytotoxicity in goldfish radial glial cells [7]

A2.1 Introduction

Dehydroabietic acid (DHAA) belongs to the resin acid family and is the most abundant and persistent resin acid found in aquatic environments found to be acutely toxic to fish (Christianson-Heiska et al., 2008; Rissanen et al., 2003). During the pulping process in wood industry DHAA is released in wastewater (Rissanen et al., 2003; Scarlett et al., 2013). In addition, DHAA has been successfully isolated and identified in oil sands process affected water (OSPW) in Alberta's Oil Sands in Canada (Jones et al., 2012). OSPW is produced during the extraction of bitumen and due to its high toxic content it is stored in basins called tailing ponds (Giesy et al., 2010). Although environmental prevalence of DHAA has increased, its toxicity and mechanisms of action have yet to be elucidated.

Trout has been widely used as an animal model for DHAA toxicity studies. Acute effects of DHAA on trout include 1) Cell membrane damage. Previous studies have demonstrated that DHAA can alter trout erythrocytes cell membrane dynamic and functions (Butterfield et al., 1994), potentially by affecting the fluidity and order of the lipid bilayer and the physical state of cytoskeletal proteins (Butterfield et al., 1994). By acting as a detergent DHAA can dissolve in the lipid layer of the erythrocyte membrane, which further increases the permeability of the membrane (Bushnell et al., 1985) causing necrosis. Furthermore, DHAA alters the conformational change of integral proteins leading to an

---

[7] *Partially based on Xing L., Gutierrez-Villagomez, J.M., Da Fonte, D.F., Venables M. and Trudeau VL. (2015). Dehydroabietic acid cytotoxicity in goldfish radial glial cells. Submitted to Toxicon. XL, designed the study, developed the methodology, conducted the majority of experiment and analysis and wrote the manuscript. GVJM, helped with antioxidant enzyme assays. DFDF, helped with cell culture and qPCR experiments. VM, gave critical comments on the manuscript. TVL, helped with the design of the study and editing the article.*

imbalance of intracellular and extracellular ion concentration, such as potassium and sodium (Toivola and Isomaa, 1991). 2) Decrease in energy production. It has been reported DHAA causes energy imbalance in rainbow trout hepatocytes and liver cells (Oikari et al., 1983; Rissanen et al., 2003). In primary cultured rainbow trout hepatocytes, DHAA induces a reduction of cellular ATP content, increased glycolytic activity, cellular oxygen consumption and heat production (Rissanen et al., 2003). Although the underlying mechanisms of failed energetic equilibrium is not clear, several studies proposed that the damage of DHAA on the cell membrane can lead to the depletion of ATP and that overconsumption of ATP may be due to the removal of DHAA from the cell (Oikari et al., 1983). 3) Oxidative damage. Due to its pro-oxidant properties, DHAA can increase lipid peroxidation (LPO) and induce an overall oxidative damage in gills of the Mediterranean mussel, potentially due to their damage on cell membrane (Gravato et al., 2005a). The elevated LPO could cause DNA damage because LPO products can directly react with DNA, resulting in genotoxicity and mutagenicity. 4) Endocrine disruption. The proposal that aquatic DHAA pollutant could act as an endocrine disruptor was supported by studies on European eel exposed to DHAA, which have shown a reduced capacity to elevate plasma cortisol after capture and handling (Teles et al., 2004). Furthermore, environmentally relevant concentrations of DHAA decrease plasma vitellogenin and testosterone levels affecting the overall reproductive physiology of zebrafish (Christianson-Heiska et al., 2008).

To our knowledge, to date no cytotoxicity studies of DHAA in central nervous system (CNS) has been performed. However, one study in African clawed frog oocytes demonstrated that DHAA acts as a positive allosteric modulator of GABA receptors and additionally displays properties of a partial agonist (Rueda et al., 2014). Through modulating

GABA receptor functions, DHAA exposure could potentially lead to severe neurotoxic damage to aquatic animals. Radial glial cells (RGCs) are the most abundant glial cell type in teleost brains. In addition to their traditional roles serving as scaffold for newborn neurons to migrate, they are also the progenitor and steroidogenic cells in the brain and involved in many functions including neuroendocrine and neurogenesis (Xing et al., 2014). Here, we take advantage of our previously established primary RGC culture model to study the cytotoxicity of DHAA on RGCs. We focus on the potential effects of DHAA on oxidative damage, steroidogenesis disruption and cellular morphology.

A2.2 Materials and Methods

A2.2.1 Cell culture and exposures

The hypothalamus and telencephalon were dissected from female goldfish and minced into small pieces. Radial glial cells were dissociated with trypsin (0.25%, Gibco) and cultured in Leibovitz's L-15 medium (Gibco) with 15% Fetal Bovine Serum (FBS, Gibco) and antibiotic-antimycotic solution. Cell culture medium was changed once a week after initial isolation. Radial glial cells were subcultured by trypsinization (0.125%) for 3 passages and then used for experiments. Passage 3 RGCs were exposed to various concentrations of DHAA (Sigma-Aldrich). After 24 hours, culture medium and cells were collected and stored at -80 °C for following experiments. DMSO was used as a vehicle to dissolve DHAA, which showed no effects.

A2.2.2 Cell viability

Cell viability of RGCs was determined by the lactate dehydrogenase (LDH) leakage

assay modified from (Feng et al., 2003; Massarsky et al., 2014). Briefly, after a 24 hr exposure, the cell media were collected and LDH activity was estimated by NADH consumption measured spectrophotometrically (SpectraMax Plus; Molecular Devices) at 340 nm in the presence of NADH (0.35 mM) and pyruvate (4.5 mM) in imidazole buffer (50 mM, pH 7.5). The reaction was monitored at 340 nm over 15 min. The activity was normalized to the control samples (n = 8).

A2.2.3 Immunocytochemistry

Cells were seeded on coverslips in 6-well plate. After 24 hr exposure to various concentrations of DHAA, RGCs were fixed in 4% paraformaldehyde (PFA) for 20 m and blocked in blocking buffer (0.3% Triton PBS containing 1% bovine serum albumin (BSA) for 45min at RT. Fixed cell slides were covered with the anti-GFAP (mouse, 1:500, Millipore, MAB360) (Forlano et al., 2001) overnight then incubated with donkey anti-mouse Alexa fluor 488 (1:500, Molecular Probes) for 1 hour at RT. Slides were washed and mounted with the antifading medium Vectashield with 4,6-diamino-2-phenylindole (DAPI). Images were taken by Nikon A1RsiMP confocal microscope with Nikon's Imaging Software NIS-Elements.

A2.2.4 Activity of antioxidant enzymes

The cells were thawed and vortexed in 50 mM potassium phosphate buffer (1:20 w/v; KPB-50; pH 7.0) and centrifuged for 15 m at 15,000 g (4 °C) in a Beckman Coulter Microfuge® R centrifuge. All enzyme assays were read on a SpectraMax Plus spectrophotometer. The following assays were adapted from (Lushchak et al., 2001; Massarsky et al., 2014): glutathione reductase (GR), glutathione peroxidase (GPx) and

glutathione S-transferase (GST). The enzyme activities were normalized to protein content assessed using the bicinchoninic acid (BCA) assay (Sigma-Aldrich).

A2.2.5 RNA extraction, cDNA synthesis and quantitative real-time RT-PCR

Cells were exposed to various concentrations of DHAA for 24 hr at various concentrations and then collected by trypsinization. The isolation of total RNA was performed by using RNeasy Micro kit (Qiagen). Total cDNA was prepared using Maxima cDNA synthesis kit (Thermo Scientific) and used as the template for the real-time RT-PCR assays. Primers used in the present study were designed using Primer3 and synthesized by Integrated DNA Technologies (Table 1). The Maxima SYBR green qPCR Master Mix (Thermo Scientific) and CFX96 Real-Time PCR Detection System (Bio-Rad) were used to amplify and detect the transcripts of interest. Data were analyzed using the Bio-Rad software package. The relative standard curve method was used to calculate relative mRNA abundance between samples based on the Cq values, which were then normalized by using NORMA-GENE algorithm (Heckmann et al., 2011). Normalized data were used to calculate fold-change against the average value of control and then presented as means + SEM of gene expression from 4 biological replicates (n = 4) (assayed in duplicate) for each group.

Table A2.1 Primer sets used for quantitative real-time PCR in RGCs.

Gene	**Primer Sequence (Forward)**	**Primer Sequence (Reverse)**
star	AGAGTGCCAATGGTGATAAGGT	GGTTCCACTCCCCCATTTGTT
cyp17	ATCTTCGGGGCAGGGGTG	AGGCTGTCTGTCTTTTCCAATCT
hsd17b4	TCAGTTCTCGCTCTTCATCGT	GTTCCAGTCTCCGCTCAATC
cyp19a1b	TGCTGACATAAGGGCAATGA	GGAAGTAAAATGGGTTGTGGA
gdnf	ATGGACTCAGGAACCAAGCA	GTCTGTGACGTTGAGGTGGA
bdnf	TTGAGGAGTTGCTTGAGGTG	GGCGTCCAGGTAGTTTTTGT

A2.2.6 Statistics

Data are presented as mean + SEM. Comparison between groups was performed using one-way analysis of variance (ANOVA) or two-way ANOVA followed by Tukey's post-hoc test or Dunnett's post-hoc test if the data did not pass homogeneity test in Graphpad Prism Version 6.

A2.3 Results

A2.3.1 DHAA is toxic to cultured RGCs

The cytotoxicity of DHAA on RGCs in culture was tested using LDH leakage assay after 24 hr exposure to various doses of DHAA. Data showed that there was a significant effect of DHAA on RGC LDH leakage when the concentration was 20 mg/L ($P < 0.05$) and higher. The concentration of 40 mg/L is lethal to RGCs since no attached cells were observed in culture. Based on the cell viability, the sub-lethal concentrations of 1 mg/L, 10 mg/L and 20 mg/L were chosen for further investigation.

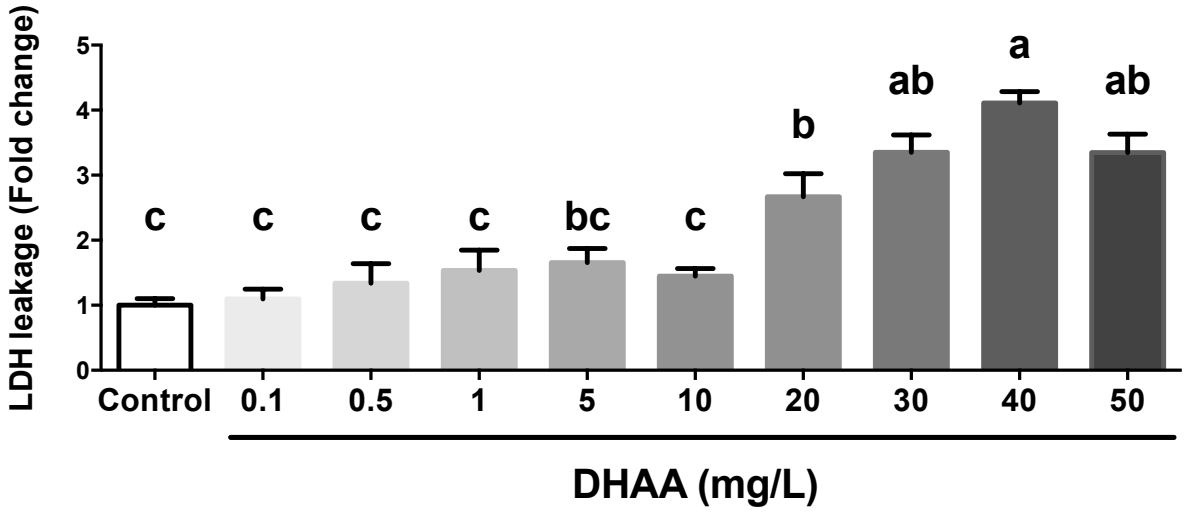

Figure A2.1 Cytotoxicity in RGCs exposed to various concentrations of DHAA for 24 hr. Cytotoxicity was assessed using LDH leakage assay. The results are expressed as fold change of control values. Data are presented as means + SEM (n = 8).

A2.3.2 Effect of DHAA on cell morphology in cultured RGCs.

We examined the RGC morphology changes following a 24 hr exposure to DHAA. The immunocytochemical analysis showed a dramatic reduction of intermediate filament protein GFAP and a severe morphological alteration induced by 20 mg/L DHAA. Compared to control group, RGCs exposed to 20 mg/L DHAA lost their characteristic bipolar shape. Most cells under the microscope exhibited round shape, and no visible processes and reduction of cell body.

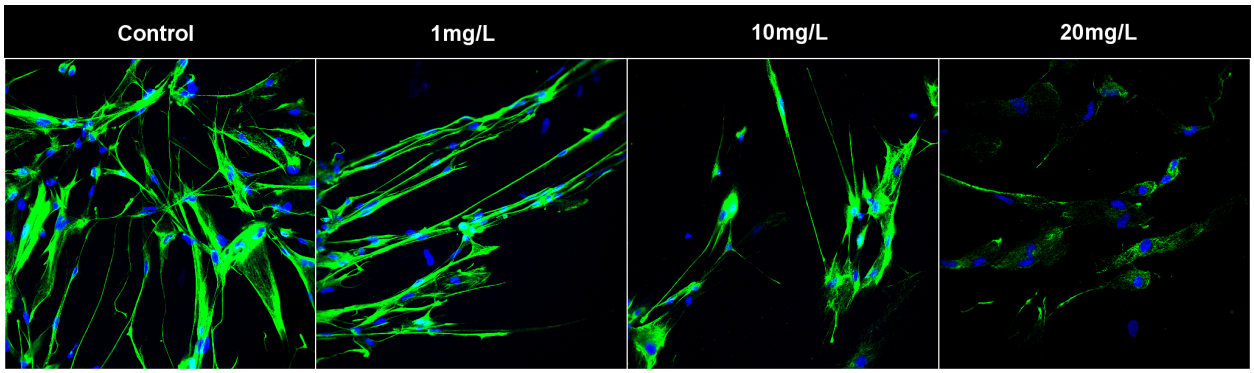

Figure A2.2 Immunocytochemical analysis of cell morphological changes induced by DHAA exposure. Cell intermediate filament was stained with anti-GFAP antibody (Green) and DAPI (Blue). Control RGCs display a typical bipolar shape with long processes extending. Cells exposed to 20mg/L DHAA showed significant decrease in GFAP protein level and cell morphological changes.

A2.3.3 Effects of DHAA on antioxidant enzyme activity

Next, we sought to measure the effects of DHAA on the activity of GST, GPx and GR. Surprisingly, there was no significant difference on the activity of GST, GPx and GR between any of the concentrations of DHAA compared to the control group ($P < 0.05$).

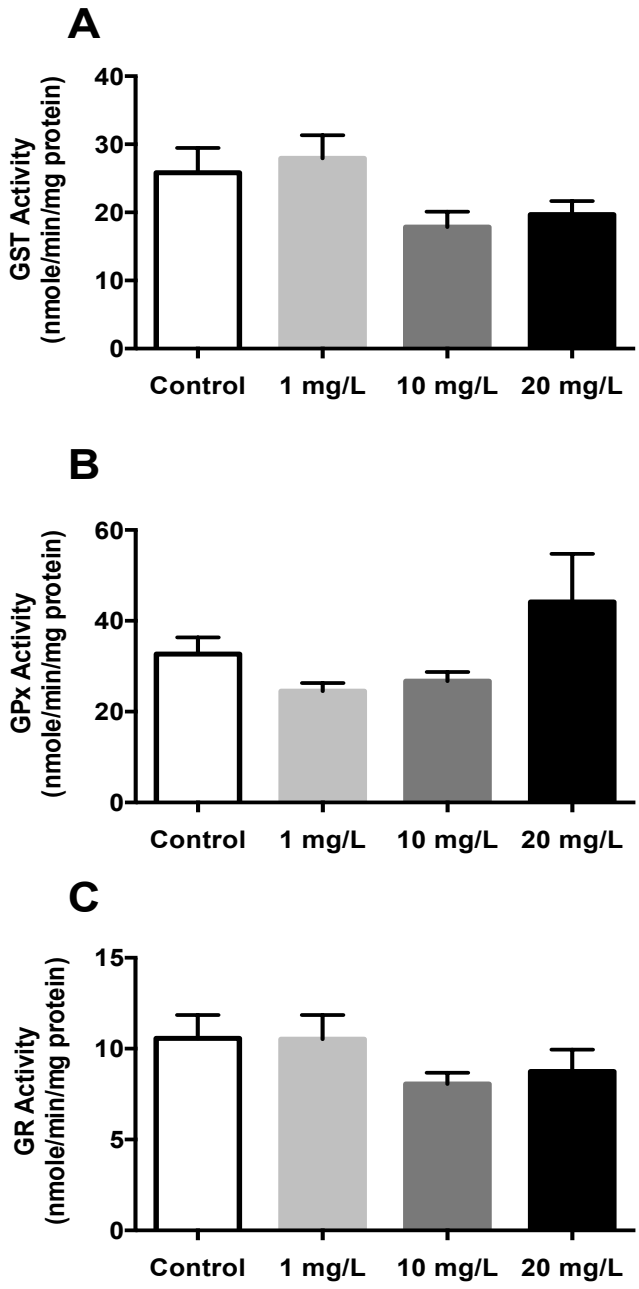

Figure A2.3 Effects of a 24hr DHAA exposure on antioxidant enzymes in cultured RGCs. The GST, GPx and GR activity levels in DHAA exposed cells showed no significant difference to control value. The bars represent the mean + SEM (n = 8).

A2.3.4 Effects of DHAA on expression of steroidogenic enzymes and neurotrophic factors

RGCs are steroidogenic cells in the fish CNS, and we hypothesize that DHAA exposure would disrupt the steoroidogenic functions of RGCs. Data from qPCR analysis showed a concentration-dependent regulation of *star* expression in cultured RGCs by DHAA, 10 mg/L DHAA and 20 mg/L reduced *star* expression to 34% ($P < 0.05$) and 21% ($P < 0.05$) of control value. The expression of *cyp17* and *hsd17b4* were increased by 20 mg/L DHAA by 9.2 fold ($P < 0.05$) and 3.2 fold ($P < 0.05$), respectively. There was no significant difference between DHAA and control groups on the expression of *cyp19a1b*, *gdnf* and *bdnf* ($P > 0.05$).

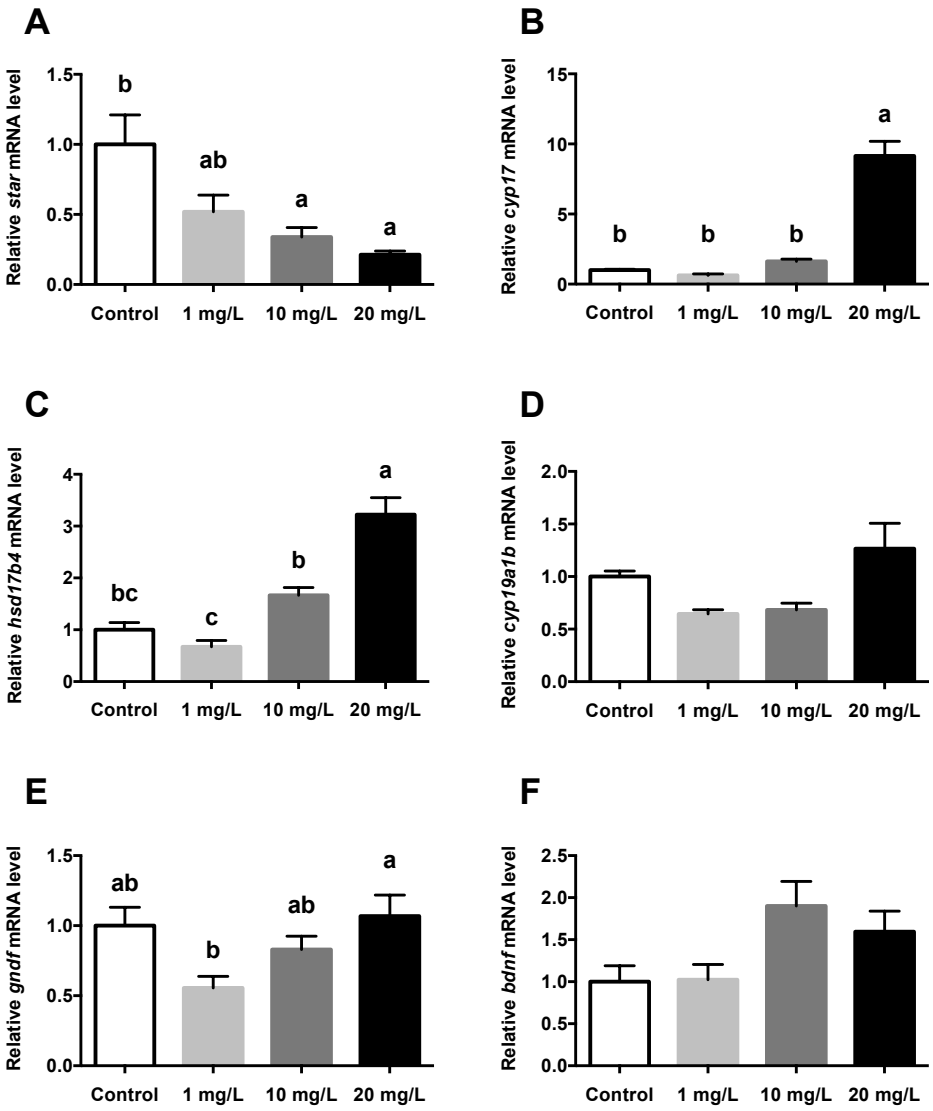

Figure A2.4. The effects of various concentrations of DHAA on the mRNA levels of steroidogenic enzymes and neurotrophic factors in cultured RGCs. Quantitative real-time PCR analysis of the mRNA levels of *star* (A), *cyp17* (B), *hsd17b4* (C), *cyp19a1b* (D), *gdnf* (E) and *bdnf* (F) in primary RGC culture after 24h exposure of different doses of DHAA. Data were defined as fold change relative to control, the bars represent the mean + SEM (n = 4), each sample was analyzed in duplicate. Groups marked by different letters are significantly different ($P < 0.05$).

A2.4 Discussion

In this study, we used a previously established culture model (Xing et al., 2015) to test the cytotoxicity of DHAA on goldfish RGCs. Data showed that DHAA is toxic to RGCs in culture after 24 hrs exposure to a 20 mg/L dosage. The effects of DHAA on RGCs include altering cell morphology and altering the expression of steroidogenic protein and enzymes like *star*, *cyp17* and *hsd17b4*, but not the activities of antioxidant enzymes such as GST, GPx and GR or the expression of neurotrophic factors like *gdnf* and *bdnf*.

In the previous study, a primary RGC culture system was established to study the RGC cell functions *in vitro*. Here, we take advantage of the culture system to investigate the cytotoxicity of DHAA on RGCs and demonstrate that 20 mg/L DHAA is toxic to RGCs *in vitro*. A wide range of doses was used in the present study to fully characterize the lethal and sub-lethal concentrations of DHAA to RGCs in culture. Data suggest that DHAA is lethal to RGCs when concentration is up to 30 mg/L. It is important to note that the DHAA concentrations (1 mg/L, 10 mg/L and 20 mg/L) used to investigate other effects of DHAA on RGCs in this study are similar and higher than the environmental concentration of ~4 mg/L measured in effluents following a resin spill in a paper mill in the United States (Makris and Banerjee, 2002). However, being relatively lipophilic and with a small molecular weight, DHAA is believed to accumulate in fish with a bioaccumulation factor of 50 to 200 and capable of reaching a concentration of 300 mg/L in fish plasma after acute exposure to a sub-lethal dosage (0.4 mg/L). Thus, the concentration of DHAA in the brain of aquatic animals is hypothesized to be higher than 20 mg/L used in this study.

As the organizer of brain structure during both development and adulthood, RGCs

differentiate into neurons and guide the newborn neuron migration (Rakic, 1971a; Zupanc and Clint, 2003). This has been reported by several studies showing the close proximity between migrating neurons with elongated cell nuclear and RGCs with extending fibers, (Barry et al., 2014; Zupanc and Sîrbulescu, 2011; Zupanc et al., 2012). The induction of morphology alteration by DHAA at sub-lethal concentrations could be extremely harmful to species with high regenerative capacity like goldfish. Due to the loss of RGC fibers, newly generated neuron precursor cells in the adult brain are not able to migrate to their final destination and maturate to functional neurons without guidance. Furthermore, the cell death caused by DHAA at lethal concentrations leads to significant reduction of progenitor cell numbers in the brain. Thus, the regenerative capacity of the brain will be compromised greatly after exposing to DHAA in the aquatic environment.

Since RGCs are steroidogenic cells in the CNS of fish, it was hypothesized that DHAA exposure would disrupt the steroidogenic functions of RGCs. The normal expression levels of steroidogenic enzymes in RGCs maintain a physiological level of steroids in the brain (Diotel et al., 2011b; Jeng et al., 2012b; Xing et al., 2014). Neurosteroids have many roles in controlling the processes, including stress, neuroprotection and neurogenesis (Elisabeth et al., 2015; Pesonen and Andersson, 1992; Pietranera et al., 2015; Waye and Trudeau, 2011). Here, our finding suggests that 20 mg/L DHAA exposure decreases *star* expression. As the first step in steroidogenesis pathway, StAR protein level determines the availability of potential substrate for steroid synthesis (Anuka et al., 2013). The reduction of *star* expression would potentially disrupt the synthesis of all steroids and have great impact on overall brain functions. However, in contrast to the changes of *star* expression, the expression of *cyp17* and *hsd17b4* were increased by DHAA after 24 hrs, which could be a compensatory

mechanism employed by RGCs to maintain normal steroid level. However, further studies are needed to investigate the steroid level alteration by DHAA exposure.

Numerous studies have reported the effects of resin acid on oxidative stress in aquatic animal and cell culture models (Butterfield et al., 1994; Christianson-Heiska et al., 2008; Gravato et al., 2005b; Pesonen and Andersson, 1992). It was our original hypothesis that DHAA induces the oxidative stress in RGC cultures. However, our data suggest that DHAA at sub-lethal concentrations do not cause oxidative stress, at least not alter the enzyme activity levels of GST, GR and GPx. In conclusion, we report that DHAA maybe toxic to goldfish RGCs at environment related levels and that lower concentrations of DHAA could alter the morphology and steroidogenic functions of goldfish RGCs *in vitro*.

Appendix 3: Supporting information

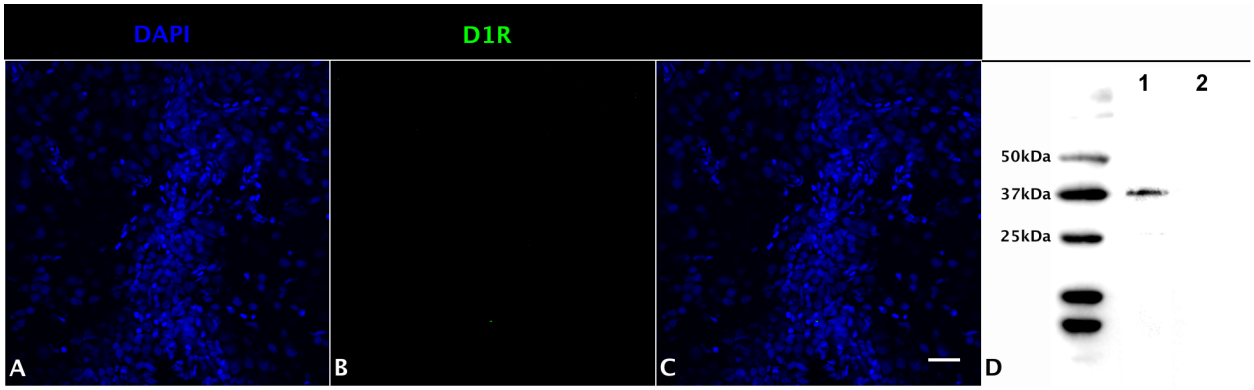

Figure A3.1. Validation of D1R antibody. The anti-D1R antibody against mouse and rat D1R was purchased from Acris Antibodies (AP09963PU-N). It was generated against a 19 amino acid sequence (IYRIAQKQIRRISALE). This short amino acid sequence is 100% identical to an equivalent portion of goldfish D1R (accession no. P35406.1). D1R control peptide (Acris, AP09963CP-N) was purchased from Acris antibodies and preabsorbed (10 µg/ml at 4°C overnight) with D1R antibody. Immunohistochemistry was performed and showed no positive staining (B). The nuclear stain DAPI (blue) is also shown (A,C). Scale bar = 20µm. To further test whether D1R antibody was recognizing D1R, western blot was performed to investigate the molecular weight of D1R antibody recognized protein. One band (40kDa) was detectable using D1R antibody (1:1000) in goldfish telencephalon tissue (D, lane 1). No band was detected after prebsorption of D1R (1:1000) and control peptide (2.5 µg/ml at 4°C overnight) (D, lane 2).

A

Gene	Primers	Product Size	Identity	Accession No.
d1r	F: TTTTTGTCTGGTTCGGATGG R: TCTATTTCCCCCTTGCTTTG	205	100%	L08602.1

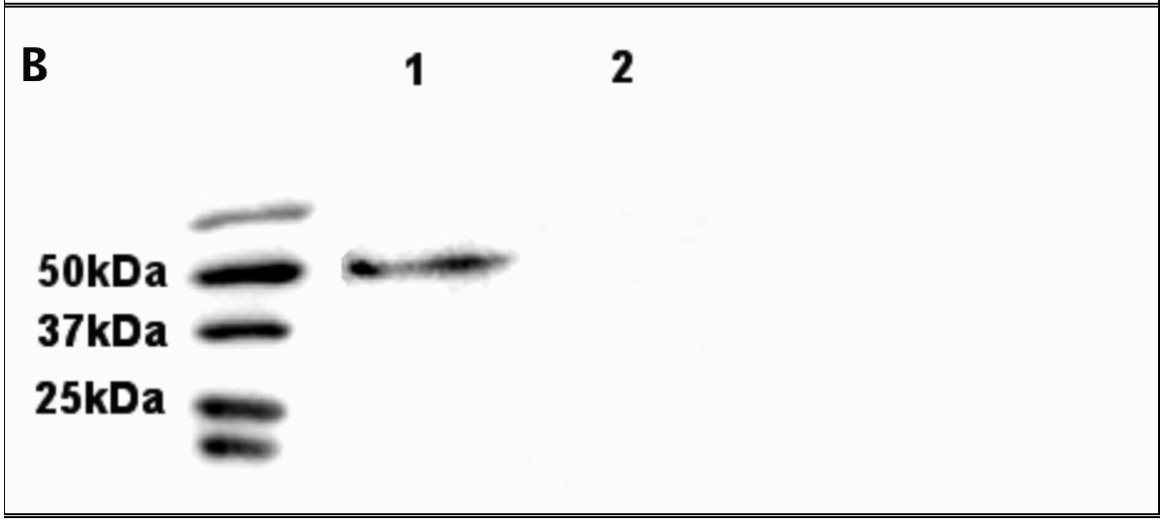

Figure A3.2. The expression of D1R in RGC cultures. Direct sequencing was performed using RGC cDNA samples to confirm the existence of D1R mRNA (A), the PCR product is 100% identical to goldfish D1R (Accession L08602.1). Western blot image shows the expression of D1R in RGC culture (B, lane 1). No band was detected after preabsorption of D1R antibody (1:1000) with control peptide (2.5 μg/ml at 4°C overnight) (B, lane 2).

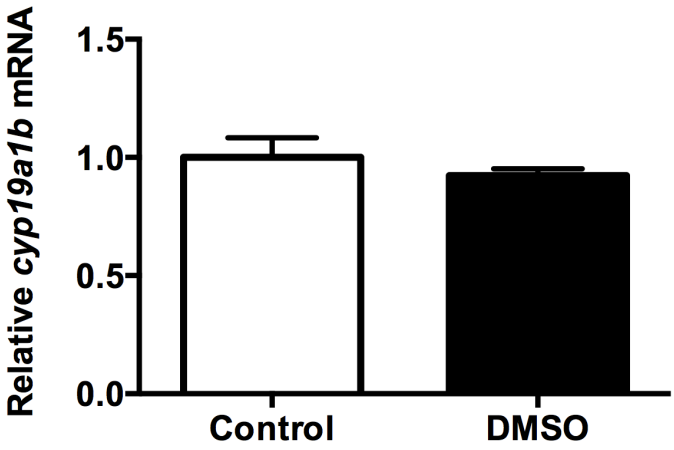

Figure A3.3. The effects of DMSO on *cyp19a1b* mRNA levels in RGC culture. Quantitative real-time PCR analysis showing the variations in the relative amounts of the *cyp19a1b* mRNA to *18s* (A) in primary RGC culture after 24h exposure of DMSO (0.1%). Data show no effects of DMSO on *cyp19a1b* mRNA levels in RGC culture (P = 0.42).

Table A3.1. Proteins quantified with unique peptides by Average TIC and NSAF that showed significant changes in abundance between control and SKF 38393-treated RGCs.

Accession	Protein ID	Average TIC		NSAF	
		P-Value	Fold change	P-Value	Fold change
gil112950077	HSP60	0.032	0.6	0.04	0.4
gil141795527	Fam114a1 protein	0.034	0.2	0.045	0.2
gil144954334	mitochondrial serine hydroxymethyltransferase	0.024	0.3	0.0078	0.2
gil156230739	Tpi1b protein	0.016	0.1	0.025	0.08
gil182890510	Hspa9 protein	0.0024	0.2	0.00075	0.1
gil197631853	capping protein (actin filament) muscle Z-line beta	0.021	0.2	0.02	0.1
gil208609645	collagen type I alpha 1	0.041	0.7	0.0053	0.4
gil208609649	collagen type I alpha 3	0.00039	0.5	0.02	0.2
gil225707292	Microtubule-associated protein RP/EB family member 1	0.012	0	0.02	0
gil28422490	Synaptotagmin binding, cytoplasmic RNA interacting protein, like	0.021	0.4	0.038	0.5
gil29436531	Ribosomal protein L4	0.027	0	0.027	0
gil308321574	endophilin-b1	0.013	0.2	0.024	0.2
gil315585122	60 kDa heat shock protein	0.00089	0.2	0.00057	0.2
gil33990002	Zgc:65956	0.0068	0.2	0.023	0.2
gil34784485	Collagen, type I, alpha 3	0.0066	0.1	0.019	0.1
gil410903448	PREDICTED: 78 kDa glucose-regulated protein-like	0.0034	0.3	0.031	0.3
gil410908016	PREDICTED: annexin A2-like	0.015	0.6	0.044	0.7
gil528508501	PREDICTED: ADP-ribosylation factor GTPase-activating protein 2 isoform X1	0.021	0.6	0.0088	0.7
gil551488208	PREDICTED: endophilin-A2-like isoform X1	0.011	0	0.014	0
gil13161384	lamin B2	0.014	0.3	0.065	0.4
gil141795754	MGC163038 protein	0.045	0.5	0.059	0.4
gil152012648	Ribosomal protein S19	0.042	0	0.058	0
gil185133062	keratin, type I cytoskeletal 18	0.037	0.6	0.19	0.7
gil190337988	Copa protein	0.031	0.4	0.18	0.5
gil190337988	Cluster of Copa protein	0.04	0.5	0.27	0.6
gil209730660	60S ribosomal protein L36	0.028	0.2	0.1	0.3
gil221220674	Fatty acid-binding protein, brain	0.049	0	0.05	0
gil26788026	novel protein similar to human proliferation-associated 2G4 protein (PA2G4)	0.02	0.2	0.24	0.4
gil2960399	40S ribosomal protein S11	0.013	0.4	0.4	0.7
gil300810921	collagen type I alpha 1	0.033	0.4	0.1	0.5
gil301033167	collagen type I alpha 2	0.0064	0.3	0.12	0.5

gil302136832	nucleobindin 2 precursor	0.043	0.6	0.75	1.1
gil31419302	Heat shock protein 5	0.022	0.6	0.066	0.5
gil31419302	Cluster of Heat shock protein 5	0.0089	0.5	0.14	0.7
gil317419458	Vinculin [Dicentrarchus labrax]	0.039	0.5	0.06	0.5
gil34783815	CAMP-regulated phosphoprotein 19a	0.029	0.3	0.27	0.5
gil37589184	Eukaryotic translation initiation factor 3, subunit 10 (theta)	0.038	0.3	0.093	0.4
gil390196251	protein disulfide-isomerase A6	0.004	0.5	0.23	0.7
gil410901675	PREDICTED: collagen alpha-1(I) chain-like isoform 1	0.035	0.7	0.17	0.7
gil528481569	PREDICTED: myosin-10 isoform X1	0.0043	0.3	0.72	0.7
gil528524154	PREDICTED: synaptopodin-like isoform X1	0.028	0.3	0.27	0.5
gil544168766	Cluster of vinculin-b, partial	0.00037	0.5	0.4	0.7
gil554805235	Cluster of PREDICTED: neuroblast differentiation-associated protein AHNAK-like	0.039	0.6	0.28	1.4
gil576887006	T-complex protein 1 subunit zeta	0.045	0.2	0.054	0.2
gil576888097	RNA-binding protein 4B	0.023	0.2	0.28	0.4
gil112419004	Nascent polypeptide-associated complex alpha polypeptide	0.038	2.4	0.025	2.7
gil145337928	Crabp2b protein	0.0059	1.3	0.013	1.7
gil145337928	Cluster of Crabp2b protein	0.0072	1.3	0.039	1.6
gil27804344	nucleolin	0.00026	6.9	0.0015	5.8
gil49902917	Ependymin related protein 1	0.011	4.9	0.012	4.8
gil528514290	PREDICTED: drebrin-like isoform X2	0.0061	2.8	0.021	3.1
gil528514290	Cluster of PREDICTED: drebrin-like isoform X2	0.006	2.9	0.021	3.1
gil152013115	Cluster of Eukaryotic translation elongation factor 1 beta 2	0.0015	1.3	0.076	1.6
gil16517097	beta tubulin	0.02	1.3	0.82	1
gil196481063	eukaryotic translation initiation factor 5A	0.028	3.2	0.21	1.8
gil196481063	Cluster of eukaryotic translation initiation factor 5A	0.03	3.2	0.18	1.9
gil197632459	myosin, light polypeptide 9, like 1	0.011	1.5	0.21	1.3
gil40807189	GTPase activating protein (SH3 domain) binding protein 1	0.0035	3	0.052	2.5
gil554818370	PREDICTED: tubulin alpha-1D chain-like isoform X1	0.0099	1.3	0.62	1.1
gil554818370	Cluster of PREDICTED: tubulin alpha-1D chain-like isoform X1	0.012	1.3	0.6	1.1
gil576893094	Tropomyosin alpha-1 chain	0.041	3.8	0.066	6.2
gil78099193	RecName: Full = Calmodulin; Short = CaM	0.0023	1.4	0.053	1.3
gil110456858	PDZ-LIM protein RIL	0.31	0.7	0.021	1.8
gil124504410	Cluster of Gfap protein	0.7	1.1	0.023	1.7
gil126631813	Ywhab1 protein	0.12	1.1	0.0014	1.9
gil150421558	RecName: Full = Glial fibrillary acidic protein; Short = GFAP	0.31	1.2	0.04	1.7
gil182889312	Txndc17 protein	0.72	1	0.011	1.3
gil209735154	Fatty acid-binding protein, adipocyte	0.77	1	0.018	1.3

gil221220434	Tropomyosin-1 alpha chain	0.97	1	0.013	1.5
gil27881886	Cluster of Tropomyosin 3	0.94	1	0.029	1.3
gil302136832	Cluster of nucleobindin 2 precursor	0.063	0.7	0.03	1.3
gil432917960	PREDICTED: tropomyosin alpha-4 chain-like	0.69	1	0.025	1.3
gil45829608	Myosin, light polypeptide 9, regulatory	0.92	1	0.03	1.3
gil46329552	Cluster of Microtubule-associated protein, RP/EB family, member 1	0.69	1	0.015	1.4
gil528480208	PREDICTED: drebrin isoform X1	0.056	0.7	0.039	1.4
gil528512244	PREDICTED: LOW QUALITY PROTEIN: afadin	0.13	2	0.049	3.1
gil528521971	PREDICTED: non-muscle caldesmon-like	0.79	1	0.038	1.4
gil109810210	histone 2A family member ZA	0.075	0.1	0.043	0.1
gil116256315	RecName: Full = Histone H3.2	0.16	0.5	0.046	0.4
gil120538141	Zgc:158450	0.11	0.7	0.04	0.5
gil15294055	40S ribosomal protein S21	0.16	0.6	0.0058	0.5
gil15528537	Cluster of elongation factor-1 alpha	0.24	0.8	0.0081	0.5
gil157422738	Proteasome (prosome, macropain) 26S subunit, ATPase, 4	0.078	0.1	0.048	0.1
gil182890016	Tkt protein	0.2	0.4	0.029	0.2
gil197631973	26S protease regulatory subunit 7	0.4	0.7	0.036	0.3
gil197632397	elongation factor-1 delta-1	0.75	0.9	0.01	0.7
gil208609645	Cluster of collagen type I alpha 1	0.086	0.8	0.012	0.6
gil213688814	annexin A4	0.18	0.4	0.049	0.2
gil27882500	Tyrosine 3-monooxygenase/tryptophan 5-monooxygenase activation protein, theta polypeptide b	0.84	1	0.021	0.7
gil298545253	unnamed protein product	0.6	0.8	0.0043	0.05
gil348543937	PREDICTED: reticulocalbin-1-like isoform X1	0.066	0	0.032	0
gil374463495	Cluster of fatty acid-binding protein	0.32	0.8	0.031	0.6
gil410931279	PREDICTED: filamin-A-like, partial	0.18	0.6	0.016	0.4
gil47605558	RecName: Full = ATP synthase subunit beta, mitochondrial; Flags: Precursor	0.066	0.7	0.021	0.4
gil47605558	Cluster of RecName: Full = ATP synthase subunit beta, mitochondrial; Flags: Precursor	0.074	0.7	0.029	0.5
gil551498431	PREDICTED: tubulin alpha chain-like	0.11	0.7	0.0066	0.5
gil8895765	alpha actin	0.053	0.4	0.0037	0.2

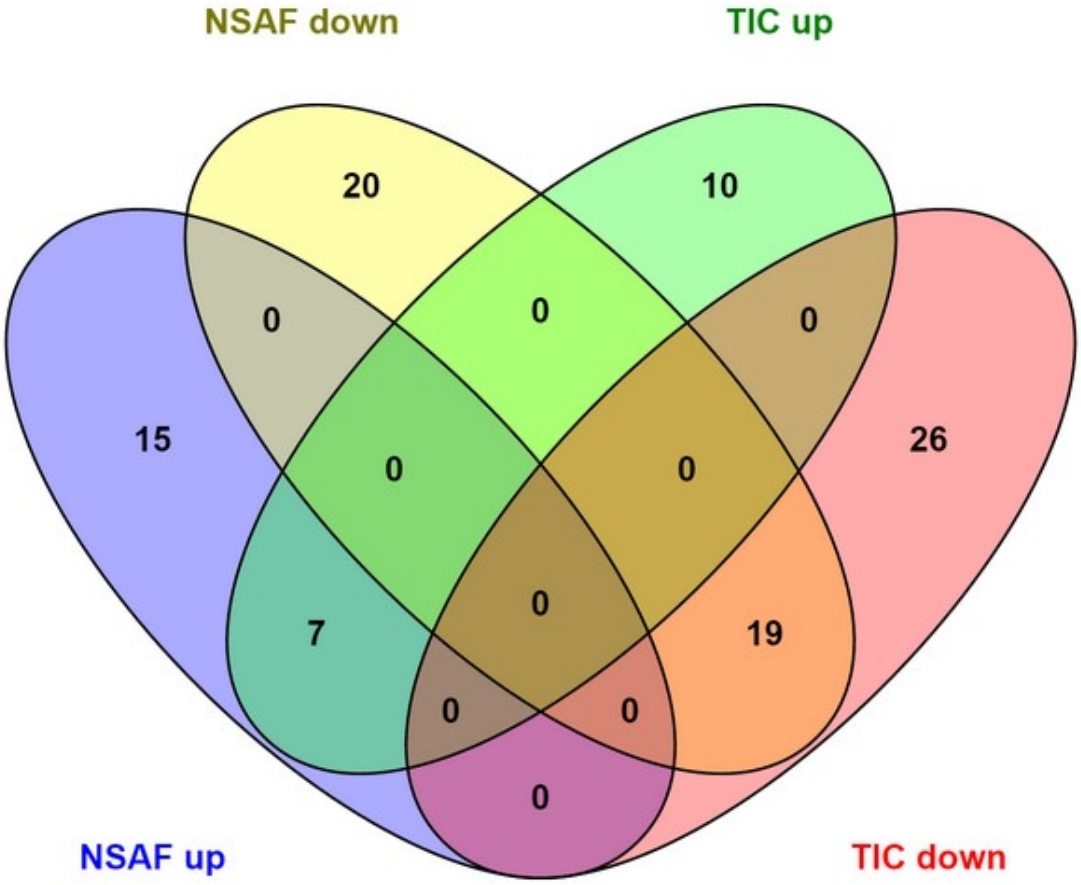

Figure A3.4 Venn Diagram summarizing the number of proteins regulated by SKF 38393 in cultured RGCs.

References

Abe-Dohmae, S., Takagi, Y., Harada, N., 1996. Neurotransmitter-mediated regulation of brain aromatase: protein kinase C- and G-dependent induction. J. Neurochem. 67, 2087-2095.

Abekawa, T., Ohmori, T., Ito, K., Koyama, T., 2000. D1 dopamine receptor activation reduces extracellular glutamate and GABA concentrations in the medial prefrontal cortex. Brain Res. 867, 250-254.

Absil, P., Foidart, A., Hemmings Jr, H.C., Steinbusch, H.W.M., Ball, G.F., Balthazart, J., 2001. Distribution of DARPP-32 immunoreactive structures in the quail brain: anatomical relationship with dopamine and aromatase. J. Chem. Neuroanat. 21, 23-39.

Addis, R.C., Hsu, F.-C., Wright, R.L., Dichter, M.A., Coulter, D.A., Gearhart, J.D., 2011. Efficient Conversion of Astrocytes to Functional Midbrain Dopaminergic Neurons Using a Single Polycistronic Vector. PLoS ONE 6, e28719.

Adolf, B., Chapouton, P., Lam, C.S., Topp, S., Tannhäuser, B., Strähle, U., Götz, M., Bally-Cuif, L., 2006. Conserved and acquired features of adult neurogenesis in the zebrafish telencephalon. Dev. Biol. 295, 278-293.

Adrover, M.F., Shin, J.H., Alvarez, V.A., 2014. Glutamate and dopamine transmission from midbrain dopamine neurons share similar release properties but are differentially affected by cocaine. J. Neurosci. 34, 3183-3192.

Al-Bader, M.D., Malatiali, S.A., Redzic, Z.B., 2011. Expression of estrogen receptor alpha and beta in rat astrocytes in primary culture: effects of hypoxia and glucose deprivation. Physiol. Res. 60, 951-960.

Alvarez-Buylla, A., Garcia-Verdugo, J.M., Tramontin, A.D., 2001. A unified hypothesis on the lineage of neural stem cells. Nat. Rev. Neurosci. 2, 287-293.

Alvarez-Buylla, A., Seri, B., Doetsch, F., 2002. Identification of neural stem cells in the adult vertebrate brain. Brain Res. Bull. 57, 751-758.

Anthony, T.E., Heintz, N., 2008. Genetic lineage tracing defines distinct neurogenic and gliogenic stages of ventral telencephalic radial glial development. Neural Dev. 3, 30.

Anthony, T.E., Klein, C., Fishell, G., Heintz, N., 2004. Radial Glia Serve as Neuronal Progenitorsin All Regions of the Central Nervous System. Neuron 41, 881-890.

Anuka, E., Gal, M., Stocco, D.M., Orly, J., 2013. Expression and roles of steroidogenic acute regulatory (StAR) protein in 'non-classica', extra-adrenal and extra-gonadal cells and tissues. Mol. Cell. Endocrinol. 371, 47-61.

Aparicio, S., 2000. Vertebrate evolution: recent perspectives from fish. Trends Genet. 16, 54-56.

Arevalo, M.A., Azcoitia, I., Garcia-Segura, L.M., 2015. The neuroprotective actions of oestradiol and oestrogen receptors. Nat. Rev. Neurosci. 16, 17-29.

Azcoitia, I., Sierra, A., Veiga, S., Garcia-Segura, L.M., 2003. Aromatase expression by reactive astroglia is neuroprotective. Ann. N. Y. Acad. Sci. 1007, 298-305.

Azcoitia, I., Yague, J.G., Garcia-Segura, L.M., 2011. Estradiol synthesis within the human brain. Neuroscience 191, 139-147.

Baillien, M., Balthazart, J., 1997. A direct dopaminergic control of aromatase activity in the quail preoptic area. J. Steroid Biochem. Mol. Biol. 63, 99-113.

Baldereschi, M., Di Carlo, A., Rocca, W.A., Vanni, P., Maggi, S., Perissinotto, E., Grigoletto, F., Amaducci, L., Inzitari, D., 2000. Parkinson's disease and parkinsonism in a longitudinal study: two-fold higher incidence in men. ILSA Working Group. Italian Longitudinal Study on Aging. Neurology 55, 1358-1363.

Balthazart, J., Baillien, M., Ball, G.F., 2002. Interactions between aromatase (estrogen synthase) and dopamine in the control of male sexual behavior in quail. Comparative Biochemistry and Physiology Part B: Biochemistry and Molecular Biology 132, 37-55.

Balthazart, J., Baillien, M., Charlier, T.D., Cornil, C.A., Ball, G.F., 2003. Multiple mechanisms control brain aromatase activity at the genomic and non-genomic level. J. Steroid Biochem. Mol. Biol. 86, 367-379.

Balthazart, J., Ball, G.F., 1998. New insights into the regulation and function of brain estrogen synthase (aromatase). Trends Neurosci. 21, 243-249.

Balthazart J, F.A., Baillien M, Harada N, Ball GF, 1998. Anatomical relationships between aromatase and tyrosine hydroxylase in the quail brain: double-label immunocytochemical studies. J. Comp. Neurol. 391, 214-226.

Balthazart, J., Foidart, A., Surlemont, C., Harada, N., 1991. Neuroanatomical specificity in the co-localization of aromatase and estrogen receptors. J. Neurobiol. 22, 143-157.

Balthazart, J., Tlemçani, O., Harada, N., Baillien, M., 2000. Ontogeny of aromatase and tyrosine hydroxylase activity and of aromatase-immunoreactive cells in the preoptic area of male and female Japanese quail. J. Neuroendocrinol. 12, 853-866.

Barry, D.S., Pakan, J.M., McDermott, K.W., 2014. Radial glial cells: key organisers in CNS development. Int. J. Biochem. Cell Biol. 46, 76-79.

Baumgarten, H.G., Bjorklund, A., Holstein, A.F., Nobin, A., 1972. Organization and ultrastructural identification of the catecholamine nerve terminals in the neural lobe and pars intermedia of the rat pituitary. Z. Zellforsch. Mikrosk. Anat. 126, 483-517.

Behl, C., Skutella, T., Lezoualc'h, F., Post, A., Widmann, M., Newton, C.J., Holsboer, F.,

1997. Neuroprotection against oxidative stress by estrogens: structure-activity relationship. Mol. Pharmacol. 51, 535-541.

Behl, C., Widmann, M., Trapp, T., Holsboer, F., 1995. 17-beta estradiol protects neurons from oxidative stress-induced cell death in vitro. Biochem. Biophys. Res. Commun. 216, 473-482.

Belcher, S.M., Zsarnovszky, A., 2001. Estrogenic actions in the brain: estrogen, phytoestrogens, and rapid intracellular signaling mechanisms. J. Pharmacol. Exp. Ther. 299, 408-414.

Beninger, R.J., 1983. The role of dopamine in locomotor activity and learning. Brain Res. 287, 173-196.

Bentivoglio, M., Mazzarello, P., 1999. The history of radial glia. Brain Res. Bull. 49, 305-315.

Berchtold, M.W., Villalobo, A., 2014. The many faces of calmodulin in cell proliferation, programmed cell death, autophagy, and cancer. Biochim. Biophys. Acta 1843, 398-435.

Berg, D.A., Kirkham, M., Wang, H., Frisen, J., Simon, A., 2011. Dopamine controls neurogenesis in the adult salamander midbrain in homeostasis and during regeneration of dopamine neurons. Cell Stem Cell 8, 426-433.

Berridge, K.C., Robinson, T.E., 1998. What is the role of dopamine in reward: hedonic impact, reward learning, or incentive salience? Brain Res. Brain Res. Rev. 28, 309-369.

Bjorklund, A., Dunnett, S.B., 2007. Dopamine neuron systems in the brain: an update. Trends Neurosci. 30, 194-202.

Blesa, J., Phani, S., Jackson-Lewis, V., Przedborski, S., 2012. Classic and new animal models of Parkinson's disease. J. Biomed. Biotechnol. 2012, 845618.

Bonfanti, L., Peretto, P., 2007. Radial glial origin of the adult neural stem cells in the subventricular zone. Prog. Neurobiol. 83, 24-36.

Bonilla, S., Hall, A.C., Pinto, L., Attardo, A., Götz, M., Huttner, W.B., Arenas, E., 2008. Identification of midbrain floor plate radial glia-like cells as dopaminergic progenitors. Glia 56, 809-820.

Bowman, C.J., Kroll, K.J., Gross, T.G., Denslow, N.D., 2002. Estradiol-induced gene expression in largemouth bass (Micropterus salmoides). Mol. Cell. Endocrinol. 196, 67-77.

Brami-Cherrier, K., Valjent, E., Garcia, M., Pages, C., Hipskind, R.A., Caboche, J., 2002. Dopamine induces a PI3-kinase-independent activation of Akt in striatal neurons: a new route to cAMP response element-binding protein phosphorylation. J. Neurosci. 22, 8911-8921.

Bressan, R.A., Crippa, J.A., 2005. The role of dopamine in reward and pleasure behaviour--review of data from preclinical research. Acta Psychiatr. Scand. Suppl., 14-21.

Brinton, R.D., 2008. The healthy cell bias of estrogen action: mitochondrial bioenergetics and neurological implications. Trends Neurosci. 31, 529-537.

Brunne, B., Zhao, S., Derouiche, A., Herz, J., May, P., Frotscher, M., Bock, H.H., 2010. Origin, maturation, and astroglial transformation of secondary radial glial cells in the developing dentate gyrus. Glia 58, 1553-1569.

Burns, R.S., Chiueh, C.C., Markey, S.P., Ebert, M.H., Jacobowitz, D.M., Kopin, I.J., 1983. A primate model of parkinsonism: selective destruction of dopaminergic neurons in the pars compacta of the substantia nigra by N-methyl-4-phenyl-1,2,3,6-tetrahydropyridine. Proc. Natl. Acad. Sci. U. S. A. 80, 4546-4550.

Bushnell, P.G., Nikinmaa, M., Oikari, A., 1985. Metabolic effects of dehydroabietic acid on rainbow trout erythrocytes. Comparative Biochemistry and Physiology Part C: Comparative Pharmacology 81, 391-394.

Butterfield, D.A., Trad, C.H., Hall, N.C., 1994. Effects of dehydroabietic acid on the physical state of cytoskeletal proteins and the lipid bilayer of erythrocyte membranes. Biochim. Biophys. Acta 1192, 185-189.

Cadet, J.L., Jayanthi, S., McCoy, M.T., Beauvais, G., Cai, N.S., 2010. Dopamine D1 receptors, regulation of gene expression in the brain, and neurodegeneration. CNS Neurol. Disord. Drug Targets 9, 526-538.

Callard, G.V., Petro, Z., Ryan, K.J., 1981. Estrogen synthesis in vitro and in vivo in the brain of a marine teleost (Myoxocephalus). Gen. Comp. Endocrinol. 43, 243-255.

Callard, G.V., Tchoudakova, A.V., Kishida, M., Wood, E., 2001. Differential tissue distribution, developmental programming, estrogen regulation and promoter characteristics of cyp19 genes in teleost fish. J. Steroid Biochem. Mol. Biol. 79, 305-314.

Calne, D.B., Kebabian, J., Silbergeld, E., Evarts, E., 1979. Advances in the neuropharmacology of Parkinsonism. Ann. Intern. Med. 90, 219-229.

Campbell, K., Götz, M., 2002. Radial glia: multi-purpose cells for vertebrate brain development. Trends Neurosci. 25, 235-238.

Cantrell, A.R., Smith, R.D., Goldin, A.L., Scheuer, T., Catterall, W.A., 1997. Dopaminergic modulation of sodium current in hippocampal neurons via cAMP-dependent phosphorylation of specific sites in the sodium channel alpha subunit. J. Neurosci. 17, 7330-7338.

Cardona-Gomez, G.P., Mendez, P., DonCarlos, L.L., Azcoitia, I., Garcia-Segura, L.M., 2001. Interactions of estrogens and insulin-like growth factor-I in the brain: implications for neuroprotection. Brain Res. Brain Res. Rev. 37, 320-334.

Caudle, W.M., Kitsou, E., Li, J., Bradner, J., Zhang, J., 2009. A role for a novel protein, nucleolin, in Parkinson's disease. Neurosci. Lett. 459, 11-15.

Chen, P.S., Peng, G.S., Li, G., Yang, S., Wu, X., Wang, C.C., Wilson, B., Lu, R.B., Gean, P.W., Chuang, D.M., Hong, J.S., 2006. Valproate protects dopaminergic neurons in midbrain neuron/glia cultures by stimulating the release of neurotrophic factors from astrocytes. Mol. Psychiatry 11, 1116-1125.

Chen, Y., Su, Y., Run, X., Sun, Z., Wang, T., Sun, S., Liang, Z., 2013. Pretreatment of PC12 cells with 17beta-estradiol prevents Abeta-induced down-regulation of CREB phosphorylation and prolongs inhibition of GSK-3beta. J. Mol. Neurosci. 50, 394-401.

Chiang, E.F.-L., Yan, Y.-L., Guiguen, Y., Postlethwait, J., Chung, B.-c., 2001. Two Cyp19 (P450 aromatase) genes on duplicated zebrafish chromosomes are expressed in ovary or brain. Mol. Biol. Evol. 18, 542-550.

Christianson-Heiska, I.L., Haavisto, T., Paranko, J., Bergelin, E., Isomaa, B., 2008. Effects of the wood extractives dehydroabietic acid and betulinol on reproductive physiology of zebrafish (Danio rerio)-a two-generation study. Aquat. Toxicol. 86, 388-396.

Corbin, J.D., Krebs, E.G., 1969. A cyclic AMP--stimulated protein kinase in adipose tissue. Biochem. Biophys. Res. Commun. 36, 328-336.

Corio, M., Peute, J., Steinbusch, W.M., 1991. Distribution of serotonin- and dopamine-immunoreactivity in the brain of the teleost *Clarias Gariepinus*
. J. Chem. Neuroanat. 4, 79-95.

Coumailleau, P., Pellegrini, E., Adrio, F., Diotel, N., Cano-Nicolau, J., Nasri, A., Vaillant, C., Kah, O., 2015. Aromatase, estrogen receptors and brain development in fish and amphibians. Biochim. Biophys. Acta 1849, 152-162.

Crocker, S.J., Frausto, R.F., Whitton, J.L., Milner, R., 2008. A novel method to establish microglia‐free astrocyte cultures: Comparison of matrix metalloproteinase expression profiles in pure cultures of astrocytes and microglia. Glia 56, 1187-1198.

Czlonkowska, A., Ciesielska, A., Gromadzka, G., Kurkowska-Jastrzebska, I., 2006. Gender differences in neurological disease: role of estrogens and cytokines. Endocrine 29, 243-256.

D'Astous, M., Gajjar, T.M., Dluzen, D.E., Di Paolo, T., 2004. Dopamine transporter as a marker of neuroprotection in methamphetamine-lesioned mice treated acutely with estradiol. Neuroendocrinology 79, 296-304.

Dauer, W., Przedborski, S., 2003. Parkinson's disease: mechanisms and models. Neuron 39, 889-909.

de Koning, T.J., Snell, K., Duran, M., Berger, R., Poll-The, B.T., Surtees, R., 2003. L-serine in disease and development. Biochem. J. 371, 653-661.

Denslow, N.D., Lee, H.S., Bowman, C.J., Hemmer, M.J., Folmar, L.C., 2001. Multiple responses in gene expression in fish treated with estrogen. Comparative Biochemistry and Physiology Part B: Biochemistry and Molecular Biology 129, 277-282.

Dhandapani, K.M., Wade, F.M., Mahesh, V.B., Brann, D.W., 2005. Astrocyte-derived transforming growth factor-{beta} mediates the neuroprotective effects of 17{beta}-estradiol: involvement of nonclassical genomic signaling pathways. Endocrinology 146, 2749-2759.

Di Paolo, T., 1994. Modulation of brain dopamine transmission by sex steroids. Rev. Neurosci. 5, 27-41.

Diotel, N., Do Rego, J.L., Anglade, I., Vaillant, C., Pellegrini, E., Gueguen, M.-M., Mironov, S., Vaudry, H., Kah, O., 2011a. Activity and expression of steroidogenic enzymes in the brain of adult zebrafish. Eur. J. Neurosci. 34, 45-56.

Diotel, N., Do Rego, J.L., Anglade, I., Vaillant, C., Pellegrini, E., Gueguen, M.M., Mironov, S., Vaudry, H., Kah, O., 2011b. Activity and expression of steroidogenic enzymes in the brain of adult zebrafish. Eur. J. Neurosci. 34, 45-56.

Diotel, N., Do Rego, J.L., Anglade, I., Vaillant, C., Pellegrini, E., Vaudry, H., Kah, O., 2011c. The brain of teleost fish, a source, and a target of sexual steroids. Front. Neurosci. 5, 137.

Diotel, N., Le Page, Y., Mouriec, K., Tong, S.K., Pellegrini, E., Vaillant, C., Anglade, I., Brion, F., Pakdel, F., Chung, B.C., Kah, O., 2010a. Aromatase in the brain of teleost fish: expression, regulation and putative functions. Front. Neuroendocrinol. 31, 172-192.

Diotel, N., Vaillant, C., Gabbero, C., Mironov, S., Fostier, A., Gueguen, M.-M., Anglade, I., Kah, O., Pellegrini, E., 2013. Effects of estradiol in adult neurogenesis and brain repair in zebrafish. Horm. Behav. 63, 193-207.

Diotel, N., Vaillant, C., Gueguen, M.-M., Mironov, S., Anglade, I., Servili, A., Pellegrini, E., Kah, O., 2010b. Cxcr4 and Cxcl12 expression in radial glial cells of the brain of adult zebrafish. J. Comp. Neurol. 518, 4855-4876.

Do Rego, J.L., Seong, J.Y., Burel, D., Leprince, J., Luu-The, V., Tsutsui, K., Tonon, M.-C., Pelletier, G., Vaudry, H., 2009. Neurosteroid biosynthesis: Enzymatic pathways and neuroendocrine regulation by neurotransmitters and neuropeptides. Front. Neuroendocrinol. 30, 259-301.

Doetsch, F., 2003. The glial identity of neural stem cells. Nat. Neurosci. 6, 1127-1134.

Dubal, D.B., Rau, S.W., Shughrue, P.J., Zhu, H., Yu, J., Cashion, A.B., Suzuki, S., Gerhold, L.M., Bottner, M.B., Dubal, S.B., Merchanthaler, I., Kindy, M.S., Wise, P.M., 2006. Differential modulation of estrogen receptors (ERs) in ischemic brain injury: a role for ERalpha in estradiol-mediated protection against delayed cell death. Endocrinology 147, 3076-3084.

Dubal, D.B., Shughrue, P.J., Wilson, M.E., Merchenthaler, I., Wise, P.M., 1999. Estradiol modulates bcl-2 in cerebral ischemia: a potential role for estrogen receptors. J. Neurosci. 19, 6385-6393.

Ehmsen, J.T., Ma, T.M., Sason, H., Rosenberg, D., Ogo, T., Furuya, S., Snyder, S.H., Wolosker, H., 2013. D-serine in glia and neurons derives from 3-phosphoglycerate dehydrogenase. J. Neurosci. 33, 12464-12469.

Elisabeth, P., Nicolas, D., Colette, V.C., Rita, P.M., Marie-Madeleine, G., Ahmed, N., Joel, C.N., Olivier, K., 2015. Steroid modulation of neurogenesis: Focus on radial glial cells in zebrafish. J. Steroid Biochem. Mol. Biol.

Elsworth, J.D., Roth, R.H., 1997. Dopamine synthesis, uptake, metabolism, and receptors: relevance to gene therapy of Parkinson's disease. Exp. Neurol. 144, 4-9.

Emsley, J.G., Menezes, J.R.L., Da Costa, R.F.M., Martinez, A.M.B., Macklis, J.D., 2012. Identification of radial glia-like cells in the adult mouse olfactory bulb. Exp. Neurol. 236, 283-297.

Episcopo, F.L., Tirolo, C., Testa, N., Caniglia, S., Morale, M.C., Marchetti, B., 2013. Reactive astrocytes are key players in nigrostriatal dopaminergic neurorepair in the MPTP mouse model of Parkinson's disease: focus on endogenous neurorestoration. Curr. Aging Sci. 6, 45-55.

Ervin, K.S., Lymer, J.M., Matta, R., Clipperton-Allen, A.E., Kavaliers, M., Choleris, E., 2015. Estrogen involvement in social behavior in rodents: Rapid and long-term actions. Horm. Behav.

Feng, Q., Boone, A.N., Vijayan, M.M., 2003. Copper impact on heat shock protein 70 expression and apoptosis in rainbow trout hepatocytes. Comp. Biochem. Physiol. C Toxicol. Pharmacol. 135C, 345-355.

Fergus, D.J., Bass, A.H., 2013. Localization and divergent profiles of estrogen receptors and aromatase in the vocal and auditory networks of a fish with alternative mating tactics. J. Comp. Neurol. 521, 2850-2869.

Figeac, N., Serralbo, O., Marcelle, C., Zammit, P.S., 2014. ErbB3 binding protein-1 (Ebp1) controls proliferation and myogenic differentiation of muscle stem cells. Dev. Biol. 386, 135-151.

Fleige, S., Pfaffl, M.W., 2006. RNA integrity and the effect on the real-time qRT-PCR performance. Mol. Aspects Med. 27, 126-139.

Forlano, P.M., Bass, A.H., 2005. Steroid regulation of brain aromatase expression in glia: female preoptic and vocal motor nuclei. J. Neurobiol. 65, 50-58.

Forlano, P.M., Deitcher, D.L., Bass, A.H., 2005. Distribution of estrogen receptor alpha

mRNA in the brain and inner ear of a vocal fish with comparisons to sites of aromatase expression. J. Comp. Neurol. 483, 91-113.

Forlano, P.M., Deitcher, D.L., Myers, D.A., Bass, A.H., 2001. Anatomical distribution and cellular basis for high levels of aromatase activity in the brain of teleost fish: aromatase enzyme and mRNA expression identify glia as source. J. Neurosci. 21, 8943-8955.

Forlano, P.M., Schlinger, B.A., Bass, A.H., 2006. Brain aromatase: new lessons from non-mammalian model systems. Front. Neuroendocrinol. 27, 247-274.

Forno, L.S., 1996. Neuropathology of Parkinson's disease. J. Neuropathol. Exp. Neurol. 55, 259-272.

Forno, L.S., DeLanney, L.E., Irwin, I., Di Monte, D., Langston, J.W., 1992. Astrocytes and Parkinson's disease. Prog. Brain Res. 94, 429-436.

Forno, L.S., DeLanney, L.E., Irwin, I., Langston, J.W., 1996. Electron microscopy of Lewy bodies in the amygdala-parahippocampal region. Comparison with inclusion bodies in the MPTP-treated squirrel monkey. Adv. Neurol. 69, 217-228.

Garcia-Segura, L.M., 2008. Aromatase in the brain: not just for reproduction anymore. J. Neuroendocrinol. 20, 705-712.

Garcia-Segura, L.M., Veiga, S., Sierra, A., Melcangi, R.C., Azcoitia, I., 2003. Aromatase: a neuroprotective enzyme. Prog. Neurobiol. 71, 31-41.

Garcia-Segura, L.M., Wozniak, A., Azcoitia, I., Rodriguez, J.R., Hutchison, R.E., Hutchison, J.B., 1999. Aromatase expression by astrocytes after brain injury: implications for local estrogen formation in brain repair. NSC 89, 567-578.

Ge, S., Pradhan, D.A., Ming, G.L., Song, H., 2007. GABA sets the tempo for activity-dependent adult neurogenesis. Trends Neurosci. 30, 1-8.

Gerke, V., Creutz, C.E., Moss, S.E., 2005. Annexins: linking Ca2+ signalling to membrane dynamics. Nat. Rev. Mol. Cell Biol. 6, 449-461.

Ghashghaei, H.T., Weimer, J.M., Schmid, R.S., Yokota, Y., McCarthy, K.D., Popko, B., Anton, E.S., 2007. Reinduction of ErbB2 in astrocytes promotes radial glial progenitor identity in adult cerebral cortex. Genes & Development 21, 3258-3271.

Giesy, J.P., Anderson, J.C., Wiseman, S.B., 2010. Alberta oil sands development. Proc. Natl. Acad. Sci. U. S. A. 107, 951-952.

Giraldez-Perez, R., Antolin-Vallespin, M., Munoz, M., Sanchez-Capelo, A., 2014. Models of alpha-synuclein aggregation in Parkinson's disease. Acta neuropathologica communications 2, 176.

Goping, G., Pollard, H.B., Adeyemo, O.M., Kuijpers, G.A., 1995. Effect of MPTP on dopaminergic neurons in the goldfish brain: a light and electron microscope study. Brain Res. 687, 35-52.

Götz, M., Huttner, W.B., 2005. The cell biology of neurogenesis. Nat. Rev. Mol. Cell Biol. 6, 777-788.

Gravato, C., Oliveira, M., Santos, M.A., 2005a. Oxidative stress and genotoxic responses to resin acids in Mediterranean mussels. Ecotoxicol. Environ. Saf. 61, 221-229.

Gravato, C., Oliveira, M., Santos, M.A., 2005b. Oxidative stress and genotoxic responses to resin acids in Mediterranean mussels. Ecotoxicol. Environ. Saf. 61, 221-229.

Gubert, F., Zaverucha-do-Valle, C., Figueiredo, F.R., Bargas-Rega, M., Paredes, B.D., Mencalha, A.L., Abdelhay, E., Gutfilen, B., da Fonseca, L.M.B., Mendez-Otero, R., Santiago, M.F., 2013. Bone-marrow cell therapy induces differentiation of radial glia-like cells and rescues the number of oligodendrocyte progenitors in the subventricular zone after global cerebral ischemia. Stem Cell Res. 10, 241-256.

Gubert, F., Zaverucha-do-Valle, C., Pimentel-Coelho, P.M., Mendez-Otero, R., Santiago, M.F., 2009. Radial glia-like cells persist in the adult rat brain. Brain Res. 1258, 43-52.

Hansen, D.V., Lui, J.H., Parker, P.R.L., Kriegstein, A.R., 2010. Neurogenic radial glia in the outer subventricular zone of human neocortex. Nature 464, 554-561.

Hartfuss, E., Galli, R., Heins, N., Götz, M., 2001. Characterization of CNS Precursor Subtypes and Radial Glia. Dev. Biol. 229, 15-30.

Hatten, M.E., 2002. New Directions in Neuronal Migration. Science 297, 1660-1663.

Hebsgaard, J.B., Nelander, J., Sabelström, H., Jönsson, M.E., Stott, S., Parmar, M., 2009. Dopamine neuron precursors within the developing human mesencephalon show radial glial characteristics. Glia 57, 1648-1659.

Heckmann, L.H., Sorensen, P.B., Krogh, P.H., Sorensen, J.G., 2011. NORMA-Gene: a simple and robust method for qPCR normalization based on target gene data. BMC Bioinformatics 12, 250.

Heikkila, R.E., Hess, A., Duvoisin, R.C., 1984. Dopaminergic neurotoxicity of 1-methyl-4-phenyl-1,2,5,6-tetrahydropyridine in mice. Science 224, 1451-1453.

Heins, N., Malatesta, P., Cecconi, F., Nakafuku, M., Tucker, K.L., Hack, M.A., Chapouton, P., Barde, Y.-A., Götz, M., 2002. Glial cells generate neurons: the role of the transcription factor Pax6. Nat. Neurosci. 5, 308-315.

Hibbert, B., Fung, I., McAuley, R., Lariviere, K., MacNeil, B., Bafi-Yeboa, N., Livesey, J., Trudeau, V., 2004. Increased GAD67 mRNA levels are correlated with in vivo GABA

synthesis in the MPTP-treated catecholamine-depleted goldfish brain. Brain Res. Mol. Brain Res. 128, 121-130.

Hickey, G.J., Krasnow, J.S., Beattie, W.G., Richards, J.S., 1990. Aromatase cytochrome P450 in rat ovarian granulosa cells before and after luteinization: adenosine 3',5'-monophosphate-dependent and independent regulation. Cloning and sequencing of rat aromatase cDNA and 5' genomic DNA. Mol. Endocrinol. 4, 3-12.

Hoglinger, G.U., Rizk, P., Muriel, M.P., Duyckaerts, C., Oertel, W.H., Caille, I., Hirsch, E.C., 2004. Dopamine depletion impairs precursor cell proliferation in Parkinson disease. Nat. Neurosci. 7, 726-735.

Hornby, P.J., Piekut, D.T., 1990. Distribution of catecholamine-synthesizing enzymes in goldfish brains: presumptive dopamine and norepinephrine neuronal organization. Brain Behav. Evol. 35, 49-64.

Hornykiewicz, O., 1989. Ageing and neurotoxins as causative factors in idiopathic Parkinson's disease--a critical analysis of the neurochemical evidence. Prog. Neuropsychopharmacol. Biol. Psychiatry 13, 319-328.

Houalla, T., Levine, R.L., 2003. The isolation and culture of microglia-like cells from the goldfish brain. J. Neurosci. Methods 131, 121-131.

Huff, R.M., 1996. Signal transduction pathways modulated by the D2 subfamily of dopamine receptors. Cell. Signal. 8, 453-459.

Hutchison, J.B., Steimer, T., 1986. Formation of behaviorally effective 17 beta-estradiol in the dove brain: steroid control of preoptic aromatase. Endocrinology 118, 2180-2187.

Itoh, K., 2002. Culture of oligodendrocyte precursor cells (NG2(+)/O1(-)) and oligodendrocytes (NG2(-)/O1(+)) from embryonic rat cerebrum. Brain Res. Brain Res. Protoc. 10, 23-30.

Iwabuchi, J., Koshimizu, K., Nakagawa, T., 2013. Expression profile of the aromatase enzyme in the Xenopus brain and localization of estradiol and estrogen receptors in each tissue. Gen. Comp. Endocrinol. 194, 286-294.

Jaber, M., Cador, M., Dumartin, B., Normand, E., Stinus, L., Bloch, B., 1995. Acute and chronic amphetamine treatments differently regulate neuropeptide messenger RNA levels and Fos immunoreactivity in rat striatal neurons. Neuroscience 65, 1041-1050.

Jeng, S.-R., Pasquier, J., Yueh, W.-S., Chen, G.-R., Lee, Y.-H., Dufour, S., Chang, C.-F., 2012a. Differential regulation of the expression of cytochrome P450 aromatase, estrogen and androgen receptor subtypes in the brain-pituitary-ovarian axis of the Japanese eel (*Anguilla japonica*) reveals steroid dependent and independent mechanisms. Gen. Comp. Endocrinol. 175, 163-172.

Jeng, S.-R., Yueh, W.-S., Pen, Y.-T., Gueguen, M.-M., Pasquier, J., Dufour, S., Chang, C.-F., Kah, O., 2012b. Expression of Aromatase in Radial Glial Cells in the Brain of the Japanese Eel Provides Insight into the Evolution of the cyp191a Gene in Actinopterygians. PLoS ONE 7, e44750.

Jing, Z., Heng, W., Xia, L., Ning, W., Yafei, Q., Yao, Z., Shulan, Z., 2015. Downregulation of phosphoglycerate dehydrogenase inhibits proliferation and enhances cisplatin sensitivity in cervical adenocarcinoma cells by regulating Bcl-2 and caspase-3. Cancer Biol. Ther. 16, 541-548.

Jones, D., West, C.E., Scarlett, A.G., Frank, R.A., Rowland, S.J., 2012. Isolation and estimation of the 'aromatic' naphthenic acid content of an oil sands process-affected water extract. J. Chromatogr. A 1247, 171-175.

Kapsimali, M., Vidal, B., Gonzalez, A., Dufour, S., Vernier, P., 2000. Distribution of the mRNA encoding the four dopamine D1 receptor subtypes in the brain of the european eel (Anguilla anguilla): Comparative approach to the function of D1 receptors in vertebrates. J. Comp. Neurol. 419, 320-343.

Kato, J., Yamada-Mouri, N., Hirata, S., 1997. Structure of aromatase mRNA in the rat brain. J. Steroid Biochem. Mol. Biol. 61, 381-385.

Kebabian, J.W., Calne, D.B., 1979. Multiple receptors for dopamine. Nature 277, 93-96.

Keefe, K.A., Gerfen, C.R., 1995. D1-D2 dopamine receptor synergy in striatum: effects of intrastriatal infusions of dopamine agonists and antagonists on immediate early gene expression. Neuroscience 66, 903-913.

Keller, A., Nesvizhskii, A.I., Kolker, E., Aebersold, R., 2002. Empirical statistical model to estimate the accuracy of peptide identifications made by MS/MS and database search. Anal. Chem. 74, 5383-5392.

Kelly, R.B., 1993. Storage and release of neurotransmitters. Cell 72 Suppl, 43-53.

Khalaj, L., Peirovi, H., Khodagholi, F., Abdi, A., Dargahi, L., Ahmadiani, A., 2011. Acute 17beta-estradiol pretreatment protects against abdominal aortic occlusion induced spinal cord ischemic-reperfusion injury. Neurochem. Res. 36, 268-280.

Kimmel, C.B., 1993. Patterning the brain of the zebrafish embryo. Annu. Rev. Neurosci. 16, 707-732.

Kinoshita, M.O., Shinoda, Y., Sakai, K., Hashikawa, T., Watanabe, M., Machida, T., Hirabayashi, Y., Furuya, S., 2009. Selective upregulation of 3-phosphoglycerate dehydrogenase (Phgdh) expression in adult subventricular zone neurogenic niche. Neurosci. Lett. 453, 21-26.

Kippin, T.E., Kapur, S., van der Kooy, D., 2005. Dopamine specifically inhibits forebrain

neural stem cell proliferation, suggesting a novel effect of antipsychotic drugs. J. Neurosci. 25, 5815-5823.

Kobayashi, M., Aida, K., Hanyu, I., 1988. Hormone changes during the ovulatory cycle in goldfish. Gen. Comp. Endocrinol. 69, 301-307.

Koh, J., Chen, S., Zhu, N., Yu, F., Soltis, P.S., Soltis, D.E., 2012. Comparative proteomics of the recently and recurrently formed natural allopolyploid Tragopogon mirus (Asteraceae) and its parents. New Phytol. 196, 292-305.

Kopin, I.J., 1985. Catecholamine metabolism: basic aspects and clinical significance. Pharmacol. Rev. 37, 333-364.

Kroehne, V., Freudenreich, D., Hans, S., Kaslin, J., Brand, M., 2011. Regeneration of the adult zebrafish brain from neurogenic radial glia-type progenitors. Development 138, 4831-4841.

Kuroki, Y., Fukushima, K., Kanda, Y., Mizuno, K., Watanabe, Y., 2001. Neuroprotection by estrogen via extracellular signal-regulated kinase against quinolinic acid-induced cell death in the rat hippocampus. Eur. J. Neurosci. 13, 472-476.

Langston, J.W., Ballard, P.A., Jr., 1983. Parkinson's disease in a chemist working with 1-methyl-4-phenyl-1,2,5,6-tetrahydropyridine. N. Engl. J. Med. 309, 310.

Lassiter, C.S., Linney, E., 2007. Embryonic expression and steroid regulation of brain aromatase cyp19a1b in zebrafish (Danio rerio). Zebrafish 4, 49-57.

Le Page, Y., Diotel, N., Vaillant, C., Pellegrini, E., Anglade, I., Merot, Y., Kah, O., 2010. Aromatase, brain sexualization and plasticity: the fish paradigm. Eur. J. Neurosci. 32, 2105-2115.

Lee, Y.H., Mungunsukh, O., Tutino, R.L., Marquez, A.P., Day, R.M., 2010. Angiotensin-II-induced apoptosis requires regulation of nucleolin and Bcl-xL by SHP-2 in primary lung endothelial cells. J. Cell Sci. 123, 1634-1643.

Lephart, E.D., 1996. A review of brain aromatase cytochrome P450. Brain Res. Brain Res. Rev. 22, 1-26.

Levitt, P., Rakic, P., 1980. Immunoperoxidase localization of glial fibrillary acidic protein in radial glial cells and astrocytes of the developing rhesus monkey brain. J. Comp. Neurol. 193, 815-840.

Li, H., Chang, Y.-W., Mohan, K., Su, H.-W., Ricupero, C.L., Baridi, A., Hart, R.P., Grumet, M., 2008a. Activated Notch1 maintains the phenotype of radial glial cells and promotes their adhesion to laminin by upregulating nidogen. Glia 56, 646-658.

Li, J., Dani, J.A., Le, W., 2009. The role of transcription factor Pitx3 in dopamine neuron

development and Parkinson's disease. Curr. Top. Med. Chem. 9, 855-859.

Li, L., Lundkvist, A., Andersson, D., Wilhelmsson, U., Nagai, N., Pardo, A.C., Nodin, C., Stahlberg, A., Aprico, K., Larsson, K., Yabe, T., Moons, L., Fotheringham, A., Davies, I., Carmeliet, P., Schwartz, J.P., Pekna, M., Kubista, M., Blomstrand, F., Maragakis, N., Nilsson, M., Pekny, M., 2008b. Protective role of reactive astrocytes in brain ischemia. J. Cereb. Blood Flow Metab. 28, 468-481.

Li, P., Shah, S., Huang, L., Carr, A.L., Gao, Y., Thisse, C., Thisse, B., Li, L., 2007. Cloning and spatial and temporal expression of the zebrafish dopamine D1 receptor. Dev. Dyn. 236, 1339-1346.

Lin, L.F., Doherty, D.H., Lile, J.D., Bektesh, S., Collins, F., 1993. GDNF: a glial cell line-derived neurotrophic factor for midbrain dopaminergic neurons. Science 260, 1130-1132.

Lindsey, B.W., Di Donato, S., Kaslin, J., Tropepe, V., 2014. Sensory-specific modulation of adult neurogenesis in sensory structures is associated with the type of stem cell present in the neurogenic niche of the zebrafish brain. Eur. J. Neurosci. 40, 3591-3607.

Liu, X., Bolteus, A.J., Balkin, D.M., Henschel, O., Bordey, A., 2006. GFAP-expressing cells in the postnatal subventricular zone display a unique glial phenotype intermediate between radial glia and astrocytes. Glia 54, 394-410.

Liu, Y., Liu, Y., Cao, J., Zhu, X., Nie, X., Yao, L., Chen, M., Cheng, X., Wang, Y., 2014. Upregulated expression of ebp1 contributes to schwann cell differentiation and migration after sciatic nerve crush. J. Mol. Neurosci. 54, 602-613.

Lonze, B.E., Ginty, D.D., 2002. Function and regulation of CREB family transcription factors in the nervous system. Neuron 35, 605-623.

Luo, Y., Kokkonen, G.C., Wang, X., Neve, K.A., Roth, G.S., 1998. D2 dopamine receptors stimulate mitogenesis through pertussis toxin-sensitive G proteins and Ras-involved ERK and SAP/JNK pathways in rat C6-D2L glioma cells. J. Neurochem. 71, 980-990.

Lushchak, V.I., Lushchak, L.P., Mota, A.A., Hermes-Lima, M., 2001. Oxidative stress and antioxidant defenses in goldfish Carassius auratus during anoxia and reoxygenation. Am. J. Physiol. Regul. Integr. Comp. Physiol. 280, R100-107.

Lykissas, M.G., Batistatou, A.K., Charalabopoulos, K.A., Beris, A.E., 2007. The role of neurotrophins in axonal growth, guidance, and regeneration. Curr. Neurovasc. Res. 4, 143-151.

Mack, A.F., Tiedemann, K., 2013. Cultures of astroglial cells derived from brain of adult cichlid fish. J. Neurosci. Methods 212, 269-275.

Makantasi, P., Dermon, C.R., 2014. Estradiol treatment decreases cell proliferation in the neurogenic zones of adult female zebrafish (Danio rerio) brain. Neuroscience 277, 306-320.

Makris, S.P., Banerjee, S., 2002. Fate of resin acids in pulp mill secondary treatment systems. Water Res. 36, 2878-2882.

Malatesta, P., Hack, M.A., Hartfuss, E., Kettenmann, H., Klinkert, W., Kirchhoff, F., Götz, M., 2003. Neuronal or glial progeny: regional differences in radial glia fate. Neuron 37, 751-764.

Malatesta, P., Hartfuss, E., Gotz, M., 2000. Isolation of radial glial cells by fluorescent-activated cell sorting reveals a neuronal lineage. Development 127, 5253-5263.

Marín, O., Rubenstein, J.L.R., 2003. Cell Migration in the Forebrain. Annu. Rev. Neurosci. 26, 441-483.

Marlatt, V.L., Martyniuk, C.J., Zhang, D., Xiong, H., Watt, J., Xia, X., Moon, T., Trudeau, V.L., 2008. Auto-regulation of estrogen receptor subtypes and gene expression profiling of 17β-estradiol action in the neuroendocrine axis of male goldfish. Mol. Cell. Endocrinol. 283, 38-48.

Maroun, M., Akirav, I., 2009. Differential involvement of dopamine D1 receptor and MEK signaling pathway in the ventromedial prefrontal cortex in consolidation and reconsolidation of recognition memory. Learn. Mem. 16, 243-247.

Martinez-Cerdeno, V., Noctor, S.C., Kriegstein, A.R., 2006. Estradiol stimulates progenitor cell division in the ventricular and subventricular zones of the embryonic neocortex. Eur. J. Neurosci. 24, 3475-3488.

Martinez-Galan, J.R., Escobar del Rey, F., Morreale de Escobar, G., Santacana, M., Ruiz-Marcos, A., 2004. Hypothyroidsm alters the development of radial glial cells in the term fetal and postnatal neocortex of the rat. Dev. Brain Res. 153, 109-114.

Martyniuk, C.J., Alvarez, S., Lo, B.P., Elphick, J.R., Marlatt, V.L., 2012. Hepatic protein expression networks associated with masculinization in the female fathead minnow (Pimephales promelas). J. Proteome Res. 11, 4147-4161.

Martyniuk, C.J., Xiong, H., Crump, K., Chiu, S., Sardana, R., Nadler, A., Gerrie, E.R., Xia, X., Trudeau, V.L., 2006. Gene expression profiling in the neuroendocrine brain of male goldfish (Carassius auratus) exposed to 17 -ethinylestradiol. Physiol. Genomics 27, 328-336.

Mashanov, V.S., Zueva, O.R., Garcia-Arraras, J.E., 2013. Radial glial cells play a key role in echinoderm neural regeneration. BMC Biol. 11, 49.

Massarsky, A., Abraham, R., Nguyen, K.C., Rippstein, P., Tayabali, A.F., Trudeau, V.L., Moon, T.W., 2014. Nanosilver cytotoxicity in rainbow trout (Oncorhynchus mykiss) erythrocytes and hepatocytes. Comp. Biochem. Physiol. C Toxicol. Pharmacol. 159, 10-21.

Matsuda, S., Kitagishi, Y., Kobayashi, M., 2013. Function and characteristics of PINK1 in mitochondria. Oxid. Med. Cell. Longev. 2013, 601587.

McCullough, L.D., Blizzard, K., Simpson, E.R., Oz, O.K., Hurn, P.D., 2003. Aromatase cytochrome P450 and extragonadal estrogen play a role in ischemic neuroprotection. J. Neurosci. 23, 8701-8705.

McEwen, B., 2002. Estrogen actions throughout the brain. Recent Prog. Horm. Res. 57, 357–384.

McKinley, E.T., Baranowski, T.C., Blavo, D.O., Cato, C., Doan, T.N., Rubinstein, A.L., 2005. Neuroprotection of MPTP-induced toxicity in zebrafish dopaminergic neurons. Brain Res. Mol. Brain Res. 141, 128-137.

Meek, J., Joosten, H.W., 1993. Tyrosine hydroxylase-immunoreactive cell groups in the brain of the teleost fish *Gnathonemus petersii*. J. Chem. Neuroanat. 6, 431-446.

Meier-Ruge, W.A., Bertoni-Freddari, C., 1997. Pathogenesis of decreased glucose turnover and oxidative phosphorylation in ischemic and trauma-induced dementia of the Alzheimer type. Ann. N. Y. Acad. Sci. 826, 229-241.

Mellon, S.H., Griffin, L.D., Compagnone, N.A., 2001. Biosynthesis and action of neurosteroids. Brain Res. Rev. 37, 3-12.

Menuet, A., Anglade, I., Le Guevel, R., Pellegrini, E., Pakdel, F., Kah, O., 2003. Distribution of aromatase mRNA and protein in the brain and pituitary of female rainbow trout: Comparison with estrogen receptor ? J. Comp. Neurol. 462, 180-193.

Menuet, A., Pellegrini, E., Anglade, I., Blaise, O., Laudet, V., Kah, O., Pakdel, F., 2002. Molecular characterization of three estrogen receptor forms in zebrafish: binding characteristics, transactivation properties, and tissue distributions. Biol. Reprod. 66, 1881-1892.

Menuet, A., Pellegrini, E., Brion, F., Gueguen, M.M., Anglade, I., Pakdel, F., Kah, O., 2005. Expression and estrogen-dependent regulation of the zebrafish brain aromatase gene. J. Comp. Neurol. 485, 304-320.

Metcalfe, W.K., Myers, P.Z., Trevarrow, B., Bass, M.B., Kimmel, C.B., 1990. Primary neurons that express the L2/HNK-1 carbohydrate during early development in the zebrafish. Development 110, 491-504.

Mi, H., Muruganujan, A., Casagrande, J.T., Thomas, P.D., 2013. Large-scale gene function analysis with the PANTHER classification system. Nat. Protoc. 8, 1551-1566.

Miller, D.B., Ali, S.F., O'Callaghan, J.P., Laws, S.C., 1998. The impact of gender and estrogen on striatal dopaminergic neurotoxicity. Ann. N. Y. Acad. Sci. 844, 153-165.

Ming, G.L., Song, H., 2011. Adult neurogenesis in the mammalian brain: significant answers and significant questions. Neuron 70, 687-702.

Missale, C., Nash, S.R., Robinson, S.W., Jaber, M., Caron, M.G., 1998. Dopamine receptors: from structure to function. Physiol. Rev. 78, 189-225.

Montminy, M., 1997. Transcriptional regulation by cyclic AMP. Annu. Rev. Biochem. 66, 807-822.

Morissette, M., Al Sweidi, S., Callier, S., Di Paolo, T., 2008. Estrogen and SERM neuroprotection in animal models of Parkinson's disease. Mol. Cell. Endocrinol. 290, 60-69.

Mouriec, K., Gueguen, M.M., Manuel, C., Percevault, F., Thieulant, M.L., Pakdel, F., Kah, O., 2009a. Androgens Upregulate cyp19a1b (Aromatase B) Gene Expression in the Brain of Zebrafish (Danio rerio) Through Estrogen Receptors. Biol. Reprod. 80, 889-896.

Mouriec, K., Lareyre, J.J., Tong, S.K., Le Page, Y., Vaillant, C., Pellegrini, E., Pakdel, F., Chung, B.C., Kah, O., Anglade, I., 2009b. Early regulation of brain aromatase (cyp19a1b) by estrogen receptors during zebrafish development. Dev. Dyn. 238, 2641-2651.

Naftolin, F., Ryan, K.J., Petro, Z., 1971. Aromatization of androstenedione by the diencephalon. J. Clin. Endocrinol. Metab. 33, 368-370.

Nagarajan, G., Aruna, A., Chang, C.-F., 2013. Neurosteroidogenic enzymes and their regulation in the early brain of the protogynous grouper Epinephelus coioides during gonadal sex differentiation. Gen. Comp. Endocrinol. 181, 271-287.

Nair, V.D., Sealfon, S.C., 2003. Agonist-specific transactivation of phosphoinositide 3-kinase signaling pathway mediated by the dopamine D2 receptor. J. Biol. Chem. 278, 47053-47061.

Nakano, I., Dougherty, J.D., Kim, K., Klement, I., Geschwind, D.H., Kornblum, H.I., 2007. Phosphoserine phosphatase is expressed in the neural stem cell niche and regulates neural stem and progenitor cell proliferation. Stem Cells 25, 1975-1984.

Namba, T., Mochizuki, H., Onodera, M., Mizuno, Y., Namiki, H., Seki, T., 2005. The fate of neural progenitor cells expressing astrocytic and radial glial markers in the postnatal rat dentate gyrus. Eur. J. Neurosci. 22, 1928-1941.

Nesvizhskii, A.I., Keller, A., Kolker, E., Aebersold, R., 2003. A statistical model for identifying proteins by tandem mass spectrometry. Anal. Chem. 75, 4646-4658.

Norris-Mullins, B., VanderKolk, K., Vacchina, P., Joyce, M.V., Morales, M.A., 2014. LmaPA2G4, a homolog of human Ebp1, is an essential gene and inhibits cell proliferation in L. major. PLoS Negl. Trop. Dis. 8, e2646.

Numakawa, Y., Matsumoto, T., Yokomaku, D., Taguchi, T., Niki, E., Hatanaka, H., Kunugi, H., Numakawa, T., 2007. 17beta-estradiol protects cortical neurons against oxidative stress-induced cell death through reduction in the activity of mitogen-activated protein kinase and in the accumulation of intracellular calcium. Endocrinology 148, 627-637.

Oikari, A., Lönn, B.-E., Castrén, M., Nakari, T., Snickars-Nikinmaa, B., Bister, H., Virtanen, E., 1983. Toxicological effects of dehydroabietic acid (DHAA) on the trout, Salmo gairdneri Richardson, in fresh water. Water Res. 17, 81-89.

Okada, M., Murase, K., Makino, A., Nakajima, M., Kaku, T., Furukawa, S., Furukawa, Y., 2008. Effects of estrogens on proliferation and differentiation of neural stem/progenitor cells. Biomedical research 29, 163-170.

Olah, J., Orosz, F., Keseru, G.M., Kovari, Z., Kovacs, J., Hollan, S., Ovadi, J., 2002. Triosephosphate isomerase deficiency: a neurodegenerative misfolding disease. Biochem. Soc. Trans. 30, 30-38.

Pasmanik, M., Callard, G.V., 1988. Changes in Brain Aromatase and 5a-Reductase Activities Correlate Significantly with Seasonal Reproductive Cycles in Goldfish. Endocrinology 122, 1349-1356.

Pecchi, E., Dallaporta, M., Charrier, C., Pio, J., Jean, A., Moyse, E., Troadec, J.-D., 2007. Glial fibrillary acidic protein (GFAP)-positive radial-like cells are present in the vicinity of proliferative progenitors in the nucleus tractus solitarius of adult rat. J. Comp. Neurol. 501, 353-368.

Pellegrini, E., Diotel, N., Vaillant-Capitaine, C., Perez Maria, R., Gueguen, M.M., Nasri, A., Cano Nicolau, J., Kah, O., 2015. Steroid modulation of neurogenesis: Focus on radial glial cells in zebrafish. J. Steroid Biochem. Mol. Biol.

Pellegrini, E., Menuet, A., Lethimonier, C., Adrio, F., Gueguen, M.-M., Tascon, C., Anglade, I., Pakdel, F., Kah, O., 2005. Relationships between aromatase and estrogen receptors in the brain of teleost fish. Gen. Comp. Endocrinol. 142, 60-66.

Pellegrini, E., Mouriec, K., Anglade, I., Menuet, A., Le Page, Y., Gueguen, M.-M., Marmignon, M.-H., Brion, F., Pakdel, F., Kah, O., 2007. Identification of aromatase-positive radial glial cells as progenitor cells in the ventricular layer of the forebrain in zebrafish. J. Comp. Neurol. 501, 150-167.

Pérez, M.R., Pellegrini, E., Cano-Nicolau, J., Gueguen, M.-M., Menouer-Le Guillou, D., Merot, Y., Vaillant, C., Somoza, G.M., Kah, O., 2013. Relationships between radial glial progenitors and 5-HT neurons in the paraventricular organ of adult zebrafish - potential effects of serotonin on adult neurogenesis. Eur. J. Neurosci. 38, 3292-3301.

Perlman, W.R., Arnold, A.P., 2003. Expression of estrogen receptor and aromatase mRNAs in embryonic and posthatch zebra finch brain. J. Neurobiol. 55, 204-219.

Pesonen, M., Andersson, T., 1992. Toxic effects of bleached and unbleached paper mill effluents in primary cultures of rainbow trout hepatocytes. Ecotoxicol. Environ. Saf. 24, 63-71.

Peterson, R.S., Lee, D.W., Fernando, G., Schlinger, B.A., 2004. Radial glia express

aromatase in the injured zebra finch brain. J. Comp. Neurol. 475, 261-269.

Peterson, R.S., Yarram, L., Schlinger, B.A., Saldanha, C.J., 2005. Aromatase is pre-synaptic and sexually dimorphic in the adult zebra finch brain. Proceedings of the Royal Society B: Biological Sciences 272, 2089-2096.

Petrova, P., Raibekas, A., Pevsner, J., Vigo, N., Anafi, M., Moore, M.K., Peaire, A.E., Shridhar, V., Smith, D.I., Kelly, J., Durocher, Y., Commissiong, J.W., 2003. MANF: a new mesencephalic, astrocyte-derived neurotrophic factor with selectivity for dopaminergic neurons. J. Mol. Neurosci. 20, 173-188.

Petrovska, S., Dejanova, B., Jurisic, V., 2012. Estrogens: mechanisms of neuroprotective effects. J. Physiol. Biochem. 68, 455-460.

Pfaus, J.G., Phillips, A.G., 1991. Role of dopamine in anticipatory and consummatory aspects of sexual behavior in the male rat. Behav. Neurosci. 105, 727-743.

Pietranera, L., Brocca, M.E., Roig, P., Lima, A., Garcia-Segura, L.M., De Nicola, A.F., 2015. Estrogens are neuroprotective factors for hypertensive encephalopathy. J. Steroid Biochem. Mol. Biol. 146, 15-25.

Pilz, G.-A., Shitamukai, A., Reillo, I., Pacary, E., Schwausch, J., Stahl, R., Ninkovic, J., Snippert, H.J., Clevers, H., Godinho, L., Guillemot, F., Borrell, V., Matsuzaki, F., tz, M.G.o., 2013. Amplification of progenitors in the mammalian telencephalon includes a new radial glial cell type. Nat. Commun. 4, 1-11.

Pinto, C., Grimaldi, M., Boulahtouf, A., Pakdel, F., Brion, F., Ait-Aissa, S., Cavailles, V., Bourguet, W., Gustafsson, J.A., Bondesson, M., Balaguer, P., 2014. Selectivity of natural, synthetic and environmental estrogens for zebrafish estrogen receptors. Toxicol. Appl. Pharmacol. 280, 60-69.

Poli, A., Gandolfi, O., Lucchi, R., Barnabei, O., 1992. Spontaneous recovery of MPTP-damaged catecholamine systems in goldfish brain areas. Brain Res. 585, 128-134.

Pollard, S., Conti, L., 2007. Investigating radial glia in vitro. Prog. Neurobiol. 83, 53-67.

Popesku, J.T., 2009. Dopaminergic regulation of gene expression in the neuroendocrine brain of the goldfish (Carassius auratus). University of Ottawa.

Popesku, J.T., Martyniuk, C.J., Denslow, N.D., Trudeau, V.L., 2010. Rapid dopaminergic modulation of the fish hypothalamic transcriptome and proteome. PLoS ONE 5, e12338.

Popesku, J.T., Martyniuk, C.J., Mennigen, J., Xiong, H., Zhang, D., Xia, X., Cossins, A.R., Trudeau, V.L., 2008. The goldfish (Carassius auratus) as a model for neuroendocrine signaling. Mol. Cell. Endocrinol. 293, 43-56.

Popesku, J.T., Martyniuk, C.J., Trudeau, V.L., 2012. Meta-type analysis of dopaminergic

effects on gene expression in the neuroendocrine brain of female goldfish. Frontiers in Endocrinology 3 30.

Radakovits, R., Barros, C.S., Belvindrah, R., Patton, B., Muller, U., 2009. Regulation of Radial Glial Survival by Signals from the Meninges. J. Neurosci. 29, 7694-7705.

Rakic, P., 1971a. Guidance of neurons migrating to the fetal monkey neocortex. Brain Res. 33, 471-476.

Rakic, P., 1971b. Neuron - glia relationship during granule cell migration in developing cerebellar cortex. A Golgi and electonmicroscopic study in Macacus rhesus. J. Comp. Neurol. 141, 283-312.

Rakic, P., 1972. Mode of cell migration to the superficial layers of fetal monkey neocortex. J. Comp. Neurol. 145, 61-83.

Rakic, P., 2003a. Developmental and evolutionary adaptations of cortical radial glia. Cereb. Cortex 13, 541-549.

Rakic, P., 2003b. Elusive radial glial cells: Historical and evolutionary perspective. Glia 43, 19-32.

Reddy, S.D., Rayala, S.K., Ohshiro, K., Pakala, S.B., Kobori, N., Dash, P., Yun, S., Qin, J., O'Malley, B.W., Kumar, R., 2011. Multiple coregulatory control of tyrosine hydroxylase gene transcription. Proc. Natl. Acad. Sci. U. S. A. 108, 4200-4205.

Reichenbach, A., Pannicke, T., 2008. Neuroscience. A new glance at glia. Science 322, 693-694.

Richards, D.L.C.a.J.S., 1997. Evidence that functional interactions of CREB and SF-1 mediate hormone regulated expression of the aromatase gene in granulosa cells and constitutive expression in R2C cells. J. Steroid Biochem. Mol. Biol. 61, 223-231.

Rissanen, E., Krumschnabel, G., Nikinmaa, M., 2003. Dehydroabietic acid, a major component of wood industry effluents, interferes with cellular energetics in rainbow trout hepatocytes. Aquat. Toxicol. 62, 45-53.

Rueda, D.C., Raith, M., De Mieri, M., Schoffmann, A., Hering, S., Hamburger, M., 2014. Identification of dehydroabietc acid from Boswellia thurifera resin as a positive GABAA receptor modulator. Fitoterapia 99, 28-34.

Ruiz-Palmero, I., Hernando, M., Garcia-Segura, L.M., Arevalo, M.A., 2013. G protein-coupled estrogen receptor is required for the neuritogenic mechanism of 17beta-estradiol in developing hippocampal neurons. Mol. Cell. Endocrinol. 372, 105-115.

Saldanha, C.J., Burstein, S.R., Duncan, K.A., 2013. Induced Synthesis of Oestrogens by Glia in the Songbird Brain. J. Neuroendocrinol. 25, 1032-1038.

Saldanha, C.J., Duncan, K.A., Walters, B.J., 2009. Neuroprotective actions of brain aromatase. Front. Neuroendocrinol. 30, 106-118.

Sanghera, M.K., Simpson, E.R., McPhaul, M.J., Kozlowski, G., Conley, A.J., Lephart, E.D., 1991. Immunocytochemical distribution of aromatase cytochrome P450 in the rat brain using peptide-generated polyclonal antibodies. Endocrinology 129, 2834-2844.

Saunders-Pullman, R., 2003. Estrogens and Parkinson disease: neuroprotective, symptomatic, neither, or both? Endocrine 21, 81-87.

Saunders-Pullman, R., Gordon-Elliott, J., Parides, M., Fahn, S., Saunders, H.R., Bressman, S., 1999. The effect of estrogen replacement on early Parkinson's disease. Neurology 52, 1417-1421.

Sawada, H., Shimohama, S., 2003. Estrogens and Parkinson disease: novel approach for neuroprotection. Endocrine 21, 77-79.

Scarlett, A.G., Reinardy, H.C., Henry, T.B., West, C.E., Frank, R.A., Hewitt, L.M., Rowland, S.J., 2013. Acute toxicity of aromatic and non-aromatic fractions of naphthenic acids extracted from oil sands process-affected water to larval zebrafish. Chemosphere 93, 415-420.

Schapira, A.H., Jenner, P., 2011. Etiology and pathogenesis of Parkinson's disease. Mov. Disord. 26, 1049-1055.

Schmechel, D.E., Rakic, P., 1979. A Golgi study of radial glial cells in developing monkey telencephalon: morphogenesis and transformation into astrocytes. Anat. Embryol. (Berl.) 156, 115-152.

Schmidt, K.L., Pradhan, D.S., Shah, A.H., Charlier, T.D., Chin, E.H., Soma, K.K., 2008. Neurosteroids, immunosteroids, and the Balkanization of endocrinology. Gen. Comp. Endocrinol. 157, 266-274.

Schnitzer, J., Franke, W.W., Schachner, M., 1981. Immunocytochemical demonstration of vimentin in astrocytes and ependymal cells of developing and adult mouse nervous system. J. Cell Biol. 90, 435-447.

Schuster, K., Dambly-Chaudiere, C., Ghysen, A., 2010. Glial cell line-derived neurotrophic factor defines the path of developing and regenerating axons in the lateral line system of zebrafish. Proc. Natl. Acad. Sci. U.S.A. 107, 19531-19536.

Scott, E., Zhang, Q.-g., Wang, R., Vadlamudi, R., Brann, D., 2012. Estrogen neuroprotection and the critical period hypothesis. Front. Neuroendocrinol. 33, 85-104.

Segura Aguilar, J., Kostrzewa, R.M., 2004. Neurotoxins and neurotoxic species implicated in neurodegeneration. Neurotox. Res. 6, 615-630.

Session, D.R., Pearlstone, M.M., Jewelewicz, R., Kelly, A.C., 1994. Estrogens and Parkinson's disease. Med. Hypotheses 42, 280-282.

Shahrokhi, N., Haddad, M.K., Joukar, S., Shabani, M., Keshavarzi, Z., Shahozehi, B., 2012. Neuroprotective antioxidant effect of sex steroid hormones in traumatic brain injury. Pakistan journal of pharmaceutical sciences 25, 219-225.

Sherwood, C.C., Stimpson, C.D., Raghanti, M.A., Wildman, D.E., Uddin, M., Grossman, L.I., Goodman, M., Redmond, J.C., Bonar, C.J., Erwin, J.M., Hof, P.R., 2006. Evolution of increased glia-neuron ratios in the human frontal cortex. Proc. Natl. Acad. Sci. U. S. A. 103, 13606-13611.

Shughrue, P.J., 2004. Estrogen attenuates the MPTP-induced loss of dopamine neurons from the mouse SNc despite a lack of estrogen receptors (ERalpha and ERbeta). Exp. Neurol. 190, 468-477.

Simpkins, J.W., Singh, M., Brock, C., Etgen, A.M., 2012. Neuroprotection and Estrogen Receptors. Neuroendocrinology 96, 119-130.

Smeets, W.J.A.J., González, A., 2000. Catecholamine systems in the brain of vertebrates: new perspectives through a comparative approach. Brain Res. Rev. 33, 308-379.

Smith, A., Zhang, J., Guay, D., Quint, E., Johnson, A., Akimenko, M.A., 2007. Gene expression analysis on sections of zebrafish regenerating fins reveals limitations in the whole-mount in situ hybridization method. Dev. Dyn. 237, 417-425.

Socorro, S., Power, D.M., Olsson, P.-E., Canario, A.V., 2000. Two estrogen receptors expressed in the teleost fish, Sparus aurata: cDNA cloning, characterization and tissue distribution. J. Endocrinol. 166, 293-306.

Squatrito, M., Mancino, M., Donzelli, M., Areces, L.B., Draetta, G.F., 2004. EBP1 is a nucleolar growth-regulating protein that is part of pre-ribosomal ribonucleoprotein complexes. Oncogene 23, 4454-4465.

Stevenson, J.A., Yoon, M.G., 1982. Morphology of radial glia, ependymal cells, and periventricular neurons in the optic tectum of goldfish (Carassius auratus). J. Comp. Neurol. 205, 128-138.

Strange, P.G., 1993. New insights into dopamine receptors in the central nervous system. Neurochem. Int. 22, 223-236.

Strobl-Mazzulla, P.H., Lethimonier, C., Gueguen, M.-M., Karube, M., Fernandino, J.I., Yoshizaki, G., Patiño, R., Strüssmann, C.A., Kah, O., Somoza, G.M., 2008. Brain aromatase (Cyp19A2) and estrogen receptors, in larvae and adult pejerrey fish Odontesthes bonariensis: Neuroanatomical and functional relations. Gen. Comp. Endocrinol. 158, 191-201.

Strobl-Mazzulla, P.H., Nunez, A., Pellegrini, E., Gueguen, M.M., Kah, O., Somoza, G.M.,

2010. Progenitor radial cells and neurogenesis in pejerrey fish forebrain. Brain Behav. Evol. 76, 20-31.

Stuart, G.W., McMurray, J.V., Westerfield, M., 1988. Replication, integration and stable germ-line transmission of foreign sequences injected into early zebrafish embryos. Development 103, 403-412.

Stuart, G.W., Vielkind, J.R., McMurray, J.V., Westerfield, M., 1990. Stable lines of transgenic zebrafish exhibit reproducible patterns of transgene expression. Development 109, 577-584.

Sundholm-Peters, N.L., Yang, H.K., Goings, G.E., Walker, A.S., Szele, F.G., 2004. Radial glia-like cells at the base of the lateral ventricles in adult mice. J. Neurocytol. 33, 153-164.

Suzuki, S., Gerhold, L.M., Bottner, M., Rau, S.W., Dela Cruz, C., Yang, E., Zhu, H., Yu, J., Cashion, A.B., Kindy, M.S., Merchenthaler, I., Gage, F.H., Wise, P.M., 2007. Estradiol enhances neurogenesis following ischemic stroke through estrogen receptors alpha and beta. J. Comp. Neurol. 500, 1064-1075.

Takeuchi, A., Okubo, K., 2013. Post-Proliferative Immature Radial Glial Cells Female-Specifically Express Aromatase in the Medaka Optic Tectum. PLoS ONE 8, e73663.

Tanapat, P., Hastings, N.B., Reeves, A.J., Gould, E., 1999. Estrogen stimulates a transient increase in the number of new neurons in the dentate gyrus of the adult female rat. J. Neurosci. 19, 5792-5801.

Tapanes-Castillo, A., Shabazz, F.S., Mboge, M.Y., Vajn, K., Oudega, M., Plunkett, J.A., 2014. Characterization of a novel primary culture system of adult zebrafish brainstem cells. J. Neurosci. Methods 223, 11-19.

Tchoudakova, A., Kishida, M., Wood, E., Callard, G.V., 2001. Promoter characteristics of two cyp19 genes differentially expressed in the brain and ovary of teleost fish. J. Steroid Biochem. Mol. Biol. 78, 427-439.

Teles, M., Maria, V.L., Pacheco, M., Santos, M.A., 2004. Anguilla anguilla L. plasma cortisol, lactate and glucose responses to abietic acid, dehydroabietic acid and retene. Environ. Int. 29, 995-1000.

Toivola, D.M., Isomaa, B., 1991. Effects of dehydroabietic acid on the erythrocyte membrane. Chem. Biol. Interact. 79, 65-78.

Tong, S.-K., Mouriec, K., Kuo, M.-W., Pellegrini, E., Gueguen, M.-M., Brion, F., Kah, O., Chung, B.-c., 2009. A cyp19a1b-gfp(aromatase B) transgenic zebrafish line that expresses GFP in radial glial cells. Genesis 47, 67-73.

Tong, S.K., Chung, B.C., 2003. Analysis of zebrafish cyp19 promoters. J. Steroid Biochem. Mol. Biol. 86, 381-386.

Tora, L., White, J., Brou, C., Tasset, D., Webster, N., Scheer, E., Chambon, P., 1989. The human estrogen receptor has two independent nonacidic transcriptional activation functions. Cell 59, 477-487.

Trudeau, V.L., 1997. Neuroendocrine regulation of gonadotrophin II release and gonadal growth in the goldfish, Carassius auratus. Rev. Reprod. 2, 55-68.

Tsuruo, Y., Ishimura, K., Osawa, Y., 1995. Presence of estrogen receptors in aromatase-immunoreactive neurons in the mouse brain. Neurosci. Lett. 195, 49-52.

Ubuka, T., Haraguchi, S., Tobari, Y., Narihiro, M., Ishikawa, K., Hayashi, T., Harada, N., Tsutsui, K., 2014. Hypothalamic inhibition of socio-sexual behaviour by increasing neuroestrogen synthesis. Nat. Commun. 5, 3061.

Untergasser, A., Cutcutache, I., Koressaar, T., Ye, J., Faircloth, B.C., Remm, M., Rozen, S.G., 2012. Primer3--new capabilities and interfaces. Nucleic Acids Res. 40, e115.

Van Den Eeden, S.K., Tanner, C.M., Bernstein, A.L., Fross, R.D., Leimpeter, A., Bloch, D.A., Nelson, L.M., 2003. Incidence of Parkinson's disease: variation by age, gender, and race/ethnicity. Am. J. Epidemiol. 157, 1015-1022.

Verwer, R.W.H., Sluiter, A.A., Balesar, R.A., Baayen, J.C., Noske, D.P., Dirven, C.M.F., Wouda, J., van Dam, A.M., Lucassen, P.J., Swaab, D.F., 2007. Mature astrocytes in the adult human neocortex express the early neuronal marker doublecortin. Brain 130, 3321-3335.

Vizziano-Cantonnet, D., Anglade, I., Pellegrini, E., Gueguen, M.M., Fostier, A., Guiguen, Y., Kah, O., 2011. Sexual dimorphism in the brain aromatase expression and activity, and in the central expression of other steroidogenic enzymes during the period of sex differentiation in monosex rainbow trout populations. Gen. Comp. Endocrinol. 170, 346-355.

Wang, L., Andersson, S., Warner, M., Gustafsson, J.A., 2001. Morphological abnormalities in the brains of estrogen receptor beta knockout mice. Proc. Natl. Acad. Sci. U. S. A. 98, 2792-2796.

Wang, W., Li, J., Ge, Y., Li, W., Shu, Q., Guan, H., Yang, K., Myatt, L., Sun, K., 2012. Cortisol induces aromatase expression in human placental syncytiotrophoblasts through the cAMP/Sp1 pathway. Endocrinology 153, 2012-2022.

Waye, A., Trudeau, V.L., 2011. Neuroendocrine disruption: more than hormones are upset. J. Toxicol. Environ. Health B Crit. Rev. 14, 270-291.

Weinreb, O., Youdim, M.B., 2007. A model of MPTP-induced Parkinson's disease in the goldfish. Nat. Protoc. 2, 3016-3021.

Wise, J.F., Berkova, Z., Mathur, R., Zhu, H., Braun, F.K., Tao, R.H., Sabichi, A.L., Ao, X., Maeng, H., Samaniego, F., 2013. Nucleolin inhibits Fas ligand binding and suppresses Fas-mediated apoptosis in vivo via a surface nucleolin-Fas complex. Blood 121, 4729-4739.

Wise, R.A., 2006. Role of brain dopamine in food reward and reinforcement. Philos. Trans. R. Soc. Lond. B Biol. Sci. 361, 1149-1158.

Wooten, G.F., Currie, L.J., Bovbjerg, V.E., Lee, J.K., Patrie, J., 2004. Are men at greater risk for Parkinson's disease than women? J. Neurol. Neurosurg. Psychiatry 75, 637-639.

Wu, T.W., Wang, J.M., Chen, S., Brinton, R.D., 2005. 17Beta-estradiol induced Ca2+ influx via L-type calcium channels activates the Src/ERK/cyclic-AMP response element binding protein signal pathway and BCL-2 expression in rat hippocampal neurons: a potential initiation mechanism for estrogen-induced neuroprotection. Neuroscience 135, 59-72.

Xing, L., Goswami, M., Trudeau, V.L., 2014. Radial glial cell: critical functions and new perspective as a steroid synthetic cell. Gen. Comp. Endocrinol. 203, 181-185.

Xing, L., McDonald, H., Da Fonte, D.F., Gutierrez-Villagomez, J.M., Trudeau, V.L., 2015. Dopamine D1 receptor activation regulates the expression of the estrogen synthesis gene aromatase B in radial glial cells. Front. Neurosci. 9, 310.

Yague, J.G., Munoz, A., de Monasterio-Schrader, P., Defelipe, J., Garcia-Segura, L.M., Azcoitia, I., 2006. Aromatase expression in the human temporal cortex. Neuroscience 138, 389-401.

Yamamoto, K., Mirabeau, O., Bureau, C., Blin, M., Michon-Coudouel, S., Demarque, M., Vernier, P., 2013a. Evolution of dopamine receptor genes of the D1 class in vertebrates. Mol. Biol. Evol. 30, 833-843.

Yamamoto, K., Mirabeau, O., Bureau, C., Blin, M., Michon-Coudouel, S., Demarque, M., Vernier, P., 2013b. Evolution of Dopamine Receptor Genes of the D1 Class in Vertebrates. Mol. Biol. Evol. 30, 833-843.

Yamamoto, K., Ruuskanen, J.O., Wullimann, M.F., Vernier, P., 2011. Differential expression of dopaminergic cell markers in the adult zebrafish forebrain. J. Comp. Neurol. 519, 576-598.

Yamasaki, M., Yamada, K., Furuya, S., Mitoma, J., Hirabayashi, Y., Watanabe, M., 2001. 3-Phosphoglycerate dehydrogenase, a key enzyme for l-serine biosynthesis, is preferentially expressed in the radial glia/astrocyte lineage and olfactory ensheathing glia in the mouse brain. J. Neurosci. 21, 7691-7704.

Yao, M., Nguyen, T.V., Pike, C.J., 2007. Estrogen regulates Bcl-w and Bim expression: role in protection against beta-amyloid peptide-induced neuronal death. J. Neurosci. 27, 1422-1433.

Yasuhara, T., Shingo, T., Date, I., 2007. Glial cell line-derived neurotrophic factor (GDNF) therapy for Parkinson's disease. Acta Med. Okayama 61, 51.

Ye, Z.C., Sontheimer, H., 1998. Astrocytes protect neurons from neurotoxic injury by serum

glutamate. Glia 22, 237-248.

Yokoyama, H., Uchida, H., Kuroiwa, H., Kasahara, J., Araki, T., 2010. Role of glial cells in neurotoxin-induced animal models of Parkinson's disease. Neurol. Sci. 32, 1-7.

Youdim, M.B., Dhariwal, K., Levine, M., Markey, C.J., Markey, S., Caohuy, H., Adeyemo, O.M., Pollard, H.B., 1992. MPTP-induced "parkinsonism" in the goldfish. Neurochem. Int. 20 Suppl, 275S-278S.

Zhang, D., Popesku, J.T., Martyniuk, C.J., Xiong, H., Duarte-Guterman, P., Yao, L., Xia, X., Trudeau, V.L., 2009a. Profiling neuroendocrine gene expression changes following fadrozole-induced estrogen decline in the female goldfish. Physiol. Genomics 38, 351-361.

Zhang, D., Xiong, H., Mennigen, J.A., Popesku, J.T., Marlatt, V.L., Martyniuk, C.J., Crump, K., Cossins, A.R., Xia, X., Trudeau, V.L., 2009b. Defining global neuroendocrine gene expression patterns associated with reproductive seasonality in fish. PLoS ONE 4, e5816.

Zhao, C., Fujinaga, R., Tanaka, M., Yanai, A., Nakahama, K., Shinoda, K., 2007. Region-specific expression and sex-steroidal regulation on aromatase and its mRNA in the male rat brain: immunohistochemical and in situ hybridization analyses. J. Comp. Neurol. 500, 557-573.

Zhao, E., Basak, A., Crump, K., Trudeau, V.L., 2006. Proteolytic processing and differential distribution of secretogranin-II in goldfish. Gen. Comp. Endocrinol. 146, 100-107.

Zupanc, G.K., 2001. A comparative approach towards the understanding of adult neurogenesis. Brain Behav. Evol. 58, 246-249.

Zupanc, G.K., 2008. Adult neurogenesis and neuronal regeneration in the brain of teleost fish. J. Physiol. Paris 102, 357-373.

Zupanc, G.K., Clint, S.C., 2003. Potential role of radial glia in adult neurogenesis of teleost fish. Glia 43, 77-86.

Zupanc, G.K.H., Sîrbulescu, R.F., 2011. Adult neurogenesis and neuronal regeneration in the central nervous system of teleost fish. Eur. J. Neurosci. 34, 917-929.

Zupanc, G.K.H., Sîrbulescu, R.F., Ilieş, I., 2012. Radial glia in the cerebellum of adult teleost fish: implications for the guidance of migrating new neurons. NSC 210, 416-430.